27 January 2006 | $10

Science

AAAS

introducing the

Time MACHINE

the MINI PREP 96

Fully Automatic plasmid and genomic DNA purification at the push of a button.

START
ENTER

Your time is valuable.

MACCONNELL RESEARCH

800.466.7949 www.macconnell.com

Proteome Profiler™ Antibody Arrays | from R&D Systems

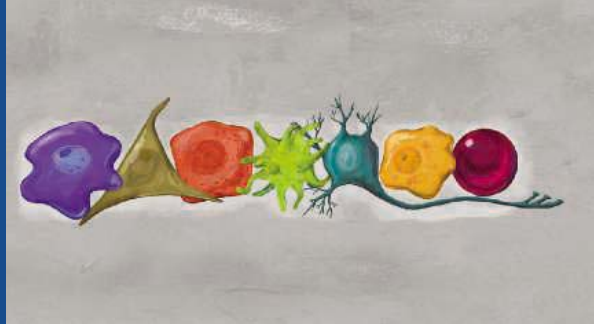

Quality | Selection | Performance | Results

	RTK Array Kit	MAPK Array Kit
PRODUCT	Proteome Profiler Phospho-Receptor Tyrosine Kinase (RTK) Array Kit	Proteome Profiler Phospho-Mitogen Activated Protein Kinase (MAPK) Array Kit
SPECIES	Human	Human
DESCRIPTION	Contains 4 arrays - each spotted (in duplicate) with antibodies to 42 different RTKs.	Contains 4 arrays - each spotted (in duplicate) with antibodies recognizing 19 different MAPKs and other kinases.
CATALOG #	ARY001	ARY002

Human Phospho-MAPK Array Panel

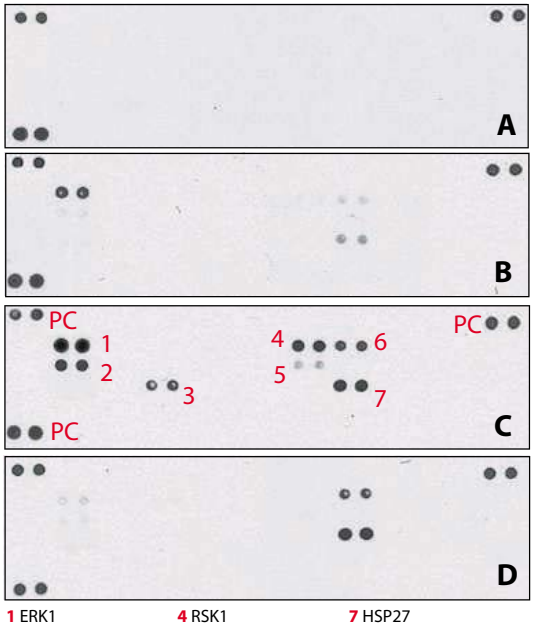

1 ERK1
2 ERK2
3 MSK2
4 RSK1
5 RSK2
6 GSK-3α/β
7 HSP27
PC Positive Control

Target	Phosphorylation Site(s)
ERK1	T202/Y204
ERK2	T185/Y187
JNK1	T183/Y185
JNK2	T183/Y185
JNK3	T221/Y223
JNK pan	T183/Y185,T221/Y223
MSK2	S360
p38α	T180/Y182
p38β	T180/Y182
p38γ	T183/Y185
p38δ	T180/Y182
RSK1	S380
RSK2	S386
p70 S6K	T421/S424
Akt1	S473
Akt2	S474
Akt3	S472
Akt pan	S473, S474, S472
GSK-3α/β	S21/S9
GSK-3β	S9
HSP27	S78/S82

FIGURE 1. HeLa cells were incubated with no additions or with 200 nM PMA for 20 minutes either with or without U0126 (a MEK1/2 inhibitor). R&D Systems Proteome Profiler Human Phospho-MAPK Arrays (Catalog # ARY002) were incubated with (A) no lysate, (B) 175 µg of lysate from untreated cells, (C) 175 µg of lysate from PMA-treated cells, or (D) 175 µg of lysate from cells treated with PMA in the presence of U0126.

Pretreatment with U0126 diminishes the PMA-induced phosphorylation of downstream MEK1/2 pathway members ERK1, ERK2, MSK2, RSK1 and RSK2, with little effect on the phosphorylation of non-members GSK-3α/β and HSP27.

R&D Systems offers new Proteome Profiler™ Antibody Arrays that are screening tools to simultaneously detect the relative level of phospho-rylation of multiple proteins in each sample. Each kit contains buffers, detection antibodies and four nitrocellulose membranes spotted with a carefully selected panel of specific capture antibodies.

www.RnDSystems.com | (800) 343-7475

U.S. & Canada
R&D Systems, Inc.
Tel: (800) 343-7475
info@RnDSystems.com

Europe
R&D Systems Europe Ltd.
Tel: +44 (0)1235 529449
info@RnDSystems.co.uk

Germany
R&D Systems GmbH
Tel: 0800 909 4455
infogmbh@RnDSystems.co.uk

France
R&D Systems Europe
Tel: 0800 90 72 49
info@RnDSystems.co.uk

GE Healthcare

Greater flexibility in histidine-tagged protein purification

Ni Sepharose™ products from GE Healthcare give you greater flexibility and the highest binding capacity available for histidine-tagged protein purification. They also assure maximum target protein activity, thanks to their tolerance of a wide range of additives and negligible nickel ion leakage.

His MultiTrap™ prepacked multiwell plates let you directly apply unclarified lysate for greater convenience and minimized degradation of sensitive target proteins. Ni Sepharose is also available prepacked in His SpinTrap™, His GraviTrap™, HisTrap™ and bulk packs to ensure maximum flexibility in histidine-tagged protein purification.

www.gehealthcare.com/his

imagination at work

YYePG Proudly Presents, Thx for Support

GE01-06

Volume 311, Issue 5760

COVER

A composite image of marine fish and invertebrate development from egg through late larval stages. As marine organisms grow beyond the egg stage, they become capable of swimming, first vertically for tens of meters, then horizontally for hundreds to thousands of meters. These behaviors influence how far they disperse. See page 522.

Image: C. Guigand

DEPARTMENTS

431 *Science* Online
432 This Week in *Science*
437 Editors' Choice
442 Contact *Science*
445 NetWatch
447 Random Samples
467 Newsmakers
482 AAAS News & Notes
542 New Products
543 *Science* Careers

EDITORIAL

435 Getting Serious About Biofuels
by S. E. Koonin
>> Review p. 484; Report p. 506

NEWS OF THE WEEK

Fraud Upends Oral Cancer Field, Casting Doubt on Prevention Trial 448
Scientists Keep Some Data to Themselves 448
U.S. Beckons Foreigners With Science Fulbrights 449
Measurement Schemes Let Physicists Tiptoe Through the Quanta 451
SCIENCESCOPE 451
Rare Tree Species Thrive in Local Neighborhoods 452
>> Report p. 527
Walk on the Wild Side Yields Supersensitive Chemical Measurements 452
I Spy ... a Cold, Little Planet 453
U.K. Backs Off Reclassifying Cannabis as a Dangerous Drug 455
Researchers Caught Between Atoll and a Hard Place 455
Donors Draw Plans to Disburse $2 Billion War Chest for Bird Flu 456
Biobank Ties Cancer Genes to Rare Developmental Syndrome 456
>> Science *Express Report by P. Rodriguez-Viciana* et al.
Genomic Analysis Hints at H5N1 Pathogenicity 457
>> Science *Express Research Article by J. C. Obenauer* et al.

NEWS FOCUS

Special: Mental Health in Developing Countries

The Unseen: Mental Illness's Global Toll 458
Mapping Mental Illness: An Uncertain Topography
China: Healing the Metaphorical Heart 462
A Spoonful of Medicine—and a Steady Diet of Normality 464

LETTERS

Where Next for Genome Sequencing? *P. Raven* et al. 468
Thinking About NASA's Future *M. Barratt; A. Hanson; J. Plescia*
Avoiding Climate Change *J. E. Hansen*
CORRECTIONS AND CLARIFICATIONS 470

BOOKS *ET AL.*

Breaking the Spell Religion as a Natural Phenomenon 471
D. C. Dennett, reviewed by M. Shermer
Plows, Plagues, and Petroleum How Humans Took Control of Climate 472
W. F. Ruddiman, reviewed by J. White

EDUCATION FORUM

The Merits of Training Mentors 473
C. Pfund et al.

PERSPECTIVES

Loop Grafting and the Origins of Enzyme Species 475
D. S. Tawfik
>> Report p. 535
Climate Change and Human Evolution 476
A. K. Behrensmeyer
Rising Mountain Ranges 478
M. A. Poage and C. P. Chamberlain
>> Report p. 511
Making Better Ceramic Composites with Ice 479
J. Halloran
>> Report p. 515
Staying Connected in a Turbulent World 480
R. S. Steneck
>> Report p. 522

CONTENTS continued >>

microRNA

Labelling - Array - Bioinformatics

miRCURY™ Array

From sample to results in 24 h

- **Use less sample**
  - *Works on <1 µg total RNA*
  - *Highly sensitive LNA™ capture probes*
- **Save time**
  - *No miRNA enrichment required*
  - *1 hour labelling protocol*
- **Get instant target prediction**
  - *Free online miRNA Resource Center*

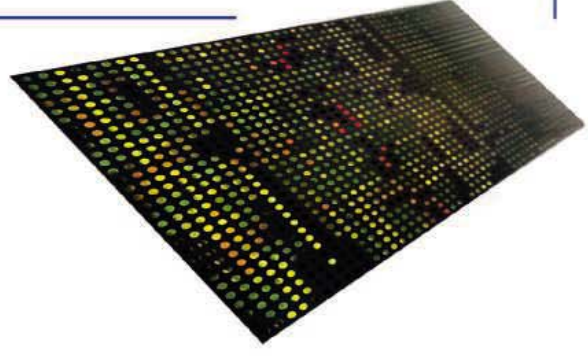

www.exiqon.com

EXIQON

THE HOME OF LNA™

Science

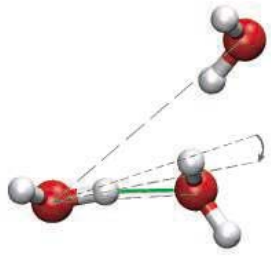

SCIENCE EXPRESS

www.sciencexpress.org

VIROLOGY

Large-Scale Sequence Analysis of Avian Influenza Isolates
J. C. Obenauer et al.
Sequences from 169 isolates of avian influenza viruses, including many different strains, reveal that all have a motif located in a nonstructural gene that is necessary for virulence.
>> News story p. 457
10.1126/science.1121586

MEDICINE

BREVIA: Prions in Skeletal Muscles of Deer with Chronic Wasting Disease
R. C. Angers et al.
Significant amounts of infectious prions are found in the muscles of deer infected with chronic wasting disease, not just in the nervous tissues as in infected cattle.
10.1126/science.1122864

CHEMISTRY

A Molecular Jump Mechanism of Water Reorientation
D. Laage and J. T. Hynes
Simulations suggest that water molecules can rotate in large jumps as the broken hydrogen bonds redistribute concertedly, not diffusively, among neighboring molecules.
10.1126/science.1122154

GENETICS

Germline Mutations in Genes Within the MAPK Pathway Cause Cardio-facio-cutaneous Syndrome
P. Rodriguez-Viciana et al.
Mutations that functionally alter an intensely studied cellular signaling pathway are found in young patients with a developmental delay disorder.
>> News story p. 456
10.1126/science.1124642

TECHNICAL COMMENT ABSTRACTS

EVOLUTION

Comment on "Reconstructing the Origin of Andaman Islanders" 470
M. g. Palanichamy et al.
full text at www.sciencemag.org/cgi/content/full/311/5760/470a

Response to Comment on "Reconstructing the Origin of Andaman Islanders"
K. Thangaraj et al.
full text at www.sciencemag.org/cgi/content/full/311/5760/470b

REVIEW

CHEMISTRY

The Path Forward for Biofuels and Biomaterials 484
A. J. Ragauskas et al.
>> Editorial p. 435; Report p. 506

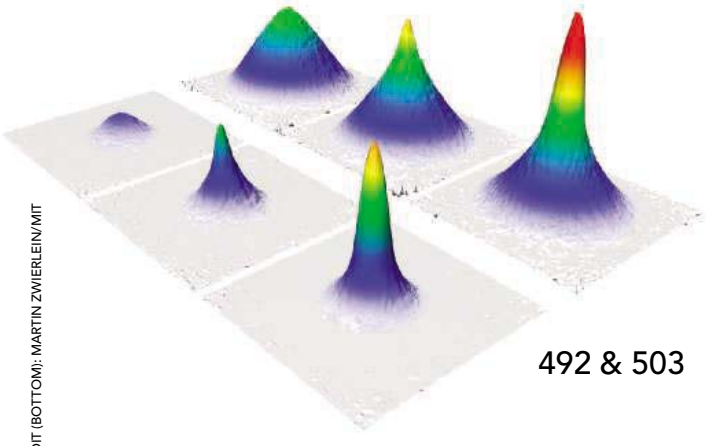

CREDIT (BOTTOM): MARTIN ZWIERLEIN/MIT

492 & 503

BREVIA

ASTRONOMY

The Orbital Period of the Ultraluminous X-ray Source in M82 491
P. Kaaret, M. G. Simet, C. C. Lang
Periodic brightening of luminous X-ray source may be due to gas supplied from a bloated star orbiting around a massive black hole.

RESEARCH ARTICLES

PHYSICS

Fermionic Superfluidity with Imbalanced Spin Populations 492
M. W. Zwierlein, A. Schirotzek, C. H. Schunck, W. Ketterle
Cold clouds of atoms with unequal populations of atomic spins can maintain a surprisingly robust superfluid state, which requires paired spins.
>> Report p. 503

MICROBIOLOGY

Community Genomics Among Stratified Microbial Assemblages in the Ocean's Interior 496
E. F. DeLong et al.
Community genomic analysis indicates that the microbes near the surface of the Northern Pacific are mobile and photosynthetic, while those below 200 meters have pili and synthesize polysaccharides and antibiotics.

REPORTS

PHYSICS

Pairing and Phase Separation in a Polarized Fermi Gas 503
G. B. Partridge, W. Li, R. I. Kamar, Y. Liao, R. G. Hulet
Cold clouds of atoms with unequal populations of atomic spins can maintain a surprisingly robust superfluid state, which requires paired spins.
>> Research Article p. 492

CONTENTS continued **>>**

PIERCE

The Protein People™

Western Blotting

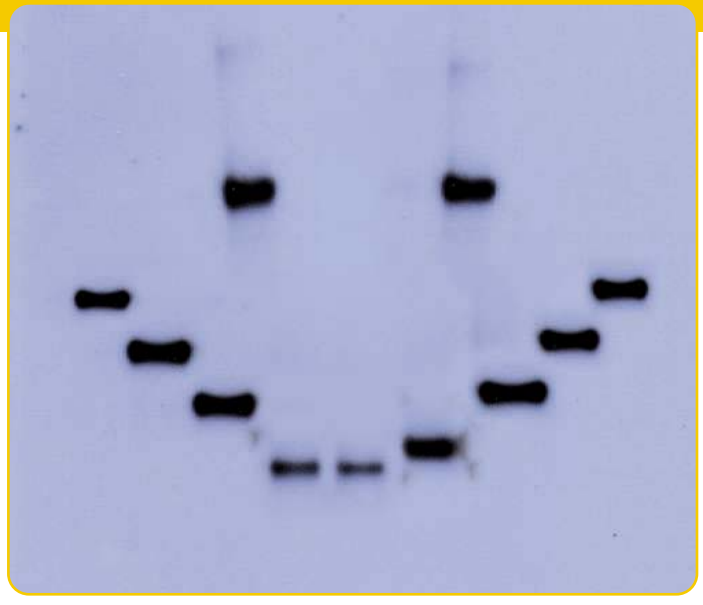

SDS-PAGE

Precise™ Precast Gels & Ranger™ MW Markers

Membrane Treatment Products

MemCode™ Stains, Qentix™ Signal Enhancer & Miser™ Antibody Extender

Blocking Buffers

StartingBlock™, SuperBlock® & SEA BLOCK Buffers; Casein and BSA

Antibodies & Other Probes

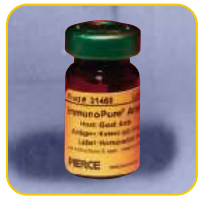

Primary and secondary antibodies with fluorescent or enzymatic labels

Enzyme Substrates

Pierce SuperSignal®, ECL and 1-Step™ Substrates

Detection & Enhancement Products

Restore™ Stripping Buffer, Erase-It® Background Eliminator and CL-XPosure™ Film

happy blotting.

Smile, and your blot smiles with you! A well-run Western blot with a strong signal-to-noise ratio will put a smile on any researcher's face. Pierce has ALL the products you need to achieve a happy Western blot.

FREE
8 Steps to Better Blotting! Log on to *www.piercenet.com* or call 800-874-3723 to request your FREE Western Blotting Handbook!

www.piercenet.com/imno22a

PIERCE

Tel: 815-968-0747 or 800-874-3723 • Fax: 815-968-7316
Technical Assistance E-mail: TA@piercenet.com • Customer Assistance E-mail: CS@piercenet.com

For distributors outside the U.S. and Europe, visit www.piercenet.com

For European offices and distributors, visit www.perbio.com

Science

REPORTS

CHEMISTRY

Ethanol Can Contribute to Energy and Environmental Goals 506

A. E. Farrell et al.

A systems analysis shows that, contrary to some studies, biofuel ethanol can yield more energy than is required for its synthesis; nevertheless, better production technologies are needed.

>> Editorial p. 435; Review p. 484

CHEMISTRY

Optical Detection of DNA Conformational Polymorphism on Single-Walled Carbon Nanotubes 508

D. A. Heller et al.

Metal ions in solution can change the way DNA wraps around a single-walled nanotube and affect the tube's fluorescence, providing a sensitive detector.

GEOCHEMISTRY

Rapid Uplift of the Altiplano Revealed Through ^{13}C-^{18}O Bonds in Paleosol Carbonates 511

P. Ghosh, C. N. Garzione, J. M. Eiler

A paleothermometer based on binding strength between rare C and O isotopes within carbonates shows that the Bolivian Altiplano rose rapidly about 8 million years ago.

>> Perspective p. 478

MATERIALS SCIENCE

Freezing as a Path to Build Complex Composites 515

S. Deville, E. Saiz, R. K. Nalla, A. P. Tomsia

Ice is used to template colloidal particles into forming bone and nacre-like structures and then is easily removed, leaving a contaminant-free substrate for further reinforcement.

>> Perspective p. 479

NEUROSCIENCE

The Cellular Basis of a Corollary Discharge 518

J. F. A. Poulet and B. Hedwig

Crickets "know" when they hear their own song because the neural circuit for singing sends a corollary discharge to auditory neurons as well as to the motor circuit for singing.

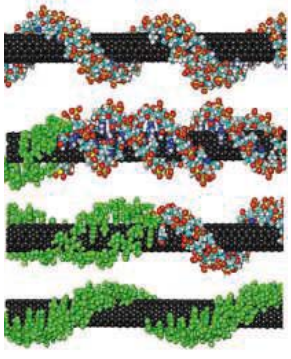

508

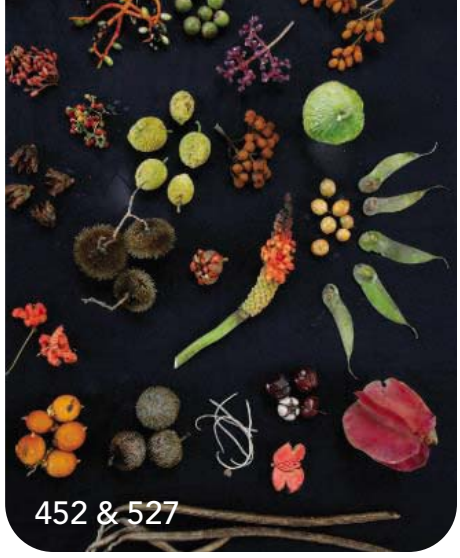

452 & 527

ECOLOGY

Scaling of Connectivity in Marine Populations 522

R. K. Cowen, C. B. Paris, A. Srinivasan

Larvae of coastal fish in the Caribbean typically disperse only 10 to 100 kilometers, less than had been thought, yielding more isolated populations.

>> Perspective p. 480

ECOLOGY

Nonrandom Processes Maintain Diversity in Tropical Forests 527

C. Wills et al.

Long-term census of trees in tropical forest plots shows that rare species survive preferentially, leading to more species diversity as forests age.

>> News story p. 452

BIOCHEMISTRY

An Architectural Framework That May Lie at the Core of the Postsynaptic Density 531

M. K. Baron et al.

A scaffolding protein, assisted by bound Zn^{2+}, can assemble into large sheets and may form a platform for the construction of the postsynaptic density.

BIOCHEMISTRY

Design and Evolution of New Catalytic Activity with an Existing Protein Scaffold 535

H.-S. Park et al.

A process that mimics natural protein evolution converts an enzyme in the metallohydrolase superfamily into a new family member with a different catalytic function.

>> Perspective p. 475

GENETICS

A Virus Reveals Population Structure and Recent Demographic History of Its Carnivore Host 538

R. Biek, A. J. Drummond, M. Poss

An innocuous virus carried by cats shows that recent cougar populations result from the expansion and merging of small isolated populations that had been reduced by hunting.

CREDIT (TOP): CHRISTIAN ZIEGLER

AAAS
ADVANCING SCIENCE, SERVING SOCIETY

SCIENCE (ISSN 0036-8075) is published weekly on Friday, except the last week in December, by the American Association for the Advancement of Science, 1200 New York Avenue, NW, Washington, DC 20005. Periodicals Mail postage (publication No. 484460) paid at Washington, DC, and additional mailing offices. Domestic individual membership and subscription (51 issues): $139 ($74 allocated to subscription). Domestic institutional subscription (51 issues): $650; Foreign postage extra: Mexico, Caribbean (surface mail) $55; other countries (air assist delivery) $85. First class, airmail, student, and emeritus rates on request. Canadian rates with GST available upon request, GST #1254 88122. Publications Mail Agreement Number 1069624. **Printed in the U.S.A.**

Change of address: Allow 4 weeks, giving old and new addresses and 8-digit account number. **Postmaster:** Send change of address to *Science*, P.O. Box 1811, Danbury, CT 06813–1811. **Single-copy sales:** $10.00 per issue prepaid includes surface postage; bulk rates on request. *Science* is indexed in the *Reader's Guide to Periodical Literature* and in several specialized indexes.

CONTENTS continued >>

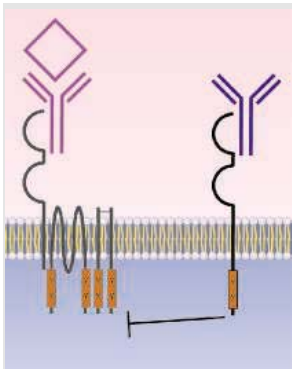

Immune receptor crosstalk.

SCIENCE'S **STKE**

www.stke.org SIGNAL TRANSDUCTION KNOWLEDGE ENVIRONMENT

REVIEW: Inhibition of Immune Responses by ITAM-Bearing Receptors
J. A. Hamerman and L. L. Lanier
Inhibitory signals propagated through ITAMs may help to set the cell's activation threshold.

EVENTS
Plan your travels with this list of meetings, workshops, and conferences related to cell signaling.

Taking the sting out of oxidants.

SCIENCE'S **SAGE KE**

www.sageke.org SCIENCE OF AGING KNOWLEDGE ENVIRONMENT

PERSPECTIVE: Prion 2005—Between Fundamentals and Society's Needs
C. Treiber
Conference goes a step further in coordinating and reinforcing international research activities.

NEWS FOCUS: The Way of the Honeybee
M. Leslie
Bees turn reproductive protein into antioxidant.

SCIENCE**NOW**

www.sciencenow.org DAILY NEWS COVERAGE

Tick, Tock: Humans Have a Slow Molecular Clock
Recent evolutionary changes may explain why humans mature slower than other primates.

Bumping Iron No Cure for Hookworms
Anemia caused by infection might actually be made worse with iron supplementation.

Green Turtles Make a Comeback
Rumors of a South Atlantic population's demise have been greatly exaggerated, says new study.

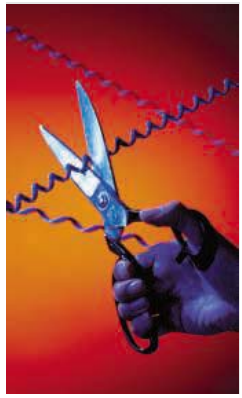

Cutting out distractions.

SCIENCE **CAREERS**

www.sciencecareers.org CAREER RESOURCES FOR SCIENTISTS

GLOBAL: Mind Matters—Driven to Distraction
I. S. Levine
Learn how to deal with personal business, chatty colleagues, and other workday distractions.

MISCINET: Educated Woman, Ch. 47—The End Is Nearer
M. P. DeWhyse
It's amazing what a few job offers will do for your morale.

US: The Other Microsoft
J. Kling
For 750 computer scientists at six facilities worldwide, Microsoft Research is a great place to work.

GRANTSNET: International Grants and Fellowship Index
A. Kotok
Get the latest listing of funding opportunities from Europe, Asia, and the Americas.

EDITED BY STELLA HURTLEY AND PHIL SZUROMI

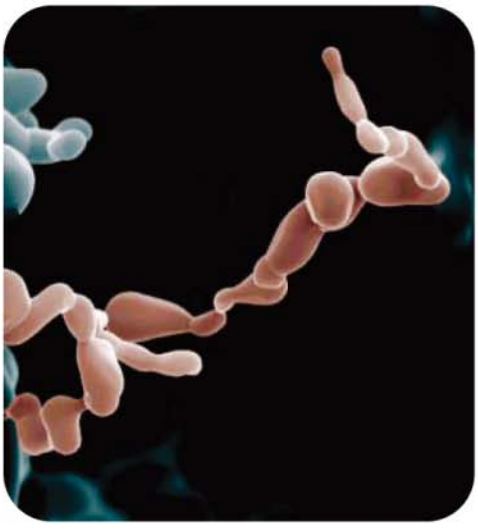

Frozen Forms

When water freezes, it can form hexagonal plates that grow at different rates in different directions, and impurities can become trapped at the water-ice interfaces. **Deville *et al.*** (p. 515; see the Perspective by **Halloran**) exploited these effects to fabricate porous materials from concentrated ceramic powder suspensions, which could also be backfilled with a second material to make composites. The colloidal particles could then be etched away to leave a porous structure composed of the second material such as alumina. Using nacre and bone as their inspirations, the authors show how they can replicate these complex composite materials.

Above-Ground Resources

With fossil-fuel supplies steadily waning, recent research has focused on using plant-derived materials as a renewable substitute (see the Editorial by **Koonin**). **Ragauskas *et al.*** (p. 484) review progress in this area, ranging from plant genetics research for enhancing supply to enzymatic and other catalytic methods for breaking down the biomass into practical fuels and fine chemical precursors. Some of the economic challenges and benefits of changing the production infrastructure on such a large scale are also addressed. Ethanol is a renewable resource already in use as a liquid fuel, but its production from corn and cellulose is energy intensive, and some analyses have found that the overall process uses more energy than it creates. **Farrell *et al.*** (p. 506) rigorously analyzed a variety of relevant investigations, and found that the studies reporting negative net energy values are flawed. All of the studies show that current corn ethanol technologies reduce petroleum use significantly relative to gasoline. However, new production methods are needed if fuel ethanol is to reduce greenhouse gas emissions significantly.

Unbalanced Superfluidity

The pairing of fermions lies at the heart of superconductivity in metals and superfluidity in helium-3, where the spin populations are generally equal. Exotic pairing states are expected to arise for imbalanced spin populations, such as in the pairing of quark matter in neutron stars and in strongly magnetized superconductors, but such systems are difficult to realize experimentally. The availability of cold atom clouds of mixed atomic spin states has allowed the crossover regime between Bose-Einstein condensates of molecules and Bardeen-Cooper-Schrieffer superfluids to be probed experimentally. Two studies now address the quantum nature and the phase transition of interacting Fermi gases of lithium-6 in which unbalanced populations of two different spins states are prepared (see the 23 December 2005 news story by **Cho**). **Zwierlein *et al.*** (p. 492, published online 22 December 2005) examined the condensate fraction and superfluidity as a function of spin imbalance and found that superfluidity is remarkably stable against population imbalance. **Partridge *et al.*** (p. 503, published online 22 December 2005) detail the spatial structure and polarization of the mixed spin system.

Tracking a Turn to the Left

Semiconducting single-walled carbon nanotubes (SWNTs) exhibit band-gap fluorescence in the near-infrared, and the dielectric environment surrounding the SWNT can modulate the band-gap energy. **Heller *et al.*** (p. 508) show that this effect is sensitive enough to distinguish whether DNA wrapped around SWNTs is in the native B form or has been shifted to lower energies when the DNA adopts the left-handed Z form in the presence of divalent metal ions such as mercury or cobalt. These shifts were seen for the several different SWNT species present in a buffer solution and were used to detect micromolar levels of Hg^{2+} in highly scattering media such as whole blood.

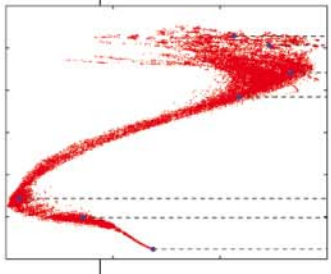

How High Was It?

Oxygen isotope fractionation in rain generally decreases with increasing temperature, and this effect can be used to determine changes in elevation of a region over geological time. However, changes in the path of storms or the season of precipitation add great uncertainty. **Ghosh *et al.*** (p. 511; see the Perspective by **Poage and Chamberlain**) have developed a thermometer based on the binding of the temperature-dependent binding of rate ^{13}C and ^{18}O isotopes in carbonate minerals. This independent estimate of temperature can be related to lapse rate and other data used to infer elevation of minerals that form in soils. An analysis of soil carbonates in Bolivia shows that the high plateau there rose between 6 and 10 million years ago.

Marine Microbial Gene Ecology

Depth stratification occurs in the open ocean not only for large planktonic creatures but also for microbial plankton. **DeLong *et al.*** (p. 496) sampled and sequenced the microorganisms in the water column in the North Pacific Subtropical Gyre with the aim of identifying sequences that tracked major environmental features. Above 200 meters, distinct photic zone sequences were found characteristic of photosynthetic and mobile microorganisms requiring iron, mostly *Prochlorococcus* (itself dividing into high- and low-light–tolerant clades) and *Peligabacter*, accompanied by Euryarchaea. Strikingly, photic zone microbes showed evidence of high rates of viral infection. Below

CREDITS (TOP TO BOTTOM): DEVILLE *ET AL.*/MATERIAL SCIENCES DIVISION,LBNL; DELONG *ET AL.*

200 meters, *Chloroflexi*, SAR202, *Planctomycetales*, and Crenarchaea were found, with sequences suggesting a predominance of "adhesive" microbes that produce pili and synthesize polysaccharides and antibiotics.

Dispersal Patterns of Marine Population

The scale of dispersal among marine populations, or "population connectivity," has been a notoriously intractable problem. **Cowen *et al.*** (p. 522, published online 15 December 2005; see the cover and the Perspective by **Steneck**) analyzed larval dispersal patterns for a suite of coastal fish species in the Caribbean Sea, a large region with complex ocean currents. Typical dispersal distances were on the scale of only 10 to 100 kilometers, and larval movement was a key factor in their dispersal potential. These robust estimates of population connectivity levels have broad relevance for the spatial management of marine resources and for understanding the spread of invasive species and disease in the marine environment.

The Not-So-Quiet Cricket

Our own behavior often generates intense sensory feedback, for example, during loud shouting. How do we prevent self-induced desensitization of our auditory pathway and distinguish between self-generated and external sounds? Inhibitory neural signals, called corollary discharges, are sent from motor to sensory areas in the brain that suppress responses at the precise time that we generate sensory information. Using singing crickets as a model system, **Poulet and Hedwig** (p. 518) identified the cellular basis for a corollary discharge that is indispensable in order to distinguish self-generated sensory feedback from external information. The corollary discharge interneuron in the cricket is driven by the song pattern generator and monosynaptically inhibits crucial elements of the auditory pathway.

Working an Active Site into an Existing Scaffold

Designing enzymes that catalyze industrial reactions is one goal of protein engineering. Although there has been progress in rational design, it is hindered by a limited understanding of structure-function relations. **Park *et al.*** (p. 535; see the Perspective by **Tawfik**) have used a strategy that mimics natural evolution to change the function of an existing protein scaffold. By insertion, deletion, and substitution of several active-site loops, followed by point mutations, they introduced β-lactamase activity into the αβ/βα metallohydrolase scaffold of glyoxalase II. Extending the process to other scaffolds may allow creation of new enzyme activities with practical applications.

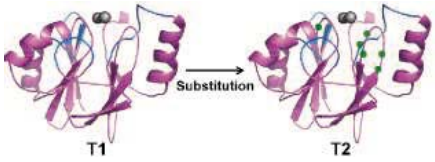

Maintaining Different Trees in the Forest

Frequency-dependent models for the maintenance of high species diversity of trees in tropical forests predict that locally rare species survive preferentially when compared with common species. **Wills *et al.*** (p. 527; see the news story by **Pennisi**) present a longitudinal survey of species frequencies from a network of large plots (50 hectares) in seven tropical forest sites in the Old and New Worlds. In all of the sites, the diversity of recruits into large size classes did increase as the forests aged. Forests suffering from limited, temporary disturbance should have the ability to recover former levels of diversity, and selection processes should favor increasing differences between species.

Viruses Reveal the Secrets of the Cougar

Conservationists and research scientists have discussed the idea that pathogens could be used as genetic tags to record changes in the demography of the host population, but until now have failed to get to grips with any specific system. **Biek *et al.*** (p. 538) have characterized the spatial and temporal distribution of nonpathogenic feline immunodeficiency virus (FIV) and its natural host, the cougar, as the cats' populations recovered from heavy hunting pressure in the first half of the 20th century. Fast-evolving RNA viruses such as FIV provide insights into what the host population has been doing on an ecological time scale, despite the slow pace of chance of the host population.

YYePG Proudly Presents, Thx for Support

CREDIT: PARK *ET AL.*

CellTiter-Glo® – The Perfect Assay.

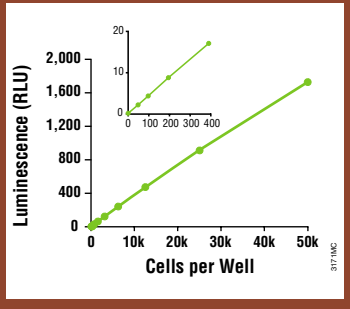

Dynamic range from less than 10 cells to over 10,000 cells.

Measure as few as 10 cells in less than 10 minutes—with a single-step protocol for quantifying intracellular ATP. From basic research to high-throughput drug screening, the CellTiter-Glo Assay is judged the best. It enables you to easily estimate cell number, measure cell viability or quantitate cytotoxic effects. Discriminating scientific minds agree; CellTiter-Glo is the perfect assay. See for yourself. For a **FREE SAMPLE** visit: **www.promega.com/celltiterglo**

Promega

PROMEGA CORPORATION • www.promega.com

Yes, Promega Proudly Presents, Thx for Support

Steven E. Koonin is chief scientist for BP, London, UK. He is a theoretical physicist from the California Institute of Technology, Pasadena, CA, USA, where he also served as provost from 1995 to 2004. E-mail: Steven.Koonin@uk.bp.com

Getting Serious About Biofuels

ALTHOUGH RUDOLF DIESEL IMAGINED THAT HIS EPONYMOUS ENGINE WOULD BE FUELED BY VEGETABLE oils, the widespread availability of inexpensive petroleum during the 20th century determined otherwise. The world is now seriously revisiting Diesel's vision, driven by surging global oil demand, the geographical concentration of known petroleum reserves, the increasing costs of finding and producing new reserves, and growing concerns about atmospheric greenhouse gas (GHG) concentrations.

Liquid hydrocarbons are well suited for transport uses because of their high energy density and handling convenience. Although fossil fuels will be required and available for many decades, producing supplementary fuels from biomass can simultaneously address three important societal concerns without requiring substantial modification of existing vehicles or of the fuel distribution infrastructure: security of supply (biofuels can be produced locally in sustainable systems), lower net GHG emissions (biofuels recycle carbon dioxide that was extracted from the atmosphere in producing biomass), and support for agriculture.

The 2% of today's transportation fuels derived from biomass and blended with fossil fuels are produced either by the fermentation to ethanol of food-derived carbohydrates (such as cane sugar or cornstarch) or by the processing of plant oils to produce biodiesel. Unfortunately, current practices based on food production models do not maximize energy or GHG benefits (because they use fossil fuels) and are not economically competitive with fossil fuels at today's energy prices.* Nevertheless, many nations (including the United States, European Union, and India) are expecting that some 5% of their road fuels will be bioderived within the next 5 years.

Credible studies show that with plausible technology developments, biofuels could supply some 30% of global demand in an environmentally responsible manner without affecting food production. To realize that goal, so-called advanced biofuels must be developed from dedicated energy crops, separately and distinctly from food. This is a multidisciplinary task in which biologists, agronomists, chemical engineers, fuel specialists, and social scientists must work to integrate and optimize several currently disjoint activities.

There are major technological challenges in realizing these goals. Genetic improvement of energy crops such as switchgrass, poplar, and jatropha has barely begun. It will be important to increase the yield and environmental range of energy crops while reducing agricultural inputs. Plant development, chemical composition, tolerance of biotic and abiotic stresses, and nutrient requirements are important traits to be manipulated. The combination of modern breeding and transgenic techniques should result in achievements greater than those of the Green Revolution in food crops, and in far less time.

The cost of biomass transport determines the supply area of a biofuels processing facility and thus its scale and economics. But unlike most food crops, there is no need to keep biomass intact. That means that in-field densification, pelletization, drying, and pyrolysis are among the technology opportunities to reduce transport costs. Fuel production from the lignocellulosic component of biomass will be a very important improvement. Its particular challenges of chemical recalcitrance and utilization of the constituent sugars to produce optimal fuel molecules and co-products are not intractable to current biotechnology. Similarly, process integration comparable to that of a modern petroleum refinery is a plausible chemical engineering goal.

Intertwined with the technology of large-scale biofuels production are the social and policy issues. The balances between natural vegetation and cultivation, arable and marginal land use, mechanized agriculture and employment opportunities, and food and energy crops will be important matters of discussion in many different forums. Whatever the outcomes, technologies will have to be sufficiently robust to accommodate a diversity of needs around the globe.

There is substantial technology "headroom" for advanced biofuels to enhance energy security, reduce GHG emissions, and provide economical transport. It exists largely because the world's scientific and engineering skills have not yet been focused coherently on the challenges involved. It is now time to do that through a coordination of government, university, and industrial R&D efforts, facilitated by responsible public policies. In the jargon of the petroleum industry, the "size of the prize" is too large to ignore.

—Steven E. Koonin

10.1126/science.1124886

*Brazil is a singular counterexample, where favorable agricultural conditions and a flexible processing infrastructure allow the majority of the world's gasoline consumption to be displaced directly with cane-derived ethanol.

CREDITS (LEFT TO RIGHT): CALTECH; BRETT HAMPTON/ARS

EndNote. Where millions of researchers, librarians and students begin.

Learn about new tools for your research and publishing—

Onfolio™
Organize RSS feeds and Web research

RefViz™
Visualize references

sciPROOF™
Proof your manuscript

800-722-1227 • 760-438-5526
Fax: 760-438-5573
rs.info@thomson.com

EndNote, used by millions of researchers, students, professors, librarians and writers worldwide, is known for introducing innovative features such as the ability to search online bibliographic databases, organize references and images, and create instant bibliographies. With EndNote 9, you can work faster with increased performance, connect to more data sources worldwide, and share customized libraries with colleagues easily. EndNote is easy to use, easy to learn and is seamlessly compatible with Microsoft® Word for Windows® and Mac® OSX. There simply is no better way to manage your references and build instant bibliographies.

Download your Free demo or buy online today.
www.endnote.com

HIGHLIGHTS OF THE RECENT LITERATURE

ECOLOGY/EVOLUTION

Taking In the Welcome Mat

Ants are ubiquitous in tropical forests, and they exhibit a wide variety of nesting and foraging behaviors that have fascinated naturalists and ecologists ever since the pioneering of scientific exploration in the tropics. Despite many decades of intense study and the high visibility of ants, Longino has managed to unearth previously unreported nesting habits in two endemic Costa Rican ant species in the genus *Stenamma*.

Nest entrance and *Stenamma alas*.

These ants build nests in the vertical clay banks of streams, and the entrance to the nest is formed by a tunnel through the center of a shallow dish sitting atop a pedestal of clay or through a similarly shaped disk of soil lying on a mound of small stones. In both types of dwelling, a spherical pebble near the entrance can be retrieved and used to plug the doorway in times of danger. Each ant colony maintains several such nests, but occupies only one at a time. Because of their colonial habit, ants attract predators, and much of their nesting repertoire revolves around defense. Hence, it appears that the elaborate constructions of *Stenamma* may minimize the chances of attack by marauding hordes of army ants, which are one of the dominant forces shaping tropical forest ecosystems. — AMS

Biotropica **37**, 670 (2005).

CREDITS (TOP TO BOTTOM): LONGINO *ET AL.*, *BIOTROPICA* **37**, 670 (2005); PHOTOS.COM

PSYCHOLOGY

Post-Testanic Potentiation

Tests are an inescapable part of schooling, though generally less prevalent now than in days of yore. Two reasons for administering tests are (i) to assess student achievement and aptitude, and (ii) to impel students to study, and presumably to learn, the subject matter.

Roediger and Karpicke demonstrate that the actual taking of a test, as opposed to simply preparing to take it, has beneficial consequences. After being allowed to study a reading comprehension passage (preparation material for the Test of English as a Foreign Language), students either were tested for retention of the ideas or allowed a second study session; students in both groups were then tested 5 min, 2 days, or 1 week later. The study-study (SS) group performed better at first but did not score as well as the study-test (ST) group on the later test dates. An expanded protocol confirmed this pattern, with SSSS students outperforming SSST and STTT students when tested right away but with the rankings reversed after 1 week. Notably, the repeated-study students had read the text four times more than the repeated-test students had, yet they retained significantly less of the information. — GJC

Taking tests to learn.

Psychol. Sci. **17**, 249 (2006).

CHEMISTRY

Using Silver to Sugarcoat DNA

One strategy for wiring nanodevices together is to make the desired connections with DNA strands, which can then be metallized. For molecular electronics, it would be useful to create metal-free gaps in these wires, and for the chemical reduction of silver with aldehyde-modified DNA, such gaps can be created by binding large proteins to the DNA, which then act as a resist.

Burley *et al*. describe an alternative approach in which modified DNA molecules are synthesized using *Pwo* polymerase with modified dTTPs bearing acetylenic groups. A protected aldehyde, in the form of a galactose that has been modified with an azide group, can then react with the acetylenic side chains via "click" chemistry. Treatment of a 318–base pair [illegible] reagent) and then with a developer solution deposited silver nanoparticles on the DNA, which was confirmed by atomic force microscopy. — PDS

J. Am. Chem. Soc. 10.1021/ja055517v (2006).

VIROLOGY

HIV Hijacks Exosomes

Understanding the mechanisms by which HIV infects cells is a key step in developing effective treatments. Wiley and Gummuluru describe how immature dendritic cells of the immune system can capture HIV particles and, soon after internalization, transmit them to T cells without themselves becoming infected.

Dendritic cells are one of the first immune cell types encountered by incoming virus particles in the mucosa. HIV particles bind to dendritic cells and are internalized, ending up in multivesicular endosomes. Dendritic cells constitutively release some of the internal vesicles from multivesicular endosomes—so-called exosomes—into the extracellular milieu. For dendritic cells that have recently internalized HIV, it appears that the exosomes contain intact infectious HIV particles, which can then infect $CD4^+$ target T cells. Indeed, the exosome-associated virus particles are up to

Continued on page 439

Enhanced RNA Amplification

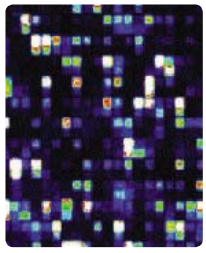

MessageAmp™ II-Biotin *Enhanced*

Single Round aRNA Amplification Kit

- **Enhanced Efficiency** – Single round of amplification from just 50 ng of RNA
- **Enhanced Yields** – Up to 10X greater yields than leading competitor
- **Enhanced Sensitivity** – Highest Present calls of any linear amplification kit
- **Enhanced Convenience** – Includes optimized NTP mix containing biotin-UTP

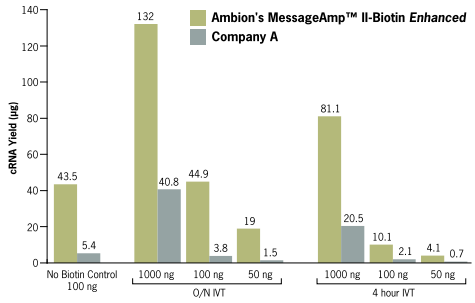

High Yields from Low Inputs. With just 50 ng of RNA input, a single round of amplification yields enough biotin labeled amplified RNA for Affymetrix® GeneChip® analysis.

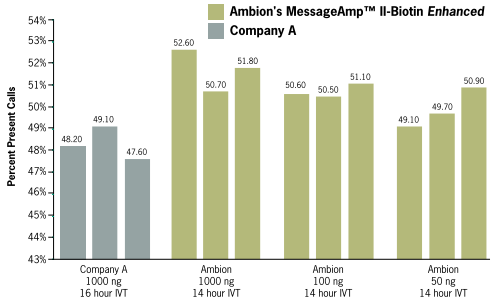

Detect More Genes. Ambion's new MessageAmp™ II-Biotin *Enhanced* kit consistently produces higher percent Present calls than the leading competitor, from 50 ng and just a single round of amplification.

Save up to 40% on Reaction Costs

MessageAmp II-Biotin *Enhanced* is a complete single round amplification and labeling kit validated for Affymetrix® GeneChip® analysis.

www.ambion.com/prod/ma2biotin

Ambion®
THE RNA COMPANY®

Ambion, Inc.
U.S. 800-888-8804 • Canada 800-445-1161
fax +1-512-651-0201

Ambion (Europe) Ltd.
tel +44 (0)1480-373-020
fax +44 (0)1480-373-010

Ambion K.K. (Japan)
tel +81 (0)3-5638-2181
fax +81 (0)3-5638-2182

For a list of Ambion direct free phone numbers and distributors in your country, go to www.ambion.com/contact

Continued from page 437

10-fold more infectious per particle than are cell-free virus preparations. The remaining dendritic cell–associated virus is transported from multivesicular endosomes to lysosomes and degraded. This exosomal pathway may explain how HIV can evade immune destruction even after having entered the wrong target cell of the immune system. The relative importance of this pathway—in comparison to the so-called infectious synapse, wherein dendritic cells directly pass HIV on to target T cells—remains to be established. — SMH

Proc. Natl. Acad. Sci. U.S.A. **103**, 738 (2006).

CHEMISTRY

A Guide to Achieving Closure

Epoxides are versatile intermediates in both enzymatic and laboratory syntheses of complex organic compounds. These three-membered rings, composed of an oxygen and two substituted carbon atoms, are strained and can be opened readily by scission of a C-O bond. Moreover, the liberated oxygen can attack another epoxide in the same molecule, forming a larger and more stable cyclic ether in the process.

In general, an epoxide can be opened via attack at either carbon, and substituents introduced to favor one path over the other can prove difficult to remove from the desired product. Simpson *et al.* have found that the tetracyclic core common to the ladder polyethers (marine natural products associated with red tides) can be prepared efficiently via a base-catalyzed epoxide-opening cascade that is guided by trimethylsilyl substituents. Attack

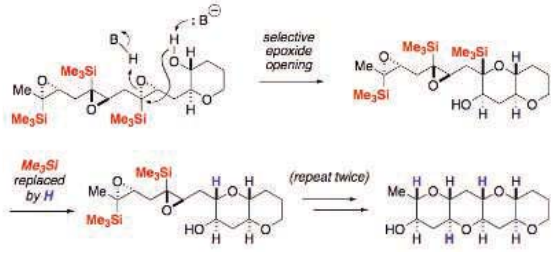

Reaction scheme yielding the tetrahydropyran core.

by the oxygen is favored at the silyl-substituted carbon of the adjacent epoxide, yielding the naturally occurring six-membered rings over the kinetically favored five-membered ones. Furthermore, including a fluoride salt in the reaction mixture has the happy consequence of eliminating the pendant trimethylsilyl group after each ring closes. — JSY

J. Am. Chem. Soc. 10.1021/ja057973p (2006).

MICROBIOLOGY

A Stomach Full

Until hints to the contrary in several recent studies, the stomach was conventionally thought of as being almost as uninhabitable as Mars. Upon analysis of small-subunit 16*S* ribosomal RNA libraries prepared from endoscopy samples collected from 23 individuals, Bik *et al.* discovered, living in the human stomach, a zoo of microorganisms of which a significant proportion had been identified previously as residing in the mouth and 10% were previously unsuspected denizens. Indeed, a member of the genus that includes the notoriously radiation-resistant *Deinococcus radiodurans* was found, perhaps reflecting the tough physicochemical environment of the stomach. Nineteen of the people were found to be positive for *Helicobacter pylori* but otherwise showed significant variation in their gastric ecosystems. In all, 128 phylotypes were discovered, with *Streptococcus* and *Prevotella* spp. being the most abundant after *H. pylori*. The authors proffer the suggestion that there are multiple ecological niches in the stomach, each with its own demographic, although currently we can only guess at the roles these organisms play in health and disease. — CA

Proc. Natl. Acad. Sci. U.S.A. **103**, 732 (2006).

APPLIED PHYSICS

Gated Spin Control in Carbon Nanotubes

The growing fields of molecular electronics and spin electronics offer the future possibility of high-density electronic devices, but with the advantage of avoiding the problem of how to dissipate the heat that builds up in such densely packed structures. Nagabhirava *et al.* have combined the two approaches using a carbon single-walled nanotube (c-SWNT) to bridge the gap between the ferromagnetic source and drain contacts. With the gap reduced to around 10 nm in order to reduce spin-scattering events along the nanotube, they show that the magnitude and sign of the magnetoresistance, a measure of the flow of polarized electrons through the carbon nanotube in response to an external magnetic field, can be reproducibly modified from +10% to −15% by application of a bias on a back gate. The results provide strong evidence for spin transport through c-SWNTs and promise for the spin transistor, a device in which a gate bias controls the flow of spin-polarized current between the source and drain contacts. — ISO

Appl. Phys. Lett. **88**, 023114 (2006).

YYePG Proudly Presents, Thx for Support

Mallinckrodt Baker.
We've been a hit with chemists for 130 years.

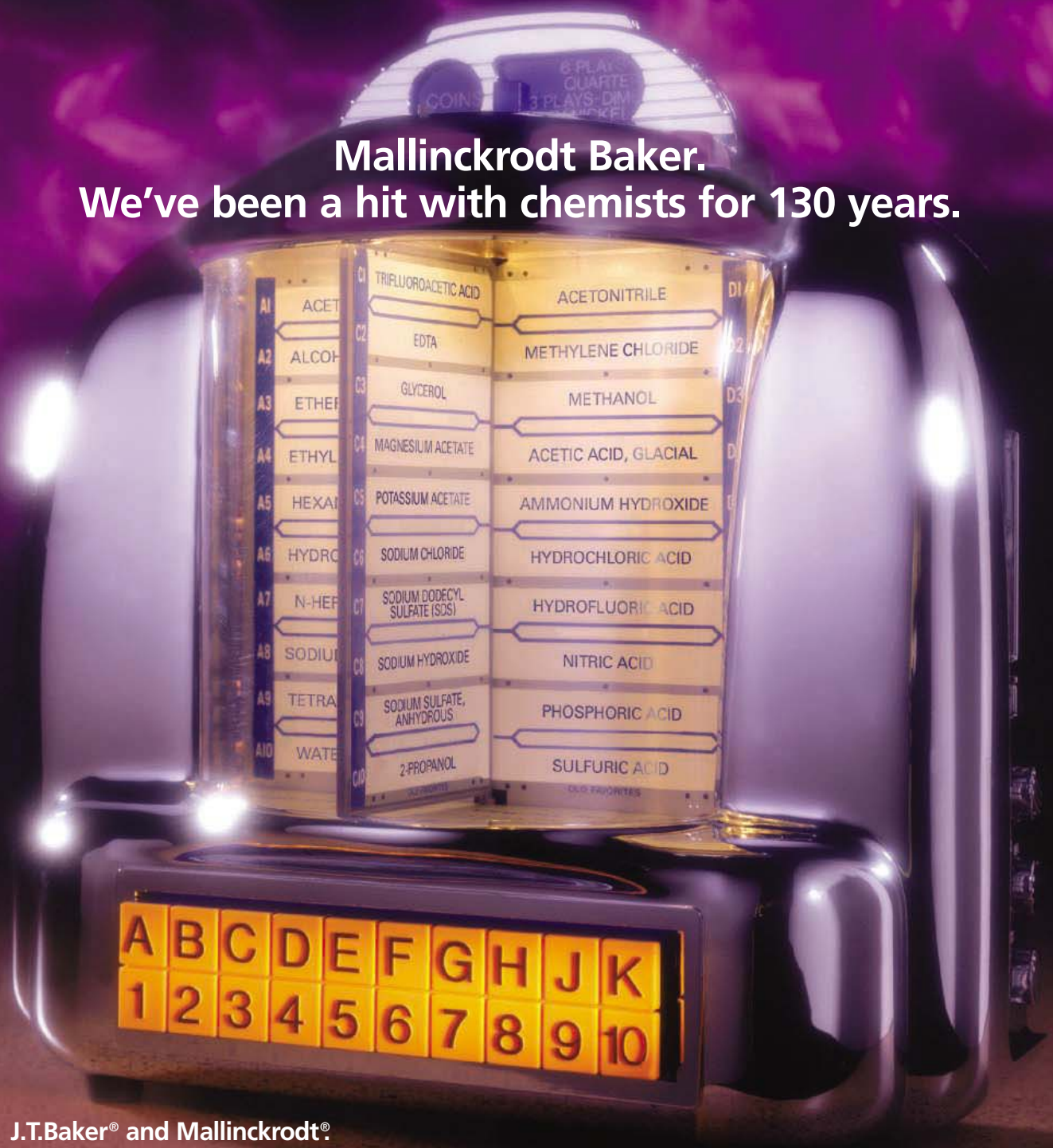

J.T.Baker® and Mallinckrodt®. Two great brands. One unique source for chemicals.

Every day, thousands of laboratories around the globe put their trust in chemicals from Mallinckrodt Baker. Our diverse product line offers a match for virtually any application you're working on. Plus, our chemicals deliver consistent results… time after time.

To request copies of the new Mallinckrodt and J.T.Baker catalogs, please visit www.mallbaker.com/lab

Mallinckrodt Baker

Quality ◆ Choice ◆ Value

YYePG Proudly Presents, Thx for Support

J.T.Baker®

Mallinckrodt® CHEMICALS

www.sciencemag.org

Science

1200 New York Avenue, NW
Washington, DC 20005
Editorial: 202-326-6550, FAX 202-289-7562
News: 202-326-6500, FAX 202-371-9227

Bateman House, 82-88 Hills Road
Cambridge, UK CB2 1LQ
+44 (0) 1223 326500, FAX +44 (0) 1223 326501

Subscription Services For change of address, missing issues, new orders and renewals, and payment questions: 800-731-4939 or 202-326-6417, FAX 202-842-1065. Mailing addresses: AAAS, P.O. Box 1811, Danbury, CT 06813 or AAAS Member Services, 1200 New York Avenue, NW, Washington, DC 20005

Institutional Site Licences please call 202-326-6755 for any questions or information

Reprints: Author Inquiries 800-635-7181
Commercial Inquiries 803-359-4578
Corrections 202-326-6501

Permissions 202-326-7074, FAX 202-682-0816

Member Benefits Bookstore: AAAS/BarnesandNoble.com bookstore www.aaas.org/bn; Car purchase discount: Subaru VIP Program 202-326-6417; Credit Card: MBNA 800-847-7378; Car Rentals: Hertz 800-654-2200 CDP#343457, Dollar 800-800-4000 #AA1115; AAAS Travels: Betchart Expeditions 800-252-4910; Life Insurance: Seabury & Smith 800-424-9883; Other Benefits: AAAS Member Services 202-326-6417 or www.aaasmember.org.

science_editors@aaas.org	(for general editorial queries)
science_letters@aaas.org	(for queries about letters)
science_reviews@aaas.org	(for returning manuscript reviews)
science_bookrevs@aaas.org	(for book review queries)

Published by the American Association for the Advancement of Science (AAAS), *Science* serves its readers as a forum for the presentation and discussion of important issues related to the advancement of science, including the presentation of minority or conflicting points of view, rather than by publishing only material on which a consensus has been reached. Accordingly, all articles published in *Science*—including editorials, news and comment, and book reviews—are signed and reflect the individual views of the authors and not official points of view adopted by the AAAS or the institutions with which the authors are affiliated.

AAAS was founded in 1848 and incorporated in 1874. Its mission is to advance science and innovation throughout the world for the benefit of all people. The goals of the association are to: foster communication among scientists, engineers and the public; enhance international cooperation in science and its applications; promote the responsible conduct and use of science and technology; foster education in science and technology for everyone; enhance the science and technology workforce and infrastructure; increase public understanding and appreciation of science and technology; and strengthen support for the science and technology enterprise.

Information for Contributors

See pages 102 and 103 of the 6 January 2006 issue or access www.sciencemag.org/feature/contribinfo/home.shtml

EDITOR-IN-CHIEF **Donald Kennedy**
EXECUTIVE EDITOR **Monica M. Bradford**
DEPUTY EDITORS **R. Brooks Hanson, Katrina L. Kelner**
NEWS EDITOR **Colin Norman**

Editorial supervisory senior editors Barbara Jasny, Phillip D. Szuromi; **senior editor/perspectives** Lisa D. Chong; **senior editors** Gilbert J. Chin, Pamela J. Hines, Paula A. Kiberstis (Boston), Beverly A. Purnell, L. Bryan Ray, Guy Riddihough (Manila), H. Jesse Smith, Valda Vinson, David Voss; **associate editors** Marc S. Lavine (Toronto), Jake S. Yeston; **online editor** Stewart Wills; **associate online editor** Tara S. Marathe; **book review editor** Sherman J. Suter; **associate letters editor** Etta Kavanagh; **information specialist** Janet Kegg; **editorial manager** Cara Tate; **senior copy editors** Jeffrey E. Cook, Harry Jach, Barbara P. Ordway; **copy editors** Cynthia Howe, Alexis Wynne Mogul, Jennifer Sills, Trista Wagoner; **editorial coordinators** Carolyn Kyle, Beverly Shields; **publication assistants** Ramatoulaye Diop, Chris Filiatreau, Joi S. Granger, Jeffrey Hearn, Lisa Johnson, Scott Miller, Jerry Richardson, Brian White, Anita Wynn; **editorial assistants** E. Annie Hall, Lauren Kmec, Patricia M. Moore, Brendan Nardozzi, Michael Rodewald; **executive assistant** Sylvia S. Kihara; **administrative support** Patricia F. Fisher

News senior correspondent Jean Marx; **deputy news editors** Robert Coontz, Jeffrey Mervis, Leslie Roberts, John Travis; **contributing editors** Elizabeth Culotta, Polly Shulman; **news writers** Yudhijit Bhattacharjee, Adrian Cho, Jennifer Couzin, David Grimm, Constance Holden, Jocelyn Kaiser, Richard A. Kerr, Eli Kintisch, Andrew Lawler (New England), Greg Miller, Elizabeth Pennisi, Robert F. Service (Pacific NW), Erik Stokstad; Katherine Unger (intern); **contributing correspondents** Barry A. Cipra, Jon Cohen (San Diego, CA), Daniel Ferber, Ann Gibbons, Robert Irion, Mitch Leslie (NetWatch), Charles C. Mann, Evelyn Strauss, Gary Taubes, Ingrid Wickelgren; **copy editors** Linda B. Felaco, Rachel Curran, Sean Richardson; **administrative support** Scherraine Mack, Fannie Groom **bureaus:** Berkeley, CA: 510-652-0302, FAX 510-652-1867, New England: 207-549-7755, San Diego, CA: 760-942-3252, FAX 760-942-4979, Pacific Northwest: 503-963-1940

Production director James Landry; **senior manager** Wendy K. Shank; **assistant manager** Rebecca Doshi; **senior specialists** Jay Covert, Chris Redwood **Preflight director** David M. Tompkins; **manager** Marcus Spiegler; **specialist** Jessie Mudjitaba

Art director Joshua Moglia; **associate art director** Kelly Buckheit; **illustrators** Chris Bickel, Katharine Sutliff; **senior art associates** Holly Bishop, Laura Creveling, Preston Huey; **associate** Nayomi Kevitiyagala; **photo researcher** Leslie Blizard

***Science* International**

Europe (science@science-int.co.uk) **editorial: international managing editor** Andrew M. Sugden; **senior editor/perspectives** Julia Fahrenkamp-Uppenbrink; **senior editors** Caroline Ash (Geneva: +41 (0) 222 346 3106), Stella M. Hurtley, Ian S. Osborne, Stephen J. Simpson, Peter Stern; **associate editor** Joanne Baker **editorial support** Alice Whaley; Deborah Dennison **administrative support** Janet Clements, Phil Marlow, Jill White; **news: international news editor** Eliot Marshall **deputy news editor** Daniel Clery; **correspondent** Gretchen Vogel (Berlin: +49 (0) 30 2809 3902, FAX +49 (0) 30 2809 8365); **contributing correspondents** Michael Balter (Paris), Martin Enserink (Amsterdam and Paris), John Bohannon (Berlin); **intern** Michael Schirber

Asia Japan Office: Asca Corporation, Eiko Ishioka, Fusako Tamura, 1-8-13, Hirano-cho, Chuo-ku, Osaka-shi, Osaka, 541-0046 Japan; +81 (0) 6 6202 6272, FAX +81 (0) 6 6202 6271; asca@os.gulf.or.jp; **asia news editor** Richard Stone +66 2 662 5818 (rstone@aaas.org) **japan news bureau** Dennis Normile (contributing correspondent, +81 (0) 3 3391 0630, FAX 81 (0) 3 5936 3531; dnormile@gol.com); **china representative** Hao Xin, + 86 (0) 10 6307 4439 or 6307 3676, FAX +86 (0) 10 6307 4358; haoxin@earthlink.net; **south asia** Pallava Bagla (contributing correspondent +91 (0) 11 2271 2896; pbagla@vsnl.com)

EXECUTIVE PUBLISHER **Alan I. Leshner**
PUBLISHER **Beth Rosner**

Fulfillment & Membership Services (membership@aaas.org) **director** Marlene Zendell; **manager** Waylon Butler; **systems specialist** Andrew Vargo; **specialists** Pat Butler, Laurie Baker, Tamara Alfson, Karena Smith, Vicki Linton; **circulation associate** Christopher Refice

Business Operations and Administration director Deborah Rivera-Wienhold; **business manager** Randy Yi; **senior business analyst** Lisa Donovan; **business analyst** Jessica Tierney; **financial analyst** Michael LoBue, Farida Yeasmin; **rights and permissions: administrator** Emilie David; **associate** Elizabeth Sandler; **marketing: director** John Meyers; **marketing managers** Darryl Walter, Allison Pritchard; **marketing associates** Julianne Wielga, Mary Ellen Crowley, Catherine Featherston, Alison Chandler; **director of international marketing and recruitment advertising** Deborah Harris; **international marketing manager** Wendy Sturley; **marketing/member services executive:** Linda Rusk; **japan sales** Jason Hannaford; **site license sales: director** Tom Ryan; **sales and customer service** Mehan Dossani, Kiki Forsythe, Catherine Holland, Wendy Wise; **electronic media: manager** Lizabeth Harman; **production associates** Sheila Mackall, Amanda K. Skelton, Lisa Stanford, Nichele Johnston; **applications developer** Carl Saffell

Advertising director worldwide ad sales Bill Moran

Product (science_advertising@aaas.org); **midwest** Rick Bongiovanni: 330-405-7080, FAX 330-405-7081 • **west coast/w. canada** B. Neil Boylan (Associate Director): 650-964-2266, FAX 650-964-2267 • **east coast/e. canada** Christopher Breslin: 443-512-0330, FAX 443-512-0331 • **uk/europe/asia** Tracey Peers (Associate Director): +44 (0) 1782 752530, FAX +44 (0) 1782 752531 **japan** Mashy Yoshikawa: +81 (0) 33235 5961, FAX +81 (0) 33235 5852 **israel** Jessica Nachlas +9723 5449123 • **traffic manager** Carol Maddox; **sales coordinator** Deiandra Simms

Classified (advertise@sciencecareers.org); **u.s.: sales director** Gabrielle Boguslawski: 718-491-1607, FAX 202-289-6742; **inside sales manager** Daryl Anderson: 202-326-6543; **west coast/midwest** Kristine von Zedlitz: 415-956-2531; **east coast** Jill Downing: 631-580-2445; **canada, meetings and announcements** Kathleen Clark: 510-271-8349; **line ad sales** Emnet Tesfaye: 202-326-6740; **sales coordinators** Erika Bryant; Rohan Edmonson Christopher Normile, Joyce Scott, Shirley Young; **international: sales manager** Tracy Holmes: +44 (0) 1223 326525, FAX +44 (0) 1223 326532; **sales** Christina Harrison, Svitlana Barnes; **sales assistant** Helen Moroney; **japan:** Jason Hannaford: +81 (0) 52 789 1860, FAX +81 (0) 52 789 1861; **production: manager** Jennifer Rankin; **assistant manager** Deborah Tompkins; **associates** Christine Hall; Amy Hardcastle; **publications assistants** Robert Buck; Natasha Pinol

AAAS Board of Directors retiring president, chair Shirley Ann Jackson; **president** Gilbert S. Omenn; **president-elect** John P. Holdren; **treasurer** David E. Shaw; **chief executive officer** Alan I. Leshner; **board** Rosina M. Bierbaum; John E. Burris; John E. Dowling; Lynn W. Enquist; Susan M. Fitzpatrick; Richard A. Meserve; Norine E. Noonan; Peter J. Stang; Kathryn D. Sullivan

AAAS
ADVANCING SCIENCE, SERVING SOCIETY

Now Available!
SNPlex™ Genotyping System on the 3130*xl* Genetic Analyzer.

Accept No Limitations.

The improved SNPlex Genotyping System now performs cost effective and customizable genotyping projects on the 3130*xl* Genetic Analyzer.

The Genetic Analyzer that does more than just sequencing:

SNPlex Genotyping System* • *De novo* sequencing • Resequencing • Comparative sequencing
Mutation/heterozygote detection • SAGE • SNP validation and screening • Genotyping • Microsatellite analysis
AFLP • Conformation analysis • T-RFLP • MLST • Relative fluorescent quantitation

Applied Biosystems 3130 and 3130*xl* Genetic Analyzers

The 4-capillary 3130 and 16-capillary 3130***xl*** Genetic Analyzers provide reference-standard data quality and sophisticated, hands-free automation capabilities across a wider range of sequencing, resequencing and fragment analysis applications. The 3130 Series systems leverage the same technology, reagents, and software interface that make our larger production-scale systems so successful, bringing superior performance within the reach of almost any lab. Learn more at: http://info.appliedbiosystems.com/3130series.

Applied Biosystems

25 YEARS ADVANCING SCIENCE

*Not supported on the 3130 Genetic Analyzer.

Take a journey

with The Journal of Biological Chemistry (JBC) and explore all the exciting and important discoveries that biochemists have made in the world of science!

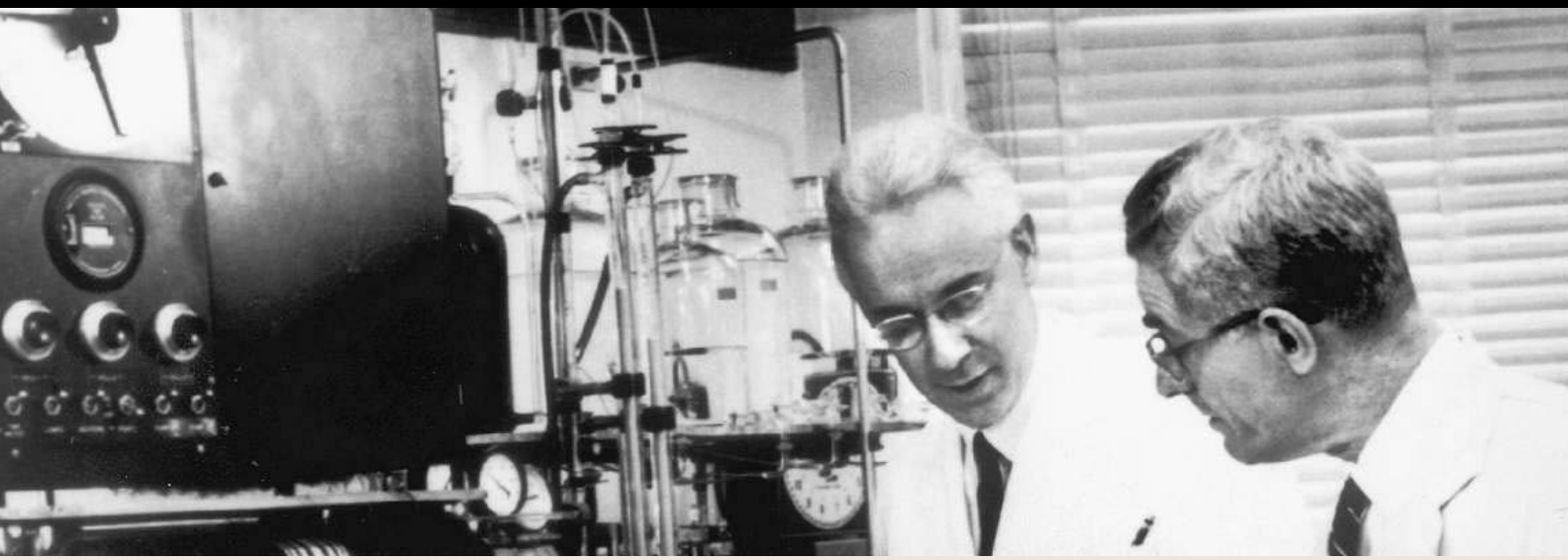

Above photograph (by Sam Vandivert, ©The Rockefeller University) shows Stanford Moore (left) and William H. Stein (right) in front of the original amino acid analyzer in 1965.

Classic Articles

In our Classic Articles you can explore original reprinted articles dating back to 1905. When completed, this series will contain over 300 original papers by the legends in biochemistry: including **Folin, Van Slyke, the Coris, Doisy, McCollum, Hastings, Lowry, Kornberg, Kennedy, Brown, Goldstein,** and many more!

Reflections

JBC Reflections were created as a celebration of JBC's 100th Birthday! We have invited premier biochemists to write about their contributions that have helped mark the many advances in biochemistry and molecular biology since 1905.

It is our hope that Classic Articles & Reflections will, in small part, share some of the personal experiences and history of biochemistry.

ASBMB & jbc 100 YEARS Chemistry of Life

Visit us at: www.jbc.org

PUBLICATIONS

Natural History Goes Digital

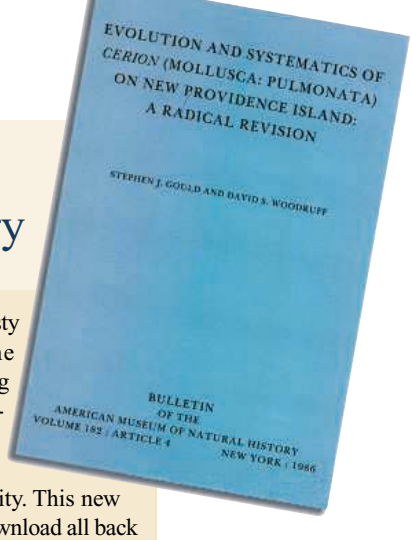

No more leafing through musty volumes or racing to the library just before closing time—at least if you're looking for publications from the American Museum of Natural History in New York City. This new virtual bookshelf lets you download all back and current issues for four of the museum's scientific titles, including its *Bulletin* and *Novitates* series. Housing papers from 1881 to the present, the archive encompasses paleontology, geology, systematics, and other fields. For instance, you'll find anthropologist Franz Boas's 1909 observations of the Kwakiutl people of Vancouver Island, Canada, and several works by evolutionist Stephen J. Gould. >> digitallibrary.amnh.org/dspace

FUN

Round and Round They Go

NASA's Satellite Tracking page is a boon for backyard astronomers and anyone who's curious about objects in the sky. The site's Java applets help users keep tabs on some of the more than 8000 humanmade structures orbiting Earth. A two-dimensional map shows the current positions of the international space station, Chandra X-ray Observatory, and a swarm of satellites. Click on the map to find out when a particular craft will pass overhead. Or for a 3D view, select the J-Track feature, which displays the orbits of some 700 satellites. Another applet pinpoints satellites that will be visible from your home tonight. >> science.nasa.gov/realtime

DATABASE

Taking the Polar Pulse >>

Canada harbors the second largest store of permanent ice in the Northern Hemisphere, and half of the country's land remains frozen year-round. All that frosty water influences weather patterns and ocean circulation and provides a sensitive indicator of climate change. Check out current ice status and follow historical trends at the State of the Canadian Cryosphere, hosted by the University of Waterloo in Ontario.

The cryosphere refers to ice and snow accumulations and includes glaciers, polar ice caps, and permafrost. A slew of maps and other graphics on the site provides snapshots of cryospheric conditions. You can get the latest measurements of Canada's snow cover and find out which lakes are frozen over. Animations track recent changes in the sea ice around the North Pole. To put the information in context, the site summarizes past variability and offers projections. The area covered by sea ice, for instance, has hit a record low due to rising temperatures, and models predict further shrinking. >> www.socc.ca

WEB TEXT

Metals With Mettle

"Organometallic" sounds like a description of the Terminator, but to chemists it denotes molecules that contain metal-carbon bonds—such as tetraethyl lead, the antiknock compound once used in gasoline. Undergraduates and others who need a refresher can consult the Organometallic HyperTextBook by Rob Toreki, a former chemistry professor at the University of Kentucky who now runs Internet start-ups. Some 40 chapters plumb the structure of these molecules and reactions such as olefin metathesis, a means of rearranging carbon double bonds using organometallic catalysts that earned last year's Nobel Prize in chemistry. Because organometallics often serve as catalysts, the site explains how a molecule's structure shapes the products. In this tricyclohexylphosphine complex (above), for instance, an organic cap partially obstructs one end of the metal (large purple ball), which restricts its reacting with other molecules. >> www.ilpi.com/organomet/index.html

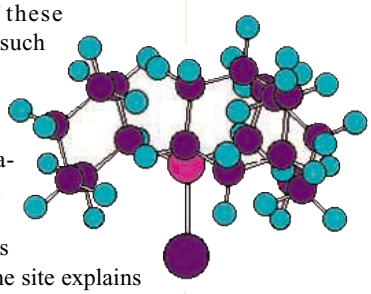

DATABASE

Cancer's Red Flags

Although cancer cells aren't foreign invaders, the immune system recognizes molecules they carry and attacks. Researchers hope that identifying these targets, or antigens, might help them devise cancer vaccines. Visitors can track down many of the antigens from abnormal cells that trigger an immune response at the Cancer Immunome Database, hosted by the international Ludwig Institute for Cancer Research. Free registration lets you peruse findings from a project that began in the 1990s and tested blood serum from cancer patients for antibodies against proteins from a variety of tumors. You can search for data on more than 1000 genes or narrow the results by tissue or cancer type. Users can also add their results to the collection. >> www2.licr.org/CancerImmunomeDB

CREDITS (TOP TO BOTTOM): AMERICAN MUSEUM OF NATURAL HISTORY; ENVIRONMENT CANADA/MSC/CANADIAN ICE SERVICE; ROB TOREKI

Send site suggestions to >> YYeeS! Proudly Presents, Thx for Support netwatch@aaas.org. Archive: www.sciencemag.org/netwatch

Big online news from *Science*

New website – retooled and redesigned.

If you're a scientist, the online version of *Science* puts a world of essential knowledge at your fingertips. And we're now proud to announce the launch of our redesigned website, which makes it even easier to keep up with the latest breakthroughs, browse journal archives, or find career advice. New features include saved searches and content, a hotlist of the most popular article downloads, and a daily science news feed – to name just a few. Discover the new online version of *Science*. Visit www.sciencemag.org today.

Science
AAAS

YYePG Proudly Presents, Thx for Support

GET THE BIG PICTURE IN *SCIENCE*

Juvenile marbled murrelet.

OVERFISHING BAD FOR BIRDS

The decline of marbled murrelets, seabirds that nest in old-growth forests, has been blamed on logging in the Pacific Northwest. But it now appears the birds are also the victims of overfishing.

Ben Becker, a marine ecologist at Point Reyes National Seashore, and Steven Beissinger of the University of California, Berkeley, compared the diets of murrelets in central California before and after the collapse in the 1940s of the Monterey Bay sardine fishery. Analyzing the feathers of living and preserved birds, they found from nitrogen and carbon-isotope measurements that contemporary birds are missing out on high-nutrient prey. Instead of dining on sardines and anchovies, the birds are forced to scrounge for krill and other creatures low on the food chain. "It takes about 80 krill to equal the energy value of a single sardine," says Beissinger, whose study is in press at *Conservation Biology*. As a result, few of the birds have enough energy to raise young, he says, and even in the best of times, fewer than half the adults are trying to reproduce.

"This is very credible work," says Kim Nelson, a wildlife biologist at Oregon State University, Corvallis, who has found marbled murrelets to be a threatened population in the Northwest. Unfortunately, she says, the U.S. Fish and Wildlife Service is proposing to remove the birds from endangered status in Washington, Oregon, and California.

Donner Party Postmortem

The newly excavated remains of a campsite have provided fresh evidence of the survival struggle of the Donner party, 81 settlers who were trapped in the snow in the winter of 1846–'47 while crossing the Sierra Nevada. About half the party survived, and contemporaneous accounts tell of cannibalism at the end.

One campsite, made by 59 travelers, was excavated more than a decade ago. Now, archaeologists have discovered the exact site 11 kilometers away where 22 others hunkered down. The research team, which described its findings earlier this month at a symposium held by the Society for Historical Archaeology in Sacramento, California, found no human burials or signs of cannibalism such as cooked human bones. (Uncooked bones would be eaten away by the acidic soil.) But signs of suffering were evident. Scattered around the campfire were nails from furniture and wagon parts that were burned. Bones from cattle, horses, and even the family dog had been chopped into small pieces and boiled to extract the last bits of fat. Pieces of china that had been unpacked from wagons show that the settlers were "being proper and … trying to normalize the situation," says Julie Schablitsky, an archaeologist affiliated with the University of Oregon, Eugene, who co-led the excavations. "They were doing everything possible to avoid cannibalism." Fragments of writing slates suggest that Tamsen Donner, a schoolteacher, may have given lessons during the months-long ordeal.

Plate fragment.

TALE OF A RAPTOR

A South African paleoanthropologist says he has "conclusive proof" that the famous Taung child, a skull of a 3-1/2-year-old hominid who died 2 million years ago, was killed and eaten by an eagle. Discovered in South Africa in 1924, the skull provided the first fossil evidence that humans originated in Africa.

Experts initially thought the child had been attacked by a big cat. In 1995, Lee Berger of the University of the Witwatersrand in Johannesburg and his colleague Ron Clarke proposed that the killer was a raptor. But critics said the skull markings were inconclusive and doubted that a bird could kill and carry off a child weighing at least 10 kg.

Berger with skull and eagle model.

Berger says he reexamined the Taung fossil last fall after reviewing a paper about eagle marks on monkey skulls. In a paper to appear in the *American Journal of Physical Anthropology*, he reports that he found two marks, including an incision in the eye orbit, that looked just like those on the monkeys. The monkey paper's author, Scott McGraw, an anthropologist at Ohio State University, Columbus, agrees that the marks seem "consistent with those we identified in the Ivory Coast monkeys, … all of whom were victims of eagles"—and some of whom weighed more than 13 kg. But at least one doubter remains. Ohio State anthropologist Jeffrey K. McKee says that the damage to the thin bone of the eye orbit could have occurred after death.

Asian Science on the Move

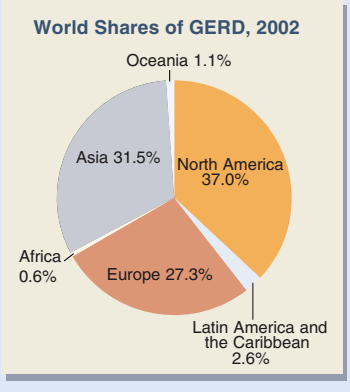

Asia is now close to spending one-third of all the money the world is devoting to R&D, according to the newly released *UNESCO Science Report 2005*. Of the world's gross expenditure on research and development (GERD) in 2002, about $2.8 trillion, Asia accounted for 31.5%, up from 27.9% in 1997. At the same time, North America's share fell from 38.2% to 37.0%, and Europe's from 28.8% to 27.3%. The Asian spurt is led by China, whose GERD went from 3.9% of the world total in 1997 to 8.7% in 2002. Recent UNESCO figures indicate that the proportion of China's gross domestic product devoted to R&D more than doubled in less than a decade, reaching 1.44% in 2004.

Rare trees thriving
452

Espying Earth-like planets
453

SCIENTIFIC MISCONDUCT

Fraud Upends Oral Cancer Field, Casting Doubt on Prevention Trial

The world of oral cancer research is reeling after one of its stars, Norwegian oncologist Jon Sudbø, admitted this week through his attorney to falsifying data in three seminal papers published by top medical journals. A fourth paper is under suspicion after editors at the *New England Journal of Medicine* (*NEJM*) found that it contains a pair of duplicate images. For one of the papers, in *The Lancet*, Sudbø also appears to have claimed funding from a nonexistent grant.

The revelations have put on hold a multimillion-dollar oral cancer prevention trial, sponsored in part by the U.S. National Cancer Institute. The affair has also raised questions about whether researchers in multi-institutional collaborations should do more to double-check the validity of data collected by others. The fraud is all the more unsettling given the recent fabrications by South Korean researcher Woo Suk Hwang in stem cell science (*Science*, 13 January, p. 156).

"Something like this, coming so hard on the stem cell revelation, is almost catastrophic," says Fadlo Khuri, an oncologist at Emory University in Atlanta, Georgia. Sudbø's results, he says, "are among the most important findings of the last decade [in] understanding the biology" of oral cancer.

Fraud exposed. Cancer researcher Jon Sudbø acknowledged faking data in three of these papers, and journal editors found a duplicated image in the fourth.

The Norwegian Radium Hospital, where Sudbø is based, has launched an investigation led by Anders Ekbom of the Karolinska Institute in Stockholm. Sudbø's 38 published articles will be reviewed, as will the role of his co-authors, one of whom is his twin brother and another his wife. Results are expected in a couple of months. "We don't have any suspicions that the other authors knew," says Stein Vaaler, director of strategy at the hospital, which has already found that hundreds of patient records were fabricated in the *Lancet* paper.

Some papers in question identified those at greatest risk of oral cancer, a disease often preceded by noncancerous mouth lesions. Just 20% to 30% of individuals with lesions develop oral cancer, confounding prevention efforts.

The earliest paper to contain false data, according to Sudbø's attorney, Erling Lyngtveit, appeared in *NEJM* in April 2004. It reported that 26 of 27 individuals with aneuploid mouth lesions, so called because they contain abnormal numbers of chromosomes, developed aggressive oral cancer and were more likely to die of the disease than were those with other types of lesions. Lyngtveit confirmed that Sudbø did not have access to death information on which the study's conclusion was based. (Sudbø is currently on sick leave and has not spoken publicly.)

That 2004 study built on one that appeared 3 years earlier in *NEJM* that identified aneuploid mouth lesions as unusually hazardous. Eighty-four percent of study volunteers with the lesions developed oral cancer. On 20 January, *NEJM* released an "Expression of Concern" stating that one of the paper's images of a mouth lesion is a magnified version of ▶

PROFESSIONAL PRACTICE

Scientists Keep Some Data to Themselves

Scientists frequently refuse to give colleagues details of their research, according to two new surveys, of life scientists and of scientists-in-training.

In the February issue of *Academic Medicine*, David Blumenthal and colleagues at Massachusetts General Hospital's Institute for Health Policy (IHP) in Boston report from a survey of 1849 life scientists that 44% of geneticists and 32% of other life scientists have engaged in some form of "withholding behavior." The behavior includes failing to mention pertinent information in a paper or a presentation. Geneticists and males are more likely to withhold information.

A related study suggests that such behaviors may stifle the growth of young scientists. A group led by IHP physician Eric Campbell surveyed 1077 graduate students and postdocs in the life sciences, computer science, and chemical engineering. About one-quarter reported that they had been denied information at some point, particularly those in "high competition" research groups or with links to industry. About half the affected respondents said the rebuff delayed their research.

"We need to inform scientists, professional associations, and universities about the impact that data withholding can have on the next generation of researchers," says Campbell.

"Sometimes it's necessary. The question is whether it's being done more [often] than it should be."

Drummond Rennie, a deputy editor of the *Journal of the American Medical Association*, notes that some data requests can be "extremely costly and very time-consuming" to fulfill. And scientists who present findings at meetings are sometimes rightfully paranoid, says sociologist Brian Martinson of Health Partners Research Foundation in Minneapolis, Minnesota. Competitors from other labs have been known to come with cameras to shoot their posters, he says.

–CONSTANCE HOLDEN

Confusion over cannabis
455

FOCUS

Special report: Mental health in the developing world
458

another in the same article. The journal, says a spokesperson, is awaiting the results from the Radium Hospital's investigation before determining how to handle both studies.

Two other reports that Sudbø's attorney told *Science* contain fabrications were published in the 20 March 2005 issue of the *Journal of Clinical Oncology* and the 15 October 2005 issue of *The Lancet*. The first concluded that smokers with mouth lesions, if told they were at high risk of oral cancer, were likelier to quit than were those without detectable lesions. The second, in *The Lancet*, claimed to draw on archived health records to show that long-term use of anti-inflammatory drugs reduced the risk of oral cancer.

That study was the first to attract suspicion. Several weeks ago, Camilla Stoltenberg, director of epidemiology at the Norwegian Institute of Public Health, noticed that the *Lancet* study relied on a database not yet available to researchers, and she alerted the Radium Hospital on 11 January. An internal investigation by the hospital concluded that Sudbø "fabricated all the data in the article," which included names, genders, diagnoses, and other variables for 908 people. The paper also cites funding from a Norwegian Cancer Society grant even though the proposal was rejected, says society spokesperson Terje Mosnesset.

An immediate casualty of the fraud may be a 360-person trial of the anti-inflammatory Celebrex, along with another drug, in healthy people with aneuploid mouth lesions. The cancer prevention trial garnered roughly $9 million from the National Cancer Institute in Bethesda, Maryland, and was to be led by Sudbø and Scott Lippman of the M. D. Anderson Cancer Center in Houston, Texas, who was a co-author on the 2004 *NEJM* paper and the *Lancet* paper. "Everything has to be put on hold," says M. D. Anderson Vice President for Research Administration Leonard Zwelling.

The hospital, he adds, will consider new ways to handle large population studies in which its researchers analyze results but may not see the raw data. "Should we have an independent board" to examine those data, Zwelling wonders.

Meanwhile, oral cancer experts are grappling with the fabrications and whether the aneuploid work will stand. Notes Richard Jordan, an oral pathologist at the University of California, San Francisco, aneuploid lesions weren't "100% predictive, but [they] were the best that anyone heard of."

–JENNIFER COUZIN AND MICHAEL SCHIRBER

GRADUATE TRAINING

U.S. Beckons Foreigners With Science Fulbrights

Twenty-five foreign graduate students in science and engineering will receive generous scholarships under a new U.S. program designed to dispel fears that tighter security following the September 2001 terrorist attacks has discouraged the world's best and brightest from studying in the United States.

The program, to be called the Fulbright Science Awards, takes the name of the prestigious intellectual exchange program between the United States and some 150 countries begun after World War II. It has not made a formal debut, but Undersecretary of State Karen Hughes mentioned it in passing at a 6 January meeting with university presidents at the State Department. The awards will be part of a proposed spending boost for academic exchanges in the president's 2007 budget request to Congress to be submitted next month.

"Several presidents told us that we needed to send a clear signal that this country is intent on welcoming foreign talent, especially future scientific and technical leaders," explained Hughes's deputy Tom Farrell. "And we felt, what better way to do that than through our most important global brand name in international education, the Fulbright program?"

The science awards will break new ground for the Fulbrights. Students will be chosen by a blue-ribbon panel of experts in a global competition rather than through the traditional bilateral agreements, and they will be funded for longer than the typical 3 years. Farrell said he hopes universities will vie for these students and that the award is intended to meet all their needs as budding scientists. "We want this scholarship to be the ne plus ultra for graduate training," says Farrell. "And we're making a commitment to support them until the completion of their Ph.D., in partnership with their university." Farrell expects the first class to be enrolled in 2007 and hopes the program, if successful, will grow in subsequent years.

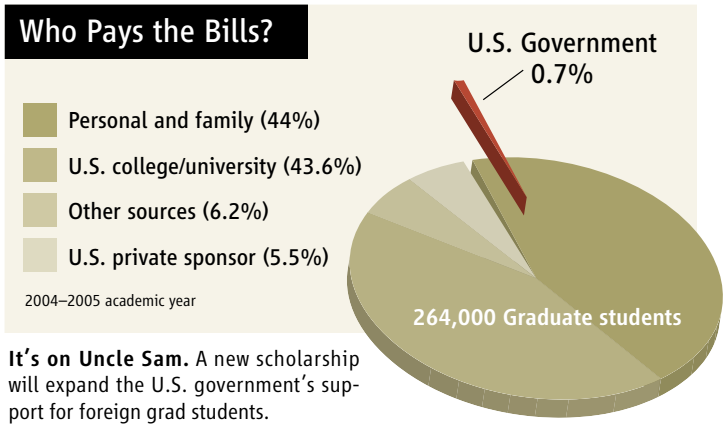

It's on Uncle Sam. A new scholarship will expand the U.S. government's support for foreign grad students.

At any likely size, the science Fulbrighters will be dwarfed by the 200,000 foreign students currently receiving graduate training in science and engineering at U.S. universities. But Association of American Universities President Nils Hasselmo, who attended the 6 January meeting, says that the new program "sends a signal" that the United States wants to attract these talented students. "To have a real impact on graduate training, the program would have to be greatly expanded," he says. "But the message is important."

That message is already getting through. Claudia Mitchell-Kernan, dean of the graduate division at the University of California, Los Angeles, reports a double-digit increase this winter in foreign applications to UCLA graduate programs. "I've heard nobody say that their applications are down," says Debra Stewart, president of the Council of Graduate Schools in Washington, D.C., whose annual survey of enrollment trends at the nation's top research institutions reported a sharp drop in applications after 9/11. Stewart credits the State Department and individual institutions for helping reverse that decline, and she predicts that the science Fulbrights will reinforce the trend.

–JEFFREY MERVIS

CREDIT: *OPEN DOORS* 2005, INSTITUTE OF INTERNATIONAL EDUCATION

TAKE CONTROL
OF MAMMALIAN GENE EXPRESSION

NEW ENGLAND BIOLABS

experience exhilarating control.

RheoSwitch®

PRECISE, VARIABLE CONTROL OF MAMMALIAN GENE EXPRESSION

Analogous to the operation of a rheostat, the RheoSwitch technology achieves precise regulation through the highly specific interaction of a synthetic inducer, RheoSwitch Ligand RSL1, and a chimeric bipartite nuclear receptor. This receptor is activated in the presence of RSL1 ligand, and the level of gene expression can be regulated by adjusting the concentration of RSL1 ligand in the tissue culture media.

Applications:

- Inducible protein expression
- Expression of toxic genes
- Overexpression/mutant rescue studies

Advantages:

- Precise control unrivaled among other expression systems
- Negligible basal expression
- Greater than 10,000 fold induction with RSL1 ligand present
- Synthetic inducer (RSL1) is non-toxic and engineered receptor eliminates non-specific side effects
- No special culture media requirements

RheoSwitch product line includes:

- Expression system
- Cell lines: NIH3T3-47, HEK293-A7
- pNEBR-X1Hygro Vector
- Ligand RSL1

RheoSwitch is a registered trademark of RheoGene, Inc.

Transcriptional control using the RheoSwitch System.

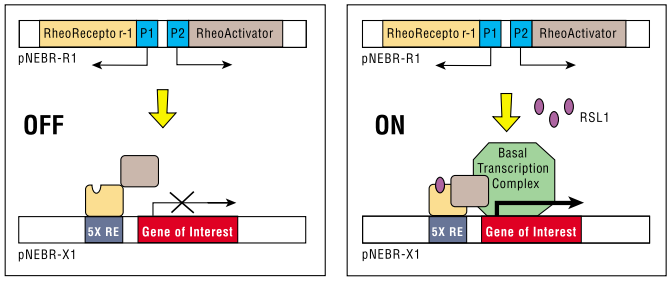

"OFF" state: *In the absence of RSL1ligand, the RheoReceptor and RheoActivator proteins exist in an inactive conformation and transcription is kept off.*

"ON" state: *In the presence of RSL1 ligand, the two proteins stably dimerize and bind to the response element of pNEBR-X1 in an active conformation and transcription is turned on.*

NEB NOW OFFERS THE RHEOSWITCH CELL LINES HEK293-A7 AND NIH3T3-47: Two stable cell lines that express optimal levels of the RheoActivator and RheoReceptor components of the RheoSwitch System.

For more information and international distribution network, please visit www.neb.com

- **New England Biolabs Inc.** 240 County Road, Ipswich, MA 01938 USA
  1-800-NEB-LABS Tel. (978) 927-5054 Fax (978) 921-1350 info@neb.com
- **Canada** Tel. (800) 387-1095 info@ca.neb.com
- **Germany** Tel. 0800/246 5227 info.de@neb.com
- **UK** Tel. (0800) 318486 info@uk.neb.com
- **China** Tel. 010-82378266 beijing@neb-china.com

NEW ENGLAND BioLabs® Inc.
the leader in enzyme technology

QUANTUM PHYSICS

Measurement Schemes Let Physicists Tiptoe Through the Quanta

In the quantum realm, information comes at a cost: Measuring the condition or "state" of a particle knocks it out of that state. Now, two groups of physicists have made the best of that tradeoff by minimizing the disturbance as they extract information from particles of light.

The "minimal disturbance measurements" probe the fundamental limits set by quantum theory and might someday help carry quantum information down optical fibers. "It's nice to know something in theory," says theorist Nicolas Cerf of the Free University of Brussels, Belgium, "but the experiment is always a crucial step."

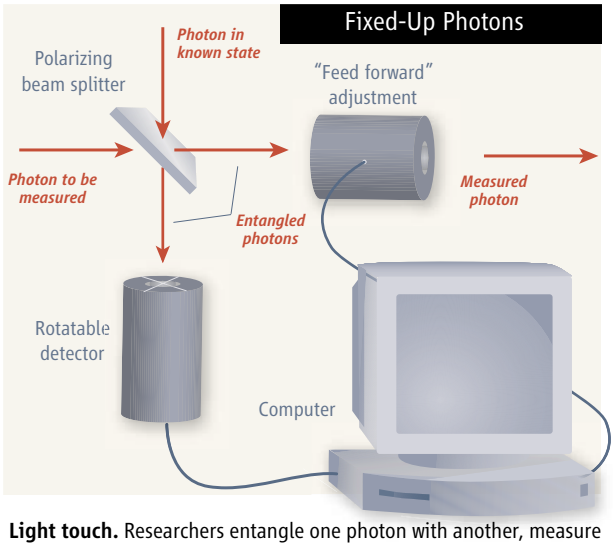

Light touch. Researchers entangle one photon with another, measure the second with an off-kilter detector, and use the result to nudge the first back toward its initial state.

According to quantum theory, a particle can be in two distinct states at once. For example, a photon can be "polarized" either vertically, horizontally, or in a combination such as seven-tenths vertical and three-tenths horizontal. An ordinary measurement doesn't reveal the weird two-way state. Instead, 70% of the time, it will show that the photon is vertically polarized, and 30% of the time it will show it as horizontally polarized. And it leaves the photon in whichever state it detected—the maximum possible disturbance.

To avoid that effect, Fabio Sciarrino and Francesco De Martini of the University of Rome "La Sapienza" and colleagues "entangled" the photon they wanted to measure with a second photon in a half-horizontal, half-vertical state and measured the second photon instead. Because of the entanglement, if one photon was measured to be vertical or horizontal, the other instantly collapsed into the same state, so measuring the second was equivalent to measuring the first directly.

But then the researchers rotated their detector away from vertical and horizontal. That loosened the connection between the photons, so that measuring the second photon no longer revealed with complete reliability whether the first was vertical or horizontal. According to the strange rules of quantum mechanics, however, that loss of information had an upside: The reading now encoded information that the researchers could use to nudge the first photon back toward its original state by applying an electric field in an automated "feed forward" scheme. As the detector rotated toward 45 degrees, the researchers reported online on 20 January in *Physical Review Letters*, the fixed-up photon approximated the original—at the cost of more and more information. "I think it's quite a fundamental achievement," De Martini says.

Meanwhile, Ulrik Andersen and Gerd Leuchs of Friedrich Alexander University of Erlangen-Nuremberg in Germany and colleagues have performed a similar experiment with different quantum states of light. Instead of studying individual photons, the researchers experimented with "coherent states," which contain an indefinite number of photons but act more like classical waves, slightly fuzzed out by quantum uncertainty. The researchers used a partially reflective mirror to split off and measure a bit of the state and used the information to tune up the remainder, they report in a paper published online in *Physical Review Letters* on the same date.

The fix-it-up methods might help restore quantum information lost or degraded by noise while passing through optical fibers in emerging quantum-communications technologies, Andersen says. His team has already performed encouraging experiments along those lines. The techniques also put an experimental handle on a conceptual issue that theorists have pondered since quantum mechanics was invented in the 1920s. "This shows us that we can get really close to the internal workings of quantum mechanics" experimentally, says Konrad Banaszek of Nicolaus Copernicus University in Torun, Poland. Alas, Banaszek says, no one expects to find a way around the information-disturbance tradeoff.

YYePG Proudly Presents, Thx for Support **ADRIAN CHO**

CREDIT: P. HUEY AND J. MOGLIA/*SCIENCE*

SCIENCESCOPE

Breeding Suspicion

NEW DELHI—The fate of a landmark nuclear pact between India and the United States hinges on whether India will allow inspections of its fast breeder reactors. The two sides will meet next month to try to resolve the impasse.

The deal, inked last July, would allow U.S. firms to sell civilian nuclear technologies and fuel to India, ending a 30-year embargo. As one concession, India would divide its nuclear complex into civilian facilities open to Western businesses—and inspectors—and closed military installations. India's draft plan to tag the bulk of its complex, including all R&D facilities, as military has created tension (*Science*, 20 January, p. 318). The U.S. Congress will review the plan before deciding whether to make changes to U.S. law needed for the pact to take effect.

The main sticking point during negotiations in New Delhi last week, *Science* has learned, is India's insistence on keeping its fast breeder reactors in Kalpakkam on the military list. India claims this is an R&D facility. The United States asserts that the technology is not novel and points out that a similar reactor in Japan is under safeguards. "This comparison is inappropriate," seethes M. R. Srinivasan of India's Atomic Energy Commission. He notes that Japan, a nonweapons state, has different safeguards obligations. It's doubtful, though, that U.S. lawmakers will buy that argument.

–PALLAVA BAGLA

Sonar Comments: Navy Listening

The public has until next week to comment on the U.S. Navy's plans to build a long-sought 1700-km^2 sonar training facility off the Atlantic coast. The Pentagon says it needs the facility, slated for the southeastern North Carolina shore, to train ships to hunt increasingly quiet submarines. But green groups opposed to the plan say the Navy's draft environmental statement downplays risks to mammals, corals, and fish.

The Natural Resources Defense Council wants to factor in a stranding of 36 whales of three species in January 2005 that occurred after Navy sonar exercises roughly 450 km away. But although it hasn't ruled sonar out as a cause, the National Oceanic and Atmospheric Administration doesn't plan to issue a report on the incident until March. The Navy has acknowledged that sonar can harm whales, but the science of mass strandings remains mysterious. A final draft of the statement will also receive comments before the Navy makes a decision on the plans.

–ELI KINTISCH

ECOLOGY

Rare Tree Species Thrive in Local Neighborhoods

Biodiversity may be threatened worldwide, but small pockets of tropical-forest trees are surprisingly becoming more diverse over time. An analysis of decades of data from seven forests across the globe, reported on page 527, indicates that, on a small scale, rare tree species are thriving, and even surviving better than common species. The forests studied were relatively pristine, but the results may apply to forests in trouble as well, if enough healthy pockets of trees persist. All over the world, "local increases in diversity are taking place," says Christopher Wills, an evolutionary biologist at the University of California, San Diego. His conclusion: "Even if an ecosystem is damaged, it can recover."

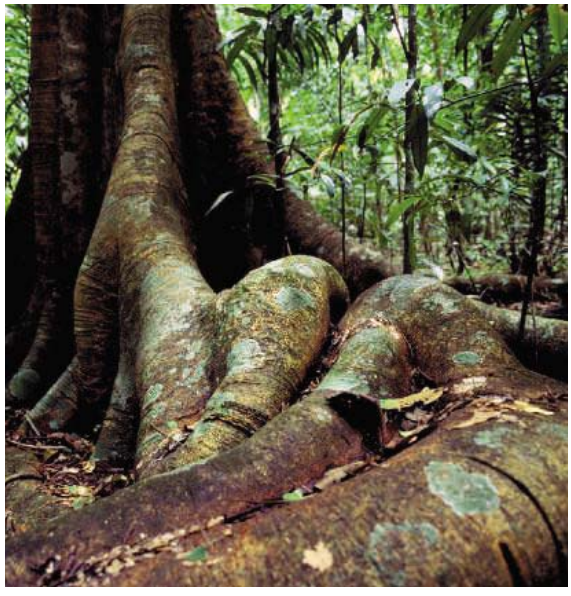

Diversity reigns. In small patches of a tropical forest, rare species often do better than common ones.

For as long as biologists have marveled at the vast number of organisms in the tropics, they have struggled to understand why such biodiversity exists. To tackle this question, Wills tapped data on seven research forests monitored by the Center for Tropical Forest Science, based at the Smithsonian Tropical Research Institute in Panama. These reserves, in India, Puerto Rico, Panama, Thailand, Sri Lanka, and Malaysia, range in size from 16 to 52 hectares and contain anywhere from 74 to 1186 tree species, depending on rainfall and other environmental conditions.

At each forest, researchers conduct 5-year or 10-year censuses, counting every tree over 1 centimeter in diameter at chest height. At the same time, they note dead trees and track the number of trees that have grown big enough to be counted. Because the local collaborators follow a common survey protocol, Wills and his colleagues were able to compare each forest's results.

The researchers did two types of analyses. To track changes in the number of species over time, they divided the forests into 10-meter squares, counted the number of tree species in each square, and calculated the density of those species. Then, to get a sense of how the findings might change depending on the size of plot studied, the researchers repeated their analyses using 20-, 30-, 40-, and 50-meter squares. The surveyed trees fell into one of four groups: recruits (trees newly counted because they had reached the minimum size), newly dead trees, younger trees, and older trees in the plot.

Within these plots, more trees of the common species died over time than did members of rarer species, increasing the relative representation of rare species. The team found ▶

CREDIT: C. WILLS *ET AL.*, *SCIENCE*

CHEMISTRY

Walk on the Wild Side Yields Supersensitive Chemical Measurements

Following the lead of astronomers who build their telescopes on remote mountaintops, German researchers have taken to the woods to generate ultrahigh-precision chemical measurements. By fleeing the magnetic interference common to civilization, a team at Forschungszentrum Jülich and Aachen University has devised a low-tech version of nuclear magnetic resonance (NMR) spectroscopy that can outperform multimillion-dollar lab instruments. The tabletop-sized device could hold the key to a new, low-cost version of NMR spectroscopy.

"It's a very beautiful piece of work," says Alexander Pines, a chemist at the University of California, Berkeley, and a pioneer in low-field NMR. His group and others have found ways to do away with expensive, high-field magnets, but only by using either other high-tech gear such as detectors or uncommonly large sample volumes (*Science*, 22 March 2002, p. 2195). By contrast, the new technique can get high-quality chemical data on a few milliliters of a liquid with standard electronic equipment. The improvement could lead to easier ways to monitor chemicals during manufacturing and track chemical spills, Pines says.

NMR works because some atomic nuclei behave like tiny bar magnets. In typical NMR experiments, researchers place a chemical sample at the center of a giant, high-field superconducting magnet that causes the nuclear spins to precess around the magnetic field at a rate that is unique for each atomic species. Next, they hit their sample with radio pulses that nudge the nuclear spins away from their normal orbit; the timing of their realignment betrays their identity and chemical neighbors. The larger the external magnetic field, the easier it is to see the signal, which makes it possible to work out the structure of larger and more complex molecules.

The new technique makes use of another NMR signal, called the "J coupling," which doesn't depend on the external field. When J coupling occurs, the spins of atomic nuclei affect the behavior of the electrons that form the chemical bonds between the atoms. This influence shows up on an NMR spectrometer as patterns that reveal the structure of the compound's bonds.

Tracking J coupling in a lab is a challenge, because even a nearby screwdriver can create imbalances in the magnetic field that wash out the J-coupling signature. Ultrasensitive superconducting detectors called SQUIDs can overcome the problem, but they are costly and need expensive cooling equipment.

So the German team—Stephan Appelt, Holger Kühn, and F. Wolfgang Häsing of the Forschungszentrum Jülich and Bernhard Blümich of Aachen University—opted to do away with extra equipment by working in a forest 5 kilometers south of Jülich. By escaping the magnetic interference of civilization and shielding their electronic gear, the scientists obtained J-coupling information at least 10 times as precise as with superconducting magnets 100,000 times more powerful, they report online this week in *Nature Physics*.

Low-field detectors will never replace high-field NMR for working out the structures of highly complex molecules such as proteins, Blümich says. But their low cost—thousands instead of millions of dollars—could push the technology rapidly into new areas of remote chemical detection. **–ROBERT F. SERVICE**

the same trend in plots of all sizes, but it was most evident in the 10-meter squares. And these results were consistent from forest to forest. "One would not expect to find such congruence unless similar processes are operating," says ecologist Theodore Fleming of the University of Miami, Florida.

What explains the success of the rarer tree species? Being closer together, common trees are more prone to deadly infections. They may also face stiffer competition for certain resources. In contrast, rarer trees, by depending on slightly different sets of resources, may not have this problem. There's a delicate balance, however, says Wills: "If [a species] gets too common, it loses advantage."

The findings challenge a theory about forest diversity. According to the so-called neutral theory, plant species are gained and lost randomly. Thus, "diversity is just an accident of history," says Wills. However, "what we are finding is that it's not neutral; [diversity] is being selected for."

Such a result should be exciting to ecologists studying grasslands, temperate forests, and perhaps even coral reefs, notes Scott Armbruster, an evolutionary ecologist at the University of Portsmouth, U.K.: "That these patterns are found to be so consistent across so many distant tropical forests suggests to me that the conclusion may eventually be found to hold for other diverse ecosystems as well."

–ELIZABETH PENNISI

EXTRASOLAR PLANETS

I Spy … a Cold, Little Planet

Applying the technique of gravitational microlensing to the search for planets beyond the solar system, a superconsortium of astronomers has detected a frozen ice ball much smaller than Neptune orbiting a faint star in the distant central bulge of the galaxy. It's the first of a new class of cold, diminutive extrasolar planets.

"It's a tremendously exciting result," says astronomer Sara Seager of the Carnegie Institution of Washington's Department of Terrestrial Magnetism in Washington, D.C. Microlensing "does things we can't do any other way," she adds. By opening a new window on "super Earths"—the least massive exoplanets yet found—it has suggested that such planets are far more common than the sizzling, Jupiter-sized gas balls that have made the news in recent years.

Not so hot. Microlensing can detect smaller planets that are far enough from their stars to avoid being roasted.

CREDIT: EUROPEAN SOUTHERN OBSERVATORY

Microlensing depends on gravity's ability to bend light, as Einstein predicted it could do. By monitoring the brightness of millions of stars at once, astronomers can tell when one star passes in front of a brighter, more distant star, gravitationally bending its light and brightening it the way a glass lens would. If the nearer or "lens" star happens to have a planet, it too will gravitationally brighten the source star. This is the only way astronomers can detect relatively small planets at some distance from their stars. The 170 "hot Jupiters"—massive, gaseous bodies orbiting scorchingly close to their stars—have been spotted by the wobble they gravitationally induce in their stars.

On 11 July of last year, the OGLE collaboration of astronomers announced that a particular star was beginning to brighten. The PLANET and MOA collaborations joined in, and, on 9 August, the combined observations revealed a small, half-day-long brightening superimposed on a slow dimming.

In this week's issue of *Nature*, the 73 astronomers of the three collaborations report that the secondary microlensing event was caused by a planet three to 10 times the mass of Earth; Neptune is 17 times Earth's mass, and Jupiter, 318 times. The exoplanet orbits its small, faint star at a distance of about three times Earth's distance from the sun and therefore is probably as cold as Pluto. In contrast, hot Jupiters swing around their stars in a matter of a few day days and reach thousands of degrees.

Microlensing's diminutive discovery implies that planets smaller than Neptune dominate between 1 and 10 astronomical units from their stars, the *Nature* authors say. That is in line with the leading theory of planet formation, in which multi-Earth-size cores of ice and rock form first and then, with luck, gather gas to form a Jupiter. All of this bodes well for future microlensing searches, as well as for finding habitable, Earth-size exoplanets.

–RICHARD A. KERR

Cell Vote a Go in MO

A Missouri judge last week ruled that stem cell advocates could begin collecting signatures for a ballot initiative that would explicitly permit research cloning, or somatic cell nuclear transfer, to generate human embryonic stem cells. The proposal would also outlaw reproductive cloning. Opponents called the proposed ballot language "misleading," but a Cole County judge called the wording "fair." The pro-research initiative must garner 150,000 signatures by 9 May to earn a fall ballot spot.

In the meantime, Republican state Senator Matt Bartle plans to introduce a bill banning the creation of a "human being" in any way other than through union of sperm and egg.

–CONSTANCE HOLDEN

Call Ourselves an Institute

PARIS AND BERLIN—A fight over a proposed 80,000-m^2 multidisciplinary institute outside Paris has pitted researchers against the French government once again. The Save French Research movement opposes plans for the European Institute of Technology in Saclay, preferring to link up and strengthen existing ones to form a multicenter European Technology Institute. Supporters say current technology labs are too dispersed and dilapidated to form a nucleus of excellence. Research Minister François Goulard, a project supporter, says he hopes it would take shape in the next few months.

Meanwhile, the German government has named 10 finalists in a competitive initiative designed to boost several universities to world-class status. Dark horse University of Bremen joined the University of Heidelberg among the finalists.

–BARBARA CASASSUS AND GRETCHEN VOGEL

Researcher Rules Eased

Easing scientists' concerns, the U.S. Department of Commerce has decided that export-control rules restricting foreign researchers in the United States from using sensitive technologies should be based on the person's most recent country of citizenship or permanent residency and not country of birth. The changes to the rules, which are aimed at preventing the transfer of sensitive technologies to countries the United States views as national security threats including China and Russia, are expected to be finalized soon.

–YUDHIJIT BHATTACHARJEE

You could be next

Yes, it *can* happen to you:
If you're making inroads in neurobiology research and you've received your M.D. or Ph.D. within the last 10 years, the Eppendorf & *Science* Prize for Neurobiology has been created for YOU!

$25,000 Prize

This annual research prize recognizes accomplishments in neurobiology research based on methods of molecular and cell biology. The winner and finalists are selected by a committee of independent scientists, chaired by the Editor-in-Chief of *Science*. Past winners include post-doctoral scholars and assistant professors.

If you're selected as next year's winner, you will receive $25,000, have your work published in the prestigious journal *Science* and be invited to visit Eppendorf in Hamburg, Germany.

What are you waiting for? Enter your research for consideration!

Deadline for entries:
June 15, 2006

For more information:
www.eppendorf.com/prize
www.eppendorfscienceprize.org

"Receiving this most prestigious prize is a milestone in my scientific career. Furthermore, it gives me the impetus to reach ever higher goals."

Pingxi Xu, M.D., Ph.D.
Postdoctoral Researcher II
University of Texas
2005 Winner

eppendorf & Science
PRIZE FOR NEUROBIOLOGY

YYePG Proudly Presents, Thx for Support

ILLEGAL DRUGS

U.K. Backs Off Reclassifying Cannabis as a Dangerous Drug

Citing recent studies that suggest cannabis use can cause schizophrenia, the U.K. government proposed taking a harsh line on the drug last year—possibly shifting it from the soft "C" class of drugs to the "B" class that includes cocaine. But after mulling the idea over for months, Britain's interior minister, Home Secretary Charles Clarke, backed off on 19 January. Following the advice of an advisory committee that told him a crackdown would be a bad move and wasn't justified by the data, Clarke left cannabis in class C. But he noted that many people have been "confused" by the debate and proposed more analysis of the drug's health risks and a "massive" education campaign.

The flap began when the U.K. government moved cannabis from class B to class C in 2004. It based this decision on a report from the Advisory Committee on the Misuse of Drugs (ACMD), which concluded that cannabis did not belong in the same category as cocaine and amphetamines. Law-enforcement costs, it found, were disproportionate to the relatively slight public health burden associated with cannabis use.

This advice prompted criticism from several researchers who argued that the panel had brushed aside recent findings indicating that cannabis use can cause mental illness. For example, psychiatrist Robin Murray of the Institute of Psychiatry at King's College London (KCL) says, "My beef with the government has not been with classification but with the message that cannabis does not induce psychosis."

Psychiatric researcher Louise Arseneault of KCL says observational studies consistently show that heavy use of cannabis, particularly in adolescence, can cause lasting mental health problems. She is part of a group led by Avshalom Caspi at KCL pursuing evidence that individuals with a variant of the *COMT* gene, which is involved in regulating neurotransmitters, have an increased risk for cannabis-induced psychosis. Such findings prompted Clarke and ACMD to review the data.

ACMD, chaired by clinical pharmacologist Michael Rawlins of the University of Newcastle upon Tyne, issued its update* on 19 January. It agreed that recent studies strongly suggest that cannabis use increases the chances of developing schizophrenia, but it also concluded that the increased risk for an individual—about 1% in a lifetime—is "very small."

Clarke, meanwhile, wants to analyze these issues once again. Within the next few weeks, he said, he plans to propose "a broad review" of the entire drug classification system.

–ELIOT MARSHALL

Mindbender. Experts continue the debate on the mental health risks of cannabis use.

* *Further consideration of cannabis under the Misuse of Drugs Act 1971*, www.drugs.gov.uk/publication-search/acmd/cannabis_reclass_2005

JAPAN-CHINA DISPUTE

Researchers Caught Between Atoll and a Hard Place

TOKYO—A maverick researcher and his former institute found themselves in troubled waters after news reports earlier this month claimed they will conduct clean-energy research off an atoll at the center of a territorial dispute between Japan and China.

No rock is an island? Calls in Japan to launch an energy experiment on Okinotorishima atoll could aggravate a territorial dispute with China.

For more than 30 years, mechanical engineer Haruo Uehara has labored to wring energy from the temperature difference between warm ocean surface waters and cooler waters several hundred meters down. In this scheme, warm surface water vaporizes ammonia in a sealed piping loop, which drives a turbine and is then condensed by cold water pumped up from the deep. Making this work year-round requires stable ocean surface temperatures of about 30°C and deep water at least 20° colder—conditions found consistently only in the tropics.

After retiring from the Institute of Ocean Energy at Saga University in Imari, Uehara has pursued the idea through a nonprofit organization he runs near Nagasaki. His idea has gained traction after proponents began lobbying to test the project off an uninhabited atoll that barely juts above high tide in the Pacific Ocean, 1740 kilometers south of Tokyo. Japan calls Okinotorishima an island, but China insists it is just a few rocks. This is not a small semantic distinction. Under United Nations conventions, an island—and a 200-nautical-mile radius of ocean surrounding it—can be claimed by a country, as Okinotorishima now is by Japan. Rocks are part of the open sea, and any nation would be free to exploit offshore fisheries or other resources, as China has around the world for decades.

Because of China's incursions, some Japanese leaders have proposed building facilities on Okinotorishima to strengthen the country's claims. In a 31 December editorial and a 5 January news article, the *Yomiuri Shimbun* newspaper wrote that the ocean thermal energy–conversion experiment might be just the thing. And it reported that an Institute of Ocean Energy demonstration project would appear in the 2006 budget, which is about to be deliberated by the legislature.

The institute's director, Masanori Monde, says the technology "really won't be ready for such a demonstration project for another 10 to 20 years." He suspects someone planted the story in an attempt to influence budget deliberations.

Uehara says he didn't do it—but insists the technology is ready for a trial. If the government provides funding, he says, he's ready to work with private sector partners to build facilities on the reef.

Even a successful experiment is unlikely to sway critics. In response to a query from *Science*, the Chinese embassy in Tokyo, in a written statement, reiterated China's view that Okinotorishima is not an island under the U.N. Convention on the Law of the Sea. "Human activity cannot change that reality," it concludes.

–DENNIS NORMILE

AVIAN INFLUENZA

Donors Draw Plans to Disburse $2 Billion War Chest for Bird Flu

BEIJING—Raising money to help fight avian influenza and prepare for the threat of a human influenza pandemic turned out to be surprisingly easy. Now, the donors and international health organizations who met here last week are trying to figure out how best to spend the $1.9 billion.

Most of the money pledged over the next 3 years is new, says John Underwood, director of country services for the World Bank, which is laying plans to coordinate spending across agencies and countries. Spending it wisely will require "transparent monitoring" of both commitments and results, adds Markos Kyprianou, European commissioner for health and consumer protection.

There is little question about the need. Since late 2003, the H5N1 avian influenza virus has decimated poultry flocks in Asia and has now spread across Eurasia as far as Turkey. The virus has killed 79 of the 148 humans it has infected, and experts project that the death toll could reach between 2 million and 7 million people if the virus acquires the ability to pass easily among humans. A yearlong pandemic could cost the global economy as much as $800 billion, according to World Bank estimates. Helping the developing countries rein in the current H5N1 avian influenza outbreak and prepare for a possible human pandemic, meanwhile, could cost between $1.2 billion and $1.4 billion worldwide over the next 3 years.

In an effort to muster those funds, the World Bank, the European Commission, and the Chinese government cosponsored the International Pledging Conference on Avian and Human Pandemic Influenza in Beijing 17 and 18 January. Pledges topped even that high estimate of needs. Donors have been "extremely generous," says James Adams, vice president of the World Bank.

One by one. Some of the new funds will be used to help developing countries vaccinate their flocks against the H5N1 influenza virus.

The top priority of the United Nations ▶

GENETICS

Biobank Ties Cancer Genes to Rare Developmental Syndrome

When Brenda Conger's second child was born, doctors knew immediately that something was wrong. The baby boy had an unusually large head, cataracts, and respiratory and feeding problems, and doctors soon identified a heart defect. But it took a 3-year medical odyssey before Clifford was diagnosed with the rare genetic disorder cardio-facio-cutaneous (CFC) syndrome.

Now, in work that should lead to faster diagnosis of the condition, Katherine Rauen of the University of California, San Francisco, and her colleagues are the first to identify mutations that cause CFC syndrome. The research, published online this week in *Science* (www.sciencemag.org/cgi/content/abstract/1124642), highlights the developmental role of a genetic pathway, called MAPK, that is more famous as a trigger for cancerous tumors. Indeed, several potential cancer drugs targeting the pathway are already in clinical trials, and Rauen says that such drugs may offer a chance to treat at least some symptoms of CFC syndrome.

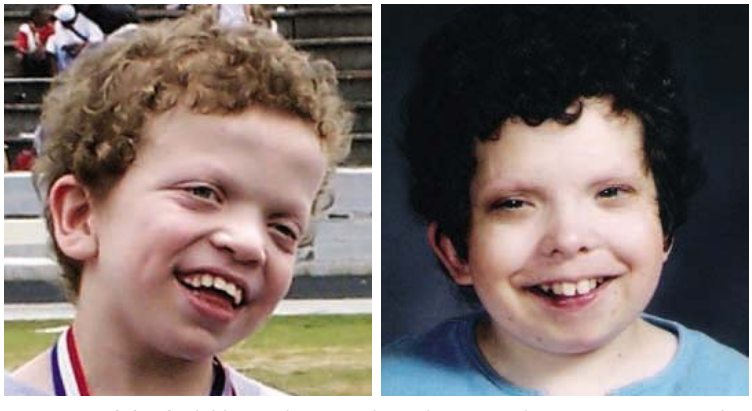

Mystery explained. Children with CFC syndrome have sporadic mutations in genes that belong to the MAPK pathway, leading to characteristic facial features, heart defects, and developmental problems.

There are fewer than 300 known cases of the syndrome, which is not fatal but causes a host of medical problems. Previous work had fingered mutations in a gene called *HRAS* as the culprit in a related, more serious condition, Costello syndrome, and defects in a gene called *PTPN11* as a cause of a milder disorder called Noonan syndrome. But CFC syndrome had remained a mystery. Some researchers even argued that it and Noonan were the same disease.

In 2004, members of CFC International, a support group for approximately 100 patients and their families, joined with several other genetic disease groups to set up a central biobank of patient records and DNA samples. "We had little pieces of our son all over the world, but no one was tying it together," says Conger, who is president of the group. Using material from the biobank, Rauen and her colleagues took only a few months to find mutations in three genes, *BRAF*, *MEK1*, and *MEK2*, that explain 21 of the 23 CFC cases they examined.

Like the genes that cause Noonan and Costello syndromes, the three are members of a complex pathway that is a main route by which a cell conveys signals from its outside to its nucleus. Among other roles, it helps the cell determine when to grow and divide. When one of the genes goes awry, the result is often a cell that divides out of control and generates a tumor.

In children with any of the three syndromes, the off-kilter signals cause heart defects; curly, brittle hair; a variety of skin conditions; slow growth; and cognitive disabilities. Although mouse studies had suggested that *MEK1* and *MEK2* mutations could cause heart and skin defects, the role for the pathway in facial development is unexpected, says Catrin Pritchard of the University of Leicester, U.K. Another surprise, Pritchard says, is that children with CFC do not seem prone to cancer, suggesting that the regulation of the pathway "is an order of complexity higher than we previously assumed." **–GRETCHEN VOGEL**

CREDITS (TOP TO BOTTOM): CHINA NEWSPHOTO/REUTERS; COURTESY OF CFC INTERNATIONAL

Food and Agriculture Organization and the World Organization for Animal Health is to provide assistance for rapid identification of the H5N1 virus and stamp out any outbreaks. For those countries where the virus is already endemic, the two organizations will help with vaccination programs. Developing countries will also need help bringing veterinary services and laboratories up to international standards.

WHO's priority for human health is its new rapid-response plan, says Peter Cordingly, spokesperson for WHO's Western Pacific Regional Office in Manila (*Science*, 20 January, p. 315). This plan aims to snuff out an incipient pandemic by identifying the first signals of human-to-human transmission and intervening with stockpiled antiviral drugs and quarantines.

The World Bank's Underwood says about $1 billion will be disbursed as grants, with the rest as loans. Cordingly adds that WHO will likely help the least developed countries define their needs. Some countries will be starting from scratch, he says. "Developing a good cadre of skilled scientists is a major issue in Laos," notes David Castellan, a poultry expert with the California Department of Food and Agriculture in Sacramento, who spent several weeks training village veterinary workers in Laos last year.

The donors—which include the United States, the European Union, and the World Bank—decided not to set up a new organization to run the massive program. Instead, the World Bank is setting up the Avian Influenza Multidonor Financing Framework to coordinate individual efforts by donor countries and agencies to minimize duplication and identify unfunded needs. On the receiving end, the World Bank will use its leverage to ensure that countries have integrated plans in place and will monitor how the money is used on the ground. "We're asking ourselves how to make sure that we don't finish up accused of squandering it," says Cordingly.

–DENNIS NORMILE AND GONG YIDONG

With reporting by Richard Stone. Gong Yidong writes for *China Features* in Beijing.

VIROLOGY

Genomic Analysis Hints at H5N1 Pathogenicity

Scientists have been puzzling over why the H5N1 avian influenza strain circulating in Asia is so much more deadly for humans than other flu viruses. Now, a new genomic analysis of hundreds of avian influenza viruses—the largest to date—hints that part of H5N1's pathogenicity may be traced to the behavior of a protein working within the infected cells.

Soon after H5N1 began sweeping across Asia, bioinformaticist Clayton Naeve and colleagues at St. Jude Children's Research Hospital in Memphis, Tennessee, realized they were sitting on a treasure trove of genomic data. The St. Jude Influenza Repository holds about 11,000 flu viruses, including 7000 avian influenza viruses, collected over 30 years by virologist Robert Webster. Naeve and colleagues started sequencing in November 2004, and online this week in *Science* (www.sciencemag.org/cgi/content/abstract/1121586), they report their first batch of results on 336 avian influenza viruses.

"Having this wealth of sequence information is very important," says Yoshihiro Kawaoka, a virologist at the University of Tokyo and the University of Wisconsin, Madison. Albert Osterhaus, a virologist at Erasmus University Medical Center in Rotterdam, the Netherlands, calls the identification of a new potential virulence determinant "quite suggestive."

Naeve says the viruses covered in the paper include isolates from a variety of wild birds and poultry collected throughout the world from 1976 to 2004. The team has almost doubled the amount of avian influenza virus sequencing data available, he says, by contributing 3.7 million base pairs of finished sequence data to the public repository GenBank. The group will continue sequencing.

For the current analysis, Naeve and colleagues combined the genetic data from their sequencing efforts with additional avian, swine, and human influenza sequencing data retrieved from GenBank. The avian influenza virus genome consists of eight RNA segments that code for 11 known proteins. In what they believe is a first, the group applied a technique called proteotyping to flu virus sequence data.

Typically, researchers create phylogenetic trees that show how the genes from the different viruses relate to one another. Proteotyping goes a step further, identifying gene variants having unique amino acid signatures. "By looking at the protein level, we see a lot of differences you wouldn't see just looking at the family tree," Naeve says.

This approach enabled them to zero in on genetic variability in their virus samples; variability typically suggests that a gene plays a key role in flu virus evolution and biology. Not surprisingly, there was a lot of variability in the *hemagglutinin* (*HA*) and *neuraminidase* (*NA*) genes, which code for two surface glycoproteins—presumably because of pressure to evolve to escape host immune response, Naeve says.

But they also found that the *NS* gene was highly variable. *NS* codes for two nonstructural proteins, NS1 and NS2. NS1 does not appear in the intact virus but rather is only produced in the infected cell, where it regulates a variety of functions during infection.

Disrupted. The H5N1 virus may be so deadly to humans because it produces a protein that can disrupt key cellular signaling pathways.

CREDIT: BOGDAN CRISTEL/AP PHOTO/POOL/REUTERS

The St. Jude researchers, led by Richard Webby, a cluster of amino acids that binds to other molecules, at one end of the NS1 molecule. If these amino acids have a certain sequence, the ligand will bind to receptors on proteins involved in many intracellular signaling pathways.

The majority of known avian NS1 proteins have this binding sequence, the researchers found, whereas the vast majority of human viruses do not. This suggests that avian viruses have the capability of disrupting key cellular processes, which human viruses leave alone, says Naeve. He speculates that, when acting in combination with other avian influenza proteins, "NS1 may be very important for the virulence of avian flu viruses when they are introduced into humans."

Kawaoka says animal experiments are needed to determine the impact of the *NS* gene variations on pathogenicity. But he says the paper provides a good example of using sequence information to develop new hypotheses. **–DENNIS NORMILE**

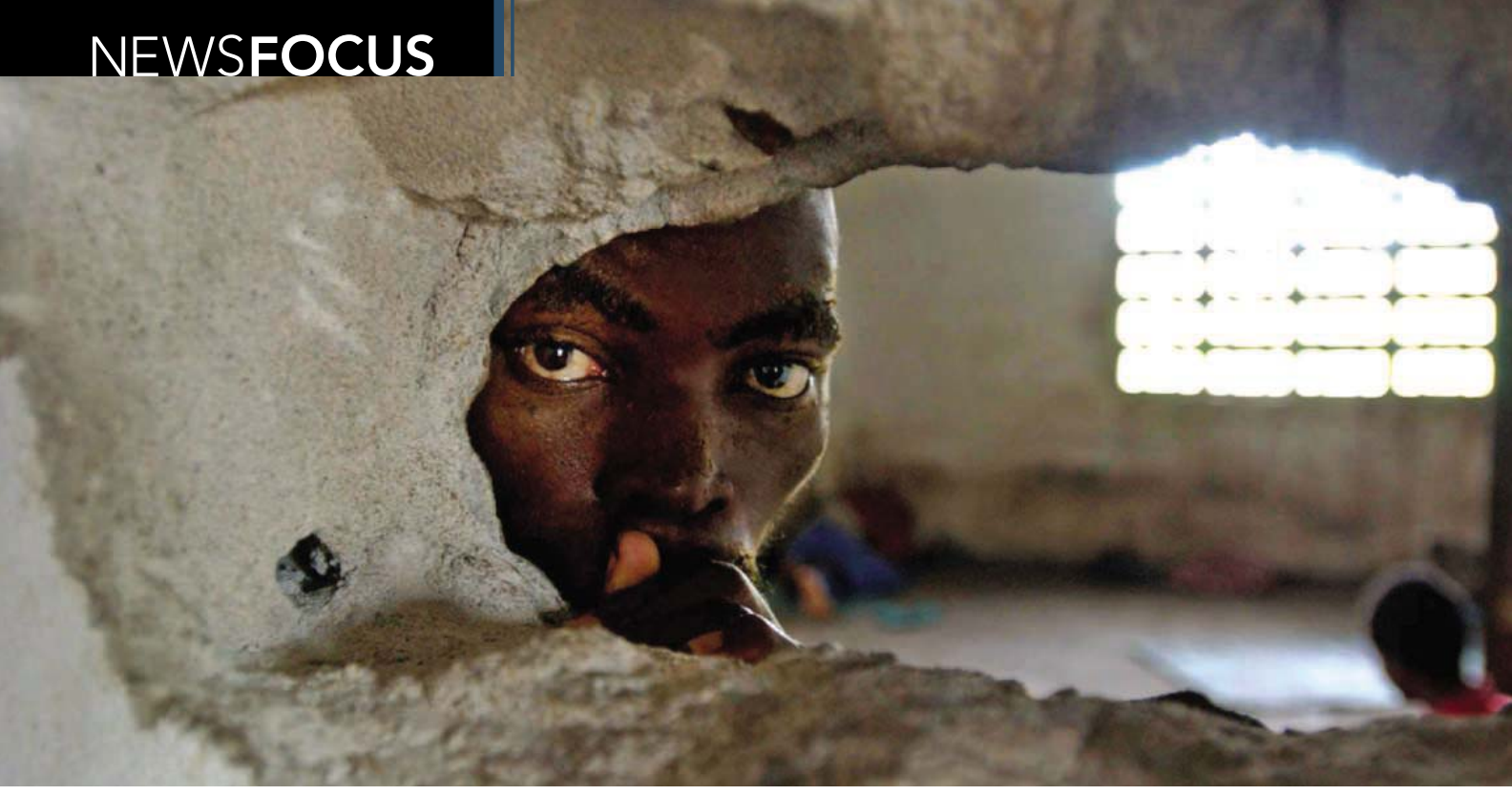

Proper care of the mentally ill often is viewed as an expendable luxury in the developing world. Recent research suggests it doesn't have to be that way

The Unseen: Mental Illness's Global Toll

LONDON—When the bloody reign of the Khmer Rouge came to an end in 1979, there were no mental health workers left in Cambodia; they had died or disappeared. For more than a decade, says Phnom Penh psychiatrist Pauv Bunthoeun, only traditional healers were available to give treatment, often administering poison or beating the patient with burning incense to drive out vexing spirits.

Conditions started to improve in 1994, Bunthoeun told a gathering of researchers and aid workers here.* That year, the Ministry of Health, aided by a team from the University of Oslo, in Norway, began training a new generation of psychiatrists. Bunthoeun was one of the first through the program, which has produced all 26 of Cambodia's psychiatrists. Bunthoeun's hospital in Phnom Penh now sees up to 200 psychiatric outpatients a day, and in July 2005 it opened a 10-bed inpatient ward—the first and only one in a country of 12 million people.

Such stories of unmet need are a common refrain among mental health workers in the developing world. The imbalance is staggering. The majority of the world's 450 million people who suffer from neuropsychiatric disorders live in developing countries, but the World Health Organization (WHO) estimates that fewer than 10% have access to treatment. In regions torn by war, poverty, and infectious disease, mental health care is often viewed as an unaffordable luxury. Nearly a third of the world's countries, including many of the poorest, have no national budget for mental health, according to WHO. Even where budgets exist in developing countries, they average only about 1% of meager health resources. The United Nations Millennium Development Goals make no mention of mental health, nor do the Bill and Melinda Gates Foundation's Grand Challenges in Global Health.

"The mentally ill are particularly disadvantaged among the poor," says Benedetto Saraceno, director of WHO's mental health department. Untreated mental illness reinforces poverty, researchers say. Yet despite the common assumption that treatments require expensive drugs and complex therapy, recent trials from developing countries on three continents have demonstrated that simple, cheap interventions for common disorders such as depression can be effective. Other recent work suggests that incorporating simple mental health interventions into anti-HIV and other public health campaigns may make them more successful.

It "really finishes off a household … when one member has a severe psychiatric problem."

—Veena Das, Johns Hopkins University

Mental health must be addressed like other basic needs, says Vikram Patel, a psychiatric epidemiologist at the London School of Hygiene and Tropical Medicine and a vocal advocate for this cause. "It is unethical to deny effective, feasible, and affordable treatment to millions of people suffering from treatable disorders," he argues. The challenge, Patel and others say, is to persuade policymakers it's a problem worth addressing.

* International Mental Health, 31 August–2 September 2005, Institute of Psychiatry, Kings College London.

CREDIT: JEHAD NGA/CORBIS

Standard care. Lockup asylums like this one in Liberia are common throughout the developing world.

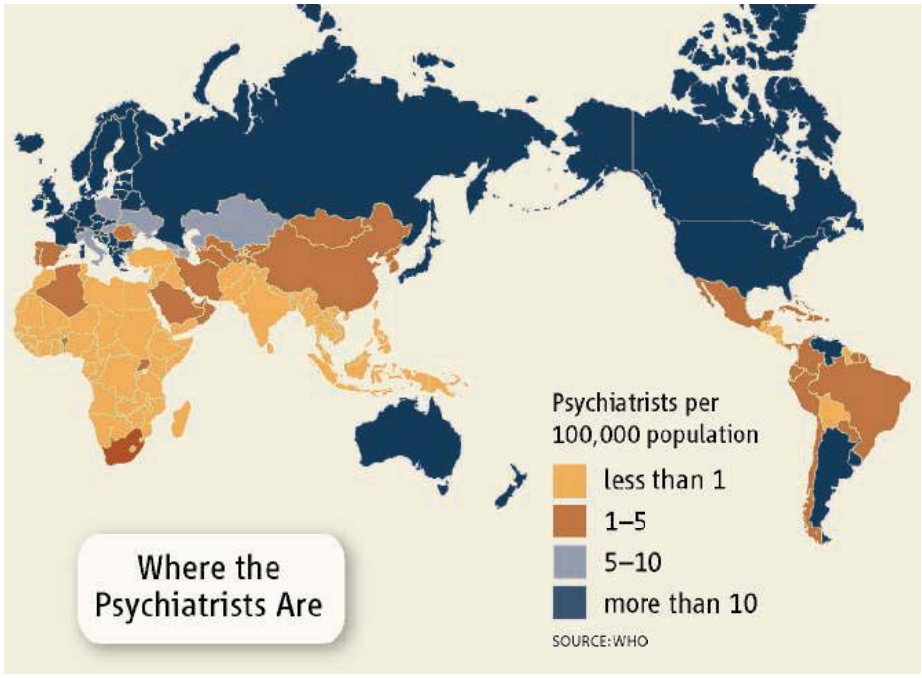

How big a burden?

A series of studies begun in the mid-1990s paints a startling picture of the global impact of mental illness. The work, led by WHO, the World Bank, and the Harvard School of Public Health, showed that although mental disorders cause fewer deaths than infectious diseases, they cause as much or more disability because they strike early and can last a long time.

Indeed, mental and behavioral disorders rank among the most burdensome disorders across the world. According to WHO's *World Health Report 2001*, for example, depression ranked fourth among all causes of disability as measured by an index called the DALY. (One disability adjusted life year is a year of healthy life lost to sickness or premature death.) The toll on the young is particularly heavy. For people aged 15 to 44, depression took the second biggest toll of all illnesses, behind only HIV/AIDS. For this age group, alcohol abuse, self-inflicted injuries, schizophrenia, and bipolar disorder also ranked among the top 10 causes of DALYs. In 2002, neuropsychiatric conditions accounted for 24% of DALYs for 15-to-44-year-olds, and 13% overall.

In some areas, particularly sub-Saharan Africa, infectious diseases and malnutrition take such a heavy toll that the share of disability from mental illness falls below the global average. Yet it is in the poorest countries that the burden of mental illness is rising most quickly, according to WHO projections. And this is where resources are thinnest. Just how thin is revealed in an inventory of mental health services described at the London meeting by Shekhar Saxena, WHO's director of mental health evidence and research (www.who.int/mental_health/evidence/atlas). In sub-Saharan Africa, many countries have one psychiatrist—if that—for every million people, compared to 137 per million in the United States.

Penalizing families

Most families in developing countries have no choice but to care for a mentally ill relative at home. And it "really finishes off a household … when one member has a severe psychiatric problem," says Veena Das, an anthropologist at Johns Hopkins University in Baltimore, Maryland, who has studied mental illness in poor neighborhoods of Delhi in India. Although decent care is available at nominal cost at government hospitals in Delhi, Das says, the hospitals are terribly overburdened. "The lines are so long that someone might go in the morning and have to leave in the evening" without seeing a doctor, she says. People with a chronic disorder such as depression can't get the regular treatment they need.

Many families turn instead to private practitioners, often wasting their money. A 2004 World Bank study concluded that incompetent practitioners in Delhi tend to congregate in poor neighborhoods. Practitioners often give out free samples from pharmaceutical company representatives rather than prescribing the most effective medicine, Das says: "You go into these really poor households, and you find that drugs have been administered in haphazard ways."

Going nowhere. This long-term patient with schizophrenia is chained to a bench at Theng Psychiatric Hospital.

The financial burden on families is huge, says Martin Knapp, a health economist at the London School of Economics. The lost income from a relative who's too sick to work is the biggest blow, but often someone works less to become a caregiver. That can have disastrous effects. "You hear about people being chained to trees so that the families can get on with subsistence," Knapp says.

But public funds are scant in the poorest countries, and siphoning money from HIV, malaria, or tuberculosis programs to put toward mental health services probably doesn't make economic sense, says Daniel Chisholm, a health economist at WHO.

Chisholm says investments in mental health services are most likely to pay off for countries a little further up the development scale. Treating common mental disorders such as depression "has similar attractiveness in terms of bang for your buck relative to … diabetes, hypertension, and cardiovascular disease," Chisholm says. Yet diabetes is commonly treated in low- to middle-income countries and depression commonly isn't, he says: "The difference comes down to stigma … [and] societal attitudes about what the priority should be."

Even in low-income countries, recent studies suggest that effective treatments may be more affordable than has been widely assumed. In 2003, three independent teams reported that low-cost interventions against depression are feasible and effective. In one study, Paul Bolton, an epidemiologist then at Johns Hopkins Bloomberg School of Public Health, and colleagues enrolled more than 200 people with depression from 30 rural villages in Uganda. Half

CREDITS (TOP TO BOTTOM): K. BUCKHEIT/*SCIENCE*; KATHARINA HESSE/GETTY IMAGES

Mapping Mental Illness: An Uncertain Topography

Mental disorders were once considered diseases of the affluent. That assumption was based on scant evidence, researchers now say. There are even reasons to suspect that the opposite might be correct, because known risk factors for poor mental health—poverty, HIV, and violence—afflict many parts of the developing world. But the true picture has been hard to nail down. Although clear geographic patterns exist for certain disorders, the figures for others are all over the map. That may reflect real geographic differences in the rates of these disorders, or it could say more about how people from different cultures think about mental health—and how they discuss it with clipboard-toting strangers.

Schizophrenia, a psychotic disorder thought to have a strong genetic component, appears to affect roughly 1% of people worldwide. People with schizophrenia seem to fare better, however, in developing countries (see p. 464). Not surprisingly, the highest rates of posttraumatic stress disorder and related problems are found in tumultuous regions of the developing world. A national survey of strife-torn Afghanistan, reported in the *Journal of the American Medical Association* (*JAMA*) in 2004, found symptoms of depression in 68% of the 407 people interviewed and symptoms of anxiety in 72%.

Dementia is another story. The prevalence of this disorder, caused mostly by Alzheimer's disease, seems similar in Latin America and in the developed West—about 2% of people aged 65 or older—but rates in India are only half as high, says Martin Prince, a psychiatric epidemiologist at the Institute of Psychiatry in London and director of Project 10/66, an effort to assess dementia and study interventions in developing countries. Prince suspects that dementia is underreported in India, perhaps because family members are reluctant to appear critical of their elders or because there are fewer demands on older people, which helps mask signs of cognitive decline. Risk of dementia rises with age, so developing countries are likely to be hit hard as their demographics shift. Today, roughly 15 million people with dementia live in developing countries; by 2040, that will rise to 57.5 million and 71% of all dementia cases worldwide, Prince and colleagues predict in a paper published 17 December 2005 in *The Lancet*.

The first batch of findings from the World Mental Health Survey, an extensive project sponsored by the World Health Organization, reveals wide variation in the prevalence of mental disorders. (Schizophrenia and dementia were not included.) Among the 14 countries analyzed so far, the prevalence of mental disorders within the last 12 months ranged from 4.3% in Shanghai, China, to 26.4% in the United States, a team led by epidemiologist Ronald Kessler of Harvard Medical School in Boston reported in June 2004 in *JAMA*. That mirrors a pattern for depression that has long intrigued researchers: It is reportedly scarce in East Asian countries, even though they have some of the highest suicide rates in the world (see p. 462). There was no systematic difference between developed and developing countries, however. Researchers found a relatively low 9% prevalence of all disorders in Japan and Germany, but 20% and 18% prevalence in Ukraine and Columbia. Kessler says the team will publish data from another 14 countries this year.

Some of the country-to-country variation can be attributed to the

participated in weekly group therapy sessions led by a local village health worker who had received 2 weeks of intensive training. After 16 weeks, the severity of symptoms had dropped sharply in the treated group, compared to far more modest spontaneous recovery in the untreated group, the team reported in the *Journal of the American Medical Association* (*JAMA*). Bolton's study was the first to show that a Western approach could be applied in a totally different setting by local people with relatively little training, says Patel.

Subsequently, researchers in Chile reported a successful trial using antidepressants and group therapy sessions led by local nurses and social workers, and a team in Goa, India, led by Patel reported promising results using antidepressants alone. Both studies appeared in *The Lancet* in 2003.

CREDITS: ATIF RAHMAN

Early disadvantage. Maternal depression appears to hinder child development in rural Pakistan.

Mind and body

Investments in mental health could pay broad public health dividends. Saraceno points out that mental disorders tend to cluster with other ailments: Depression is a risk factor for heart disease, cancer, and alcohol abuse. At the same time, depression is more common in people with physical ailments. WHO estimates that as many as 45% of people with HIV or tuberculosis develop depression. A 2001 study published in *JAMA* found that depression hastened the progression of disease and more than doubled the mortality rate in HIV-positive women.

The HIV-depression link has worrying implications, says Melvyn Freeman, a clinical psychologist at the Human Sciences Research Council in Pretoria, South Africa. "Someone with depression is not going to take the same precautions as someone who's well and cares about their life," says Freeman. Moreover, he adds, studies from developed countries show that people with depression and other mental disorders are less likely to adhere to complex anti-HIV therapy—which involves an extended course of multiple drugs, some with nasty side effects. Noncompliance is a serious problem because it squanders scant resources and because partial treatment could enable drug-resistant HIV strains to proliferate. Freeman and colleagues have developed a plan for training health care workers to incor-

difficulty of adapting diagnostic interviews to different cultures, Kessler says. Another difficulty is getting people to talk about their inner turmoil. In some places, "people think if they give a wrong answer to one of our questions the government is going to come and shoot them," Kessler says. Survey teams work through local religious and community leaders to allay such concerns. Even so, Kessler suspects that teams may be getting underestimates outside of Europe and North America: "We're working … to improve the way we ask questions about emotional problems in these countries, but we're not far enough along to know what we will find."

At the same time, other researchers suspect that surveys overestimate the prevalence of mental illness in wealthy countries. "It's an absurdity to say 50% of Americans will have a mental disorder in the course of their lifetime," says Arthur Kleinman, a medical anthropologist at Harvard Medical School, referring to an estimate Kessler and colleagues published in June 2005 in the *Archives of General Psychiatry*. To Kleinman, the high prevalence figures suggest that the surveys are too sensitive, picking up common unhappiness as well as clinical cases of depression in some populations. "We now have a strange situation in epidemiology," he says, where mental illness is overestimated in some places and underestimated in others.

–G.M.

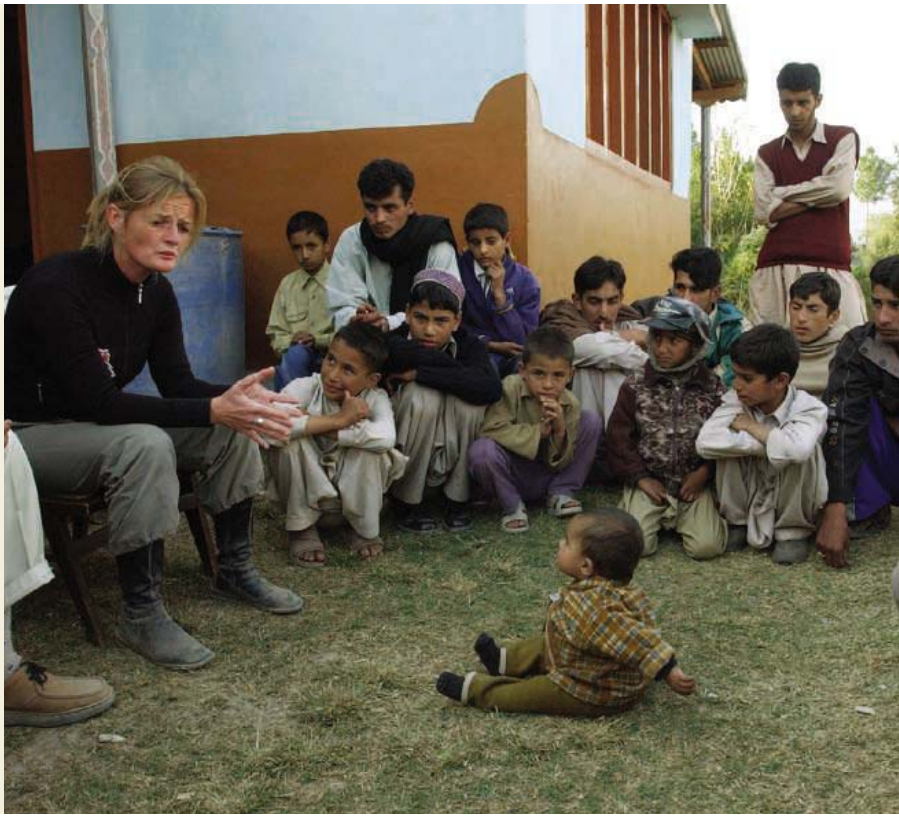

Kashmir. War and natural disasters increase the need for mental health support.

CREDITS: ASSOCIATED PRESS

porate basic mental health interventions into anti-HIV programs.

In south Asia, a similar strategy might improve low birth weight and stunted childhood development. Several recent studies have found a high prevalence of maternal depression—up to 30% of new mothers—in India and Pakistan. In 2004, Atif Rahman, a child psychiatrist at the University of Manchester, U.K., and colleagues reported in the *Archives of General Psychiatry* that children born to depressed mothers in Rawalpindi, Pakistan, have lower birth weights and slower growth in the first year of life. Such children also are more likely to have diarrheal disease and less likely to receive a complete set of vaccinations. Rahman suspects that depressed mothers may breastfeed less, or even produce less breast milk—a hypothesis his team plans to test.

At the same time, Rahman's group will evaluate a modest mental health program by enrolling 900 expecting mothers in a randomized trial. Half will receive the usual visits from a village health worker, the other half will receive a combination of counseling and nutrition advice from a health worker who has attended a 2-day workshop put on by Rahman's team. The researchers will check how the babies are faring 6 and 12 months after birth. They have approached the issue of depression obliquely because "treating women for depression, no matter how you sell it, isn't sellable" in this rural area of Pakistan, Rahman says. His team has billed the project as a child-development effort.

Rahman's work shows how mental health is relevant to development goals, says the organizer of the London conference, Martin Prince, a psychiatric epidemiologist at Kings College London. He and others say the best solution is to shift the emphasis away from centralized hospitals to care by well-trained community workers.

People with depression and other mental disorders are less likely to adhere to complex anti-HIV therapy.

—Melvyn Freeman, Human Sciences Research Council

Uphill battle

But many officials who control the purse strings are not convinced. The World Bank's position is that there's not enough evidence to recommend investments in mental health services in poor countries, says Florence Baingana, a Ugandan psychiatrist who advises the bank on mental health issues. (Baingana says she personally believes such investments are warranted.) Convincing the skeptics will require demonstrating the economic costs of untreated illness more clearly and countering the persistent view that a person with a mental disorder will never function at a normal level, Baingana says: "When we can show that people with neuropsychiatric disorders, if properly treated, can [illegible] we will have greater interest."

Governments in the developing world are reluctant to devote resources to mental health—or even to ensure basic rights for people with mental illness, says Saxena. A mental disorder is grounds for denying the right to vote in some countries; in others, it can be grounds for annulling a marriage. Conditions in many government-run asylums are deplorable. In September 2005, the Washington, D.C.–based Mental Disability Rights International released a report documenting the use of electroconvulsive therapy, without anesthesia or muscle relaxants, as punishment for unruly patients in a Turkish psychiatric hospital.

Often it takes a disaster to get mental health on the agenda. For example, a fire at Erwadi Dharga, a religious healing center in southern India, in 2001 claimed the lives of 25 mental patients who'd been chained to their beds. It made international headlines. Afterward, India cracked down on private asylums—inspecting and certifying them according to laws that have been on the books for years but were rarely enforced. More recently, the Asian tsunami spurred countries in the region to improve mental health services (*Science*, 12 August 2005, p. 1030). The evidence may be there, but until something terrible happens, most politicians don't think about mental health, Saxena says. "Our job," he says, "is systematically shaming them into thinking about it." **–GREG MILLER**

Reporting for this series was supported by a fellowship from the Carter Center.

Sign of the times. China's rapid development has brought new stresses and mental health risks.

China: Healing the Metaphorical Heart

Eastern and Western concepts of mental health clash as psychiatrists seek to reconcile China's apparent scarcity of mental illness with its high suicide rate

HONG KONG—Dominic Lee declines an offer of chili sauce as he tucks into wonton soup and stir-fried greens. Over lunch at a bustling indoor market near his office at the Chinese University of Hong Kong (CUHK), Lee, a psychiatrist and researcher, explains that chilies tend to make him agitated because they are metaphysically hot. Although trained in the Western medical tradition, Lee incorporates the notion of balance between opposing forces—cold and hot, yin and yang—a tenet of traditional Chinese medicine (TCM), into his personal life and professional practice.

In TCM, mental distress falls into a category of diagnoses that involve weakness of the heart, or bad interactions between the heart and other organs, Lee explains: "The heart is part of the metaphorical mind." The idea is rooted in thousands of years of Chinese culture, and even now it shapes how Chinese talk about their mental life. "There are more than 100 Chinese characters for emotion that contain the heart symbol in combination with others," Lee says. His research has found, for example, that people with symptoms of depression often insist that their distress centers on the heart.

The tendency to express emotional distress in physical rather than mental terms is much stronger in China than in most Western cultures. It may help explain why mental disorders are diagnosed less frequently here. And it could have implications for understanding China's alarmingly high suicide rate. At the same time, Lee and others note that the public health picture is changing as social and economic changes sweep China and more and more people become familiar with Western concepts of mental illness.

Depression by any other name?

Many epidemiologists have reported low rates of depression and other mood disorders in East Asia, including in China (see sidebar, p. 460). A survey coordinated by the World Health Organization (WHO) found that roughly one in 50 people in Shanghai and Beijing suffered from a diagnosable mood disorder over a recent 12-month period. In the United States, one in 10 had, according to the survey, published in the 2 June 2004 issue of the *Journal of the American Medical Association*. However, surveys of this sort have a flaw that may skew results: They are designed to detect disorders as experienced by Westerners, says Arthur Kleinman, a medical anthropologist at Harvard Medical School in Boston.

A generation ago, depression as a clinical diagnosis was unheard of in China, says Kleinman, who has done research in Taiwan and mainland China since 1968. The most common psychiatric diagnosis was neurasthenia, characterized by lethargy, poor concentration, headache, and other symptoms. But in 1982, Kleinman published a landmark study in which he found that 87% of patients with neurasthenia at a Hunan hospital met criteria for depression. Since then, neurasthenia has faded as a clinical diagnosis. Depression has become more common, although not nearly as prevalent as in the West.

In one recent study, Lee interviewed 40 psychiatric outpatients at a clinic in Guangzhou, the capital of southern Guangdong province. Although all the patients had the telltale signs of depression listed in Western diagnostic manuals, including loss of appetite, impaired concentration, and feelings of hopelessness, they also told of other experiences not covered in Western texts. Many described discomfort or distress in the heart, using terms like *xinhuang* (heart panic), *xinfan* (heart vexed), and *xintong* (heart pain). Patients also reported distress at the social disharmony caused by their illness, citing disruptions to relationships with families and colleagues. Some patients acknowledged they were sad or depressed but insisted the depression was a side effect of their primary problem—sleeplessness—thereby turning on its head the Western notion that insomnia is a symptom of depression.

Such studies reveal important differences in the language Chinese and Western people use to describe their experience with depression, Kleinman says. This type of knowledge can improve the ability to recognize mental illness. It can also help psychiatric epidemiologists fine-tune surveys, he says. Indeed, in a recent survey designed to be more sensitive to Chinese expressions of mental pain, a team led by Michael Phillips, a psychiatrist at Hui Long Guan Hospital in Beijing, found that 8.6% of nearly 15,000 people interviewed in Zhejiang province met Western criteria for a mood disorder, roughly quadruple the prevalence reported by the WHO study.

At the same time, Phillips and Kleinman suspect that there is more to the cultural difference than using different words to describe the same experience. "The differences are not just linguistic," says Kleinman. "There really are differences in the lived experience of [mental] disorders."

Depression versus despair

Low reported rates of depression in China have led some researchers to conclude that mental illness is not the main factor in most suicides here, as it is thought to be in

Yiyuzheng. The Chinese word for depression is rarely used outside of the clinic.

the West. China has one of the highest suicide rates in the world: Nearly 300,000 people take their own lives each year. It is also one of only a handful of countries in which more women than men kill themselves.

Studies in China have found that fewer than half of those who attempt or commit suicide have a diagnosable mental illness at the time. One exception, a study by Phillips and colleagues that employed more culturally sensitive methods, found mental illness in 63% of suicides, the team reported in *The Lancet* in 2002. Even the higher figure falls short of those typically seen in the West, however, where at least 90% of suicides are blamed on mental illness. The authors of *The Lancet* study concluded that "many suicides are impulsive acts by people who do not have a mental illness" but face acute stress.

In China, there is no strong moral taboo against suicide, Phillips says, and many people see it as an acceptable way out of a bad situation. His team recently did a survey in which they presented subjects with 26 stressful scenarios such as getting a divorce or failing an important exam. Only 15% said they would never consider suicide in any of the circumstances. Twice that number said they would definitely consider it in at least one of the scenarios, Phillips says.

They may not spend much time deliberating, however. Phillips reported in 2004 that 45% of suicides in China were contemplated for 10 minutes or less. Easy access to pesticides—used in more than half the suicides in that study—helped convert impulse into lethal action. Women in particular are prone to such "low-planned" suicides, Phillips and colleagues reported in 2005 in *Psychological Medicine*.

Social and financial stresses are often the root cause of suicide in Hong Kong, says Lee. "We have some patients who develop severe depression and kill themselves out of the blue, without any social stress—but that's very uncommon," he says. Lee and colleagues recently investigated how worries over finances influenced the suicide rate in Hong Kong following the handover from Britain to China in 1997. After years of prosperity in the 1980s and 1990s, the city's economy nosedived in the late '90s. The change in fortune hit people hard, Lee says, and the suicide rate rose to a historic high.

Although a link between economic hard times and suicides is generally accepted, few studies have examined this trend in detail, Lee says. He and colleagues tried to do this for a highly publicized rash of suicides following the handover. In November 1998, a woman sealed herself inside her bedroom and lit a charcoal fire on a grill, poisoning herself with carbon monoxide. By January 2000, 160 Hong Kong residents had killed themselves this way. Lee's team reviewed coroners' records for all 160 and interviewed 25 people who survived attempted charcoal suicides. They also interviewed families and survivors of other suicide methods. People who killed themselves by charcoal fumes had one thing in common that the others did not: serious debt.

CREDIT: LI JIN

Locus of pain. In traditional Chinese medicine, mental illness is often attributed to maladies of the heart.

Banks, looking for new revenue streams during the posthandover recession, provided easier access to consumer credit, Lee says. In early 2002, the average family with a credit card carried a balance equivalent to 85% of their annual income, according to the Hong Kong Monetary Authority. Vivid media coverage of the charcoal suicides, often including photos of necessary equipment, popularized the method and made it seem like a way out for people in dire straits, the researchers reported in January 2005 in the *British Journal of Psychiatry*.

A balancing act

In Lee's small but impeccably neat office at CUHK, a corner cabinet holds a stockpile of puer tea, prized by connoisseurs for its complex, earthy aroma. Lee stores the tea at his office because at home it might absorb cooking odors that would ruin the flavor. On the wall, a framed cover of *The New Yorker* portrays four people in suits, apparently commuters on a train. Three are busy working on cell phones and laptops. Lee says he identifies with the fourth man, who smiles with anticipation at a toaster in his lap. "He's taking time out to enjoy something in the middle of a hectic world," he says.

Life for many Chinese is growing more hectic. In some ways that's a good thing. The booming economy has created jobs that have improved the fortunes of millions. At the same time, development has ushered in new stresses. In 1995, the Chinese Medical Association added *lutu jing-shenbing* or traveling psychosis to the Chinese Classification of Mental Disorders to describe the symptoms—including delusions, hallucinations, disordered speech, confusion, or catatonia—sometimes suffered by rural peasants traveling hundreds or even thousands of kilometers on overcrowded trains to the economically vibrant coastal cities.

The infiltration of Western media and changing roles of women contributed to a sharp rise in eating disorders in Hong Kong in the 1990s, says CUHK psychiatrist Sing Lee (no relation to Dominic). "When I was a trainee 20 years ago, I didn't see eating disorders," he says. Now, he says he's seen anorexia patients as young as 10. "In the traditional Chinese view, beauty is all in the face. Now it's the body," Lee says, tracing an hourglass in the air with his hands. In addition to the stress of being homemakers, women now are more likely to work and face occupational stress as well.

The westernization trend also extends to concepts of depression. "Just in the last 10 years, depression has become a term that people in urban areas understand," Kleinman says. It's also a term that's increasingly familiar to primary-care doctors, thanks in part to "educational" programs offered by Western drug companies. With patent protection running out on the blockbuster antidepressant selective serotonin reuptake inhibitors, companies see China as a vast untapped market, Kleinman and others say.

Chinese psychiatrists say it lessens the stigma of mental disease if they convey to patients a physical root of their illness. "If I make a diagnosis of postnatal depression, the family will think the mother is mad, but with TCM, you can make a diagnosis without stigma so that people retain their social support," Dominic Lee says. "I'll say, 'Have you heard of postnatal depression?' and explain what that means, and I'll also say 'In TCM, this is how your condition is viewed' and encourage them to see an herbalist."

To Lee, Eastern and Western views of mental health aren't in competition. Both have their advantages, and both have their place in his practice. They're just two contrasting forces in need of balance. **–GREG MILLER**

Men at work. Schizophrenia patients in Chennai spend most of the day in organized activities.

A Spoonful of Medicine—And a Steady Diet of Normality

Private hospitals in India are showing that the best treatment for mentally ill patients is to lend purpose to their lives

CHENNAI, INDIA—Incense wafts around two dozen men standing in a circle stomping, clapping, and chanting to the rhythm of a drum. This ceremony for the Hindu god Krishna wouldn't seem out of place in a temple, but this evening the venue is a rehab clinic, and the men are patients with schizophrenia.

Earlier, the men were hard at work here at the Schizophrenia Research Foundation (SCARF), making chalk sticks or fashioning sturdy shopping bags from old newspapers. The clinic sells the items, along with dolls and candles made by female patients, to local shops in Chennai, a sweltering city of 6 million on India's southeast coast, and shares the proceeds with the patients. The buzz of activity makes SCARF feel more like a summer camp than a psychiatric ward. About 40 patients live at SCARF's Chennai headquarters, and several dozen others spend their days here and return home at night.

Although the patients take antipsychotic drugs, it's the healing power of social interventions that has given SCARF an international reputation as a leader in schizophrenia treatment. The clinic's success at rehabilitating patients—many of whom recover enough to hold down a full-time job, marry, and otherwise lead fairly normal lives—offers a powerful lesson on the benefits of going beyond the standard biomedical approach. "If I become psychotic, I'd rather be in India than in Switzerland," confesses Shekhar Saxena, director of mental health research at the World Health Organization (WHO) in Geneva.

Some Western psychiatrists argue that social activities such as those employed at SCARF and other Indian nongovernmental organizations (NGOs) are too often shunned in the pursuit of pharmacological solutions. "One of the great disgraces of American psychiatry is that we're very, very invested in medications," says Paul Fink, a psychiatrist at Temple University in Philadelphia, Pennsylvania, and a former president of the American Psychiatric Association. Despite decades of research indicating that mentally ill patients respond best to a combination of drugs and social programs, Fink and others see few signs that U.S. psychiatric institutions are moving to integrate more social interventions into treatment regimens.

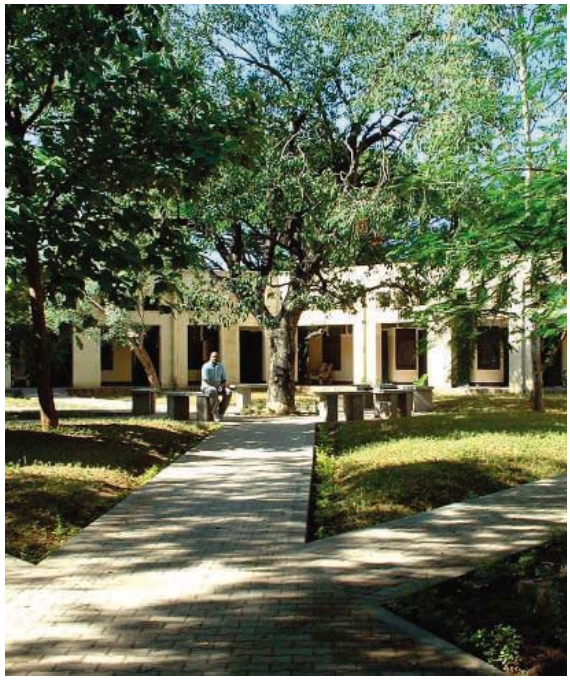

Relative peace. Mentally ill patients live with family members at a private hospital in Chennai.

Family ties

Narendran, a handsome, animated man in his 30s, lives at SCARF's home for men in Mamallapuram, about 50 kilometers down the coast from Chennai. Sitting at a table in the center's cafeteria, Narendran, who like many Indians goes by a single name, explains how the activities at SCARF give him a sense of purpose. Captaining the center's cricket team has brought out his competitive side, he says. During the day, Narendran tends the gardens at a nearby office complex. He's proud to be able to spend part of his earnings on political biographies for a niece. At SCARF, finding a job is viewed as essential to a patient's recovery; family members are advised to bribe employers—typically friends or relatives—if necessary.

SCARF's philosophy taps into an emphasis on family and community long flagged as an explanation for evidence that schizophrenia patients fare better in developing countries than in wealthier countries. These findings are especially remarkable because most people with a severe mental illness in India, for example, receive little if any specialized care; extremely few are lucky enough to get into a program such as SCARF's. The country has only 25,000 psychiatric hospital beds—a third of which are in a single state, Maharashtra—for 15 million people sick enough to need them, including about 3 million with schizophrenia.

Yet a long string of studies, beginning with WHO's International Pilot Study of Schizophrenia, launched in 1967, have reported that patients in India and other developing countries are more likely to have long-term remission of symptoms and fewer relapses than patients in the developed world. Subsequent studies with refined methodologies have concluded the same, says Assen Jablensky, a psychiatric epidemiologist at Western Australia University in Perth who led one of the largest follow-ups, a 10-country project that wrapped up in the early 1990s. He chalks

CREDITS (TOP TO BOTTOM): SCARF; PRATHAP THARYAN

up the difference to better social support in more traditional societies.

Indeed, out of necessity, about 99% of Indians with schizophrenia live with their families, says psychiatrist R. Thara, SCARF's director. In developed countries, estimates range from 15% to 25%; most patients live alone or in a hospital or an assisted-living facility. In the United States, about 6% of people with schizophrenia are homeless, and a similar percentage are in prison. In one study in Chennai, three-quarters of patients got married and held jobs—considerably more than in Western countries, Thara and colleagues reported in the August 2004 issue of the *Canadian Journal of Psychiatry*. Thara involves the patients' social network in their care. "We have a much more global view of the patient," she says.

Other illnesses also appear to respond to this holistic strategy, says Prathap Tharyan, head of psychiatry at Christian Medical College (CMC) in Vellore, about 150 kilometers west of Chennai. Tharyan will only admit a patient on the condition that at least one family member stays in an on-campus apartment with the sick relative. CMC may be the first psychiatric hospital in the world to insist on this arrangement, Tharyan says. "It's absolutely crucial to have the family involved."

Like many Eastern psychiatrists, Tharyan shares the view of Western medicine that mental illness is a neurobiological problem. "I have no doubt that schizophrenia is caused by something that goes wrong in the brain," he says. But Western medicine often overlooks how mental illness disrupts social networks, Tharyan says: "It affects the entire function of the family and the individual's role in the family."

Drug culture

That idea is more studied than practiced in the West, particularly in the United States. Researchers have identified at least half a dozen interventions—including work training and placement programs, education and support for families, and programs that teach social skills—that improve the lives of schizophrenia patients, says Wayne Fenton, director of adult translational research at the U.S. National Institute of Mental Health (NIMH) in Bethesda, Maryland.

The problem is that these findings don't make it into the clinic. A 2001 study in *Schizophrenia Bulletin* found that although 61% of schizophrenia patients in the United States want to work, fewer than 20% find employment. A 1998 study funded by NIMH and the Agency for Health Care Policy and Research hints at the reason. It found that only one in four schizophrenia patients in the United States receive employment assistance. In addition, less than 10% of patients participate in community-based programs that help prevent relapses and hospitalization, and less than 10% of families receive education and support. Moreover, U.S. psychiatric facilities aren't designed to reduce social isolation or facilitate reintegration into the outside world, says William Carpenter, director of the Maryland Psychiatric Research Center in Baltimore. "If you go into a hospital, you get pretty much cut off from other things."

Ironically, part of the reason may lie in the importance attached to patients' rights in Western countries, Carpenter and others say. Under the U.S. Health Insurance Portability and Accountability Act, privacy restrictions limit communication between clinicians and patients' families, says Fenton. "If you have an 18-year-old child that's hospitalized for psychiatric reasons, the hospital can send you a bill, but they can't tell you if the child has been admitted to the hospital, unless the patient gives permission," Fenton says. "If patients are suspicious or hostile, the hospitals are constrained in getting a family's help."

Work programs such as those at SCARF are rare in the United States, in part because of lingering memories of peonage at mental institutes. In the 1930s, long-stay mental hospitals were often little more than sweatshops in which patients toiled without pay, says Carpenter. Work programs at long-term care facilities began dying out around midcentury as word of abuses leaked out and advocates insisted that patients receive minimum wage for their work, making many programs unaffordable, Carpenter says.

Another big impediment to weaving social interventions into care is unbridled enthusiasm for drugs. Although Western psychiatrists agree that drugs are essential for stabilizing severely ill patients to give other therapies a chance to work, many clinicians support a bullet. "The trend is to give a medication for each symptom," says Fink. "You can find patients with six or seven psychiatric pills, and it doesn't make sense, it's terrible." The U.S. system is biased toward short appointments and profuse prescriptions, some psychiatrists say. Insurance companies are happy to reimburse for psychiatric drugs, Carpenter adds, but getting them to pony up for social interventions can be difficult.

Paradigm shift?

Even in India, institutions such as SCARF and CMC are far from the norm. Severely ill patients who don't live at home often end up in giant state-run mental hospitals. "All that is done in a typical state hospital is to ask, 'How are you doing? Are you still hearing voices?' and give them medicine," Thara says. She would like to see hundreds of organizations such as SCARF spread across the country.

System under stress. Crowded government hospitals deter many Indian patients and their families from seeking care.

CREDITS: TAUSEEF MUSTAFA/GETTY IMAGES

It's an idea worth considering, says the World Bank's Benjamin Loevinsohn. He coauthored a review published in *The Lancet* last August that concluded that NGOs often provide higher quality service at lower cost than governments do, and he thinks this would apply to mental health NGOs, too.

On an annual budget of about $70,000, SCARF provides low-cost care for 140 inpatients and up to 100 outpatients a day. Most of the 25 permanent staff are psychiatric social workers. "SCARF has a truly innovative way of doing social interventions without highly trained people" such as psychiatrists, who are in short supply in India, says Vikram Patel, a psychiatrist at the London School of Hygiene and Tropical Medicine. It's a lesson worth noting for rich and poor countries alike.

–GREG MILLER

EDITED BY YUDHIJIT BHATTACHARJEE

Misconduct

GROUNDED AND CANCELED. With the unraveling of the Korean cloning scandal, stem cell researcher Woo Suk Hwang has lost his title as the country's "top scientist," $3 million in government funding, and police protection. Now the Seoul National University professor is losing another privilege earned through his fraudulent research claims: free travel on the nation's flagship airline, Korean Air.

Last June, after Hwang published his now-discredited paper in *Science* claiming that he'd cloned patient-specific embryonic stem cells, the company said he and his wife could fly first class, for free, for 10 years to promote his research (*Science*, 1 July 2005, p. 49). Although the offer hasn't been officially withdrawn, Korean Air spokesperson Seo Dong-il told *The Korea Times* last week that Hwang had effectively been grounded. "Because his stem cell research was found to be fabricated and there are no cloned stem cells at all, he will not be able to meet the preset conditions of research-purpose trips," the newspaper quoted Dong-il as saying. Hwang isn't likely to need an overseas ticket anytime soon: Korean prosecutors have forbidden him from leaving the country.

To add to his ignominy, Korea's postal service has decided to end sales of stamps issued last year in honor of Hwang's achievements. The stamp shows a man springing out of his wheelchair, presumably after receiving cloned stem cells to treat his spinal cord injury.

AWARDS

JAPAN PRIZES. Weather and cholesterol were on the minds of the Japan Prize judges this year.

John Houghton, an atmospheric physicist at the Hadley Centre for Climate Prediction and Research in Exeter, U.K., was honored in the "Global Change" category for developing satellite-based remote-sensing techniques for mapping atmospheric temperatures in three dimensions and tracking the distribution and circulation of ozone, methane, and water vapor.

For his role in discovering and developing statins, a key component of cholesterol-lowering drugs, Akira Endo of Biopharm Research Laboratories in Tokyo won for "Development of Novel Therapeutic Concepts and Technologies." The judges said Endo's work has helped those with atherosclerotic vascular diseases, a leading cause of death in developed countries. Each winner receives $450,000.

EUROPEAN HONOR. A Finnish cancer biologist and a French geneticist have been named winners of the 2006 medicine prize awarded by the Louis-Jeantet Foundation in Geneva, Switzerland. Kari Alitalo, a professor at the Finnish Academy of Sciences in Helsinki, receives the prize for his discovery of a growth factor involved in the formation of lymphatic vessels, and Christine Petit, a professor at the Pasteur Institute in Paris, wins the award for identifying the genes responsible for hereditary deafness. The two will share a research award of $1 million and take home an individual prize of $90,000 each.

PUBLIC SERVICE. Norman Augustine, former CEO of Lockheed Martin Corp., has been awarded the Public Welfare Medal by the National Academy of Sciences. The 70-year-old aeronautical engineer receives the honor for helping the U.S. government and industry understand the role of fundamental research in the country's "long-term security and economic prosperity."

Nonprofit World >>

WELL-TROD PATH. John Boslego next week becomes the third senior vaccine developer at Merck & Co. to pack his bags and join a nonprofit. Boslego, who heads the company's clinical research on vaccines and other biologics, is going to direct vaccine development at PATH, a Seattle, Washington–based organization with close ties to the Bill and Melinda Gates Foundation. "It's an opportunity to do something broader in the vaccine arena," says Boslego, 57.

Boslego hopes to contract with biotech and pharmaceutical companies to develop a much-needed vaccine for poor countries that protects against pneumococcus, a bacteria that causes severe pneumonia in children and kills as many as 1 million each year. Although a pneumococcal vaccine already exists for children, it's expensive, difficult to produce, and has limited effectiveness against bacterial strains in many poor countries.

Boslego follows Emilio Emini, who stepped down as director of Merck's HIV vaccine effort in 2004 to work at the International AIDS Vaccine Initiative (which he subsequently left for Wyeth), and Jerald Sadoff, who gave up another top vaccine job at Merck in 2003 to head the Aeras Global TB Vaccine Foundation.

YYePG Proudly Presents, Thx for Support

Got a tip for this page? E-mail people@aaas.org

CREDITS (CLOCKWISE FROM TOP LEFT): LEE JAE-WON/REUTERS; REUTERS; GRACE GREGORIO; JSTF

The power of belief 471

Benefits of mentoring 473

LETTERS

edited by Etta Kavanagh

Where Next for Genome Sequencing?

THE SUCCESSFUL SEQUENCING OF THE HUMAN GENOME, ALONG WITH those of *Arabidopsis thaliana* and rice, raises the question of what we should do next with the significant sequencing infrastructure and technical capacity that has been developed. Although the costs of sequencing are falling, sequencing eukaryotic genomes still requires a minimum commitment of U.S. $5 million to $10 million. For those who can raise such funds, the resulting information will provide an invaluable resource, underpinning research and technology development in their chosen organism and related species for decades to come.

It is easy to justify the scientific value of large-scale, publicly available sequencing projects. Our concern is to ensure that this powerful capacity directly addresses the needs of the majority of the world's people. By the year 2050, 90% of humankind will live in developing countries, where agriculture remains the most important economic activity. Crops grown by small farmers are central to food security, health, economic growth, poverty reduction, and social stability in these regions. In determining how best to exploit the existing capacity for genome sequencing, therefore, we believe that crops essential to resource-poor farmers in developing countries should be given highest priority.

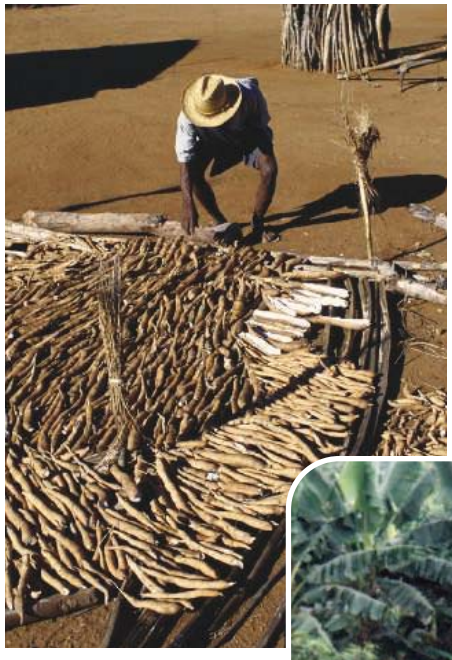

Man drying cassava in a desert village in Madagascar (above), and peeling of cassava in Ivory Coast, West Africa (inset).

Cassava (*Manhiot esculenta* Crantz) offers one such important opportunity. Grown throughout tropical Africa, Asia, and the Americas for its starchy storage roots, cassava feeds an estimated 600 million people each day. Farmers choose it for its high productivity and its ability to withstand conditions in which other crops fail. Cassava is now the most important source of dietary calories in the tropics after rice and maize.

Cassava retains a largely untapped potential for genetic improvement. Worldwide, average yields barely attain 1/10 of the demonstrated potential. The Global Cassava Partnership (GCP-21), an alliance of the world's leading cassava researchers and developers operating under the auspices of the Food and Agriculture Organization, has proposed that sequencing *M. esculenta* should be a priority. We agree. Realizing the full genetic potential of cassava to meet the needs of developing countries will require both conventional breeding methods and modern molecular technologies. Sequencing its 770-Mb genome would boost both approaches.

Sequencing the cassava genome would also bring it into the mainstream of plant science research. The community resources required to fully benefit from sequence analysis of the cassava genome are already being established by a small but dedicated group of scientists under the aegis of GCP-21. Large collections of publicly available germ plasm, including wild related species, are available, as are modest but significant EST collections, BAC libraries, and molecular genetic maps. In addition to enhancing the value of these resources, sequencing data will make it possible to interface with existing plant genome databases, and to exploit the biodiversity within cultivated and wild *Manihot* species more effectively. In this way, genes that impart important agronomic qualities will become increasingly accessible for transfer into elite breeding lines and varieties preferred by farmers.

For a fraction of the cost of other, much larger genomic and postgenomic projects, sequencing cassava could bring this important crop to the forefront of modern science, generating new possibilities for its agronomic improvement. So where next with genome sequencing? It's time to harness part of our technical capacity to advance crops like cassava that are central to the livelihoods and health of half a billion people.

PETER RAVEN,[1] CLAUDE FAUQUET,[2] M. S. SWAMINATHAN,[3] NORMAN BORLAUG,[4] CRISTIÁN SAMPER[5]

[1]Missouri Botanical Gardens, 2345 Tower Grove Avenue, Post Office Box 299, St. Louis, MO 63110, USA. [2]Danforth Plant Science Center, 975 North Warson Road, St. Louis, MO 63132, USA. [3]M. S. Swaminathan Research Foundation, 3rd Cross Street, Chennai, Madras, India. [4]Texas A&M University, College Station, TX 77843, USA. [5]National Museum of Natural History, Smithsonian Institution, 10th and Constitution Avenue, NW, Washington, DC 20560, USA.

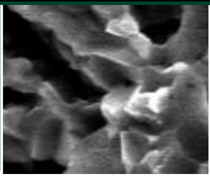

Ice makes better composite materials

479

Thinking About NASA's Future

AS A SPACE MEDICINE SPECIALIST NOW TRAINING for long-duration spaceflight, I read with consternation the Editorial by Donald Kennedy "NASA: Back to eating seed corn" (Editorial, 25 Nov. 2005, p. 1245), which contained this remarkable statement: "But will the basic and applied science be done beforehand that is necessary to keep the explorers safe and healthy, or will these professionals seem more like participants in another extreme sport?" This underscores a long-standing disconnect between much of the life sciences community and the actual world of spaceflight. A cursory look at history shows that it is not the issues addressed by the life sciences community that make spaceflight an "extreme sport," it is the physical barriers that must be overcome to leave and return to the planet and the machines we build to overcome them, which function necessarily near the limits of their performance capabilities.

The legitimacy of basic life sciences research should stand alone. Observations made in spaceflight have challenged our basic understanding of human physiology, such as persistent inhomogeneity in pulmonary ventilation and perfusion (*1*) and the counterintuitive decrease in central venous pressure upon arrival into weightlessness (*2*). Understanding the fundamental physiology of weightlessness will form a basis upon which to practice clinical space medicine and develop better countermeasures against adverse effects of weightlessness on bone, muscle, and other systems, and will diminish the risk of space travel in the long run. It is doubtful there will be a similar laboratory of such size and capability as the International Space Station in Earth orbit for some time, and it is a sincere hope that such research will be conducted there. However, to suggest at this point that basic and applied life science research will take us out of the extreme sport category or is necessary for the safe conduct of spaceflight inaccurately portrays spaceflight and adds undue hyperbole to an inherently meritorious research agenda.

MICHAEL BARRATT

NASA Johnson Space Center, 2101 NASA Parkway, Houston, TX 77058, USA.

References

1. G. K. Prisk, *J. Appl. Physiol.* **89**, 385 (2000).
2. J. C. Buckey *et al.*, *J. Appl. Physiol.* **81**, 19 (1996).

IN RESPONSE TO DONALD KENNEDY'S EDITORIAL "NASA: Back to eating seed corn" (25 Nov. 2005, p. 1245), I'd like to offer a student perspective. As president of the American Society for Gravitational and Space Biology (ASGSB) Student Association, I represent the current inspired generation of young scientists, who would not be here but for the thrill of space exploration and expertise of veteran researchers.

Well over 10,000 students have toiled diligently in NASA's quest to develop life support systems, understand spaceflight bone and muscle loss, define mechanisms of plant growth in microgravity, and understand basic gravity-dependent processes. Until recently, space life science has been listed as a top priority to enable further space exploration. But now NASA is dismantling this research and training infrastructure, or as Kennedy puts it, "eating seed corn." With these losses and an aging workforce approaching retirement, we are stifling our technical competency and relinquishing key institutional memory.

"[W]e cannot send humans to the Moon and Mars without a robust research program to address safety, adaptation, and long-term habitation."

—Andrea Hanson

Without forging ahead in research supporting healthy space travel now, all the efforts to bring people to the Moon and Mars will have been in vain. We will lose valuable time, people, and resources that must be reinvented later at a much higher cost. Our small space life science community has been criticized for not speaking up in our own defense. If we are not being heard, it's because NASA is not listening. Hear this—we cannot send humans to the Moon and Mars without a robust research program to address safety, adaptation, and long-term habitation. I believe space life science programs are the key to survival of those in space now, future space travelers, and the space program as a whole.

ANDREA HANSON

President, ASGSB-SA, University of Colorado, Boulder, CO 80309, USA. E-mail: andrea.hanson@colorado.edu

DONALD KENNEDY'S EDITORIAL "NASA: BACK to eating seed corn" (25 Nov. 2005, p. 1245) states that the cost of shuttle flights through 2010 was underestimated by NASA and implies that this would cripple basic science and force cancellation of robotic missions. In fact, the difference between the required funds and those being suggested by the Administration is the result of the Office of Management and Budget reducing the budget because they do not understand the cost aspects of the Shuttle program (it takes almost as much money to launch one as it does 10 shuttles: the hardware costs are minimal and the primary costs are people).

NASA Administrator Michael Griffin stated last week at the American Geophysical Union (AGU) Meeting in San Francisco that Earth and space sciences are important and will continue and that the exploration initiative will not consume the Science Mission Directorate resources. Science will, however, have to deal with its problems within its budgetary guidelines as will exploration. NASA has often committed itself to robotic missions that were significantly undercosted with the resulting pressure on other programs. Mary Cleave, Science Mission Directorate Associate Administrator, indicated last week at the AGU Meeting that NASA will no longer allow such decisions to be made.

In a perfect world, NASA would focus not only on its near-term goal of the Moon but also on long-term goals such as Mars, and would fund a variety of activities aimed at, among other things, understanding human aspects of space flight and development of technologies. Given the limited budget available, priorities must be established and near-term objectives must be satisfied.

The primary programmatic objective of Griffin is to set the agency on a course with the long-term goal of the Vision for Space Exploration (VSE). Without such a long-term goal, NASA is likely to simply disappear. The costs and risks of sending humans to the International Space Station on the Shuttle simply to spend time there cannot be sustained, nor should they.

NASA cannot do everything it wants nor all of what the scientific community wants within a fixed budget; priorities must be established. Without a long-term human spaceflight theme, NASA will not continue. To assume that if the exploration initiative and human spaceflight went away, that space science would receive a fiscal windfall is sophomoric.

JEFFREY PLESCIA

Applied Physics Laboratory, Johns Hopkins University, 11100 Johns Hopkins Road, MS MP3-E163, Laurel, MD 20723, USA.

Avoiding Climate Change

THE QUOTE CREDITED TO ME IN THE RANDOM Samples item "Ice ages as history" (23 Dec. 2005, p. 1900) ("Anthropogenic climate change will basically produce another planet…. Earth won't have another ice age until humans go extinct.") was constructed from two statements that I made at the 6 December 2005 meeting of the American Geophysical Union: "business-as-usual scenarios will produce basically another planet" and "another ice age cannot occur unless humans become extinct."

The printed construction provides no hint of my conclusion that large climate change can be avoided via a scenario that includes actions to improve energy efficiency and reduce non-CO_2 climate forcings. These actions require

strong policy leadership and international cooperation, but they have multiple practical benefits for the environment, human health, and economic development.

I suggest (my talk is available at www.columbia.edu/~jeh1) that special interests have been a roadblock to this end, wielding undue influence over policy-makers. The public has the power to override special interests, but scientists need to communicate the full climate story to the public in a credible, understandable fashion.

JAMES E. HANSEN

Columbia University Earth Institute, New York, NY 10025, USA.

TECHNICAL COMMENT ABSTRACTS

Comment on "Reconstructing the Origin of Andaman Islanders"

Malliya gounder Palanichamy, Suraksha Agrawal, Yong-Gang Yao, Qing-Peng Kong, Chang Sun, Faisal Khan, Tapas Kumar Chaudhuri, Ya-Ping Zhang

On the basis of mitochondrial DNA sequence analyses, Thangaraj *et al*. (Brevia, 13 May 2005, p. 996) proposed that Andaman islanders descended from the first humans to migrate out of Africa. We identified mitochondrial DNA from two northeast Indian Rajbanshi individuals that shares three specific mutations with the M31a lineage observed in the Great Andamanese, which suggests that the predecessor of haplogroup M31 originated on the Indian subcontinent.

Full text at www.sciencemag.org/cgi/content/full/311/5760/470a

Response to Comment on "Reconstructing the Origin of Andaman Islanders"

Kumarasamy Thangaraj, Gyaneshwer Chaubey, Toomas Kivisild, Alla G. Reddy, Vijay Kumar Singh, Avinash A. Rasalkar, Lalji Singh

The mitochondrial DNA coding region substitutions shared by the Andamanese and two Rajbanshi individuals suggests the early split of M31 from some continental Indian mitochondrial DNA lineages at the time depth 11/14 of the age of haplogroup M. This is still consistent with the ancient isolation of these gene pools, albeit not as early as the initial phase of human migration out of Africa.

Full text at www.sciencemag.org/cgi/content/full/311/5760/470b

CORRECTIONS AND CLARIFICATIONS

News of the Week: "Plants may be hidden methane source" by E. Stokstad (13 Jan., p. 159). Michael Keller is based at the University of New Hampshire, but he works for the U.S. Forest Service.

News Focus: "A dead spot for the tsunami network?" by P. Bagla (9 Dec. 2005, p. 1604). Contrary to what was reported, the Indian government's Integrated Coastal and Marine Area Management (ICMAM) project directorate in Chennai is leading the Indian government's effort to develop tsunami inundation maps, not the National Institute of Oceanography, Goa.

Letters: "Attribution of disaster losses" by R. A. Pielke Jr. (9 Dec. 2005, p. 1615). There should have been an additional sentence at the end of the second paragraph reading "In 2005 several studies reported an increase in the intensity of tropical cyclones (*8, 9*); however, long-term records of economic damages show no upward trend, once the data are normalized to remove the effects of societal changes (*10, 11*)." The references cited here are:
8. K. Emanuel, *Nature* **436**, 686 (2005).
9. P. Webster *et al*., *Science* **309**, 1844 (2005).
10. S. Raghavan, S. Rajesh, *Bull. Am. Meteorol. Soc.* **84**, 635 (2003).
11. R. Pielke Jr., *Nature*, in press.
The reference cited in the last paragraph should be:
12. R. Pielke Jr. *et al.*, *Bull. Am. Meteorol. Soc.* **86**, 1481 (2005).

Letters to the Editor

Letters (~300 words) discuss material published in *Science* in the previous 6 months or issues of general interest. They can be submitted through the Web (www.submit2science.org) or by regular mail (1200 New York Ave., NW, Washington, DC 20005, USA). Letters are not acknowledged upon receipt, nor are authors generally consulted before publication. Whether published in full or in part, letters are subject to editing for clarity and space.

SCIENCE AND RELIGION

Believing in Belief

Michael Shermer

In a 1997 episode of the animated television series *The Simpsons*, Lisa Simpson discovers a fossil angel. Suspecting a hoax, she takes a piece of the fossil to the natural history museum, where Harvard paleontologist Stephen Jay Gould (playing himself) analyzes it. The age-old conflict between science and religion then plays out in this ne plus ultra of pop culture. When Gould announces that the test results are "inconclusive," Reverend Lovejoy boasts: "Well, it appears science has failed again, in front of overwhelming religious evidence." Marge counsels Lisa's skepticism with motherly wisdom: "There has to be more to life than just what we see, Lisa. Everyone needs something to believe in." Lisa's rejoinder is classic skepticism: "It's not that I don't have a spiritual side. I just find it hard to believe there's a dead angel hanging in our garage." The Scopes-like trial that ensues ends when the judge issues a restraining order: "Religion must stay 500 yards from science at all times."

Breaking the Spell
Religion as a Natural Phenomenon

by Daniel C. Dennett

Viking, New York, 2006. 464 pp. $25.95, C$36. ISBN 0-670-03472-X.

This is, in fact, Gould's conciliatory solution (*1*), which he called non-overlapping magisteria, and it is the primary target of Tufts University philosopher Daniel C. Dennett in *Breaking the Spell*. All restraining orders are off, as Dennett calls for "a forthright, scientific, no-holds-barred investigation of religion as one natural phenomenon among many." The spell to be broken is the taboo that science will render incapable "the life-enriching enchantment of religion itself."

So sensitive is Dennett to the potential reaction on the part of his audience (which he maintains is the general public, over 90 percent of whom believe in God) that the book's first 55 pages are devoted to an apologia for scientific research on religion. My concern is that religious adherents will take offense at Dennett's rationale before they get to the heart of the book, where the author really shines. In one passage, for example, he tells believers that their repugnance to science is misdirected but admits that his attempt to convince them otherwise "is a daunting task, like trying to persuade your friend with the cancer symptoms that she really ought to see a doctor *now*, since her anxiety may be misplaced and the sooner she learns that the sooner she can get on with her life, and if she does have cancer, timely intervention may make all the difference." The deeply devout will not take kindly to their beliefs (about either science or religion) being equated with cancer.

Breaking the Spell is really written for scientists and scholars who have thought little on the subject of religion as a natural phenomenon. Dennett's starting point is the "rational choice" theory of religion, proffered by sociologist Rodney Stark and his colleagues, which holds that the beliefs, rituals, customs, commitments, and sacrifices associated with religion are best understood as a form of exchange between believers and gods or God. Where resources and rewards are scarce (e.g., rain for crops) or nonexistent (e.g., immortality) through secular sources, then religion steps in to act as the exchange intermediary (*2*–*4*). To an evolutionist like Dennett, such exchanges demand that we look for a deeper causal vector: "Any such regular expenditure of time and energy has to be balanced by something of 'value' obtained, and the ultimate measure of evolutionary 'value' is *fitness*: the capacity to replicate more successfully than the competition does."

What is the value of religion to evolutionary fitness? In two books (*5*, *6*), I have outlined at least four such values: (i) mythmaking to explain apparently inexplicable phenomena in the world, (ii) redemption (forgiveness in this life) and resurrection (immortality in the next life), (iii) morality (reinforcement of prosocial behavior and punishment of anti-social behavior), and (iv) sociality (encouragement of within-group amity and between-group enmity). Do such values explain religion? We don't know yet, Dennett admits, but the rest of his book presents a plausible explanation that I summarize as follows.

Humans have brains that are big enough to be both self-aware and aware that others are self-aware. This "theory of mind" leads to a "hyperactive agent detection device" (HADD) that not only alerts us to real dangers, such as poisonous snakes, but also generates false positives, such as believing that rocks and trees are imbued with intentional minds or spirits. "The memorable nymphs and fairies and goblins and demons that crowd the mythologies of every people are the imaginative offspring of a hyperactive habit of finding agency wherever anything puzzles or frightens us." This is animism that, in the well-known historical sequence, leads to polytheism and, eventually, monotheism. In other words, God is a false positive generated by our HADD.

Around these animistic entities our ancestors created folk religions, which, between the Neolithic revolution and the rise of cities, evolved into the organized religions we recognize today. During this transition there was competition among the countless god memes (each of whom were believed to control some tiny part of the world), out of which emerged the winner: a single God meme believed to control everything. Concomitant with God's triumph was a corresponding belief in belief—not just belief in God, but belief in belief in God. This, says Dennett, was the coup de grace: religion no longer had to depend on uniformity of belief, only uniformity of professing belief.

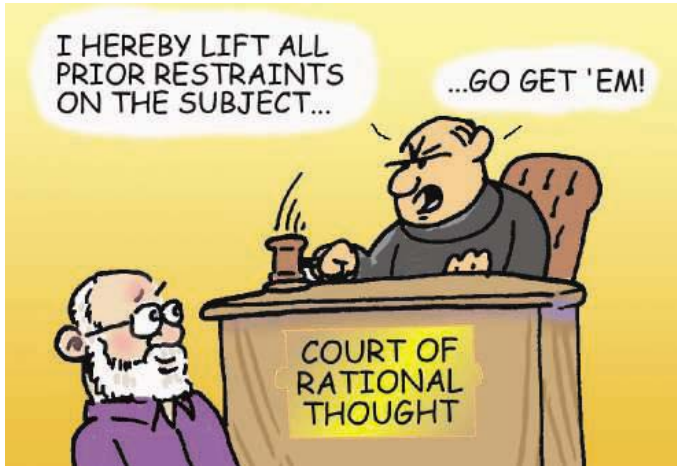

CREDIT: JOE SUTLIFF

Dennett's dangerous idea is his concept of belief in belief, but it is a two-edged sword. On the one side, it not only grants believers some elbow room for doubt (as long as you still believe in belief in God), it allows atheists like myself (and Dennett) to profess that I believe in God—that is, I believe in the God that exists in the minds of people who themselves believe in the existence of an omniscient and omnipotent deity. That God is so powerful that He can get believers to bomb abortion clinics and fly planes into buildings.

On the flip side, perspicacious believers may perceive that an ontological trap is being

The reviewer is at *Skeptic* magazine, 2761 North Marengo Avenue, Altadena, CA 91001, USA. E-mail: skepticmag@aol.com

set: belief in belief implies that the God in your head doesn't actually exist. I predict that in the competitive memescape that is the human mind, the belief in God meme will beat out the belief in belief meme, as much as I would like to believe otherwise.

References

1. S. J. Gould, *Rocks of Ages: Science and Religion in the Fullness of Life* (Ballantine, New York, 1999).
2. R. Stark, W. S. Bainbridge, *A Theory of Religion* (Rutgers Univ. Press, New Brunswick, NJ, 1987).
3. R. Stark, *Religion, Deviance, and Social Control* (Routledge, New York, 1997).
4. R. Stark, R. Finke, *Acts of Faith: Explaining the Human Side of Religion* (Univ. California Press, Berkeley, CA, 2000).
5. M. Shermer, *How We Believe: Science, Skepticism, and the Search for God* (Henry Holt, New York, 2000).
6. M. Shermer, *The Science of Good and Evil* (Henry Holt, New York, 2004).

10.1126/science.1123433

CLIMATE

Early and Profound Human Impact?

James White

One evening in the midst of reading William Ruddiman's *Plows, Plagues and Petroleum: How Humans Took Control of Climate*, I took a break to watch a PBS program on climate change with my 10-year-old daughter, Molly. About halfway through the program, in which the pop musician Alanis Morissette tells us that human-caused climate change is measurably upon us and not at all a good thing, Molly asked to switch to another station. When I asked her why—this is a kid who has sat with me through many hours of educational TV without complaint—she said the program scared her. Scared her.

Well, if Alanis scared her with tales of modern human intervention in the climate system, I wonder what Molly would think of Ruddiman's hypothesis, which he lays out in the book, that humans caused climate change thousands of years in the past by inadvertent interference with greenhouse gases and that these actions thwarted an approaching ice age and led to the unusually long interglacial period we currently enjoy. Would it comfort her to know that human actions can cause both beneficial (to humans, at least) changes such as a delayed ice age as well as negative impacts such as sea level rise or abrupt climate changes? Or is human intervention with climate inherently a bad thing?

If you're not familiar with Ruddiman's hypothesis, you should be. He argues that as far back as 6000 to 8000 years ago, humans began adding carbon dioxide and methane to the atmosphere through such practices as clearing forests, farming rice, and raising domesticated animals. That in itself is not controversial, but his interpretation gets really interesting in the claim that human actions thwarted a cyclical drop in these gases, a conclusion that is tied to greatly increased estimates of the human-caused fluxes. He then goes on to postulate that our added greenhouse gases stopped an ice age that, he insists, should have been upon us several thousand years ago. Is this Gaia with human daisies or pure dumb luck? Or is Ruddiman wrong? Whatever the answer, he offers wonderful food for thought.

Ruddiman's ideas have not been greeted with open arms by the scientific community. All scientific hypotheses should be poked and prodded, tested and retested, and made to stand up to the available observations. Ruddiman embraces this process cheerfully. Given the highly politicized nature of the debate about modern climate, I found his approach refreshing. At a time when some scientists seem to fear that open criticism will give the public the impression that we disagree about the facts on climate change—that it is real, caused in part by humans, and increasingly unavoidable—it is good to read of Ruddiman's faith in the scientific method and his willingness to let the process unfold as it should, even if that means he takes a few lumps along the way.

Plows, Plagues, and Petroleum is excellent reading for scientist and nonscientist alike. Whether or not one agrees with Ruddiman's most recent hypothesis, he has much to say and his ideas provoke thought. Readers may be tempted to skip to where Ruddiman lays out his hypothesis, but that would be a mistake. The first third of the book offers a valuable, entertaining, and highly informative account of the author's view of the history of climate science, including his own, important part in that history. The study of Earth's climate is a fairly young field, and in the heads of the pioneers—people like Wally Broecker, John Imbrie, Nick Shackleton, and, yes, Ruddiman—lie great stories that should be told. Do not skip this part.

In the last third of the book, the author gets personal, writing about his encounters with climate change naysayers and what he thinks are the key issues for future climate change. I liked his reference to "Glacierless National Park," but we should have a national contest to rename the park—maybe Yosemite would bring more people the reality of climate change.

So would Ruddiman's ideas make Molly feel better? I doubt it. I think that her fear has to do with control, a central issue in Ruddiman's book, and one of the few places I disagree with him. Ruddiman uses "control" frequently (including in the subtitle) but I believe incorrectly. My 10-year-old is tall enough to reach the pedals and smart enough to mimic the actions of driving our car. As Ruddiman uses the word, she could control the vehicle. But when she presses down on the accelerator and the car speeds off, control, as I define it, would be lost. Molly, who can't see over the steering wheel, has the intelligence to take charge of the vehicle but not the skills to control it. Humans and climate are in much the same position. We have the ability to take charge of climate but not the skill (yet) to control it. The distinction is important. In Ruddiman's world, humans stopped an ice age. But our ancestors did not know what they were doing. Today we haven't progressed far. We're like a 10-year-old speeding down the road in that car, unable to see where we're going, increasingly aware that maybe we should back off the accelerator and that maybe even if we did it might be too late, but too full of ourselves and proud of our ability to drive to change course. So we continue to accelerate.

Maybe we will be fortunate and not wreck. After all, if Ruddiman's right, we have a history of good luck.

10.1126/science.1121900

Plows, Plagues, and Petroleum
How Humans Took Control of Climate
by William F. Ruddiman
Princeton University Press, Princeton, NJ, 2005. 216 pp. $24.95, £15.95. ISBN 0-691-12164-8.

A source of warmth. Cultivated fields, Guizhou Province, China.

CREDIT: GEORG GERSTER/PHOTO RESEARCHERS

The reviewer is at the Environmental Studies Program, University of Colorado, 1560 30th Street, Boulder, CO 80309, USA. E-mail: james.white@colorado.edu

PROFESSIONAL SKILLS

The Merits of Training Mentors

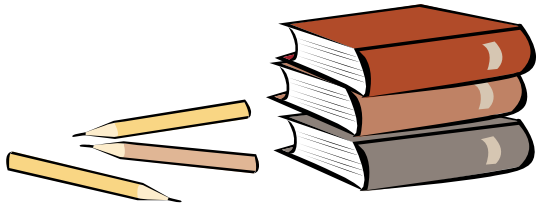

Christine Pfund,[1,2] Christine Maidl Pribbenow,[3] Janet Branchaw,[4] Sarah Miller Lauffer,[1] Jo Handelsman[1,3]*

Good mentoring can be learned.

In research universities and colleges, mentoring is one of the most important skills for faculty because it affects both research productivity and the quality of training for undergraduate students, graduate students, and postdoctoral researchers. Moreover, the diversity of science is dependent on the quality of mentored research, because this experience is a key to attracting underrepresented groups to science (*1*–*5*). In the past, many faculty learned skills such as mentoring on the job. In recent years, various organizations have developed training programs to help prospective and new faculty learn skills such as grant writing, laboratory management, and classroom teaching, but mentoring has been largely absent. In response to this need, we developed and evaluated a mentor-training seminar. The seminar is intended to improve mentors' skills and to enhance the research experiences of undergraduate students.

Enhanced online at www.sciencemag.org/cgi/content/full/311/5760/473

In research universities, graduate students and postdoctoral researchers often serve as the primary mentors for undergraduate researchers (see photograph, this page). This arrangement provides undergraduates with guidance from a person who is accessible and whose primary focus is laboratory work. It also provides graduate students and postdoctoral researchers with experience as mentors. Therefore, our seminar focused on training graduate students and postdoctoral researchers as mentors, but it is also suitable for developing mentoring skills of faculty.

The Wisconsin Mentoring Seminar

The Wisconsin Mentoring Seminar was developed using an iterative approach of design, testing, evaluation, and revision. The seminar (table S1) reflects participation of eight cohorts of mentors led by four facilitators at the University of Wisconsin–Madison (*6*). This version of the seminar has since been implemented and evaluated at 11 research universities including UW-Madison. The objectives of the Wisconsin Mentoring Seminar are to train mentors to communicate effectively, to consider issues of human diversity, to discuss mentoring approaches, and to apply a "scientific teaching" approach to mentoring (*7*). The seminar consists of eight sessions of discussion facilitated by faculty or staff using a collaborative, problem-solving format. The participants read articles and case studies, write biographies of their undergraduate students, compare their goals with those of their undergraduate researchers, explore time-management strategies, and write mentoring philosophies.

Communication skills are addressed with the use of exercises that include interviews with their undergraduate researchers. The aim is to help the mentors to recognize and reconcile differing expectations about time commitment, independence, and skill proficiency. Mentors learn the value of discussing mentoring issues with peers and faculty through discussion in the seminar itself and discussions they are required to initiate with their research advisers.

The mentors discuss the value of and accommodations for diversity in the laboratory. Consideration of how their own work habits, cognitive styles, attitudes, gender, ethnicity, physical ability, educational background, and nationality differ from that of their mentees complements readings of research on stereotypes and unconscious prejudices. The group brainstorms about approaches to overcoming cultural biases.

The mentors are encouraged to approach teaching with the same rigor and spirit of experimentation that they bring to research (*7*). They develop their own systematic approaches by identifying objectives and approaches to overcome associated impediments. They evaluate their approaches through feedback from their undergraduate researchers, peers in the laboratory, and research advisers.

Mentors design strategies to help undergraduates develop understanding, support, and confidence, creativity, and independence. In addition to discussing their own scientific and ethical standards and effective ways to transmit those standards to their students, the mentors grapple with the challenge of reconciling high standards with flexibility and personal style.

Mentoring in microbiology. Graduate student Courtney Robinson (left) participated in the Wisconsin Mentoring Seminar while she mentored undergraduate researcher Yolied Ramos at the University of Wisconsin–Madison.

Implementation and Evaluation

Over the past 2½ years, the mentoring seminar has been run 22 times at 11 institutions. To evaluate the impact of the seminar, we gathered data about mentors who either did or did not participate in the seminar and the undergraduate researchers under their supervision at UW-Madison. Although we were unable to conduct a randomized experiment, we reduced the impact of self-selection by using as the untrained comparison group entire cohorts of mentors who were not offered the opportunity to participate in the mentoring seminar and compared them with cohorts in which all members were required to participate. Five of the seminars were conducted concurrently with summer undergraduate research programs. Three of the mentoring seminars at UW-Madison were offered in conjunction with a semester-long program in which research laboratory experience partially replaced an introductory biology laboratory course requirement. From these cohorts, we surveyed 85 mentors and 84 undergraduate researchers. In addition, we interviewed 10 undergraduate researchers and 11 graduate students and postdoctoral mentors about their experiences. We have since surveyed trained mentors and the facilitators of the mentoring seminar from 11 institutions. The surveys used in this study are available (*6*).

Graduate students, postdoctoral researchers, and research scientists served as the primary mentors, and each seminar was facilitated by a faculty or staff member. The facilitator was provided with a manual, "*Entering Mentoring*,"

[1]Wisconsin Program for Scientific Teaching, Department of Plant Pathology, [2]Center for the Integration of Research, Teaching, and Learning, [3]Women in Science and Engineering Leadership Institute, [4]Center for Biology Education, University of Wisconsin, Madison, WI 53706, USA.

*To whom correspondence should be addressed. E-mail: joh@plantpath.wisc.edu

that contains reading material and detailed instructions for facilitating the seminar (*6*). All of the respondent facilitators found "*Entering Mentoring*" useful and interesting (table S2).

Surveys of 12 facilitators of the mentoring seminar from nine institutions indicated that all considered facilitating the seminar to be a positive experience that they would recommend to a colleague (table S3). Most (64%) indicated that their own philosophy of mentoring changed as a result of facilitating the seminar. Several facilitators said they were more aware of their students' needs and had more ideas about how to address these needs. One professor commented, "The mentors empowered me to be more bold in my own mentoring."

Our results indicate that the mentoring seminar was successful in achieving the set objectives: Mentors who participated in the seminar ("trained mentors") were significantly more likely to discuss expectations with their undergraduate researchers, to consider issues of diversity, and to discuss mentoring with peers and faculty than were those who did not participate in the seminar ("untrained mentors") (see graph, this page). The mentors trained at UW-Madison and eight other research universities self-reported gains in a number of areas (table S4, A and B), and 87% said they would recommend the seminar to their peers. Mentors reported satisfaction with each of the discussion topics in the mentoring seminar, as shown in table S5. In addition, when mentors reflected on their mentoring after the training, they noted their intentions to work harder in future mentoring in many of the areas covered in the training, including setting clear expectations, regularly assessing their student's understanding, fostering independence, and asking colleagues for advice when confronted with a challenge in mentoring. Such insights about their mentoring were also reflected in their mentoring philosophies (table S6).

The mentoring seminar favorably influenced the undergraduate research experience. Students who had been previously mentored were asked to compare their experiences, and they consistently reported that mentors who participated in the seminar were more available to them, were more interested in them as individuals, and gave them more independence.

In the quantitative analysis, we found no significant difference between responses from undergraduates whose mentors did or did not participate in the mentoring seminar, in part because the undergraduate researchers had positive experiences regardless of the status of their mentor. Our results confirm published studies to this effect (*1*, *2*), showing self-reported gains in 19 categories, with the greatest gains in "developing a research project" and "working independently on research" (table S7A).

Comparison of how undergraduates themselves and their trained or untrained mentors assessed the progress of the undergraduates (table S7, A and B) shows that trained mentors' assessments more closely matched the undergraduates' self-assessments (table S7C). Undergraduates working with trained mentors were more likely to agree with the statement that their mentor "regularly assessed the skills and knowledge that they had gained in the lab" ($P < 0.05$). We conclude that the seminar enhanced the ability of the mentors to assess the skills of their students and likely enhanced the accuracy of the undergraduate students' assessment of their own skills. Because alignment of mentee and mentor skill ratings is an important measure of the validity of self-reported data (*3*), mentor training may have the unexpected benefit of increasing the reliability of assessments based on self-reporting, which are often used to evaluate undergraduate research programs.

At the conclusion of the summer programs at UW-Madison, 80% of the mentors who participated and none of those who had not participated in the mentoring seminar said that their view of their own adviser was altered by the summer mentoring experience (table S8), enhancing the mentors' understanding of their advisers' mentoring strategies and their empathy for the challenges faced by undergraduate

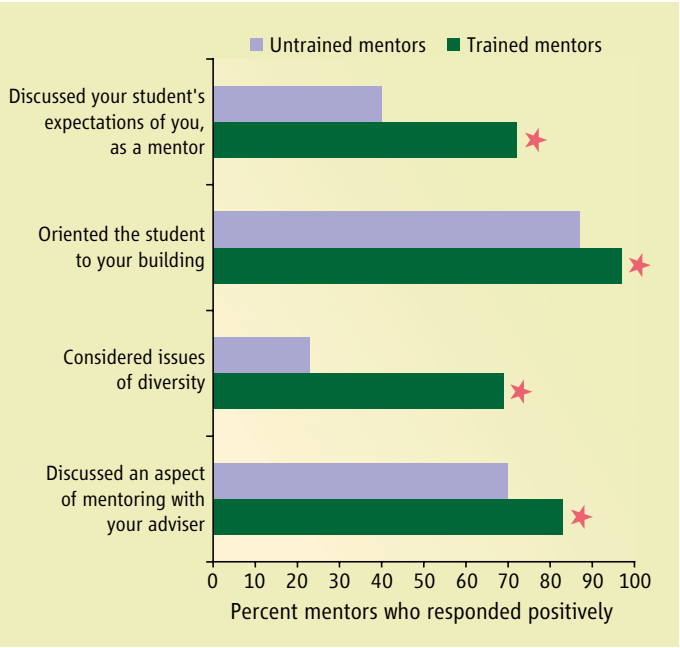

Behaviors of trained and untrained mentors. Percentage of mentors who indicated that they engaged in the noted activity while mentoring an undergraduate researcher. Stars indicate that the difference between the trained and untrained mentors was significant ($P < 0.05$).

Conclusion

We developed a seminar on mentoring that fills a critical gap in graduate education and training of future faculty. Evaluation of the seminar suggests that it is an effective means of improving communication and evaluation skills that are essential to good mentoring.

Mentoring relationships between faculty and students are often cited as critical in the decisions of undergraduates to pursue graduate education, but the effective elements of those relationships are not clear (*4*, *8*–*10*). In our study, undergraduate researchers who compared experiences with trained and untrained mentors stressed communication as a key feature of good mentoring.

The mentored research experience represents an intersection of many aspects of research and education in our research universities, offering an opportunity for generating multiple effects with a single intervention. The most direct effect is an improvement in the quality of the undergraduate research experience, which has been shown to be pivotal in attracting students in general, but especially racial minorities, to science (*1*–*5*). But we anticipate other effects, including an improved quality of undergraduate research, resulting in greater faculty satisfaction and perhaps a greater willingness to host undergraduate researchers. Training graduate students and postdoctoral researchers in mentoring might also produce a new generation of scientists who enter the professoriate as skilled mentors. The minimal resources required to teach this seminar seem worth investing to achieve these diverse outcomes.

References and Notes

1. Reviewed in E. Seymour *et al.*, *Sci. Educ.* **88**, 493 (2004).
2. D. Lopatto, *Cell Biol. Educ.* **3**, 270 (2004).
3. C. M. Kardash, *J. Educ. Psychol.* **92**, 191 (2000).
4. R. S. Hathaway, B. A. Nagda, S. R. Gregerman, *J. Coll. Stud. Dev.* **43**, 614 (2002).
5. B. A. Nagda *et al.*, *Rev. Higher Educ.* **22**, 55 (1998).
6. J. Handelsman, C. Pfund, S. M. Lauffer, C. Pribbenow, *Entering Mentoring: A Seminar to Train a New Generation of Scientists* (Univ. of Wisconsin Press, Madison, 2005).
7. J. Handelsman *et al.*, *Science* **304**, 521 (2004).
8. A. W. Astin, *What Matters in College? Four Critical Years Revisited* (Jossey-Bass, San Francisco, 1993).
9. E. T. Pascarella, P. T. Terezini, *How College Affects Students* (Jossey-Bass, San Francisco, 1991).
10. J. C. Hearn, *Res. Higher Educ.* **27**, 119 (1987).
11. We thank J. Heitz and the Biology 152 staff and the undergraduate researchers, mentors, and faculty who participated in this program. Supported by the University of Wisconsin–Madison and the Howard Hughes Medical Institute through a grant to J.H. from the Howard Hughes Medical Institute Professors Program. J.B. was supported by NSF grant no. 0402549.

Supporting Online Material

www.sciencemag.org/cgi/content/full/311/5760/473/DC1
10.1126/science.1123806

BIOCHEMISTRY

Loop Grafting and the Origins of Enzyme Species

An enzyme with completely new function can be created in the lab by mimicking natural evolutionary processes that both alter and preserve protein architecture.

Dan S. Tawfik

Understanding the emergence of new protein functions is no less a challenge than unraveling the origins of the organisms in which they occur. Proteins, enzymes in particular, exhibit spectacular performance unequaled by any human-made catalyst. Highly proficient and robust apparatuses are usually neither versatile nor easily modifiable. Enzymes, however, exhibit a remarkable evolutionary adaptability. New enzymes have emerged throughout the natural history of this planet. These did not simply turn up, nor were they the subject of "intelligent design." They evolved through Darwinian processes of mutation and selection. In fact, new functions can evolve in a matter of a few decades or even months, as with enzymes that degrade synthetic chemicals (nonexistent on this planet until the 20th century) and the alarming evolution of drug resistance (in which an enzyme evolves to avoid a drug designed to block it).

On page 535 of this issue, Park *et al.* (*1*) provide insights regarding the emergence of new enzyme functions. They mimicked, in the laboratory and in real time, the divergence of a new, human-made member of a large family of enzymes that has diverged in nature time and again. The work demonstrates that a switch in enzyme function that involves a dramatic change in amino acid sequence and active-site architecture boils down to replacing several of the enzyme's surface loop structures.

The structures of more than 30,000 proteins taught us that nature made use of a rather limited repertoire of core structural platforms, or "scaffolds" (on the order of a few thousand), to mediate an amazingly large diversity of functions (*2*). This diversity had presumably emerged from a small number of progenitor proteins, each with a different basic scaffold, thus creating enzyme families and superfamilies. The vestiges of this process are the scaffold and active-site architecture (or "key catalytic residues") shared by all family members (*3*).

Millions of years of evolutionary drift resulted in sequence changes that largely obscure the precise routes by which these enzymes diverged. Pointing out a route by sequence and structure comparisons is an essential step, but its resolution is inevitably low (imagine the deconvolution of a complex movie plot from a few snapshots). The ultimate test of our understanding, in the view of skeptical experimentalists, is reproducing these routes in the laboratory. In Thomas Edison's words, "Until man duplicates a blade of grass, nature will laugh at his so-called scientific knowledge." Although alteration of enzymatic function through point mutations has become a matter of routine, the reshaping of active sites through insertion and/or deletion of entire polypeptide segments was scarcely exercised (*4*). There is little doubt, however, that major switches in function demand major sequence rearrangements including insertion, deletion, and recombination (*5*).

Through extensive sequence changes, including the deletion and insertion of several structural loops in the active site, Park *et al.* converted one member of the αβ/βα metallohydrolase superfamily (glyoxalase II) into a new family member with a different catalytic function (degradation of a β-lactam antibiotic). Hundreds of natural enzymes belong to the metallohydrolase superfamily, mediating a myriad of different reactions. Despite this diversity of function, they all share the same scaffold and key catalytic residues—a bimetal (typically zinc) active center ligated to the enzyme's scaffold through different residues. These metallo centers activate both the substrate and a water molecule, thereby accelerating the hydrolytic breakdown of the former. Thus, all family members share the same chemistry, although the substrates and the detailed reaction pathways differ. These common themes, which characterize all enzyme superfamilies (*3*), imply that when a need for a new hydrolytic function emerged, nature recruited existing members of hydrolase superfamilies and tinkered with their active sites to fit the new substrate.

In accordance with this scenario, Park *et al.* maintained the basic scaffold and chemistry, whereas the switch in function was triggered by extensive changes in four active-site loops. The resulting protein (evMBL8) bears little resemblance (25% sequence identity) to IMP-1, a natural β-lactamase from the same superfamily, although its active-site architecture is probably close to that of IMP-1 (*1*). Thus, as in nature, sequence diverged much further than structure.

From an engineering perspective, this work extends the powers of protein engineering, one of the first achievements of which (*6*) had been the

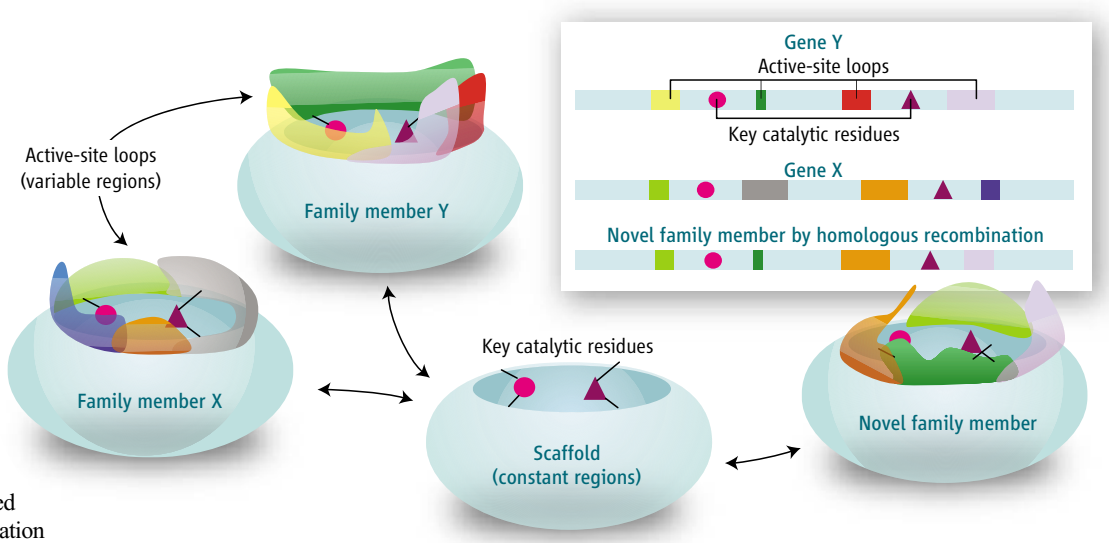

Loop grafting yields new enzymes. Park *et al.* (*1*) demonstrate that replacing several active-site loops (variable regions) of an enzyme, while retaining its scaffold and key catalytic residues (constant regions; red circle and pink triangle), can yield a family member with new reaction specificity. In nature, the conserved scaffold and key catalytic residues constitute obvious crossover points for homologous gene recombination and may enable the shuffling of active-site loops between family members and the emergence of new enzymatic functions.

The author is in the Department of Biological Chemistry, Weizmann Institute of Science, Rehovot 76100, Israel. E-mail: tawfik@weizmann.ac.il

10.1126/science.1124166

grafting of antigen binding loops from rodent into human antibody scaffolds (*7*). Grafting enzyme loops is far more tricky an exercise. As demonstrated by Park *et al.* (*1*), the combination of rational design (or "rationalized design," i.e., deciding which loops to replace and the simultaneous insertion of several loops containing randomized sequences) and directed evolution has proven useful. However, the engineering of artificial enzymes with catalytic efficiencies that rival those of natural enzymes remains a challenge. The engineered enzyme (evMBL8) is inferior to its natural counterparts by a factor of 1000—and so are other designed enzymes (*8*). Future work may provide additional examples, improved design rules, and computational algorithms that direct the grafting of active-site loops or even replace the scaffold (*9*).

From an evolutionary point of view, the key to success seems to be the preservation of scaffold and chemistry. Notably, the latter is mediated by the key catalytic residues that are often associated with the scaffold, whereas the active-site loops vary from one family member to another. This hierarchy of enzyme structure is seen in many enzymes and is probably one of the keys to enzyme evolvability (*10*). Two important questions remain, however. First, can loop swapping be exercised in nature? Homologous recombination of genes encoding different family members seems a most feasible mechanism (see the figure). Second, an essence of Darwinian processes is that they occur gradually while maintaining organism fitness throughout. But the first steps toward evMBL8 led to a complete loss of function. Can a switch in enzyme function that involves multiple and drastic changes in sequence evolve gradually? Well, nature's starting point might have been an enzyme that promiscuously exhibits low levels of the desired function. Indeed, promiscuous activities, or cross-reactivities, are often observed between members of the same superfamily (*11*, *12*). The next step may involve mutations that increase this promiscuous function while maintaining the original function, thereby providing a bifunctional evolutionary intermediate (*10*). Gene duplication could then lead to the divergence of the new gene through recombination with homologous family members and further mutation and selection. Individual steps along these routes have been demonstrated in the laboratory, but reproducing this process in its entirety remains a challenge.

References

1. H.-S. Park *et al.*, *Science* **311**, 535 (2006).
2. R. Service, *Science* **307**, 1555 (2005).
3. J. A. Gerlt, P. C. Babbitt, *Annu. Rev. Biochem.* **70**, 209 (2001).
4. F. Pries, A. J. van den Wijngaard, R. Bos, M. Pentenga, D. B. Janssen, *J. Biol. Chem.* **269**, 17490 (1994).
5. L. D. Bogarad, M. W. Deem, *Proc. Natl. Acad. Sci. U.S.A.* **96**, 2591 (1999).
6. J. A. Brannigan, A. J. Wilkinson, *Nat. Rev. Mol. Cell Biol.* **3**, 964 (2002).
7. P. T. Jones, P. H. Dear, J. Foote, M. S. Neuberger, G. Winter, *Nature* **321**, 522 (1986).
8. M. A. Dwyer, L. L. Looger, H. W. Hellinga, *Science* **304**, 1967 (2004).
9. B. Kuhlman *et al.*, *Science* **302**, 1364 (2003).
10. A. Aharoni *et al.*, *Nat. Genet.* **37**, 73 (2005).
11. D. M. Schmidt *et al.*, *Biochemistry* **42**, 8387 (2003).
12. C. Roodveldt, D. S. Tawfik, *Biochemistry* **44**, 12728 (2005).

10.1126/science.1123883

ATMOSPHERE

Climate Change and Human Evolution

What can we learn about cause and effect relationships between climate and human evolution from the late Cenozoic?

Anna K. Behrensmeyer

Climate and biological evolution have interacted throughout Earth's history, together creating many small and a few major transformations in the planet's atmosphere and biota. The role of climate in the origin and adaptations of humans relates not only to our past but also, potentially, to our future (*1*). A number of hypotheses propose that climate-driven environmental changes during the past 7 million years were responsible for hominin speciation, the morphological shift to bipedality, enlarged cranial capacity, behavioral adaptability, cultural innovations, and intercontinental immigration events (*2–9*). These hypotheses are based on correlations between global-scale climate shifts documented in oceanic deposits and events in hominin evolution recorded in continental fossil-bearing strata. Establishing cause-effect relationships between climate and human evolution is tantalizing but presents many challenges for paleoanthropology and the geological sciences.

The biggest challenge involves how to relate different types and scales of paleoclimatic evidence between the marine and terrestrial realms. Marine-core records show that a cooler, drier, and more variable global climate regime began about 3.0 million years ago (Ma), gradually intensifying into northern continental glacial cycles by 1.0 Ma (*10–12*). The climate shift between ~3.0 and 2.5 Ma thus marks the onset of Northern Hemisphere glaciation (*10–13*), and this coincides generally with the timing of the origin of the genus *Homo* [reviewed in (*8*, *14*)] (see the figure). Fluctuations in continent-derived dust and biomarkers in the marine record indicate that climate shifts recorded in the oceans affected the land as well (*12*, *15*). However, in the continental basins that preserve hominin fossils, the record of climate change is much harder to decipher. Paleoclimatic proxy evidence includes stable isotope (*8*, *16*, *17*), pollen (*18*), mammal faunas (*7*), and lake versus land deposits (*9*, *19*, *20*). Although these signals are documented in many vertebrate fossil-bearing localities (*17*, *21–23*), each stratigraphic sequence represents only limited portions of the time-space framework of hominin evolution. In addition, the proxy records are subject to local tectonic and climatic processes that often obscure or completely overprint global-scale climate signals. Thus, we must confront the problem of relating a fossil record preserved in strata dominated by local- to regional-scale paleoenvironmental signals to a marine record dominated by continental- to global-scale signals. Long cores from deep African lakes could provide more continuous data and a stronger bridge between oceanic and continental climate records, but these are only beginning to be tapped (*24*).

Another challenge is deciding what constitutes a strong case for a causal link between a climate change and an evolutionary event. We can't step into a laboratory to test the impact of climate change on the human genome, but we do have the results of natural experiments—the proxy evidence for environmental changes in continental rock sequences, as well as many fossils of hominins and other organisms that were evolving on different continents during that same time period. There is a rich body of data to draw upon, but hypotheses are often structured around an assumption that "synchronous" events in the geological and paleontological record constitute evidence for cause and effect. These hypotheses, while seductive in their simple explanation of how our species came to be, do not do justice to the complexity of the climate-evolution problem (see the figure) or to the full range of evidence and scientific methodologies that now can be brought to bear on this problem.

Research into human origins, as well as other fields of science, uses probability-based evidence to test cause-effect hypotheses. Establishing a

The author is a research curator in the Department of Paleobiology, Smithsonian Institution, Washington, DC 20560, USA. E-mail: behrensa@si.edu

credible cause-effect relationship between events or trends in the geological record requires (i) a clear definition of what "synchronous" means, (ii) consideration of the mechanism for transmitting climatic cause to evolutionary effect, and (iii) multiple lines of proxy evidence supporting interpretations of the climatic trends or events. A recently proposed link between climate and human evolution provides an example of how these criteria can be used to assess hypotheses.

A new compilation of paleolimnological evidence concludes that lake levels were high in the East African Rift between 2.7 and 2.5 Ma (*9*) based on two generally synchronous lacustrine deposits in Kenya and southern Ethiopia [see the figure, land record (left)]. Radiometric dating shows that the two phases of lacustrine deposition occurred within a period of about 200,000 years (*9*). It is tempting to speculate [as in (*9*)] that there may be a cause and effect between this wet climate phase and the origin of *Homo*, but let us consider this in light of the three criteria above. There is debate about the precise time and place of the origin of the genus *Homo* (*8*, *14*), with time estimates ranging from 2.6 to 1.7 Ma. Synchrony of the climatic signal and the evolutionary event thus remains in question. The related notion that fluctuating lake levels provided environmental stress that drove speciation does not provide a mechanism for how this could have exerted selective pressure on the immediate ancestor of *Homo* and resulted in the emergence of a new genus and species. Other proposals instead have linked human evolution with increasing aridity and climate variability (*4*, *6*, *25*). Finally, other paleoclimatic evidence indicates drier rather than wetter climatic conditions between 2.7 and 2.5 Ma (*8*, *17*, *26*) [see the figure, land record (center)], bringing into question the extent of a prolonged high lake phase throughout East Africa. Although the multibasin approach to establishing regional paleoclimate trends is commendable, the proposed causal link between a wet climate phase and the origin of *Homo* is not yet supported by sufficient evidence to establish its credibility.

The way forward is to carefully match the quality and scale of the data with the scale of the question. We cannot expect to link global- or continental-scale climate processes to major events and trends in human evolution without first disentangling basin- and regional-scale environmental signals in strata that contain the hominin fossil record (*17*, *27*, *28*). This complexity can work in our favor, however. A multibasin, multiproxy approach is now possible because paleoclimate data and chonostratigraphic correlations are becoming available for a large number of rock sequences (*9*, *29*, *30*). If many stratigraphic sequences and independent climate proxies show similar, synchronous environmental shifts, this would be strong evidence for climate change affecting large regions of a continent, particularly when such trends can be matched to the marine core data. On the other hand, if basins show independent patterns of environmental change, this

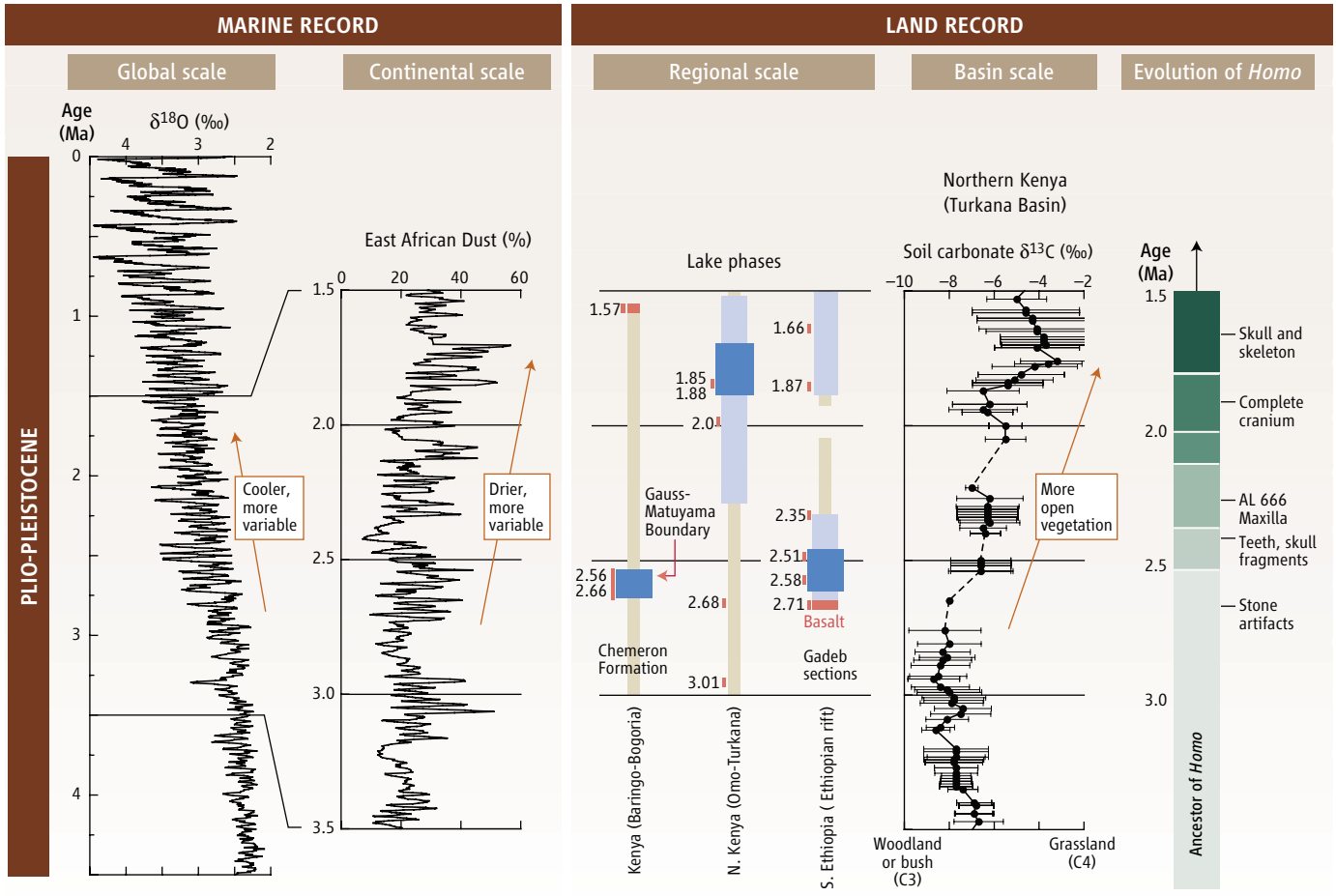

Marine and land records showing paleoclimatic trends during human evolution. Marine record: **(Left)** Global ice volume trend based on composite oxygen stable isotope ($\delta^{18}O$) data from seven different marine cores (*31*). **(Right)** Cycles of aridity in the Sahara Desert, based on percent terrigenous dust in the ODP (Ocean Drilling Program) Site 721/722 core from the Arabian Sea (*32*). Land records: **(Left)** Multibasin records of lake phases. Darkest vertical bars indicate deep lakes, lighter bars indicate shallow lakes, and lightest bars indicate land; red bars mark radiometric dating levels (*9*). **(Center)** Carbon stable isotope ($\delta^{13}C$) record of closed (woodland or bush) versus open (grassland) vegetation in the Turkana Basin of northern Kenya (*8*) (same basin as central lake phase record); **(right)** milestones in the fossil and archaeological record that are used as evidence for the timing of the appearance of *Homo* (*14*). There is no simple translation of the marine Plio-Pleistocene global climate shifts into the continental records, but future integration of marine and land-based evidence will allow rigorous testing of the impact of global change on the environments and evolutionary trajectories of our ancestors.

implies that they were locally buffered against larger-scale climate forcing, or that the available evidence is not sufficient to resolve small- versus large-scale environmental processes. The hominin fossil and cultural record could be reconsidered in light of such paleoclimatic meta–data sets. The strength of this approach depends on the number of sample points (that is, different basins and regions), accurate interpretations of climatic proxies, well-resolved correlations between basins, and a healthy dose of devil's advocacy before making a leap to global-scale interpretations. It is also worth remembering that climate was only one of many factors affecting human evolution; biological processes including genetic innovation, interspecies competition, and dispersal ability also could have played defining roles (*14*).

Rather than a simple story of global climate drumbeat and evolutionary response, more informative and exciting revelations about the 7-million-year development of hominin morphology, behavior, and culture will likely come from detailing the prolonged tension between local ecosystems and global climate change. This is also a strikingly relevant theme for the future of our species.

References and Notes

1. National Research Council Committee on the Geological Record of Biosphere Dynamics, The Geological Record of Ecological Dynamics: Understanding the Biotic Effects of Future Environmental Change (National Academies Press, Washington, DC, 2005).
2. L. F. Laporte, A. L. Zihlman, *S. Afr. J. Sci.* **79**, 96 (1983).
3. S. M. Stanley, *Paleobiology* **18**, 237 (1992).
4. E. S. Vrba, in *Paleoclimate and Evolution with Emphasis on Human Origins*, E. S. Vrba, G. H. Denton, T. C. Partridge, L. H. Burckle, Eds. (Yale Univ. Press, New Haven, CT, 1995), pp. 24–45.
5. R. Potts, *Humanity's Descent: The Consequences of Ecological Instability* (Morrow, New York, 1996).
6. R. Potts, *Yrbk. Phys. Anthropol*. **41**, 93 (1998).
7. R. Bobe, A. K. Behrensmeyer, R. Chapman, *J. Hum. Evol.* **42**, 475 (2002).
8. J. G. Wynn, *Am. J. Phys. Anthropol.* **123**, 106 (2004).
9. M. H. Trauth, M. A. Maslin, A. Deino, M. R. Strecker, *Science* **309**, 2051 (2005).
10. R. Tiedemann, M. Sarnthein, N. J. Shackleton, *Paleoceanography* **9**, 619 (1994).
11. J. Zachos, M. Pagani, L. Sloan, E. Thomas, K. Billups, *Science* **292**, 686 (2001).
12. P. B. deMenocal, *Earth Planet. Sci. Lett.* **220**, 3 (2004).
13. N. J. Shackleton, in *Paleoclimate and Evolution with Emphasis on Human Origins*, E. S. Vrba, G. H. Denton, T. C. Partridge, L. H. Burckle, Eds. (Yale Univ. Press, New Haven, CT, 1995), pp. 242–248.
14. R. Potts, in *Hominid Environments in the East African Pliocene: An Assessment of the Faunal Evidence*, R. Bobe, Z. Alemseged, A. K. Behrensmeyer, Eds. (Kluwer, New York, in press).
15. S. J. Feakins, P. B. deMenocal, T. I. Eglinton, *Geology* **33**, 977 (2005).
16. T. E. Serling, *Palaeogeogr. Palaeoclimatol. Palaeoecol.* **97**, 241 (1992).
17. N. E. Levin, J. Quade, S. W. Simpson, S. Semaw, M. Rogers, *Earth Planet. Sci. Lett.* **219**, 93 (2004).
18. R. Bonnefille, R. Potts, F. Chalié, D. Jolly, O. Peyron, *Proc. Natl. Acad. Sci. U.S.A.* **101**, 12125 (2004).
19. R. B. Owen, in *Sedimentation in Continental Rifts*, R. W. Renaut, G. M. Ashley, Eds. (Special Publication No. 73, Society for Sedimentary Geology, Tulsa, OK, 2002), pp. 233–246.
20. C. S. Feibel, in *African Biogeography, Climate Change, and Human Evolution*, T. G. Bromage, F. Schrenk, Eds. (Oxford Univ. Press, Oxford, 1999), pp. 276–281.
21. A. Hill, A. Deino, J. Kingston, "Hominids and paleoenvironments: The view from the Tugen Hills, Kenya," (Geological Society of America Annual Meeting Abstracts with Program 73-6 (2003) .
22. M. H. Trauth, A. L. Deino, A. G. N. Bergner, M. R. Strecker, *Earth Planet. Sci. Lett.* **206**, 297 (2003).
23. C. J. Lepre, R. L. Quinn, *Paleoanthropology* (abstr.), p. A38 (2005).
24. A. S. Cohen, C. A. Scholz, T. C. Johnson, *J. Paleolimnol.* **24**, 231 (2000).
25. R. Bobe, A. K. Behrensmeyer, *Palaeogeogr. Palaeoclimatol. Palaeoecol.* **207**, 399 (2004).
26. P. B. deMenocal, J. Bloemendal, in *Paleoclimate and Evolution with Emphasis on Human Origins*, E. S. Vrba, G. H. Denton, T. C. Partridge, L. H. Burckle, Eds. (Yale Univ. Press, New Haven, CT, 1995), pp. 262–288.
27. C. S. Feibel, *GSA Today* **7**, 1 (1997).
28. R. L. Quinn, C. J. Lepre, *Eos Trans. AGU* **85** (Fall Meet. Suppl. Abstr.), U21A-0707 (2004).
29. P. B. deMenocal, F. H. Brown, in *Hominoid Evolution and Climate Change in Europe*, J. Agusti, L. Rook, P. Andrews, Eds. (Cambridge Univ. Press, Cambridge, UK, 1999), vol. 1, pp. 23–54.
30. C. J. Campisano, A. K. Behrensmeyer, R. Bobe, N. Levin, *Paleoanthropology* (abstr.), p. A34 (2004).
31. L. E. Lisiecki, M. E. Raymo, *Paleooceanography* **20**, PA1003 (2005).
32. P. B. deMenocal, *Science* **270**, 53 (1995).

33. I thank R. Potts, C. Campisano, C. Feibel, N. Levin, and P. deMenocal for useful discussions. Research funding has been provided by NSF grant 0218511.

10.1126/science.1116051

GEOCHEMISTRY

Rising Mountain Ranges

Michael A. Poage and C. Page Chamberlain

Stable isotope measurements of ancient soil minerals reveal the elevation history of a mountainous region in the Bolivian Andes.

Mountain ranges and plateaus are among the largest and most alluring physiographic features on Earth's surface. Their elevational histories are important in understanding tectonic processes as well as ancient climate change. Determining the timing and magnitude of surface uplift—paleoaltimetry—has been notoriously difficult because of a lack of direct elevation proxies in the geologic record. Consequently, estimates for the timing of mountain range formation often differ by millions of years, even for geologically young regions.

Geoscientists have developed several methods to constrain estimates of paleoelevation (*1*–*3*). Each has limitations, and the applicability of any method to a specific region depends in part on the availability of appropriate samples and the ability to account for confounding factors. On page 511 of this issue, Ghosh *et al.* (*4*) report their reconstruction of the elevation history of the Altiplano of the Bolivian Andes. They achieve this by combining data from a new geochemical technique, the "clumped isotope thermometer" (*5*), with conventional stable isotopic data (*6*) from ancient soil minerals. Their novel approach addresses several long-standing problems facing the field of paleoaltimetry.

Fundamental to many paleoaltimetry studies is an understanding of changes in the stable isotopic composition of precipitation through time (*7*–*10*). As air masses rise across a high region, continual rainout creates an oxygen isotope composition gradient in the precipitation ($\delta^{18}O_P$) quantitatively related to the elevation of the land surface (see the figure). In the case of a rising mountain range or plateau, changes in elevation at a given location will influence $\delta^{18}O_P$ accordingly. The isotopic composition of ancient precipitation can be preserved in the geologic record by oxygen-containing minerals formed in equilibrium with precipitation-derived waters (e.g., soil water or shallow groundwater). For example, the $\delta^{18}O$ of soil-formed (pedogenic) calcite ($CaCO_3$) is related to the $\delta^{18}O$ of precipitation-derived soil water by a temperature-dependent isotopic fractionation factor. Isotopic analysis of an established chronosequence of proxy minerals such as calcite allows for a first-order reconstruction of changes in $\delta^{18}O_P$ through time. Using the modern incremental change in $\delta^{18}O_P$ with elevation, researchers can then place constraints on a region's elevational history (*3*).

Natural systems are complex, however, with uncertainties and confounding factors often muddling the reconstruction of paleoelevation. Ghosh *et al.* (*4*) specifically address several aspects of this complexity in their analysis of a pedogenic calcite chronosequence from the Bolivian Altiplano. They use the clumped isotope thermometer, which involves measuring the abundance of ^{13}C-^{18}O bonds in carbonate minerals, to determine a sample-specific calcite growth temperature (*5*). When combined with the $\delta^{18}O$ from the same calcite sample, this paleotemperature permits precise evaluation of the $\delta^{18}O$ of the soil water present during sample growth.

Isotope paleoaltimetry studies have typically relied on less direct temperature estimates to relate the $\delta^{18}O$ of a proxy mineral to the $\delta^{18}O$ of the water from which it formed. The resultant iso-

M. A. Poage is in the Geoscience Department, Indiana University of Pennsylvania, Indiana, PA 13705, USA. E-mail: mpoage@iup.edu C. P. Chamberlain is in the Department of Geological and Environmental Science, Stanford University, Stanford, CA 94305, USA. E-mail: chamber@pangea.stanford.edu

topic record forms one basis for interpreting paleoelevation change. Because the authors' chronosequence of samples developed on a rising surface, they are also able to generate an independent temperature-based elevational history using values from the clumped isotope thermometer. This second history couples changes in mineral growth temperature through time with knowledge of the modern temperature change with elevation. The temperature-based and isotope-based histories together provide corroborating and convincing evidence to suggest that the Bolivian Altiplano uplifted ~3700 m between 10.3 million and 6.7 million years ago (*4*).

Other processes that affect either temperature or $\delta^{18}O_P$ can complicate elevational reconstructions of this type. For example, changes in global climate, annual proportions of precipitation derived from different moisture sources, or seasonal distribution of precipitation can all occur independent of elevation change. With creative insight, the authors develop a framework in which to evaluate the likelihood that observed changes in paleotemperature and $\delta^{18}O_P$ are specifically due to elevation change. They demonstrate that the trend in temperature versus $\delta^{18}O_P$ inferred from their sequence of calcite samples closely parallels the temperature versus $\delta^{18}O_P$ trend measured from a modern elevation transect. If either of these variables were influenced by processes other than elevation change, this would cause these trends to plot obliquely. Such a framework, which enables a distinction between temperature and/or isotopic variations caused by elevation change versus other processes, represents an exciting refinement in paleoaltimetry that will improve our understanding of the evolution of mountain ranges.

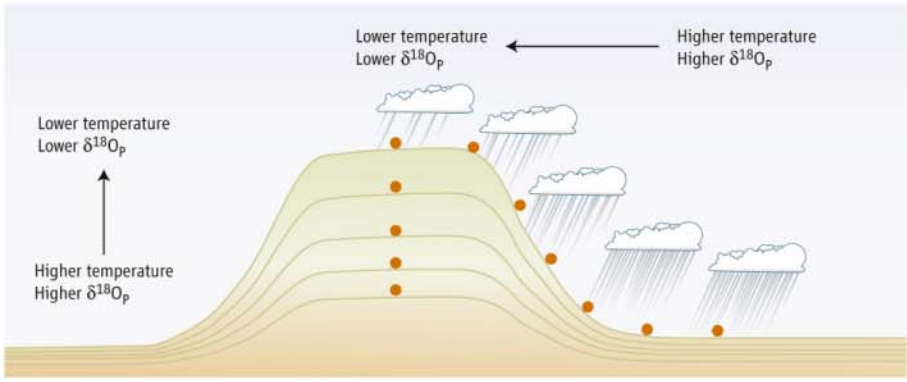

Measuring mountain uplift. Mountain ranges cause air masses to rise and lose moisture. Thus, a gradient exists for warmer temperatures and higher $\delta^{18}O_P$ values at lower elevations to cooler temperatures and lower $\delta^{18}O_P$ values at higher elevations (horizontal arrow; red dots denote hypothetical samples). Pedogenic minerals formed on a rising surface and preserved in the rock record will initially record warmer temperatures and higher $\delta^{18}O_P$ values, progressing toward cooler temperatures and lower $\delta^{18}O_P$ values as elevation increases (vertical arrow).

Paleoaltimetry is a rapidly developing field, especially as interest increases in the connections and feedbacks among tectonics, geomorphology, and climate change. Despite these and other recent advances, there are still many challenges ahead and limitations to current techniques. The geologic histories of mountainous regions are sufficiently variable that any single paleoaltimetry technique is unlikely to prove effective in all (or even most) cases. Rather, it is more likely that our understanding will reflect a consensus from multiple techniques applied to a particular region.

References and Notes

1. D. L. Sahagian, J. E. Maus, *Nature* **372**, 449 (1994).
2. J. A. Wolfe *et al.*, *Science* **276**, 1672 (1997).
3. D. B. Rowley *et al.*, *Earth Planet. Sci. Lett.* **188**, 253 (2001).
4. P. Ghosh *et al.*, *Science* **311**, 511 (2006).
5. P. Ghosh *et al.*, *Geochim. Cosmochim. Acta*, in press.
6. The relative proportion of an element's stable isotopes (e.g. ^{16}O,^{18}O; ^{12}C,^{13}C) in a given material is measured as the per mil (‰) deviation from a standard using conventional δ notation, for example, $\delta^{18}O = [[(^{18}O/^{16}O)_{sample}/(^{18}O/^{16}O)_{standard}] - 1] \times 1000‰$.
7. C. P. Chamberlain *et al.*, *Chem. Geol.* **155**, 279 (1999).
8. C. N. Garzione *et al.*, *Geology* **28**, 339 (2000).
9. H. C. Fricke, *Geol. Soc. Am. Bull.* **115**, 1088 (2003).
10. A. Mulch *et al.*, *Geology* **32**, 525 (2004).

10.1126/science.1123215

MATERIALS SCIENCE

Making Better Ceramic Composites with Ice

The tough structure of shellfish nacre has been replicated in a ceramic by a simple water-freezing method.

John Halloran

Modern ceramics are very strong but brittle, and so are unsuitable for most load-bearing applications. Ceramics fail by sudden catastrophic fracture, which is not a trait that engineers find endearing. These materials behave in this way because they absorb very little energy during fracture. A good example is glass, which is one of the strongest manufactured materials when the surfaces are free from flaws (as with glass fibers), but under ordinary conditions "glass" is a metaphor for fragility. Since the classic work by Griffith (*1*), there has been remarkable progress on the mechanics of fracture (*2*, *3*), but strength must still be treated with statistics describing the severity of the flaws that are present. Few designers are willing to accept the risk of working with inherently unreliable ceramics. These difficulties could be alleviated if it were possible to build energy-absorbing mechanisms into the microstructure to increase toughness. Some specific examples are known, such as the use of phase transformations in zirconium oxide to absorb energy (*4*), but only a few materials can be "transformation toughened" in this way (*5*). A general strategy for toughening ceramics has been sought by a generation of materials scientists.

Previous reports of the extraordinary toughness through [illegible] have inspired much research because the shells, consisting of 99% calcium carbonate ($CaCO_3$), are hundreds of times tougher than simple polycrystalline limestone. These remarkable properties are related to the fine-scale structure of the shell, a laminate of thin calcium carbonate crystallite layers and tough biopolymers, arranged in an energy-absorbing hierarchical microstructure (*7*), as recently reviewed by Meyer (*8*). Calcium carbonate is a fine material for the nacre in shellfish, but is not particularly useful in jet turbine engines. How can the nacre structure be obtained in more durable materials? How can it be manufactured by fast, economical methods? A number of bio-inspired techniques, working both from bottom-up (*9*) and top-down methods, produced laminates (*10*) and

The author is in the Department of Materials Science and Engineering, University of Michigan, Ann Arbor, MI 48109, USA. E-mail: peterjon@umich.edu

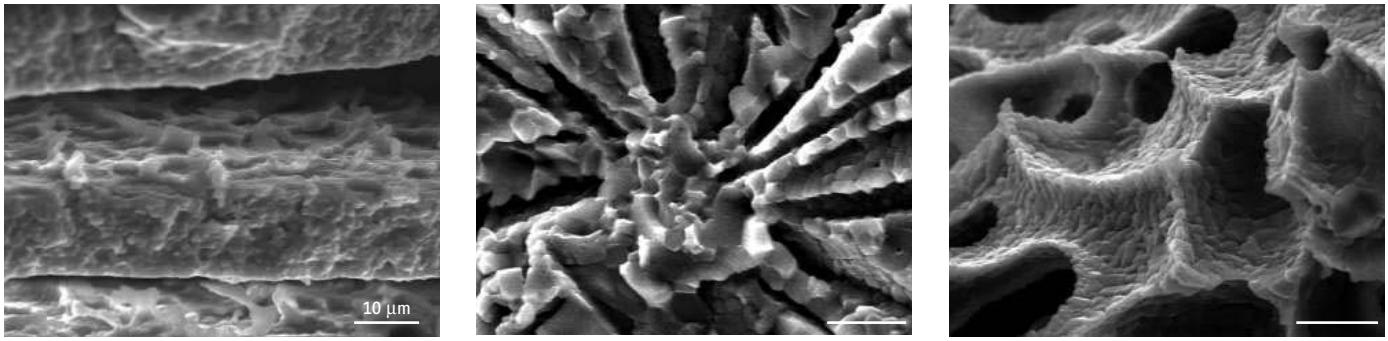

Ice templates. (Left) Nacre-like layers after removal of ice dendrites from solidification of alumina suspension in water. [Adapted from (*12*)] (**Center**) Starburst voids after removal of naphthalene dendrites from solidification of alumina suspension in camphor-naphthalene, which do not provide a template for tough composites. (**Right**) Branching voids after removal of camphor dendrites from solidification of alumina suspension in camphor-naphthalene.

fibrous laminates (*11*) that were in fact much tougher ceramics. However, these were tedious to manufacture and limited in the suite of materials. On page 515 of this issue, Deville *et al.* report a better route, using simple freezing (*12*).

Deville *et al*. have shown how to replicate the nacre structure of shells using controlled freezing of mixtures of water and ceramic powder. The composites made by this route have remarkably improved mechanical properties. The researchers achieve this by combining conventional manufacturing approaches that are already part of the engineering toolkit. These are as follows: (i) fine powder processing, the mainstay of the ceramic industry; (ii) controlled solidification, the core capability for metal casting and the frozen-food industry; and (iii) freeze-drying, a routine technique in the chemical, food, and coffee industries. Their nacre-like composites start with a lamellar template assembled by ice crystals. Water freezes as lamellar dendrites (*13*), and the ice dendrites push the ceramic particles into the interdendritic regions, making layers on the same scale as the ice. After the ice is removed by freeze-drying, the ceramic keeps the shape of the interdendritic layers, forming a template for subsequent injection of tough metal or polymer. The choice of water is clever, as the lamellar ice dendrites make an excellent template for nacre (see the figure, left panel). Other media are not useful templates, forming starburst dendrites as with naphthalene (see the figure, middle panel) or branched dendrites as with camphor (see the figure, right panel).

The technology for controlling dendrites is commonly used in applications ranging from the improvement of exotic jet-engine alloys to creating a tastier texture in frozen desserts. With the scale and arrangement of dendrites determined by well-known physics, and pattern formation well understood, there are many opportunities to build on the ideas of templating composites with ice. The methods of Deville *et al.* promise a flexible strategy for combining what people can do in factories with design concepts inspired by biology.

References

1. A. A. Griffith, *Philos. Trans. R. Acad*. **A221**, 163 (1920).
2. B. Lawn, *Fracture of Brittle Solids* (Cambridge Univ. Press, Cambridge, UK, 1993).
3. D. Green, *An Introduction to the Mechanical Properties of Ceramics* (Cambridge Univ. Press, Cambridge, UK, 1998).
4. R. C. Garvie, R. H. Hannick, R. T. Pascoe, *Nature* **258**, 703 (1975).
5. A. H. Heuer, *J. Am. Ceram. Soc.* **70**, 689 (1987).
6. J. D. Curry, A. J. Kohn, *J. Mater. Sci*. **11**, 1615 (1976).
7. S. Kamat, X. Su, R. Ballarini, A. H.Heuer, *Nature* **405**, 1036 (2000).
8. G. Meyer, *Science* **310**, 1144 (2005).
9. Z. Tang, N. A. Kotov, S. Magonov, B. Ozturk, *Nat. Mater.* **2**, 413 (2003).
10. K. Kendall, N. M. Alford, W. J. Clegg, J. D. Birchall, *Nature* **339**, 130 (1989).
11. D. Kovar, B. H. King, R. W. Trice, J. W. Halloran, *J. Am. Ceram. Soc.* **80**, 2471 (1997).
12. S. Deville, E. Saiz, R. K. Nalla, A. P. Tomsia, *Science* **311**, 515 (2006).
13. S. W. Sofie, F. Dogan, *J. Am. Ceram. Soc.* **84**, 1459 (2001).

10.1126/science.1123220

ECOLOGY

Staying Connected in a Turbulent World

The swimming behavior of fish larvae limits their dispersal among coral reef populations more than previously thought. This stands to affect the design of protected marine ecosystems.

Robert S. Steneck

Globally, coral reefs are endangered ecosystems that continually frustrate marine resource managers and policymakers charged with their protection and restoration. Sadly, we know much more about the frequency, intensity, and scale of coral reef degradation (*1*) than we do about the processes that drive their recovery (*2*). This is most noticeable among Caribbean coral reefs that have particularly low resilience in both resisting phase shifts to degraded states (*3*) and, once degraded, in returning to their previous state (*4*). A study by Cowen *et al.* on page 522 in this issue (*5*) offers new insights into the spatial scale and rate of larval supply necessary to sustain Caribbean reef fish populations. Cowen *et al*. improved on past population "connectivity" models by developing a coupled biological-physical approach that integrates factors such as the duration of development and swimming behavior of larvae, together with a well-validated model of ocean currents. They determined that connectivity, or the nexuses among disjunct populations of reef fish, is more local and regionally more variable than previously thought. Thought-provoking results influence the scale at which coral reefs should be managed and identify regions that will likely be more resilient or more vulnerable to the effects of fishing. The results scale up to regional (ocean-basin scale) considerations of biogeography, genetic isolation, and invasions of nonnative species that apply to fish and potentially to other reef-dwelling organisms, including corals.

The model developed by Cowen *et al.* improves upon the work of Roberts (*6*), a highly influential paper on connectivity and the management of Caribbean coral reefs, that considered primarily passive transport of fish larvae via ocean currents in order to estimate

The author is at the School of Marine Sciences, University of Maine, Darling Marine Center, Walpole, ME 04573, USA. E-mail: steneck@maine.edu

YOGI GT Proudly Presents, Thx for Support

the maximum range of larval connectivity among coral reefs. Roberts viewed many populations of marine organisms as being relatively open with substantial subsidies from distant upstream populations. In contrast, Cowen *et al*. have determined that larval transport via passive-diffusion cannot sustain reef fish at current levels unless there is substantial self-recruitment that results from the behavior of fish larvae themselves. The more realistic connectivity model of Cowen *et al*. provides the first robust estimates of the distance larvae will probably travel to successfully recruit to a specific reef [called the dispersal kernel (see the figure)]. Because a large portion of the larvae are recruiting at or near the reef where their eggs were hatched (that is, "self-recruiting" to the reef of larval origin) and because larval mortality will diminish the number of surviving larvae with time and distance from the larval source (*7*), the dispersal kernel will usually be greatest near the region where eggs were hatched and decline with distance. Conversely, passive advective-diffusion models will result in larvae being transported, and thus their kernel dispersed, some distance away from their places of origin. The Cowen *et al*. model operates at several spatial scales and identifies distinct subregions within the Caribbean that have different levels of larval subsidies and self-recruitment. The finding that larval subsidies are very limited in some regions suggests that marine resource managers must directly manage their reefs on a local scale and not depend on substantial larval subsidies from distant upstream sources.

Another advantage of the Cowen *et al*. biological-physical model over past contributions is the specific spatial and organismal precautionary advice provided for marine resource managers. The authors determine that subsidies are more likely in some Caribbean regions such as the Bahamas than in others such as the Windward Islands and Mexico's Caribbean Yucatan coast, because many of the reefs in the latter regions are beyond the dispersal kernel emanating from adjacent reefs. In effect, the discontinuous distribution of coral reefs provides a network of "stepping-stones" if reefs fall within the dispersal kernel of adjacent reefs (see the figure). However, as reef habitat and its associated reproductive fish populations decline (*3*, *8*, *9*), the distances between stepping-stones may increase to the point where they exceed the larval dispersal kernel, causing connectivity to decline (*9*).

The natural-history characteristics of fish species are also critical to their sustainability in a world increasingly influenced by human activities. Whereas short-lived fish may require regular recruitment to sustain their populations, longer lived species persist with periodic pulsed recruitment events. However, fishing pressure on reefs reduces both the population density and body size of harvested species (*10*, *11*), which can, in turn, reduce larval abundance and thus shrink the dispersal kernel and effective connectivity distance (see the figure).

Although Cowen *et al*. focus on several common groups of reef fish with different larval durations and swimming behaviors, their conclusions apply to most occupants of coral reef ecosystems. Understanding what drives connectivity in these diverse ecosystems helps us to understand their resilience. For example, in recent decades, reefs suffered widespread coral mortality owing to diseases and thermally induced bleaching (*1*). However, recovery may be limited by the generally short dispersal kernels of most corals owing to their brief period of larval development while planktonic (*12*). Because some corals provide essential habitat for some reef fish (*13*), limited connectivity among corals may limit the recovery of dependent species of reef fish.

Reef management should integrate this new understanding of the geography of resilience. The Cowen *et al*. model predicts that some reefs might be more susceptible to the effects of overfishing than others elsewhere in the Caribbean. Similarly, different reef-dwelling organisms such as corals, fish, and lobsters have vastly different larval durations [that is, short (few days to weeks), medium (months), to very long (a year or more), respectively], which add to the challenge of managing these diverse ecosystems.

The growing movement toward ecosystem-based management (*3*, *14*) and for networks of unfished or "no-take" fish reserves requires that they be spaced for connectivity. The approach illustrated by Cowen *et al*. should be broadly applicable because the inputs to their models—larval duration and behavior and the physical oceanography—apply to most organisms in most marine ecosystems. Finally, as these authors point out, their model suggests testable hypotheses with specific predictions that will allow the science of ecosystem-based management to move forward adaptively (*2*).

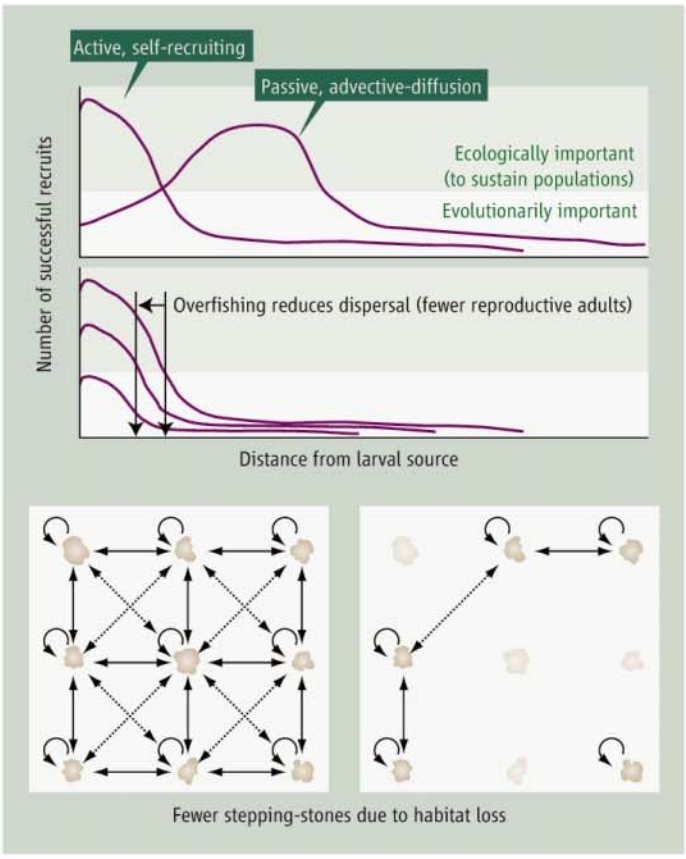

Sustaining Caribbean reef fish populations. Shrinking larval dispersal kernels and connectivity due to (**top graphs**) increased proportion of self-recruiting larvae and declining abundance of reproductive populations, and (**bottom graphs**) diminished abundance of stepping-stones within the dispersal region for larvae. Horizontal shading in top graphs represent the ecologically important number of larval recruits necessary to sustain fish populations demographically, whereas the lower, unshaded portions represent the evolutionarily important number of larvae necessary to connect populations genetically. Arrowed lines in bottom denote connectivity among populations within or between adjacent reefs. Dotted arrowed lines represent limited or sporadic connectivity. [Modified from (*9*), copyright 2005, with permission from Elsevier]

References

1. J. Pandolfi *et al*., *Science* **307**, 1725 (2005).
2. P. F. Sale *et al*., *Trends Ecol. Evol.* **20**, 74 (2005).
3. D.R. Bellwood *et al.*, *Nature* **429**,827(2004).
4. J. C. Connell, *Coral Reefs* **16**, S101 (1997).
5. R. K. Cowen, C. B. Paris, A. Srinivasan, *Science* **311**, 522 (2006); published online 15 December 2005 (10.1126/science.1122039).
6. C. M. Roberts, *Science* **278**, 1454 (1997).
7. R. K. Cowen *et al*., *Science* **287**, 857 (2000).
8. T. A. Gardner *et al*., *Science* **301**, 958 (2003).
9. T. P. Hughes *et al*., *Trends Ecol. Evol.* **20**, 380 (2005).
10. N. V. C. Polunin, C. M. Roberts, *Mar. Ecol. Prog. Ser.* **1000**, 167 (1993).
11. C. Birkeland, P. K. Dayton, *Trends Ecol. Evol.* **20**, 356 (2005).
12. P. W. Sammarco, J. C. Andrews *Science* **239**, 1422 (1988).
13. G. P. Jones *et al*., *Proc. Natl. Acad. Sci. U.S.A.* **101**, 8251 (2004).
14. E. K. Pikitch *et al*., *Science* **305**, 346 (2004).

10.1126/science.1123541

SCIENCE AND HEALTH

Scholars at First Abelson Seminar Urge Focus on Chronic Disease

Influential experts in medicine and public health warned a AAAS audience that heart disease, cancer, diabetes, and other chronic diseases have emerged as the world's dominant health threat, posing a greater human and economic risk than infectious diseases, hunger, and afflictions related to childbearing and early childhood combined.

Speaking at the first AAAS Philip Hauge Abelson Advancing Science Seminar, several of the experts stressed that prevention strategies and treatments are available to prevent millions of deaths from chronic disease. And developments at the frontiers of medicine may mean dramatic and effective future treatments for such illness.

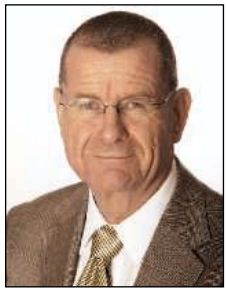

Robert Beaglehole

Susan Raymond

"We can stop already the global pandemic of chronic disease, and conservatively and relatively easily save 36 million lives between now and the year 2015," said Robert Beaglehole, director of Chronic Diseases and Health Promotion for the World Health Organization (WHO). "The solutions are inexpensive, they're cost-effective, and they're widely applicable."

But, the speakers said, health, research, and funding agencies must develop a new appreciation of the global threat posed by chronic disease and invest more in addressing it. Too often, the agencies still see the world as it was a half-century ago, when poverty, high infant mortality, and low life-expectancy were overwhelming threats outside the developed world, said Susan Raymond, senior managing director for research, evaluation, and strategic planning at Changing Our World Inc., a New York–based philanthropic service company.

"New Directions in Health: The Global Burden of Chronic Disease" was held 8 December 2005 at AAAS headquarters in Washington, D.C.; it was the inaugural event in a series named for Abelson, who died in 2004 after a career that included research in physics and biology and 22 years as the editor of *Science*. The seminar series is expected to focus on the frontiers of science and technology and address major social challenges.

Indeed, several speakers focused on the science of battling chronic disease, describing research that could revolutionize future health policy and treatment.

Eric J. Topol, provost of the Cleveland Clinic Lerner College of Medicine, described how future heart attacks could be prevented by early intervention into families with genes that make them vulnerable. Michael Sefton, professor of biomedical engineering at the University of Toronto, described efforts now under way to grow new tissues, new organs—even new hearts—to address the ravages of chronic disease and other afflictions.

Beaglehole, the opening speaker, and Raymond, the closing speaker, combined to paint a picture of dramatic changes in the global health profile, with chronic disease rising along with living standards in developing countries—but with medical, research, and funding agencies failing to take heed.

Poverty, infant mortality, and population growth are down sharply since 1950, Raymond said. In all but the least developed countries, people are more likely to be working, better fed, and living longer. But that creates more opportunity for chronic diseases that arise with poor dietary habits, physical inactivity, and tobacco use. For example, Beaglehole cited "a very frightening statistic": Worldwide, 22 million children under the age of 5 are obese. That means more future risk of obesity-related chronic diseases.

Raymond said the workforce in some developing countries could be "devastated" by chronic disease, with ripple effects exacting a human and multibillion-dollar toll on families, communities, and economies. "Dealing with chronic diseases at the onset of a stroke is a lot more expensive than dealing with the problem when it's at an earlier stage," she added.

"We need to invest seriously in a broad-based approach to the prevention and control of chronic disease," Beaglehole concluded. "The way forward is clear. It is up to us all now to take appropriate action."

Paul Recer contributed to this report.

ANNUAL MEETING

Teachers on the Front Line

Jeff Corwin, a wildlife biologist and host of "The Jeff Corwin Experience" on the Animal Planet cable TV station, will be among the top-flight speakers at "Evolution on the Front Line," a forum for teachers at the 2006 Annual Meeting in St. Louis. Register now for the 19 February event at www.aaasmeeting.org/evolution.

AAAS

Call for Nomination of AAAS Fellows

AAAS Fellows who are current members of the Association are invited to nominate members for election as Fellows. A Fellow is defined as "a Member whose efforts on behalf of the advancement of science or its applications are scientifically or socially distinguished." A nomination must be sponsored by three AAAS Fellows, two of whom must have no affiliation with the nominee's institution.

Nominations undergo review by the Steering Groups of the Association's sections (the Chair, Chair-Elect, Retiring Chair, Secretary, and four Members-at-Large of each section). Each Steering Group reviews only those nominations designated for its section. Names of Fellow nominees who are approved by the Steering Groups are presented to the AAAS Council for election.

Nominations with complete documentation must be received by 12 May 2006. Nominations received after that date will be held for the following year. The nomination form and a list of current AAAS Fellows can be found on the AAAS Web site at www.aaas.org/aboutaaas/fellows. To request a hard copy of the nomination form, please contact Linda McDaniel at the AAAS Executive Office, 1200 New York Avenue, NW, Washington, DC, 20005, at 202-326-6635, or at Lmcdanie@aaas.org.

Results of the 2005 Election of AAAS Officers

Following are the results of the 2005 election. Terms begin on 21 February 2006.

General Offices
President-Elect: David Baltimore. *Board of Directors:* Alice P. Gast, Thomas D. Pollard. *Committee on Nominations:* Elizabeth Blackburn, Peter G. Brewer, Claire M. Fraser, Pauline O. Lawrence.

Section on Agriculture, Food, and Renewable Resources
Chair-Elect: James L. Van Etten. *Member-at-Large:* Eugene Nester. *Electorate Nominating Committee:* Thomas J. Guilfoyle, George E. Seidel Jr. *Council Delegate:* Jeffrey C. Silvertooth.

Section on Anthropology
Chair-Elect: A. Theodore Steegmann Jr. *Member-at-Large:* Cynthia M. Beall. *Electorate Nominating Committee:* John Kappelman, Lynnette Leidy Sievert.

Section on Astronomy
Chair-Elect: Alyssa A. Goodman. *Member-at-Large:* Julie Lutz. *Electorate Nominating Committee:* Karen S. Bjorkman, Steven Kilston.

Section on Atmospheric and Hydrospheric Sciences
Chair-Elect: Thomas P. Ackerman. *Member-at-Large:* Peter J. Webster. *Electorate Nominating Committee:* David D. Houghton, David A. Randall.

Section on Biological Sciences
Chair-Elect: Virginia Walbot. *Member-at-Large:* Marian Carlson. *Electorate Nominating Committee:* Daphne Preuss, Barbara T. Wakimoto.

Section on Chemistry
Chair-Elect: John C. Hemminger. *Member-at-Large:* Patricia A. Thiel. *Electorate Nominating Committee:* Marisa C. Kozlowski, David A. Tirrell.

Section on Dentistry and Oral Health Sciences
Chair-Elect: Ann Progulske-Fox. *Member-at-Large:* Beverly A. Dale-Crunk. *Electorate Nominating Committee:* Susan Kinder Haake, Philip Stashenko.

Section on Education
Chair-Elect: James H. Stith. *Member-at-Large:* Penny J. Gilmer. *Electorate Nominating Committee:* Sandra K. Abell, Bonnie J. Brunkhorst.

Section on Engineering
Chair-Elect: Gail H. Marcus. *Member-at-Large:* Herbert H. Richardson. *Electorate Nominating Committee:* Sangeeta N. Bhatia, Frank L. Huband. *Council Delegates:* James J. Duderstadt, Winfred M. Phillips.

Section on General Interest in Science and Engineering
Chair-Elect: Lynn E. Elfner. *Member-at-Large:* Linda Trocki. *Electorate Nominating Committee:* Jack O. Burns, Robert D. Crangle.

Section on Geology and Geography
Chair-Elect: James C. Knox. *Member-at-Large:* Greg Ravizza. *Electorate Nominating Committee:* Paul A. Baker, Debra A. Willard.

Section on History and Philosophy of Science
Chair-Elect: James R. Fleming. *Member-at-Large:* Douglas Allchin. *Electorate Nominating Committee:* Corinna Treitel, Virginia Trimble. *Council Delegate:* Sara Joan Miles.

Section on Industrial Science and Technology
Chair-Elect: Charles L. Liotta. *Member-at-Large:* Max G. Lagally. *Electorate Nominating Committee:* Thomas W. Eagar, Kenneth A. Jackson. *Council Delegate:* Steven W. Popper.

Section on Information, Computing, and Communication
Chair-Elect: Bryant W. York. *Member-at-Large:* Joel Moses. *Electorate Nominating Committee:* Barbara J. Grosz, Fred W. Weingarten.

Section on Linguistics and Language Science
Chair-Elect: Patricia K. Kuhl. *Member-at-Large:* Barbara Abbott. *Electorate Nominating Committee:* Jeanette K. Grundel, Richard T. Oehrle.

Section on Mathematics
Chair-Elect: Carl Pomerance. *Member-at-Large:* David Isaacson. *Electorate Nominating Committee:* Sheldon Axler, T. Christine Stevens.

Section on Medical Sciences
Chair-Elect: Jay A. Berzofsky. *Member-at-Large:* Judy Lieberman. *Electorate Nominating Committee:* H. Kim Bottomly, Phillip Scott. *Council Delegates:* Gail A. Bishop, Carol D. Blair, Ashley T. Haase, Paul A. Insel, Gary J. Nabel, Joann B. Sweasy.

Section on Neuroscience
Chair-Elect: Mary E. Hatten. *Member-at-Large:* Leslie P. Tolbert. *Electorate Nominating Committee:* Gail Mandel, Robert H. Wurtz.

Section on Pharmaceutical Sciences
Chair-Elect: Margaret O. James. *Member-at-Large:* Robert P. Hanzlik. *Electorate Nominating Committee:* William F. Elmquist, Anthony J. Hickey.

Section on Physics
Chair-Elect: Lawrence M. Krauss. *Member-at-Large:* Peter D. Barnes. *Electorate Nominating Committee:* Dawn A. Bonnell, Leonard C. Feldman.

Section on Psychology
Chair-Elect: Lynn Nadel. *Member-at-Large:* Roberta L. Klatzky. *Electorate Nominating Committee:* Richard J. Davidson, Barbara L. Finlay. *Council Delegate:* Robert A. Rescorla.

Section on Social, Economic, and Political Sciences
Chair-Elect: Linda G. Martin. *Member-at-Large:* Jeffrey D. Sachs. *Electorate Nominating Committee:* Michael Brintnall, Beth J. Soldo. *Council Delegate:* Charles F. Manski.

Section on Societal Impacts of Science and Engineering
Chair-Elect: Susan Hackwood. *Member-at-Large:* Elizabeth Chornesky. *Electorate Nominating Committee:* Donna Gerardi Riordan, Albert H. Teich.

Section on Statistics
Chair-Elect: Ron Brookmeyer. *Member-at-Large:* Juliet Popper Shaffer. *Electorate Nominating Committee:* Carol K. Redmond, James L. Rosenberger.

The Path Forward for Biofuels and Biomaterials

Arthur J. Ragauskas,[1]* Charlotte K. Williams,[4] Brian H. Davison,[6] George Britovsek,[4] John Cairney,[2] Charles A. Eckert,[3] William J. Frederick Jr.,[3] Jason P. Hallett,[3] David J. Leak,[5] Charles L. Liotta,[1] Jonathan R. Mielenz,[6] Richard Murphy,[5] Richard Templer,[4] Timothy Tschaplinski[7]

Biomass represents an abundant carbon-neutral renewable resource for the production of bioenergy and biomaterials, and its enhanced use would address several societal needs. Advances in genetics, biotechnology, process chemistry, and engineering are leading to a new manufacturing concept for converting renewable biomass to valuable fuels and products, generally referred to as the biorefinery. The integration of agroenergy crops and biorefinery manufacturing technologies offers the potential for the development of sustainable biopower and biomaterials that will lead to a new manufacturing paradigm.

We are apt to forget the gasoline shortages of the 1970s or the fuel price panic after Hurricane Katrina, but these are but harbingers of the inevitable excess of growing demand over dwindling supplies of geological reserves. Before we freeze in the dark, we must prepare to make the transition from nonrenewable carbon resources to renewable bioresources. This paper is a road map for such an endeavor.

Among the earliest drivers of chemical and biochemical research were the benefits to be gained from converting biomass into fuels and chemical products. At the beginning of the 20th century, many industrial materials such as dyes, solvents, and synthetic fibers were made from trees and agricultural crops. By the late 1960s, many of these bio-based chemical products had been displaced by petroleum derivatives (*1*). The energy crisis of the 1970s sparked renewed interest in the synthesis of fuels and materials from bioresources. This interest waned in the decades that followed as the oil price abated. However, this meant that global consumption of liquid petroleum tripled in the ensuing years (*2*). Indeed, energy demand is projected to grow by more than 50% by 2025, with much of this increase in demand emerging from several rapidly developing nations. Clearly, increasing demand for finite petroleum resources cannot be a satisfactory policy for the long term.

Hoffert *et al*. (*3*) and others (*4*) have provided a global perspective on these energy challenges and their relationship to global climate stability. As these authors point out, future reductions in the ecological footprint of energy generation will reside in a multifaceted approach that includes nuclear, solar, hydrogen, wind, and fossil fuels (from which carbon is sequestered) and biofuels. These concerns have also been advanced by the recent Joint Science Academies' statement to the Gleneagles G8 Summit in July 2005, *Global Response to Climate Change*, which asserts that the warming of the planet can be attributed to human activities and identifies the need for action now to pinpoint cost-effective steps to contribute to substantial and long-term reductions in net greenhouse gas emissions (*5*).

Shifting society's dependence away from petroleum to renewable biomass resources is generally viewed as an important contributor to the development of a sustainable industrial society and effective management of greenhouse gas emissions. In the United States, bioethanol derived primarily from corn contributes ~2% to the total transportation fuels mix; another ~0.01% is based on biodiesel. The U.S. Department of Energy has set goals to replace 30% of the liquid petroleum transportation fuel with biofuels and to replace 25% of industrial organic chemicals with biomass-derived chemicals by 2025 (*2*, *6*). The European Union Directive 2003/30/EC ("the Biofuels Directive") adopted in 2003 targeted 2% of all petrol and diesel transport fuels to be biomass-derived by December 2005 and 5.75% by December 2010. This directive was motivated by concerns to ensure the security of the European energy supply, environmental sustainability, and achievement of Kyoto Protocol targets (*2*). These biomaterials and biofuels production targets are certainly achievable; Parikka (*7*) has reported the current sustainable global biomass energy potential at ~10^{20} joules per year, of which ~40% is currently used.

Given these accomplishments, a key question is "When will biorefineries be ready to make a major contribution?" One answer, coming from a forum at the 27th Symposium on Biotechnology for Fuels and Chemicals, was that some applications are ready now, but their impact will be limited with current technologies and feedstocks (*8*). We need commercialization and policy support for current and near-term opportunities to grow the industry from its present base. Equally important, we need research and development to increase the impact, efficiency, and sustainability of biorefinery facilities. The current production and use of bioethanol and biodiesel processes are a starting point. It is our belief that the next generational change in the use of bioresources will come from a total integration of innovative plant resources, synthesis of biomaterials, and generation of biofuels and biopower (Fig. 1).

Innovative Plant Design via Accelerated Domestication

"More, Bigger, and Better," the mantra of modern consumerism, also summarizes—ironically—the goals of research aimed at modifying plant species for use in sustainable biomass production. Interrelated plant traits such as higher yield, altered stature, resilience to biotic and abiotic challenge, and biomass composition will increase industrial crop value in terms of biofuels and biomaterials. The challenge is to weave these different strands of research into an integrated production strategy.

Currently, the global yield for all biomass crops, including woody and herbaceous crops growing in temperate and subtropical regions, varies from ~8 dry Mg ha^{-1} $year^{-1}$ (for willow in Sweden) to 10 to 22 dry Mg ha^{-1} $year^{-1}$ (for short-rotation woody crops in the United States). Some commercial plantations in Brazil have reported up to 20 dry Mg ha^{-1} $year^{-1}$. A conservative global biomass average would be ~10 dry Mg ha^{-1} $year^{-1}$, although some small-scale field trials have reported four times this level of biomass production (*9*, *10*). The grand challenge for biomass production is to develop crops with a suite of desirable physical and chemical traits while increasing biomass yields by a factor of 2 or more. Although many annual crops benefit from centuries of domestication efforts, perennial species that could play a central role in providing a renewable source of feedstock for conversion to fuels and materials have not had such attention to date. Doubling the global productivity of energy crops will depend on identifying the fundamental constraints on productivity and addressing those constraints with modern genomic tools (Fig. 2).

An obvious target is manipulation of photosynthesis to increase the initial capture of light energy, which at present is less than 2%. Recently, this approach has had some success using engineered genes from plants and photosynthetic bacteria. For example, ribulose-1,5-

[1]School of Chemistry and Biochemistry, [2]School of Biology, [3]School of Chemical and Biomolecular Engineering, Georgia Institute of Technology, Atlanta, GA 30332, USA. [4]Department of Chemistry, [5]Division of Biology, Imperial College London, London SW7 2AZ, UK. [6]Life Sciences Division, [7]Environmental Sciences Division, Oak Ridge National Laboratory, Oak Ridge, TN 37831, USA.

*To whom correspondence should be addressed. E-mail: arthur.ragauskas@chemistry.gatech.edu

bisphosphate carboxylase-oxygenase (RuBisCO), the plant enzyme that converts CO_2 to organic carbon by carboxylation during photosynthesis, also conducts a competing, less efficient oxygenation reaction. When an inorganic carbon transporter gene from cyanobacteria was expressed in plants, the more efficient carbon-fixing photosynthetic reaction of RuBisCO was favored. In another approach, the cyanobacterial versions of two rate-limiting enzymes in the chloroplast's carbon-fixing "dark reaction" were overexpressed in tobacco, resulting in an elevated rate of photosynthesis and increased plant dry weight (*11*).

In addition to manipulating photosynthesis to increase the initial capture of light energy, the manipulation of genes involved in nitrogen metabolism has also been a successful approach to increasing biomass. For example, in a 3-year field trial of transgenic poplar (*P. tremula* × *P. alba*) overexpressing a glutamine synthase gene (*GS1*), tree height increased to 141% that of control plants by the third year of the study (*12*). The potential of *GS1* for engineering biomass increase is further emphasized by results showing that quantitative trait loci for yield in maize and maritime pine map to the location of *GS1*. Similar possibilities are evident in the overexpression of a bacterial glutamate dehydrogenase, which increased the biomass of tobacco plants under both laboratory and field conditions (*13*).

Much research has been devoted to protecting food and fiber supplies from biological and environmental stress by transferring genetically engineered versions of plant defense genes to crop plants. By this method, different plant lines have been generated that, relative to controls, grow at elevated rates under drought and high- and low-temperature stress; they also survive pathogen attack (*14*). Furthermore, plants typically invest considerable energy in making reproductive structures, and if flowering can be delayed or prevented, this energy may be transferred into increasing the overall biomass of the plant. In addition, by delaying or shortening the winter dormancy of plants, the growth phase of plants can be extended; regulators for this process are being investigated.

Additional research has revealed the coregulation of lignin and cellulose biosynthesis in several studies (*15*). Repressing a single lignin biosynthetic gene, *4-CL*, resulted in a reduction in lignin content with a concomitant increase in cellulose, an effect that can be amplified by cotransformation of multiple genes (*16*). Conversely, an *Arabidopsis* CESA3 mutant, impaired in cellulose biosynthesis, had altered lignin synthesis. In several cases, manipulation of the expression of lignin biosynthesis genes resulted in alteration in lignin structure rather than alteration in quantity. Because the efficiency of biomass conversion depends on hydrolyzing agents gaining access to plant polysaccharides, alteration of plant cell wall structure could yield important advantages. For example, when the lignin biosynthesis gene *CCR* is down-regulated in poplar, the cellulose component of the plant cell wall is more easily digested by the bacterium *Clostridium*

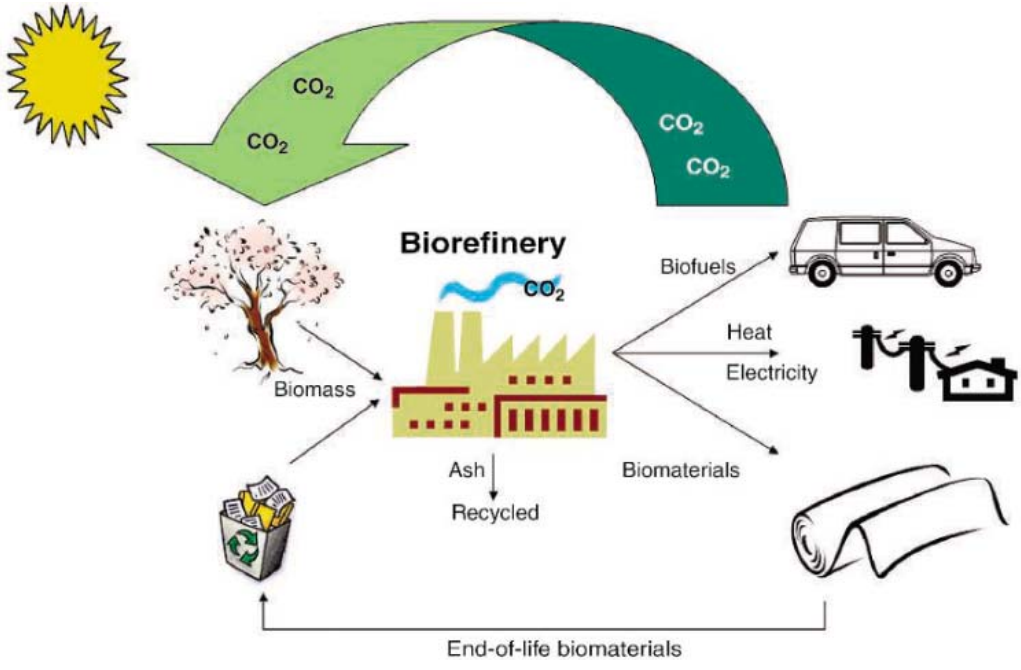

Fig. 1. The fully integrated agro-biofuel-biomaterial-biopower cycle for sustainable technologies.

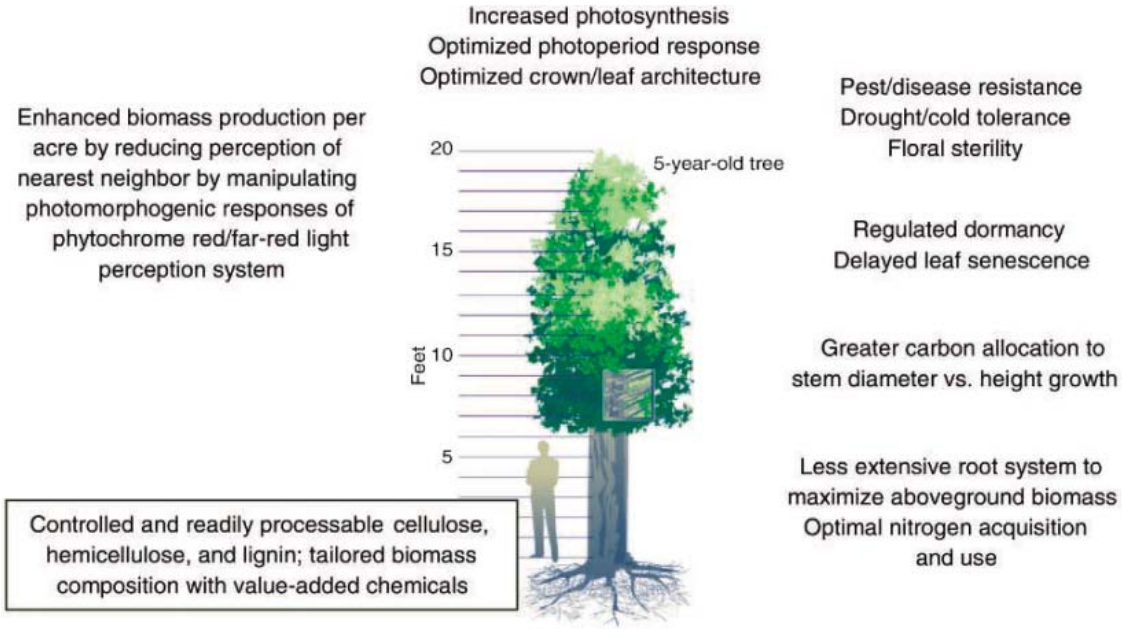

Fig. 2. Overview of plant traits that can be targeted by accelerated domestication for enhanced plant biomass production and processing.

cellulolyticum, and twice as much sugar is released (*15*). The intensive genetic engineering used to alter lignin structure and content with the goal of improving wood and papermaking quality shows the potential of these approaches (*15*). In summary, advances in plant sciences and genetics are providing researchers with the tools to develop the next generation of agro-energy/material crops having increased yield and utility tailored for modern biorefinery operations.

Biomaterials from Biorefineries

These advances in plant sciences will need to be captured in subsequent biorefinery operations. In essence, the modern biorefinery parallels the petroleum refinery: An abundant raw material consisting primarily of renewable polysaccharides and lignin (Fig. 3) enters the biorefinery and, through an array of processes, is fractionated and converted into a mixture of products including transportation fuels, co-products, and direct energy.

The power of the biorefinery concept is supported by economies of scale and by efficient use of all incoming bioresources. A key aspect of the biorefinery concept is the imbalance between commodity chemical needs and transportation fuels. Using the petroleum industry as an illustrative example, ~5% of the total petroleum output from a conventional refinery goes to chemical products; the rest is used for transportation fuels and energy. Most visions for integrated biorefineries do not expect this ratio to change (*17*).

The paradigm shift from petroleum hydrocarbons to highly oxygen-functionalized, bio-based feedstocks will create remarkable opportunities for the chemical processing industry. For example, the use of carbohydrates as chemical raw materials will eliminate the need for several capital-intensive, oxidative processes used in the petroleum industry. Biomass carbohydrates will provide a viable route to products such as alcohols, carboxylic acids, and esters. These natural products are also stereo- and regiochemically pure, thereby reducing dependence on expensive chiral catalysts and complex syntheses that are currently required to selectively install chemical functionality in petrochemicals.

Bio-based feedstocks are already having an impact on some practical applications, including solvents, plastics, lubricants, and fragrances. Bio-derived plastics such as polylactic acid are attracting attention, in part because of their biological compatibility and hydrolytic degradation, which enables them to successfully replace petrochemicals as well as open up new applications. Polylactic acid is currently manufactured on a million-kilogram scale in the United States and on a smaller scale in Europe and Japan (*18*). This process ferments corn dextrose to produce lactic acid that is subsequently dimerized, polymerized, and used in several applications, including food packaging and the apparel industry. The production of lactic acid by fermentation is economically competitive with its chemical synthesis from acetaldehyde and hydrogen cyanide. Further reductions in cost are expected with improvements in the fermentation process and the use of waste agricultural materials as feedstocks. Another example is the production of 1,3-propanediol by the fermentation of carbohydrates. This process is being exploited to supplement the use of petrochemically derived 1,3-propanediol to make poly(trimethylene terephthalate), a polymer fiber with properties related to nylon and polyethylene terephthalate. These commercially viable processes do, however, require purified feedstocks. The major impediment to biomass use is the development of methods to separate, refine, and transform it into chemicals and fuels.

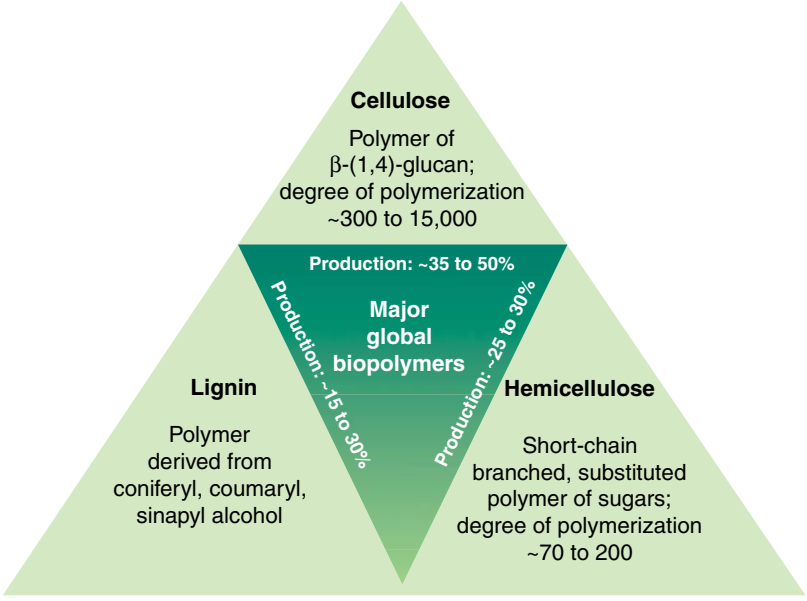

Fig. 3. Key global biomass resources from agricultural residues, wood, and herbaceous energy crops.

One of these steps, separation, currently accounts for 60 to 80% of the process cost of most mature chemical processes. As we progress from the oil refinery to the biorefinery, the challenges associated with separation will change, but not diminish, in importance. In the petroleum industry, distillation is the unit operation that dominates the refinery separation scheme. For chemicals derived from biomass, this dominance will be transferred to solvent-based extraction. This is a result of the non-volatile nature of most biomass components and the fact that other separation techniques, such as chromatography or membranes, do not yet have the same economies of scale.

Future biorefinery operations will first extract high-value chemicals already present in the biomass, such as fragrances, flavoring agents, food-related products, and high-value nutraceuticals that provide health and medical benefits (*19*). Once these relatively valuable chemicals are extracted, the biorefinery will focus on processing plant polysaccharides and lignin into feedstocks for bio-derived materials and fuels. This requires the development of innovative separation and depolymerization process chemistries. Supercritical CO_2, near-critical water, and gas-expanded liquids are well suited to these challenges (*20*, *21*). These tunable solvents offer distinct green chemistry processing advantages (*22*) that could be exploited in the processing of renewable bioresources. Supercritical fluids exhibit outstanding transport properties coupled with highly tunable solvent properties (such as solvent power and polarity) and ease of solvent removal. Near-supercritical fluids are also highly tunable and generally offer better transport than liquids and better solvent power than supercritical fluids. Gas-expanded liquids are mixtures of a gas with an organic liquid such as methanol or acetone; in our context the gas is CO_2, which is completely miscible with most organics. These solvents exhibit highly tunable solvent power, as small pressure changes yield large changes in composition, and they give much greater solubilities and operate at much lower pressures than supercritical fluids. All of these solvents result in advantages for downstream processing in terms of product purification and/or catalyst recycling.

Water is arguably the most environmentally benign and food-safe solvent that can be used in chemical synthesis. However, the range of water-soluble substrates is quite limited, making ambient water an unsuitable medium for many chemical syntheses. Near-critical water (200° to 300°C) exhibits a reduction in dielectric constant (20 to 30) and density (0.7 to 0.8 g/cm^3) relative to ambient water; its ability to dissolve both nonpolar organic molecules and inorganic salts is comparable to that of the popular organic solvent acetone. In addition, under these conditions, the dissociation constant of water into hydroxide and hydrogen ions rises

by more than three orders of magnitude, so that near-critical water also acts as a self-neutralizing acid or base catalyst, eliminating salt waste generation (*23*). Further, the use of near-critical water in place of organic solvents greatly simplifies product isolation, as nonpolar products are insoluble after cooling. The utility of this medium has been demonstrated for a diverse group of organic syntheses (*24*). High-temperature water has already been proposed for the depolymerization of cellulosic waste materials in the Biometics process for producing levulinic acid (*25*).

The sugars in the biorefinery process can be transformed into building-block chemicals by fermentation as well as by enzymatic and chemical transformations. The key building block chemicals will include ethanol, C3 to C6 carboxylic acids (e.g., hydroxypropanoic acid, glucaric acid), and alcohols such as glycerol and sorbitol. It is noteworthy that the current cost of many carbohydrates and their derivatives is already competitive with petrochemicals and solvents such as toluene, aniline, and acetaldehyde (*26*). The U.S. Department of Energy recently published a comparative study on the top 12 chemicals from carbohydrate biomass, identifying several particularly promising compounds including sorbitol, levulinic acid, and glycerol (*27*). The effective production and use of these chemicals rely on the development of innovative enzymatic and catalytic green chemistries that will yield a viable range of new bioderived products.

Biofuels: Biopower from Biorefineries

After extracting value-added chemicals from biomass in the early stages of a biorefinery, the separations and chemical operations will need to be shifted to the production of biofuels. Today's bioethanol plant process relies largely on the fermentation of starch from corn in the United States or from sugar cane in Brazil (*2*, *7*). Enhancing the cost structure of bioethanol generation has moved research attention away from plant grains and more toward corn stovers, trees, and other low-cost agricultural and municipal waste materials (*28*, *29*). These biomaterials typically have higher amounts of cellulose and hemicellulose, and their efficient, cost-effective depolymerization remains a key challenge in their use.

One important tool in reducing the cost of this depolymerization is pretreatment of lignocellulosics to make the biomass matrix more accessible to enzymes. The tailoring of chemical and physical pretreatments for specific biomass resources is a field of growing interest and practicality (*30*). These pretreatment benefits are leveraged with recent research efforts that have reduced the cost of cellulase by a factor of 5 to 10 (*31*). Future cost reductions in bioprocessing will be accomplished by combining cellulase/hemicellulase treatments with other process steps. For example, researchers have proposed combining cellulase production with the fermentation steps via modified microorganisms capable of both cellulase production and ethanol fermentation, which could provide just-in-time delivery of the optimal mixture of the hydrolytic enzymes (*32*).

The endogenous production of such polysaccharide hydrolyase enzymes could also be coupled with enhanced plant biomass production made possible by recent advances in molecular farming (*33*). Exogenous depolymerization enzymes used in the bioethanol process could be replaced with plants that are capable of synthesizing these enzymes in situ. Carbohydrate depolymerase enzymes, such as cellulase, could be triggered for plant biosynthesis when an inducer is applied to the plant. A signal sequence from a cell wall protein could be spliced onto the cellulase gene to ensure that the cellulase synthesized by the plant is localized to the plant cell wall. The cellulase signal sequence-coding region would be attached to a chemically induced promoter that would switch on the cellulase gene. Once the modified cellulase transgene is introduced into a host plant, seeds could be produced, planted, and cultivated normally. Just before harvest, the crop would be sprayed with the chemical inducer. The cellulase would then be produced and transported to the cell wall, where it would start to break down the cellulose. After harvesting, the residual plant material would be collected and transported to a biorefinery, during which the in situ–generated cellulase would continue to depolymerize cellulose to glucose. An added feature of this approach is that additional depolymerization enzymes could be brought to bear for further, no-cost conversion of plant polysaccharides to mono- or oligosaccharides, facilitating subsequent separation or fermentation operations.

Currently, the fermentation of a mixture of hexoses and pentoses is inefficient because no wild organisms have been found that can convert all sugars at high yield into ethanol. Recently, several groups have made great advances in this field by genetically modifying microorganisms. One promising strategy has been to take a natural hexose ethanologen and add the pathways to convert other sugars. This strategy has been effective in adding pentose conversion to *Saccharomyces cerevisiae* and to *Zymomonas mobilis* (*34*, *35*). The other primary strategy has been to modify a host capable of converting multiple sugars to produce only ethanol from glycolysis. Other remaining microbiological challenges include the need to understand and manipulate ethanol and sugar tolerance and resistance to potential inhibitors generated in presaccharification treatments. Solutions to these issues also will need to accommodate the variability in biomass resources.

Biological processing is not the only refining approach, however. Although biological protocols of converting polysaccharides to bioethanol are among the most developed process technologies available for biofuels, other burgeoning chemical technologies are being pursued and present promising alternatives. These biofuels technologies are centered on the removal of oxygen from carbohydrates to obtain oxygenated hydrocarbons. As summarized in Fig. 4, controlled elimination of water from sugars has been extensively studied and can provide 5-hydroxymethyl-2-furfural (HMF), levulinic acid, and other organic acids.

Although these materials are too polar for direct liquid fuel applications, they could be used as a resource for subsequent conversion to alternative fuels. For example, controlled decarboxylation and dehydration of hexoses could yield structures such as valerolactone or 2-methylfuran. These relatively nonpolar compounds could be considered as components for novel gasoline blends, which are typically dependent on ~C5 to C10 hydrocarbons. The controlled decarboxylation and dehydration of sugars is an essential objective of this process, as overdehydration will lead to polymeric materials that have little value as biofuels. These proposed products will not provide a viable diesel supplement because diesel fuel typically relies on C12 to C20 hydrocarbons. Given the higher vapor pressure requirements of diesel fuel, these issues could be addressed by subsequent dimerization of HMF, valerolactone, or related compounds, which will increase the chain length of these biodiesel precursors.

Dumesic and co-workers recently demonstrated the potential of this pathway (*36*). Using a catalytic system containing both acidic and noble metal catalysts, they were able to dehydrate and hydrogenate an aqueous stream of sorbitol to hexane. They also showed that an aldol-crossed condensation between HMF and acetone leads to C9 to C15 alkanes when performed under a hydrogen atmosphere in the presence of a Pt/SiO_2-Al_2O_3 catalyst. This field of study is ripe for further rapid advances as the revolution in catalysis, computational modeling, and combinatorial chemistry will lead to a suite of catalytic systems that will facilitate the conversion of biomass polysaccharides to liquid alkanes and oxyalkanes for fuel applications.

For the biorefinery approach to be widely applicable, the lignin component of lignocellulosics must also be addressed (*37*). Residual lignin from paper pulping is now burned for heat and power, but lignin thermal-cracking studies using temperatures of ~250° to 600°C have demonstrated the potential of generating low molecular weight feedstocks for further processing (*28*). These high temperatures suggest that the use of cracking catalysts could lower conversion temperatures and provide improved control over product distributions. Shabtai *et al*. (*29*) have highlighted this potential in a process whereby a two-stage catalytic reaction with lignin produces a reformulated, partially

oxygenated gasoline-like product. Lignin is first depolymerized by a base-catalyzed treatment into a series of low molecular weight phenolic compounds. This mixture is then subjected to hydroprocessing, which primarily yields a mixture of alkylbenzenes useful as a potential liquid biofuel.

This pyrolysis approach to biofuels from lignin is also being pursued with biomass in general, with and without a catalyst; it provides about 58 to 77% conversion of biomass to a condensable gas, 13 to 28% noncondensable gases, and 6 to 13% char formation. The condensable gases can be refined to fuels and chemicals, and the noncondensables can be steam-reformed to synthesis gas (syngas), a mixture of CO and H_2, which can also be used to produce fuels and chemicals (*38*).

Regardless of which process technologies are incorporated into a biorefinery, almost all will generate some waste products that will be intractable and difficult to convert to value-added biomaterials or biofuels. These spent-biomass residues will contain fragments from lignin, residual carbohydrates, and other organic matter. This residue will need to be treated in an environmentally compatible manner, with the smallest ecological footprint. Such wastes and residues offer important energy sources within the biorefinery, given their chemical energy content, and are an ideal candidate for thermochemical conversion to syngas (*39*). Syngas is an intermediate in the production of ammonia, methanol, and Fischer-Tropsch hydrocarbons. Production of syngas from coal, natural gas, and other carbonaceous sources is well established. Coal is normally gasified in entrained-flow reactors at temperatures exceeding 1400°C at 20 to 70 bar. Biomass is more reactive than coal and is usually gasified at temperatures between 800° and 1000°C at 20 to 30 bar.

The greatest challenge in producing syngas from biomass is the need to avoid poisoning the noble metal catalysts used in the subsequent downstream conversion to fuels and chemicals. Potential problem products are the alkali metals, halides, sulfur gases, and especially the tars. A high quantity of tar is produced as the organic components of biomass decompose. Evolution of tar from primary to tertiary species is rapid, but tertiary tar species are degraded slowly to CO and H_2 by water vapor or CO_2 at temperatures below 1100°C. Catalytic conversion of tar in raw syngas to CO and H_2 is practiced, but the quantities of tar that must be converted are large, and robust catalysts that are insensitive to alkali metals, halides, sulfur, and nitrogen need to be developed.

Chloride, the predominant halide in biomass, is converted to HCl or submicrometer aerosols of potassium and sodium during gasification, which poses a corrosion issue. Most of the alkali metal chlorides are removed by filtering the cooled syngas. Sulfur gases can be removed by absorption. Remaining alkali metal chlorides and sulfur gases are removed by reaction with ZnO in a packed-bed filter. Although these advances in syngas purification technologies are necessary for the catalytic conversion of syngas to other fuels or chemicals, they add further complications and increase the overall cost.

Anaerobic fermentation of syngas into biofuels is a promising competing technology that is far more tolerant of tar and trace contaminants than noble metal catalysts (*40*). Development of enhanced bioagents, reactor designs with improved mass transfer of the syngas into the liquid phase, and enhanced gas and liquid separation methods are needed if the biochemical route is to become economically viable. As these challenges are addressed, the final component of the integrated biorefinery will become available, and the resulting residue products from the biorefinery will become a valuable resource for biopower, biofuels, and biomaterial generation.

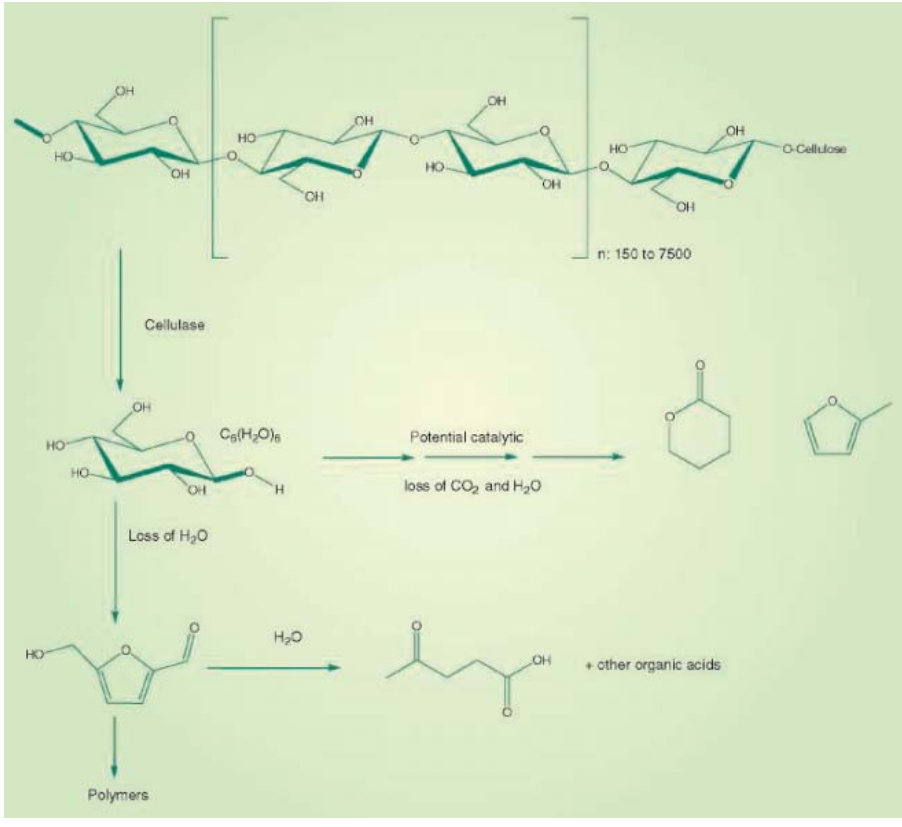

Fig. 4. Dehydration-decarboxylation chemistry of hexoses.

Concluding Remarks

In view of changing world energy needs, a research road map for the biorefinery of the 21st century is vital. This biorefinery vision will contribute to sustainability not only by its inherent dependence on sustainable bioresources, but also by recycling waste, with the entire process becoming carbon neutral. It leverages our knowledge in plant genetics, biochemistry, biotechnology, biomass chemistry, separation, and process engineering to have a positive impact on the economic, technical, and environmental well-being of society.

An integrated biorefinery is an approach that optimizes the use of biomass for the production of biofuels, bioenergy, and biomaterials for both short- and long-term sustainability. The demands of future biorefineries will stimulate further advances in agriculture in which tailored perennial plants and trees will provide increasing amounts of bioresources, as highlighted in the "Billion-Ton" report (*10*). The advances in plant science will certainly be influenced by societal policies, land use practices, accelerated plant domestication programs, and research funding to develop this vision. Nonetheless, given humanity's dependence on diminishing nonrenewable energy resources, this is a challenge that must be addressed—and we need to get on with it!

References and Notes

1. J. P. van Wyk, *Trends Biotechnol.* **19**, 172 (2001).
2. A. B. Lovins *et al.*, in *Winning the Oil Endgame: Innovation for Profits, Jobs, and Security*, B. T. Aranow, Ed. (Rocky Mountain Institute, Snowmass, CO, 2004), pp. 1–122.
3. M. I. Hoffert *et al.*, *Science* **298**, 981 (2002).
4. S. Pacala, R. Socolow, *Science* **305**, 968 (2004).
5. *Global Response to Climate Change* (available at www.g8.gov.uk/servlet/Front?pagename=OpenMarket/Xcelerate/ShowPage&c=Page&cid=1123951048479).
6. H. L. Chum, R. P. Overend, *Adv. Solar Energy* **15**, 83 (2003).
7. M. Parikka, *Biomass Bioenergy* **27**, 613 (2004).
8. Program and Abstracts, 27th Symposium on Biotechnology for Fuels and Chemicals, Golden, CO,

1 to 4 May 2005 (available at www.eere.energy.gov/biomass/biotech_symposium).
9. G. Berndes, C. Azar, T. Kaberger, D. Abrahamson, *Biomass Bioenergy* **20**, 371 (2001).
10. R. D. Perlack *et al.*, *Biomass as Feedstock for a Bioenergy and Bioproducts Industry: The Technical Feasibility of a Billion-Ton Annual Supply* (U.S. Department of Energy and U.S. Department of Agriculture, April 2005; available at feedstockreview.ornl.gov/pdf/ billion_ton_vision.pdf).
11. W. Van Camp, *Curr. Opin. Biotechnol.* **16**, 147 (2005).
12. Z. P. Jing *et al.*, *New Phytol.* **164**, 137 (2004).
13. A. G. Good, A. K. Shrawat, D. G. Meunch, *Trends Plant Sci.* **12**, 597 (2005).
14. B. Vinocur, A. Altman, *Curr. Opin. Biotechnol.* **16**, 123 (2005).
15. A. M. Boudet, S. Kajita, J. Grima-Pettanati, D. Goffner, *Trends Plant Sci.* **8**, 576 (2003).
16. L. Li *et al.*, *Proc. Natl. Acad. Sci. U.S.A.* **100**, 4939 (2003).
17. B. Kamm, M. Kamm, *Appl. Microbiol. Biotechnol.* **64**, 137 (2004).
18. R. Auras, B. Harte, S. Selke, *Macromol. Biosci.* **4**, 835 (2004).
19. P. Morandini, F. Salamini, P. Gantet, *Curr. Med. Chem. Immun. Endocr. Metab. Agents* **5**, 103 (2005).
20. S. A. Nolen, C. L. Liotta, C. A. Eckert, *Green Chem.* **5**, 663 (2003).
21. C. A. Eckert, C. L. Liotta, D. Bush, J. S. Brown, J. P. Hallett, *J. Phys. Chem. B* **108**, 18108 (2004).
22. S. K. Ritter, *Chem. Eng. News* **82** (28), 4 (2004).
23. T. S. Chamblee, R. R. Weikel, S. A. Nolen, C. L. Liotta, C. A. Eckert, *Green Chem.* **6**, 382 (2004).
24. N. Akiya, P. E. Savage, *Chem. Rev.* **102**, 2725 (2002).
25. S. W. Fitzpatrick, Patent Cooperation Treaty (PCT) International Application, WO 9640609 A1 19961219 CAN 126:117739 (1996).
26. F. W. Lichtenthaler, *Acc. Chem. Res.* **35**, 728 (2002).
27. T. Werpy *et al.*, *Top Value Added Chemicals From Biomass, Volume 1—Results of Screening for Potential Candidates from Sugars and Synthesis Gas* (U.S. Department of Energy, Oak Ridge, TN, August 2004; available at www.eere.energy.gov/biomass/pdfs/35523.pdf).
28. P. F. Britt, A. C. Buchanan, M. J. Cooney, D. R. Martineau, *J. Org. Chem.* **65**, 1376 (2000).
29. J. S. Shabtai, W. W. Zmierczak, E. Chornet, D. Johnson, USA Patent Application 972,461 (2003).
30. N. Mosier *et al.*, *Bioresour. Technol.* **96**, 673 (2005).
31. Cellulase Cost-Reduction Contracts (Biomass Program, Office of Energy Efficiency and Renewable Energy, U.S. Department of Energy; available at www.eere.energy.gov/biomass/cellulase_cost.html).
32. Y.-H. Zhang, L. R. Lynd, *Proc. Natl. Acad. Sci. U.S.A.* **102**, 7321 (2005).
33. A. S. Rishi, N. D. Nelson, A. Goyal, *J. Plant Biochem. Biotechnol.* **10**, 1 (2001).
34. S. S. Helle, A. Murray, J. Lam, D. R. Cameron, S. J. B. Duff, *Bioresour. Technol.* **92**, 163 (2004).
35. H. G. Lawford, J. D. Rousseau, *Appl. Biochem. Biotechnol.* **98-100**, 429 (2002).
36. G. W. Huber, J. N. Chheda, C. J. Barrett, J. A. Dumesic, *Science* **308**, 1446 (2005).
37. F. S. Chakar, A. J. Ragauskas, *Ind. Crop. Prod.* **20**, 131 (2004).
38. A. A. Boateng, K. B. Hicks, K. P. Vogel, *J. Anal. Appl. Pyrolysis,* in press.
39. V. Sricharoenchaikul, P. Agrawal, W. J. Frederick Jr., *Ind. Eng. Chem. Res.* **41**, 5640 (2002).
40. M. D. Bredwell, P. Srivastava, R. M. Worden, R. Mark, *Biotechnol. Prog.* **15**, 834 (1999).
41. Supported by NSF Performance for Innovation Program grant EEC0525746, NSF Plant Genome Program grant 0217594, and USDA Novel Biomass Processing Chemistry grant USDA 2003-35504-13620. We thank T. Welton for his guidance and input on several issues in this paper. This work was partially supported by Oak Ridge National Laboratory, operated for the U.S. Department of Energy under contract DE-AC05-00OR22725.

10.1126/science.1114736

Thank you

to all of the sponsors and supporters of the 2006 AAAS Annual Meeting.

SUBARU

Premier Sponsor

MONSANTO imagine®

Principal Sponsor

SIGMA-ALDRICH

NATIONAL SCIENCE FOUNDATION

Johnson & Johnson PHARMACEUTICAL RESEARCH & DEVELOPMENT, L.L.C.

MERCK Research Laboratories

THE GEOLOGICAL SOCIETY OF AMERICA

L'ORÉAL

SUPPORTERS:

The British Consulate General —Chicago & UK Trade & Investment

Glenn Medical Research Foundation

Merck/AAAS Undergraduate Science Research Program

Prologue Ventures

U.S. Department of Agriculture, Agricultural Research Service, Office of Scientific Quality Review

Visit our Web site for full meeting details:
www.aaasmeeting.org

YYePG Proudly Presents, Thx for Support

AAAS
ADVANCING SCIENCE, SERVING SOCIETY

The Orbital Period of the Ultraluminous X-ray Source in M82

Philip Kaaret,* Melanie G. Simet, Cornelia C. Lang

Intermediate-mass black holes (*1*), which have masses in the range 10^2 to 10^4 solar masses ($M_\odot$)—larger than can be produced in the collapse of a single normal star and smaller than the supermassive black holes found in galactic nuclei—would be a new class of astrophysical object and may be important in the formation of supermassive black holes (*2*). The brightest x-ray source in the nearby starburst galaxy M82 has an apparent luminosity reaching 10^{41} erg s^{-1}, indicating a mass exceeding 500 $M_\odot$ (*2*, *3*). Its displacement from the galaxy nucleus indicates a mass less than 10^5 $M_\odot$ because of dynamical friction (*3*). The source also shows quasiperiodic x-ray oscillations at frequencies of 0.05 to 0.1 Hz, suggestive of a mass near 100 to 1000 $M_\odot$ (*4*).

We monitored the x-ray emission from M82 every other day for 240 days with the Proportional Counter Array on the Rossi X-ray Timing Explorer satellite (*5*). We found that the x-ray flux from M82 is modulated (Fig. 1), with a peak-to-peak amplitude corresponding to an isotropic luminosity of 2.4×10^{40} erg s^{-1} in M82 and a period of 62.0 ± 2.5 days. The peak arrival times appear periodic to the accuracy of measurement.

X-ray modulations at the orbital period are known from several black hole x-ray binaries (*6*–*9*). Therefore, we interpret the x-ray periodicity from M82 as the orbital period of the ultraluminous x-ray source (ULX). Superorbital modulations in black hole x-ray binaries occur with periods of 162 to 600 days, which are longer than the observed period.

The high inferred luminosity indicates that the black hole is gravitationally pulling mass directly from the outer surface of its companion star via Roche-lobe overflow (*10*). Because of the geometry of the binary system, the orbital period is related to the companion star density $\rho \approx 115\ P^{-2}$ g cm^{-3}, where P is the period in hours (*11*). For a 62-day orbital period, the mean density of the companion star is 5×10^{-5} g cm^{-3}. This excludes normal main-sequence stars, which are denser than 10^{-2} g cm^{-3}, but is compatible with giant or supergiant stars.

The ULX in M82 lies close to (as projected on the sky) and possibly within the super star cluster MGG 11 (*10*, *12*). An intermediate-mass black hole may have been formed by stellar collisions in the extremely dense core of MGG 11 (*12*). Infrared spectroscopy of MGG 11 shows that its near-infrared light is dominated by red supergiant stars (*13*, *14*). Hence, the cluster has existed long enough for the ULX companion star to evolve to the giant stage.

When the companion star of an intermediate-mass black hole evolves through the giant phase, mass transfer causes the orbit to widen, and the orbital period increases through 10 to 100 days as the mass transfer rate reaches 10^{-4} $M_\odot$ $year^{-1}$ for an initial companion mass near 15 $M_\odot$ (*15*, *16*). This mass transfer rate is sufficient to power an x-ray luminosity of 10^{41} erg s^{-1}. The lifetime of this phase is short, of order 10^5 years, compared with the companion age of 10^7 years, suggesting that we are fortunate to see the M82 ULX during a brief and unusually bright phase of its evolution and that other ULXs reaching such extreme luminosities, near 10^{41} erg s^{-1}, should be rare.

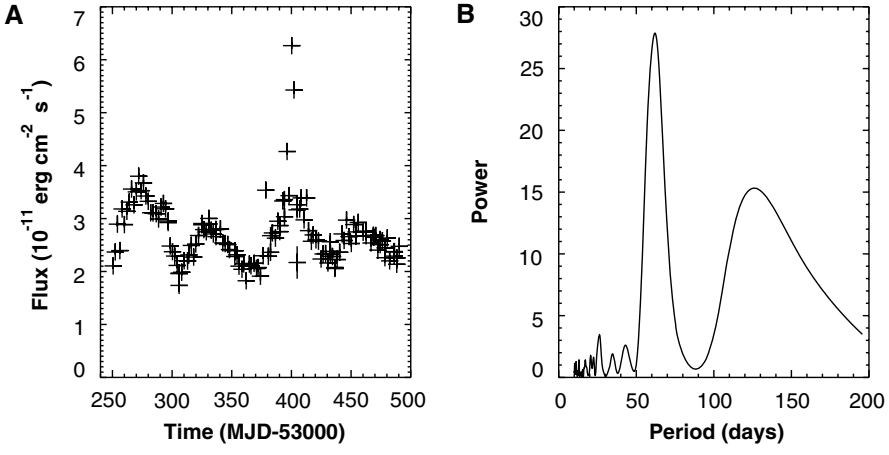

Fig. 1. (**A**) X-ray light curve of M82. The x-ray flux in the 2- to 10-keV band from M82 was measured with the Proportional Counter Array on the Rossi X-ray Timing Explorer is shown versus time in modified Julian days (MJD). A periodicity near 60 days is evident with a peak-to-peak flux of 1.5×10^{-11} erg cm^{-1} s^{-1}. There is an x-ray flare at MJD 53400.2. (**B**) A periodogram of the data in (A) and two earlier data points from MJD 53098.9 and 51153.7. The peak at 62.0 ± 2.5 days has a power of 27.9 (*17*). The chance probability of occurrence, taking into account the number of trials, is 1.1×10^{-10}. Removing the two early data points or points with fluxes above 4×10^{-11} erg cm^{-1} s^{-1} does not significantly shift the peak. There is a secondary peak at 125.7 days with a power of 15.3.

References and Notes

1. E. J. M. Colbert, R. F. Mushotzky, *Astrophys. J.* **519**, 89 (1999).
2. A. Ptak, R. Griffiths, *Astrophys. J.* **517**, L85 (1999).
3. P. Kaaret *et al.*, *Mon. Not. R. Astron. Soc.* **321**, L29 (2001).
4. T. Strohmayer, R. F. Mushotzky, *Astrophys. J.* **586**, L61 (2003).
5. H. V. Bradt, R. E. Rothschild, J. H. Swank, *Astron. Astrophys. Suppl. Ser.* **97**, 355 (1993).
6. R. F. Elsner *et al.*, *Astrophys. J.* **239**, 355 (1980).
7. P. T. Boyd, A. P. Smale, J. F. Dolan, *Astrophys. J.* **555**, 822 (2001).
8. D. M. Smith, W. A. Heindl, J. H. Swank, *Astrophys. J.* **578**, L132 (2002).
9. R. H. D. Corbet, *Astrophys. J.* **595**, 1086 (2003).
10. P. Kaaret *et al.*, *Mon. Not. R. Astron. Soc.* **348**, L28 (2004).
11. J. Frank, A. R. King, D. J. Raine, *Accretion Power in Astrophysics* (Cambridge Univ. Press, Cambridge, 1992).
12. S. F. Portegies Zwart, H. Baumgardt, P. Hut, J. Makino, S. L. W. McMillan, *Nature* **428**, 724 (2004).
13. N. McCrady, A. M. Gilbert, J. R. Graham, *Astrophys. J.* **596**, 240 (2003).
14. The proximity of the M82 ULX to MGG 11 will make isolation of an optical/infrared counterpart difficult.
15. X.-D. Li, *Astrophys. J.* **616**, L119 (2004).
16. S. F. Portegies Zwart, J. Dewi, T. Maccarone, *Mon. Not. R. Astron. Soc.* **355**, 413 (2004).
17. Power is a measure of the amplitude of modulation at a given frequency. Details of the correct definition of power for unevenly sampled data are discussed in (*18*).
18. H. J. Horne, S. L. Baliunas, *Astrophys. J.* **302**, 757 (1986).
19. We thank X.-D. Li for discussing his binary evolution calculations. Grants from NASA and a faculty scholar award from the University of Iowa supported this research.

6 October 2005; accepted 18 November 2005
Published online 5 January 2006;
10.1126/science.1121067
Include this information when citing this paper.

Department of Physics and Astronomy, University of Iowa, Van Allen Hall, Iowa City, IA 52242, USA.

*To whom correspondence should be addressed. E-mail: philip-kaaret@uiowa.edu

Fermionic Superfluidity with Imbalanced Spin Populations

Martin W. Zwierlein,* André Schirotzek, Christian H. Schunck, Wolfgang Ketterle

We established superfluidity in a two-state mixture of ultracold fermionic atoms with imbalanced state populations. This study relates to the long-standing debate about the nature of the superfluid state in Fermi systems. Indicators for superfluidity were condensates of fermion pairs and vortices in rotating clouds. For strong interactions, near a Feshbach resonance, superfluidity was observed for a broad range of population imbalances. We mapped out the superfluid regime as a function of interaction strength and population imbalance and characterized the quantum phase transition to the normal state, known as the Pauli limit of superfluidity.

Fermionic superfluidity, whether it occurs in superconductors, helium-3, or inside a neutron star, requires pairing of fermions, particles with half-integer spin. In an equal mixture of two states of fermions ("spin up" and "spin down"), pairing can be complete and the entire system will become superfluid. When the two populations of fermions are unequal, however, not every particle can find a partner, raising the question of whether superfluidity can persist in response to such a population imbalance. This problem arises in many different fields of physics—for example, in the study of superfluidity of quarks in the dense matter of the early universe, where charge neutrality and differing masses impose unequal quark densities. In superconductors, an applied magnetic field could in principle imbalance the densities of spin up and spin down electrons. As first discussed by Clogston in 1962 (*1*), there exists an upper limit for this magnetic field, beyond which superconductivity with equal spin densities will break down. Fulde and Ferrell (*2*), and independently Larkin and Ovchinnikov (*3*), proposed a more stable configuration of the superconductor that allows for unequal densities, the FFLO or LOFF state containing nonzero-momentum Cooper pairs. The true ground state of imbalanced fermionic superfluids has been the subject of debate for decades (*4*, *5*), and experimental studies are highly desirable. However, superconductors are charged fermionic superfluids, and imbalancing the electron densities by applying magnetic fields is hindered by the Meissner effect. The fields are either fully shielded from the superconductor, or they enter in the form of quantized flux lines or vortices. Only in special materials can these effects be suppressed, such as in heavy-fermion superconductors (*6*–*8*) or in quasi–two-dimensional (2D) organic superconductors (*6*). In the neutral superfluid helium-3, one can mismatch the Fermi surfaces by a magnetic field and thus destroy interspin pairing. However, superfluidity persists due to (p-wave) pairing between equal spins (*9*).

Fermionic superfluids of atom pairs. The recently discovered fermionic superfluids in ultracold atomic gases (*10*–*19*) provide an exciting new possibility of exploring unequal mixtures of fermions, because populations in two hyperfine states of the fermionic atom can be freely chosen. In addition, the (s-wave) interactions between two atoms in different states and the binding energy of atom pairs can be tuned via Feshbach resonances. In equal mixtures of fermions, this tunability gives access to the crossover from a Bose-Einstein Condensate (BEC) of molecules to a Bardeen-Cooper-Schrieffer (BCS) superfluid of loosely bound pairs (*13*–*19*). At zero temperature, this crossover is smooth (*20*–*22*), the system stays

Department of Physics, Massachusetts Institute of Technology (MIT)–Harvard Center for Ultracold Atoms, and Research Laboratory of Electronics, MIT, Cambridge, MA 02139, USA.

*To whom correspondence should be addressed. E-mail: zwierlei@mit.edu

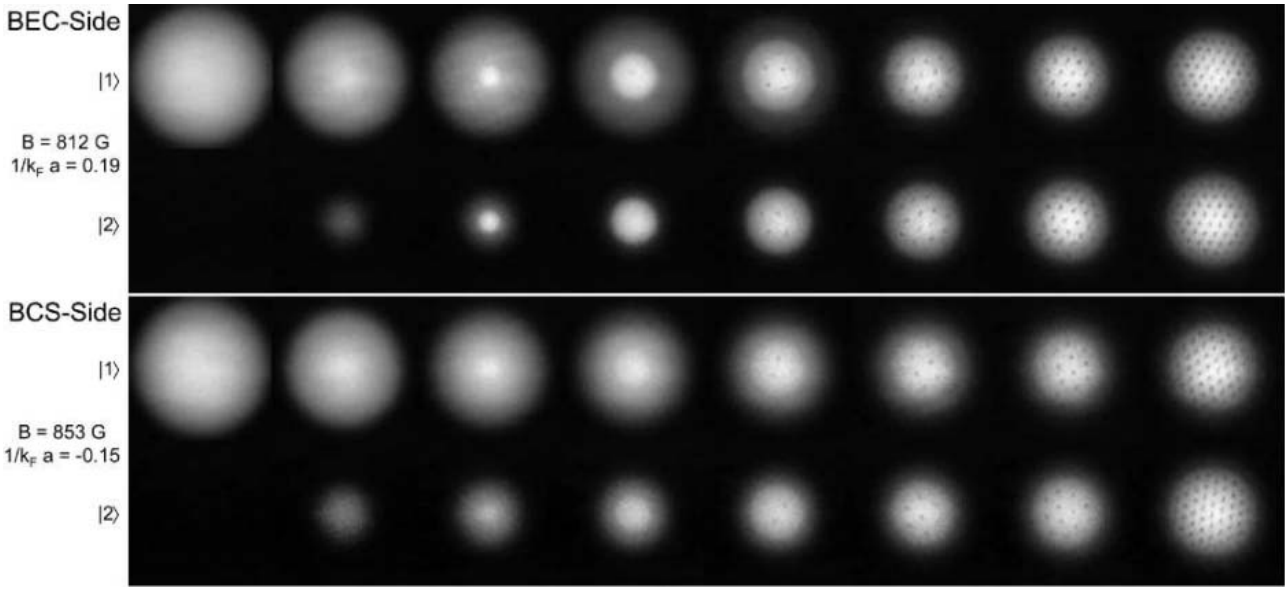

Fig. 1. Superfluidity in a strongly interacting Fermi gas with imbalanced populations. The upper (lower) pair of rows shows clouds prepared at 812 G, on the BEC side (853 G, BCS side), where $1/k_F a = 0.2$ ($1/k_F a = -0.15$). In each pair of rows, the upper image shows state $|1\rangle$, the lower one state $|2\rangle$. For the 812-G data, the population imbalance $\delta = (N_2 - N_1)/(N_1 + N_2)$ between N_1 atoms in state $|1\rangle$ and N_2 in state $|2\rangle$ was (from left to right) 100, 90, 80, 62, 28, 18, 10, and 0%. For the 853-G data, the imbalance was 100, 74, 58, 48, 32, 16, 7, and 0%. For different values of δ, the total number of atoms varied only within 20% around $N = 7 \times 10^6$, with the exception of the end points $\delta = 100\%$ ($N = 1 \times 10^7$) and $\delta = 0\%$ ($N = 1.2 \times 10^7$). The field of view of each image is 1.4 mm by 1.4 mm.

superfluid even for arbitrarily weak interactions, and no phase transition occurs. In the case of unequal mixtures, the phase diagram is predicted to be much richer (*23*–*28*). In the molecular limit of tight binding, all fermions in the less populated spin state will pair up with atoms in the other state. The resulting molecular condensate will spatially coexist with the remaining Fermi sea of unpaired atoms. As the repulsive interaction between atoms and molecules is increased, the condensate will start to expel unpaired atoms, leading to a phase separation of the superfluid from the normal phase (*24*–*26*, *29*, *30*). This picture is expected to extend into the BCS limit of weakly bound pairs, where the pairing gap Δ prevents unpaired atoms from entering the BCS superfluid (*24*–*26*, *31*). As the binding energy and hence the pairing gap is further reduced, Δ will eventually become small compared to the chemical potential difference $\delta\mu = \mu_2 - \mu_1$ between the two spin states, allowing unpaired excess atoms to enter the superfluid region. Close to this point, superfluidity will cease to exist. In the weakly interacting BCS limit, the pairing gap is exponentially small compared to the Fermi energy; hence, an exponentially small population imbalance can destroy superfluidity.

This superfluid-to-normal transition is an example of a quantum phase transition, which occurs even at zero temperature, when all thermal fluctuations are frozen out and only quantum fluctuations prevail. It can also be driven by increasing the mismatch in chemical potentials between the two spin states to the critical value of $\delta\mu \approx \Delta$, inducing collapse into the normal state. In this context the phase transition is known as the Pauli or Clogston limit of superfluidity (*1*). However, its exact nature—whether there is one or several first- and/or second-order transitions—remains the subject of debate (*6*, *27*, *28*).

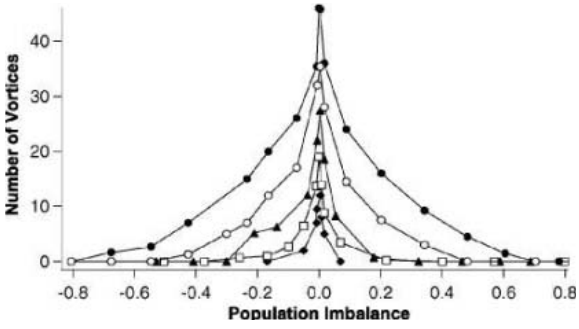

Fig. 2. Vortex number versus population imbalance for different interaction strengths. Results are shown for 812 G or $1/k_F a = 0.2$ (●), 853 G ($1/k_F a = -0.15$, ○), 874 G ($1/k_F a = -0.3$, ▲), 896 G ($1/k_F a = -0.4$, □), and 917 G ($1/k_F a = -0.5$, ♦).

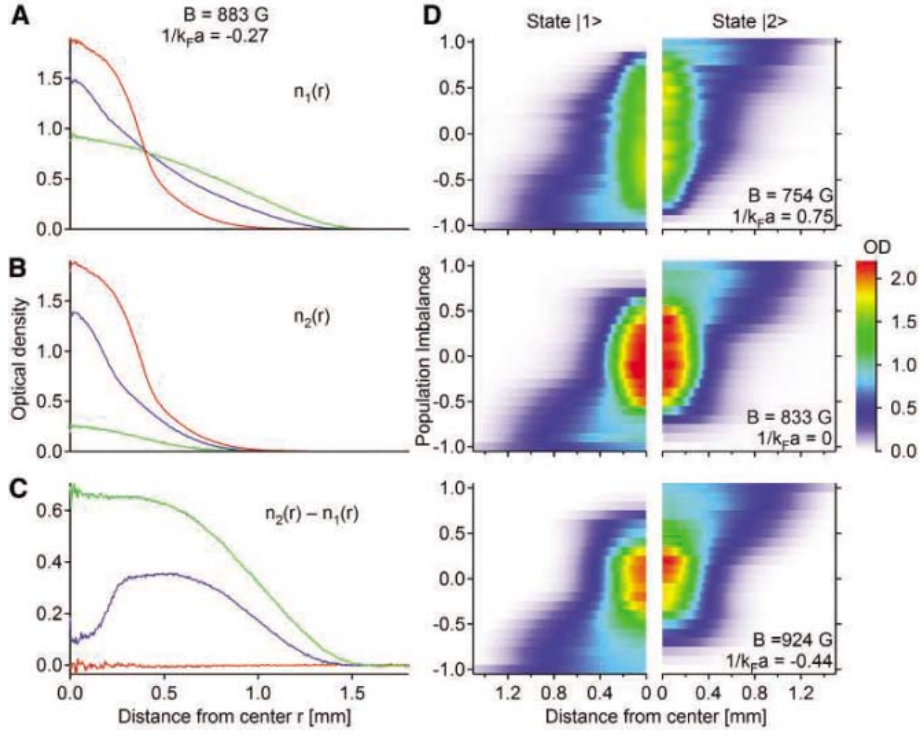

Fig. 3. Radial density profiles of the two components of a strongly interacting Fermi gas mixture with unequal populations. The profiles are azimuthal averages of the axially integrated density. (**A** and **B**) Profiles of the component in state $|1\rangle$ and $|2\rangle$, respectively, originating from 883 G ($1/k_F a = -0.27$). The imaging procedure, as detailed in the text and in (*32*), involves a magnetic-field sweep and ballistic expansion. The population imbalance was $\delta = 0\%$ (red), $\delta = 46\%$ (blue), and $\delta = 86\%$ (green). (**C**) Difference between the distributions in state $|1\rangle$ and $|2\rangle$. The total number of atoms was $N = 2.3 \times 10^7$. The clear dip in the blue curve caused by the pair condensate indicates phase separation of the superfluid from the normal gas. (**D**) Color-coded profiles of clouds prepared at three different interaction strengths. The condensate is clearly visible as the dense central part surrounded by unpaired fermions or uncondensed molecules. Spin-polarized clouds ($\delta = \pm 100\%$) are not in thermal equilibrium, owing to Pauli suppression of collisions. OD, optical density.

Imbalanced spin populations. As the starting point of our experiments, we prepared a degenerate Fermi gas of spin-polarized ^{6}Li atoms, using methods of laser cooling, sympathetic cooling by sodium atoms, and optical trapping (*32*). A radiofrequency sweep with an adjustable sweep rate created a variable spin mixture of the two lowest hyperfine states, labeled $|1\rangle$ and $|2\rangle$. Interactions between these two states are strongly enhanced around a 300-G-wide Feshbach resonance located at $B_0 = 834$ G. At lower values of the magnetic-bias field B, two isolated fermions can bind into a stable molecule (BEC side), whereas at higher values fermion pairs can exist only in the stabilizing presence of the surrounding gas (BCS side). The interaction is described by the parameter $1/k_F a$, where a is the scattering length and k_F is defined as the Fermi momentum of a noninteracting, equal spin mixture.

For the study of vortices and superfluid flow as a function of population imbalance, the spin mixture was set in rotation on the BEC side, using two laser beams that rotated symmetrically around the cloud (*19*, *32*). Starting with either a rotating or a nonrotating cloud, we then varied the interaction strength by ramping the magnetic field B to several values around the Feshbach resonance. To image the fermion pair condensates, the cloud was released from the optical trap and the binding energy of the pairs was increased by switching the magnetic field to the BEC side, far away from resonance (*13*, *14*, *19*, *32*). This revealed the center-of-mass wave function of the pairs and thus, for rotating clouds, the eventual presence of vortices.

Figure 1 shows images of the two spin states for varying population imbalance, originating from the BEC side ($B < 834$ G) and from the BCS side ($B > 834$ G) of the resonance. Starting with a pure Fermi sea in state $|1\rangle$, we see how gradually, for increasing numbers in the second spin state $|2\rangle$, first a normal (uncondensed) cloud of fermion pairs emerges, then a condensate peak appears within the normal cloud (see also Fig. 3, A and B). The condensate can be clearly distinguished in the minority cloud as the dense

central region (appearing as white in the image) surrounded by the lower density normal component (appearing as gray). As the condensate size increases and the friction due to the normal component decreases, vortices appear in the rotating cloud, a direct and unambiguous signature of superfluid flow. As expected, the largest condensates with the largest number of vortices are obtained for an equal mixture. However, superfluidity in the strongly interacting Fermi gas is clearly not constrained to a narrow region around the perfectly balanced spin mixture, but is observed for large population asymmetries.

Figures 1 and 2 summarize our findings for rotating spin mixtures and displays the number of detected vortices versus the population imbalance between the two spin states. The vortex number measures qualitatively how deep the system is in the superfluid phase: The higher the nonsuperfluid fraction, the faster the condensate's rotation will damp given the nonvanishing anisotropy $[(\omega_x - \omega_y)/(\omega_x + \omega_y) \approx 1.5\%]$ of our trap (*19*, *33*, *34*). Figure 2 therefore shows the shrinking of the superfluid region with decreasing interaction strength on the BCS side, closing in on the optimal situation of equal populations.

The fraction of condensed fermion pairs. Close to the breakdown of superfluidity, vortices are strongly damped and difficult to observe. Therefore, the presence of vortices provides only a lower bound on the size of the superfluid window. A more detailed map of the superfluid phase as a function of interaction strength and temperature was obtained from a study of condensate fractions, determined from cloud profiles such as those shown in Fig. 3. Throughout the whole crossover region, pair condensation occurred for a broad range of population imbalances. As expected, this range was even wider than that obtained from the observation of vortices.

An intriguing property of the superfluid state with imbalanced populations is the clear depletion in the excess fermions of the majority component (Fig. 3C). The profiles in Fig. 3 present the axially integrated density; hence, the true depletion in the 3D density is even stronger. The condensate seems to repel the excess fermions. This feature was observed after expansion at 690 G, where interactions are still strong (initially $1/k_F a \approx 2.0$). The expansion, at least in the region around the condensate, is hydrodynamic and should proceed as a scaling transformation (*35*, *36*). Therefore, the depletion observed in expansion hints at spatial phase separation of the superfluid from the normal state. This effect was observed throughout the resonance region, and on resonance even when no magnetic field ramps were performed during expansion. After submission of our work, depletion of excess fermions in the center of the trap was reported (*37*). However, to distinguish a phase-separated state with equal densities in the superfluid region from more exotic states allowing unequal densities, a careful analysis of the 3D density, reconstructed from the integrated optical densities, will be necessary.

We did not observe (by simultaneously imaging along the long and short axis) a modulation in the condensate density as would be predicted for the FFLO state (*23*, *38*, *39*). However, this state is predicted to be favored only in a narrow region of parameter space and might have escaped our attention.

The condensate fraction was determined from the minority component, which in all cases is very well fit by a Gaussian for thermal molecules and unpaired atoms, plus a Thomas-Fermi profile for the condensate (fig. S2) (*32*). Figure 4 shows the condensate fraction obtained for varying population difference and temperature, and for several magnetic fields (i.e., interaction strengths) around resonance. The data for 754 G, on the BEC side of the resonance, show condensation over almost the entire range of population imbalance. As the interaction strength is increased toward resonance, the condensate fraction for equal mixtures grows (*14*). However, for large population asymmetries, the condensate disappears. The window of condensation shrinks further as we cross the resonance and move to the BCS side (Fig. 4, 833 to 924 G).

The temperature varied with number imbalance, as indicated in the insets of Fig. 4. The temperature maximum for equal mixtures at 754 G is likely due to the greater energy release when more deeply bound molecules were formed and explains the smaller condensate fraction for equal mixtures found at this field. For higher fields, the temperature changes much less with the spin composition (*32*). The observed critical population imbalance was only weakly dependent on temperature. This may reflect the fact that well below the critical temperature for superfluidity, the pairing gap is only weakly dependent on temperature (*40*). The critical imbalance at our coldest temperatures will thus essentially coincide with its value at zero temperature.

On resonance, where the scattering length a diverges, the system is in the unitary regime (*41*), where the only remaining energy scales of the system are the Fermi energies $E_{F,1}$ and $E_{F,2}$ of the two spin components (*42*). The breakdown of

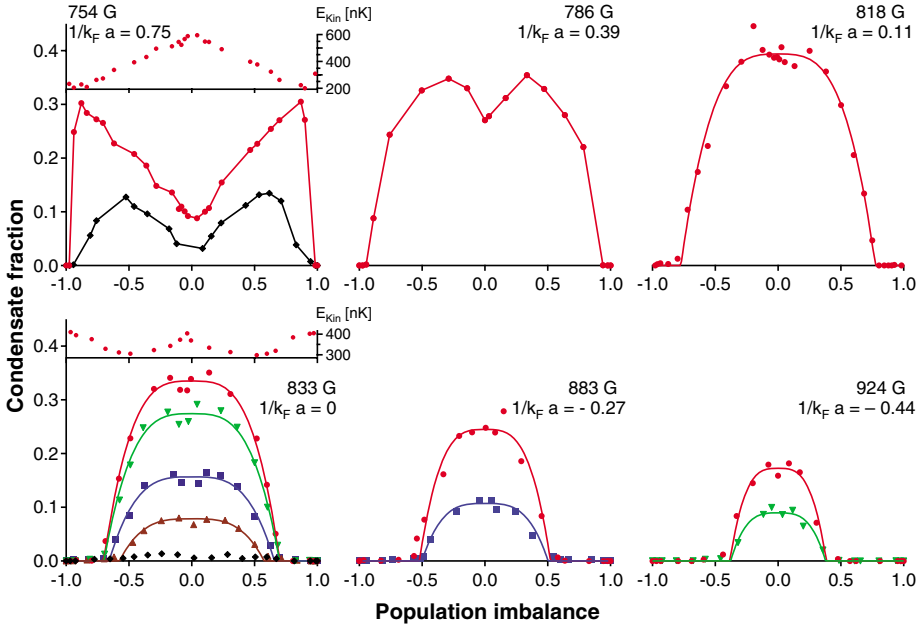

Fig. 4. Condensate fraction versus population imbalance for several temperatures and interaction strengths. The total number of atoms $N = 2.3 \times 10^7$ is constant to within 20% for all data points ($T_F = 1.9\ \mu K$ for an equal mixture) (*32*). For a given population imbalance, the uppermost curves for different magnetic fields are approximately isentropically connected. The different symbols correspond to different evaporation ramps. The average radial kinetic energy per molecule of thermal clouds in the minority component serves as an indicator for temperature and is shown in the insets for 754 G (upper) and 833 G (lower) for the coldest data. On resonance, for a population asymmetry of 50%, we measure an energy of $k_B \times 300$ nK (circles) (k_B is the Boltzmann constant), 345 nK (inverted triangles), 390 nK (squares), 420 nK (triangles), and 505 nK (diamonds). The critical population imbalance δ_c for the breakdown of condensation at 754 G is about $\delta_c^{754} \approx 96\%$, and at 786 G it is $\delta_c^{786} \approx 95\%$. For the data at higher magnetic fields, we determine δ_c through a threshold fit to the first three data points with nonzero condensate fraction for each sign of asymmetry. Although we could have used any reasonable threshold function, empirically, it was found that the function $n_c(1 - |\delta/\delta_c|^{3.3})$ (n_c – maximum condensate fraction) provided a good fit to all data points. Therefore, it was used for the threshold fits and is shown as a guide to the eye.

superfluidity occurs for a certain universal ratio of these two or equivalently, in a harmonic trap, for a certain critical population imbalance. We determine this universal number to be $\delta_c \approx \pm 70(3)\%$ for our approximately harmonic trapping potential. In (*37*), depletion of excess fermions was reported up to an imbalance of 85% and was interpreted as indirect evidence for superfluidity. However, superfluidity was not directly observed, and our data show that the system is normal at this imbalance.

The critical imbalance δ_c corresponds to a Fermi energy difference $\delta E_F = E_{F,2} - E_{F,1} = [(1 + \delta_c)^{1/3} - (1 - \delta_c)^{1/3}]E_F = 0.53(3)E_F$, where E_F is the Fermi energy of an equal mixture of noninteracting fermions. The standard BCS state is predicted (*1*) to break down for a critical chemical-potential difference $\delta\mu = \sqrt{2}\,\Delta$. On resonance, however, Monte-Carlo studies predict (*24*) the superfluid breakdown to occur when $\delta\mu = 2.0(1)\Delta = 1.0(1)E_F$. Only in the weakly interacting regime do the chemical potentials equal the Fermi energies. Quantitative agreement with the Monte-Carlo study would require that $\delta\mu \approx 2\delta E_F$. This is not unreasonable given that interactions will reduce the chemical potential of the minority component. In a preliminary analysis, we indeed find close agreement with theory.

Figure 5 summarizes our findings, showing the critical mismatch in Fermi energies for which we observed the breakdown of superfluidity as well as the pairing gap Δ versus the interaction parameter $1/k_F a$. Far on the BEC side of the resonance, the superfluid is very robust with respect to population imbalance. Here, pairing is dominantly a two-body process: The smallest cloud of atoms in state $|1\rangle$ will fully pair with atoms in state $|2\rangle$ and condense at sufficiently low temperatures. On the BCS side of the resonance, however, pairing is purely a many-body effect and depends on the density of the two Fermi clouds. As the density of the minority component becomes smaller, the net energy gain from forming a pair condensate will decrease. Even at zero temperature, this eventually leads to the breakdown of superfluidity and the quantum phase transition to the normal state. We have experimentally confirmed the qualitative picture that fermionic superfluidity breaks down when the difference in chemical potentials between the two species becomes larger than the pairing gap.

Concluding remarks and outlook. We have observed superfluidity with imbalanced spin populations. Contrary to expectations for the weakly interacting case, superfluidity in the resonant region is extremely stable against population imbalance. As the asymmetry is increased, we observe the quantum phase transition to the normal state, known as the Pauli limit of superfluidity. Our observation opens up intriguing possibilities for further studies on Fermi systems with mismatched Fermi surfaces. One important aspect concerns the density distribution in the superfluid regime. Standard BCS theory allows only equal spin densities, which would entail complete phase separation of the superfluid from the normal density. More exotic solutions (*6*) allow superfluidity also with imbalanced densities, most notably the FFLO state. A more detailed scan of the parameter space and precise measurements of spatial profiles might resolve the long-standing question of the true ground state. Equally fascinating is the nature of the strongly correlated normal state slightly below resonance. For sufficient population imbalance, we have the remarkable situation in which bosonic molecules, stable even in isolation, do not condense at zero temperature, owing to the presence of the Fermi sea.

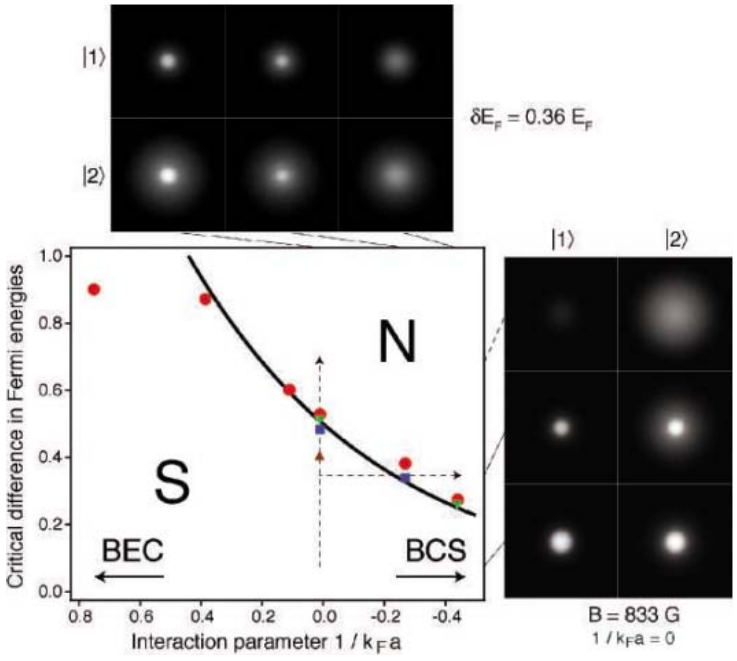

Fig. 5. Critical difference in Fermi energies δE_F between the two spin states for which the superfluid-to-normal transition is observed. δE_F for each interaction strength and temperature is obtained from the critical population imbalance determined in Fig. 3 using $\delta E_F/E_F = (1 + \delta_c)^{1/3} - (1 - \delta_c)^{1/3}$. The symbols are defined in Fig. 3. The line shows the expected variation of the pairing gap Δ, where the value on resonance has been taken from (*24*) and the exponential behavior in the BCS regime, $\Delta \sim e^{-\pi/2k_F|a|}$, was assumed. Although the trend of δE_F is expected to follow that of Δ, the close agreement is coincidental. Representative density profiles illustrate the quantum phase transition for fixed interaction and for fixed population imbalance along the dashed lines.

References and Notes

1. A. M. Clogston, *Phys. Rev. Lett.* **9**, 266 (1962).
2. P. Fulde, R. A. Ferrell, *Phys. Rev.* **135**, A550 (1964).
3. A. J. Larkin, Y. N. Ovchinnikov, *Zh. Eksp. Teor. Fiz.* **47**, 1136 (1964) [*Sov. Phys. JETP* **20**, 762 (1965)].
4. G. Sarma, *J. Phys. Chem. Solids* **24**, 1029 (1963).
5. W. V. Liu, F. Wilczek, *Phys. Rev. Lett.* **90**, 047002 (2003).
6. R. Casalbuoni, G. Nardulli, *Rev. Mod. Phys.* **76**, 263 (2004).
7. H. A. Radovan *et al.*, *Nature* **425**, 51 (2003).
8. A. Bianchi, R. Movshovich, C. Capan, P. G. Pagliuso, J. L. Sarrao, *Phys. Rev. Lett.* **91**, 187004 (2003).
9. D. Vollhardt, P. Wölfle, *The Superfluid Phases of Helium 3* (Taylor & Francis, London, 1990).
10. C. A. Regal, C. Ticknor, J. L. Bohn, D. S. Jin, *Nature* **424**, 47 (2003).
11. S. Jochim *et al.*, *Science* **302**, 2101 (2003).
12. M. W. Zwierlein *et al.*, *Phys. Rev. Lett.* **91**, 250401 (2003).
13. C. A. Regal, M. Greiner, D. S. Jin, *Phys. Rev. Lett.* **92**, 040403 (2004).
14. M. W. Zwierlein *et al.*, *Phys. Rev. Lett.* **92**, 120403 (2004).
15. T. Bourdel *et al.*, *Phys. Rev. Lett.* **93**, 050401 (2004).
16. J. Kinast, S. L. Hemmer, M. E. Gehm, A. Turlapov, J. E. Thomas, *Phys. Rev. Lett.* **92**, 150402 (2004).
17. C. Chin *et al.*, *Science* **305**, 1128 (2004).
18. G. B. Partridge, K. E. Strecker, R. I. Kamar, M. W. Jack, R. G. Hulet, *Phys. Rev. Lett.* **95**, 020404 (2005).
19. M. W. Zwierlein, J. R. Abo-Shaeer, A. Schirotzek, C. H. Schunck, W. Ketterle, *Nature* **435**, 1047 (2005).
20. D. M. Eagles, *Phys. Rev.* **186**, 456 (1969).
21. A. J. Leggett, in *Modern Trends in the Theory of Condensed Matter. Proceedings of the XVIth Karpacz Winter School of Theoretical Physics, Karpacz, Poland, 1980* (Springer-Verlag, Berlin, Karpacz, Poland, 1980), pp. 13–27.
22. P. Nozières, S. Schmitt-Rink, *J. Low Temp. Phys.* **59**, 195 (1985).
23. A. Sedrakian, J. Mur-Petit, A. Polls, H. Müther, *Phys. Rev. A.* **72**, 013613 (2005).
24. J. Carlson, S. Reddy, *Phys. Rev. Lett.* **95**, 060401 (2005).
25. C.-H. Pao, S.-T. Wu, S.-K. Yip, preprint available at http://xxx.lanl.gov/abs/cond-mat/0506437.
26. D. E. Sheehy, L. Radzihovsky, preprint available at http://xxx.lanl.gov/abs/cond-mat/0508430.
27. D. T. Son, M. A. Stephanov, preprint available at http://xxx.lanl.gov/abs/cond-mat/0507586.
28. K. Yang, preprint available at http://xxx.lanl.gov/abs/cond-mat/0508484.
29. L. Viverit, C. J. Pethick, H. Smith, *Phys. Rev. A.* **61**, 053605 (2000).
30. S. Powell, S. Sachdev, H. P. Büchler, *Phys. Rev. B* **72**, 024534 (2005).
31. P. F. Bedaque, H. Caldas, G. Rupak, *Phys. Rev. Lett.* **91**, 247002 (2003).

32. Materials and methods are available as supporting material on *Science* Online.
33. J. R. Abo-Shaeer, C. Raman, W. Ketterle, *Phys. Rev. Lett.* **88**, 070409 (2002).
34. D. Guéry-Odelin, *Phys. Rev. A.* **62**, 033607 (2000).
35. Y. Kagan, E. L. Surkov, G. V. Shlyapnikov, *Phys. Rev. A.* **55**, R18 (1997).
36. C. Menotti, P. Pedri, S. Stringari, *Phys. Rev. Lett.* **89**, 250402 (2002).
37. G. B. Partridge, W. Li, R. I. Kamar, Y.-a. Liao, R. G. Hulet, *Science*, **311**, 503 (2006); published online 22 December 2005 (10.1126/science.1122876).
38. T. Mizushima, K. Machida, M. Ichioka, *Phys. Rev. Lett.* **94**, 060404 (2005).
39. P. Castorina, M. Grasso, M. Oertel, M. Urban, D. Zappalà, *Phys. Rev. A.* **72**, 025601 (2005).
40. A. A. Abrikosov, L. P. Gorkov, I. E. Dzyaloshinski, *Methods of Quantum Field Theory in Statistical Physics* (Dover, New York, 1975).
41. G. Bertsch, INT Workshop on Effective Field Theory in Nuclear Physics (Seattle, WA, February 1999).
42. T. D. Cohen, *Phys. Rev. Lett.* **95**, 120403 (2005).
43. We thank G. Campbell for critical reading of the manuscript and X.-G. Wen, E. Demler, and S. Sachdev for stimulating discussions. This work was supported by the NSF, Office of Naval Research, Army Research Office, and NASA.

Supporting Online Material
www.sciencemag.org/cgi/content/full/1122318/DC1
Materials and Methods
Figs. S1 and S2
References and Notes

7 November 2005; accepted 14 December 2005
Published online 22 December 2005;
10.1126/science.1122318
Include this information when citing this paper.

Community Genomics Among Stratified Microbial Assemblages in the Ocean's Interior

Edward F. DeLong,[1]* Christina M. Preston,[2] Tracy Mincer,[1] Virginia Rich,[1] Steven J. Hallam,[1] Niels-Ulrik Frigaard,[1] Asuncion Martinez,[1] Matthew B. Sullivan,[1] Robert Edwards,[3] Beltran Rodriguez Brito,[3] Sallie W. Chisholm,[1] David M. Karl[4]

Microbial life predominates in the ocean, yet little is known about its genomic variability, especially along the depth continuum. We report here genomic analyses of planktonic microbial communities in the North Pacific Subtropical Gyre, from the ocean's surface to near–sea floor depths. Sequence variation in microbial community genes reflected vertical zonation of taxonomic groups, functional gene repertoires, and metabolic potential. The distributional patterns of microbial genes suggested depth-variable community trends in carbon and energy metabolism, attachment and motility, gene mobility, and host-viral interactions. Comparative genomic analyses of stratified microbial communities have the potential to provide significant insight into higher-order community organization and dynamics.

Microbial plankton are centrally involved in fluxes of energy and matter in the sea, yet their vertical distribution and functional variability in the ocean's interior is still only poorly known. In contrast, the vertical zonation of eukaryotic phytoplankton and zooplankton in the ocean's water column has been well documented for over a century (*1*). In the photic zone, steep gradients of light quality and intensity, temperature, and macronutrient and trace-metal concentrations all influence species distributions in the water column (*2*). At greater depths, low temperature, increasing hydrostatic pressure, the disappearance of light, and dwindling energy supplies largely determine vertical stratification of oceanic biota.

For a few prokaryotic groups, vertical distributions and depth-variable physiological properties are becoming known. Genotypic and phenotypic properties of stratified *Prochlorococcus* "ecotypes" for example, are suggestive of depth-variable adaptation to light intensity and nutrient availability (*3*–*5*). In the abyss, the vertical zonation of deep-sea piezophilic bacteria can be explained in part by their obligate growth requirement for elevated hydrostatic pressures (*6*). In addition, recent cultivation-independent (*7*–*15*) surveys have shown vertical zonation patterns among specific groups of planktonic *Bacteria*, *Archaea*, and *Eukarya*. Despite recent progress however, a comprehensive description of the biological properties and vertical distributions of planktonic microbial species is far from complete.

Cultivation-independent genomic surveys represent a potentially useful approach for characterizing natural microbial assemblages (*16*, *17*). "Shotgun" sequencing and whole genome assembly from mixed microbial assemblages has been attempted in several environments, with varying success (*18*, *19*). In addition, Tringe *et al.* (*20*) compared shotgun sequences of several disparate microbial assemblages to identify community-specific patterns in gene distributions. Metabolic reconstruction has also been attempted with environmental genomic approaches (*21*). Nevertheless, integrated genomic surveys of microbial communities along well-defined environmental gradients (such as the ocean's water column) have not been reported.

To provide genomic perspective on microbial biology in the ocean's vertical dimension, we cloned large [~36 kilobase pairs (kbp)] DNA fragments from microbial communities at different depths in the North Pacific Subtropical Gyre (NPSG) at the open-ocean time-series station ALOHA (*22*). The vertical distribution of microbial genes from the ocean's surface to abyssal depths was determined by shotgun sequencing of fosmid clone termini. Applying identical collection, cloning, and sequencing strategies at seven depths (ranging from 10 m to 4000 m), we archived large-insert genomic libraries from each depth-stratified microbial community. Bidirectional DNA sequencing of fosmid clones (~10,000 sequences per depth) and comparative sequence analyses were used to identify taxa, genes, and metabolic pathways that characterized vertically stratified microbial assemblages in the water column.

Study Site and Sampling Strategy

Our sampling site, Hawaii Ocean Time-series (HOT) station ALOHA (22°45' N, 158°W), represents one of the most comprehensively characterized sites in the global ocean and has been a focal point for time series–oriented oceanographic studies since 1988 (*22*). HOT investigators have produced high-quality spatial and time-series measurements of the defining physical, chemical, and biological oceanographic parameters from surface waters to the seafloor. These detailed spatial and temporal datasets present unique opportunities for placing microbial genomic depth profiles into appropriate oceanographic context (*22*–*24*) and leverage these data to formulate meaningful ecological hypotheses. Sample depths were selected, on the basis of well-defined physical, chemical, and biotic characteristics, to represent discrete zones in the water column (Tables 1 and 2, Fig. 1; figs. S1 and S2). Specifically, seawater samples from the upper euphotic zone (10 m and 70 m), the base of the chlorophyll maximum (130 m), below the base of the euphotic zone (200 m), well below the upper mesopelagic (500 m), in the core of the dissolved oxygen minimum layer (770 m), and in the deep abyss, 750 m above the seafloor (4000 m), were collected for preparing microbial community DNA libraries (Tables 1 and 2, Fig. 1; figs. S1 and S2).

The depth variability of gene distributions was examined by random, bidirectional end-sequencing of ~5000 fosmids from each depth, yielding ~64 Mbp of DNA sequence total from the 4.5 Gbp archive (Table 1). This represents raw sequence coverage of about 5 (1.8 Mbp sized) genome equivalents per depth. Because we surveyed ~180 Mbp of cloned DNA (5000 clones by

[1]Massachusetts Institute of Technology, Cambridge, MA 02139, USA. [2]Monterey Bay Aquarium Research Institute, Moss Landing, CA 95064, USA. [3]San Diego State University, San Diego, CA 92182, USA. [4]University of Hawaii Honolulu, HI 96822, USA.

*To whom correspondence should be addressed. E-mail: delong@mit.edu

~36 kbp/clone per depth), however, we directly sampled ~100 genome equivalents at each depth. We did not sequence as deeply in each sample as a recent Sargasso Sea survey (*19*), where from 90,000 to 600,000 sequences were obtained from small DNA insert clones, from each of seven different surface-water samples. We hypothesized, however, that our comparison of microbial communities collected along well-defined environmental gradients (using large-insert DNA clones), would facilitate detection of ecologically meaningful taxonomic, functional, and community trends.

Vertical Profiles of Microbial Taxa

Vertical distributions of bacterial groups were assessed by amplifying and sequencing small subunit (SSU) ribosomal RNA (rRNA) genes from complete fosmid library pools at each depth (Fig. 2; fig. S3). Bacterial phylogenetic distributions were generally consistent with previous polymerase chain reaction–based cultivation-independent rRNA surveys of marine picoplankton (*8*, *15*, *25*). In surface-water samples, rRNA-containing fosmids included those from *Prochlorococcus*; *Verrucomicrobiales*; *Flexibacteraceae*; Gammaproteobacteria (SAR92, OM60, SAR86 clades); Alphaproteobacteria (SAR116, OM75 clades); and Deltaproteobacteria (OM27 clade) (Fig. 2). Bacterial groups from deeper waters included members of *Deferribacteres*; *Planctomycetaceae*; *Acidobacteriales*; *Gemmatamonadaceae*; *Nitrospina*; *Alteromonadaeceae*; and SAR202, SAR11, and Agg47 planktonic bacterial clades (Fig. 2; fig. S2). Large-insert DNA clones previously recovered from the marine environment (*9*, *10*) also provide a good metric for taxonomic assessment of indigenous microbes. Accordingly, a relatively large proportion of our shotgun fosmid sequences most closely matched rRNA-containing bacterioplankton artificial clones previously recovered from the marine environment (fig. S3).

Taxonomic bins of bacterial protein homologs found in randomly sequenced fosmid ends (Fig. 2; fig. S4) also reflected distributional patterns generally consistent with previous surveys in the water column (*8*, *15*). Unexpectedly large amounts of phage DNA were recovered in clones, particularly in the photic zone. Also unexpected was a relatively high proportion of Betaproteobacteria-like sequences recovered at 130 m, most sharing highest similarity to protein homologs from *Rhodoferax ferrireducens*. As expected, representation of *Prochlorococcus*-like and *Pelagibacter*-like genomic sequences was high in the photic zone. At greater depths, higher proportions of *Chloroflexi*-like sequences, perhaps corresponding to the co-occurring SAR202 clade, were observed (Fig. 2). *Planctomycetales*-like genomic DNA sequences were also highly represented at greater depths.

All archaeal SSU rRNA–containing fosmids were identified at each depth, quantified by macroarray hybridization, and their rRNAs sequenced

Table 1. HOT samples and fosmid libraries. Sample site, 22°45′ N, 158°W. All seawater samples were pre-filtered through a 1.6-μm glass fiber filter, and collected on a 0.22-μm filter. See (*35*) for methods.

Depth (m)	Sample date	Volume filtered (liters)	Total fosmid clones	Total DNA (Mbp)	
				Archived	Sequenced
10	10/7/02	40	12,288	442	7.54
70	10/7/02	40	12,672	456	11.03
130	10/6/02	40	13,536	487	6.28
200	10/6/02	40	19,008	684	7.96
500	10/6/02	80	15,264	550	8.86
770	12/21/03	240	11,520	415	11.18
4,000	12/21/03	670	41,472	1,493	11.10

Table 2. HOT sample oceanographic data. Samples described in Table 1. Oceanographic parameters were measured as specified at (*49*); values shown are those from the same CTD casts as the samples, where available. Values in parentheses are the mean ± 1 SD of each core parameter during the period October 1988 to December 2004, with the total number of measurements collected for each parameter shown in brackets. The parameter abbreviations are Temp., Temperature; Chl a, chlorophyll a; DOC, dissolved organic carbon; N+N, nitrate plus nitrite; DIP, dissolved inorganic phosphate; and DIC, dissolved inorganic carbon. The estimated photon fluxes for upper water column samples (assuming a surface irradiance of 32 mol quanta m^{-2} d^{-1} and a light extinction coefficient of 0.0425 m^{-1}) were: 10 m = 20.92 (65% of surface), 70 m = 1.63 (5% of surface), 130 m = 0.128 (0.4% of surface), 200 m = 0.07 (0.02% of surface). The mean surface mixed-layer during the October 2002 sampling was 61 m. Data are available at (*50*). *Biomass derived from particulate adenosine triphosphate (ATP) measurements assuming a carbon:ATP ratio of 250. ND, Not determined.

Depth (m)	Temp. (°C)	Salinity	Chl a (μg/kg)	Biomass* (μg/kg)	DOC (μmol/kg)	N + N (nmol/kg)	DIP (nmol/kg)	Oxygen (μmol/kg)	DIC (μmol/kg)
10	26.40	35.08	0.08	7.21 ± 2.68	78	1.0	41.0	204.6	1,967.6
	(24.83 ± 1.27)	(35.05 ± 0.21)	(0.08 ± 0.03)	[78]	(90.6 ± 14.3)	(2.6 ± 3.7)	(56.0 ± 33.7)	(209.3 ± 4.5)	(1,972.1 ± 16.4)
	[2,104]	[1,611]	[320]		[140]	[126]	[146]	[348]	[107]
70	24.93	35.21	0.18	8.51 ± 3.22	79	1.3	16.0	217.4	1,981.8
	(23.58 ± 1.00)	(35.17 ± 0.16)	(0.15 ± 0.05)	[86]	(81.4 ± 11.3)	(14.7 ± 60.3)	(43.1 ± 25.1)	(215.8 ± 5.4)	(1,986.9 ± 15.4)
	[1,202]	[1,084]	[363]		[79]	[78]	[104]	[144]	[84]
130	22.19	35.31	0.10	5.03 ± 2.30	69	284.8	66.2	204.9	2,026.5
	(21.37 ± 0.96)	(35.20 ± 0.10)	(0.15 ± 0.06)	[90]	(75.2 ± 9.1)	(282.9 ± 270.2)	(106.0 ± 49.7)	(206.6 ± 6.2)	(2,013.4 ± 13.4)
	[1,139]	[980]	[350]		[86]	[78]	[68]	[173]	[69]
200	18.53	35.04	0.02	1.66 ± 0.24	63	1,161.9 ± 762.5	274.2 ± 109.1	198.8	2,047.7
	(18.39 ± 1.29)	(34.96 ± 0.18)	(0.02 ± 0.02)	[2]	(64.0 ± 9.8)	[7]	[84]	(197.6 ± 7.1)	(2,042.8 ± 10.5)
	[662]	[576]	[97]		[113]			[190]	[125]
500	7.25	34.07	ND	0.48 ± 0.23	47	28,850	2,153	118.0	2197.3
	(7.22 ± 0.44)	(34.06 ± 0.03)		[107]	(47.8 ± 6.3)	(28,460 ± 2210)	(2,051 ± 175.7)	(120.5 ± 18.3)	(2,200.2 ± 17.8)
	[1,969]	[1,769]			[112]	[326]	[322]	[505]	[134]
770	4.78	34.32	ND	0.29 ± 0.16	39.9	41,890	3,070	32.3	2323.8
	(4.86 ± 0.21)	(34.32 ± 0.04)		[107]	(41.5 ± 4.4)	(40,940 ± 500)	(3,000 ± 47.1)	(27.9 ± 4.1)	(2,324.3 ± 6.1)
	[888]	[773]			[34]	[137]	[135]	[275]	[34]
4,000	1.46	34.69	ND	ND	37.5	36,560	2,558	147.8	2325.5
	(1.46 ± 0.01)	(34.69 ± 0.00)			(42.3 ± 4.9)	(35,970 ± 290)	(2,507 ± 19)	(147.8 ± 1.3)	(2,329.1 ± 4.8)
	[262]	[245]			[83]	[108]	[104]	[210]	[28]

(figs. S5 and S6). The general patterns of archaeal distribution we observed were consistent with previous field surveys (*15*, *25*, *26*). Recovery of "group II" planktonic *Euryarchaeota* genomic DNA was greatest in the upper water column and declined below the photic zone. This distribution corroborates recent observations of ion-translocating photoproteins (called proteorhodopsins), now known to occur in group II *Euryarchaeota* inhabiting the photic zone (*27*). "Group III" *Euryarchaeota* DNA was recovered at all depths, but at a much lower frequency (figs. S5 and S6). A novel crenarchaeal group, closely related to a putatively thermophilic *Crenarchaeota* (*28*), was observed at the greatest depths (fig. S6).

Vertically Distributed Genes and Metabolic Pathways

The depths sampled were specifically chosen to capture microbial sequences at discrete biogeochemical zones in the water column encompassing key physicochemical features (Tables 1 and 2, Fig. 1; figs. S1 and S2). To evaluate sequences from each depth, fosmid end sequences were compared against different databases including the Kyoto Encyclopedia of Genes and Genomes (KEGG) (*29*), National Center for Biotechnology Information (NCBI)'s Clusters of Orthologous Groups (COG) (*30*), and SEED subsystems (*31*). After categorizing sequences from each depth in BLAST searches (*32*) against each database, we identified protein categories that were more or less well represented in one sample versus another, using cluster analysis (*33*, *34*) and bootstrap resampling methodologies (*35*).

Cluster analyses of predicted protein sequence representation identified specific genes and metabolic traits that were differentially distributed in the water column (fig. S7). In the photic zone (10, 70, and 130 m), these included a greater representation in sequences associated with photosynthesis; porphyrin and chlorophyll metabolism; type III secretion systems; and aminosugars, purine, proponoate, and vitamin B6 metabolism, relative to deep-water samples (fig. S7). Independent comparisons with well-annotated subsystems in the SEED database (*31*) also showed similar and overlapping trends (table S1), including greater representation in photic zone sequences associated with alanine and aspartate; metabolism of aminosugars; chlorophyll and carotenoid biosynthesis; maltose transport; lactose degradation; and heavy metal ion sensors and exporters. In contrast, samples from depths of 200 m and below (where there is no photosynthesis) were enriched in different sequences, including those associated with protein folding; processing and export; methionine metabolism; glyoxylate, dicarboxylate, and methane metabolism; thiamine metabolism; and type II secretion systems, relative to surface-water samples (fig. S7).

COG categories also provided insight into differentially distributed protein functions and categories. COGs more highly represented in photic zone included iron-transport membrane receptors, deoxyribopyrimidine photolyase, diaminopimelate decarboxylase, membrane guanosine triphosphatase (GTPase) with the lysyl endopeptidase gene product LepA, and branched-chain amino acid–transport system components (fig. S8). In contrast, COGs with greater representation in deep-water samples included transposases, several dehydrogenase categories, and integrases (fig. S8). Sequences more highly represented in the deep-water samples in SEED subsystem (*31*) comparisons included those associated with respiratory dehydrogenases, polyamine adenosine triphosphate (ATP)–binding cassette (ABC) transporters, polyamine metabolism, and alkylphosphonate transporters (table S1).

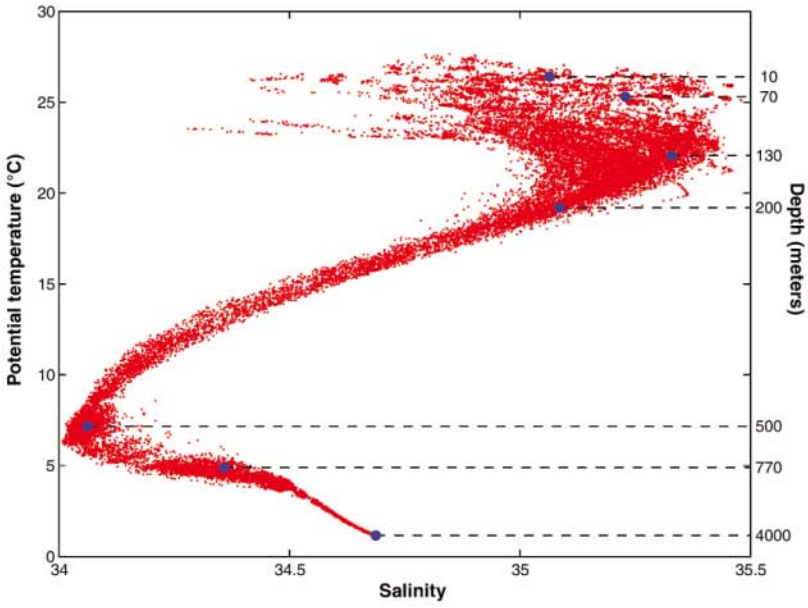

Fig. 1. Temperature versus salinity (T-S) relations for the North Pacific Subtropical Gyre at station ALOHA (22°45′N, 158°W). The blue circles indicate the positions, in T-S "hydrospace" of the seven water samples analyzed in this study. The data envelope shows the temperature and salinity conditions observed during the period October 1988 to December 2004 emphasizing both the temporal variability of near-surface waters and the relative constancy of deep waters.

Habitat-enriched sequences. We estimated average protein sequence similarities between all depth bins from cumulative TBLASTX high-scoring sequence pair (HSP) bitscores, derived from BLAST searches of each depth against every other (Fig. 3). Neighbor-joining analyses of a normalized, distance matrix derived from these cumulative bitscores joined photic zone and deeper samples together in separate clusters (Fig. 3). When we compared our HOT sequence datasets to previously reported Sargasso Sea microbial sequences (*19*), these datasets also clustered according to their depth and size fraction of origin (fig. S9). The clustering pattern in Fig. 3 is consistent with the expectation that randomly sampled photic zone microbial sequences will tend on average to be more similar to one another, than to those from the deep-sea, and vice-versa.

We also identified those sequences (some of which have no homologs in annotated databases) that track major depth-variable environmental features. Specifically, sequence homologs found only in the photic zone unique sequences (from 10, 70, and 130 m), or deepwater unique sequences (from 500, 770, and 4000 m) were identified (Fig. 3). To categorize potential functions encoded in these photic zone unique (PZ) or deep-water unique (DW) sequence bins, each was compared with KEGG, COG, and NCBI protein databases in separate analyses (*29*, *30*, *36*).

Some KEGG metabolic pathways appeared more highly represented in the PZ than in DW sequence bins, including those associated with photosynthesis; porphyrin and chlorophyll metabolism; propanoate, purine, and glycerphospholipid metabolism; bacterial chemotaxis; flagellar assembly; and type III secretion systems (Fig. 4A). All proteorhodopsin sequences (except one) were captured in the PZ bin. Well-represented photic zone KEGG pathway categories appeared to reflect potential pathway interdependencies. For example the PZ photosynthesis bin [3% of the total (Fig. 4A)] contained *Prochlorococcus*-like and *Synechococcus*-like photosystem I, photosystem II, and cytochrome genes. In tandem, PZ porphyrin and chlorophyll biosynthesis sequence bins [~3.9% of the total (Fig. 4A)] contained high representation of cyanobacteria-like cobalamin and chlorophyll biosynthesis genes, as well as photoheterotroph-like bacteriochlorophyll biosynthetic genes. Other probable functional interdependencies appear reflected in the corecovery of sequences associated with chemotaxis (mostly methyl-accepting chemotaxis proteins), flagellar biosynthesis (predominant-

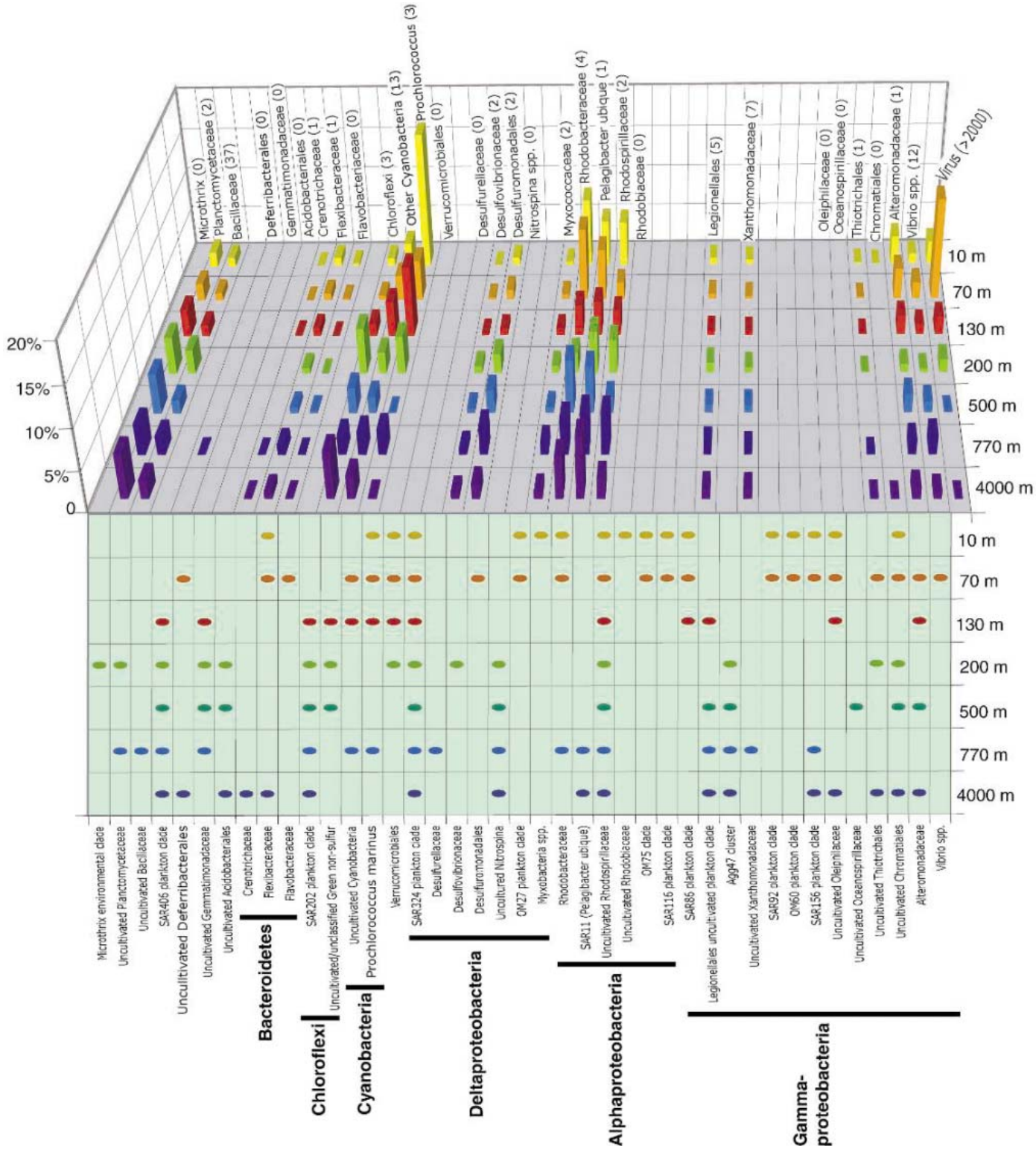

Fig. 2. Taxon distributions of top HSPs. The percent top HSPs that match the taxon categories shown at expectation values of $\leq 1 \times 10^{-60}$. Values in parentheses indicate number of genomes in each category, complete or draft, that were in the database at the time of analysis. The dots in the lower panel tabulate the SSU rRNAs detected in fosmid libraries from each taxonomic group at each depth (*35*) (figs. S3 and S6).

ly flagellar motor and hook protein-encoding genes), and type III secretory pathways (all associated with flagellar biosynthesis) in PZ (Fig. 4A).

DW sequences were enriched in several KEGG categories, including glyoxylate and dicarboxylate metabolism (with high representation of isocitrate lyase– and formate dehydrogenase–

like genes); protein folding and processing (predominantly chaperone and protease like genes); type II secretory genes (~40% were most similar to pilin biosynthesis genes); aminophospho-

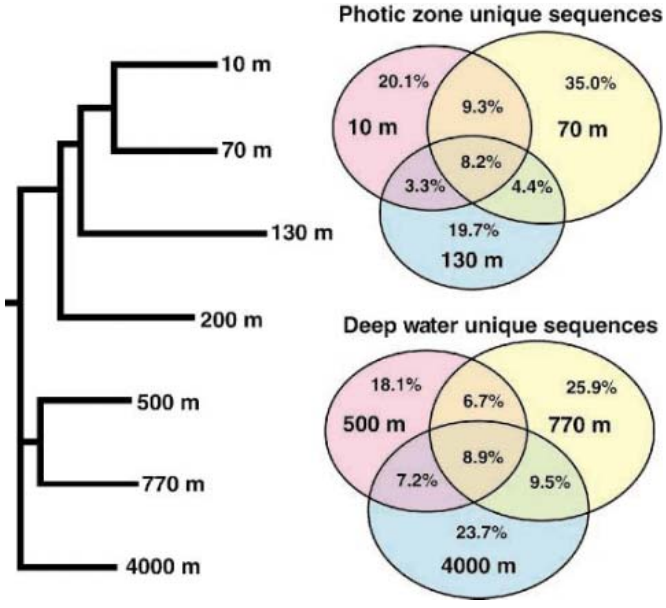

Fig. 3. Habitat-specific sequences in photic zone versus deep-water communities. The dendrogram shows a cluster analysis based on cumulative bitscores derived from reciprocal TBLASTX comparisons between all depths. Only the branching pattern resulting from neighbor-joining analyses (not branch-lengths) are shown in the dendrogram. The Venn diagrams depict the percentage of sequences that were present only in PZ sequences (n = 12,713) or DW sequences (n = 14,132), as determined in reciprocal BLAST searches of all sequences in each depth versus every other. The percentage out of the total PZ or DW sequence bins represented in each subset is shown. See SOM for methods (*35*).

nate, methionine, and sulfur metabolism; butanoate metabolism; ion-coupled transporters; and other ABC transporter variants (Fig. 4B). The high representation in DW sequences of type II secretion system and pilin biosynthesis genes, polysaccharide, and antibiotic synthesis suggest a potentially greater role for surface-associated microbial processes in the deeper-water communities. Conversely, enrichment of bacterial motility and chemotaxis sequences in the photic zone indicates a potentially greater importance for mobility and response in these assemblages.

Similar differential patterns of sequence distribution were seen in COG categories (Fig. 4B). COGs enriched in the PZ sequence bin included photolyases, iron-transport outer membrane proteins, Na^+-driven efflux pumps, ABC-type sugar-transport systems, hydrolases and acyl transferases, and transaldolases. In deeper waters, transposases were the most enriched COG category (~4.5% of the COG-categorized DW), increasing steadily in representation with depth from 500 m to their observed maximum at 4000 m (Fig. 4B; fig. S9). Transposases represented one of the single-most overrepresented COG categories in deep waters, accounting for 1.2% of all fosmids sequenced from 4000 m (fig. S8). Preliminary analyses of the transposase variants and mate-pair sequences indicate that they represent a wide variety of different transposase families and originate from diverse microbial taxa. In contrast, other highly represented COG categories appeared to reflect specific taxon distribution and abundances. For example, the enrichment of transaldolases at 70 m (Fig. 4B; fig. S9) were mostly derived from abundant cyanophage DNA that was recovered at that depth (see discussion below).

Sargasso Sea surface-water microbial sequences (*19*) shared, as expected, many more homologous sequences with our photic zone sequences than those from the deep sea (fig. S10). There were 10 times as many PZ than DW sequences shared in common with Sargasso Sea samples 5 through 7 (*19*) (fig. S10). In contrast, PZ-like sequences were only three times higher in DW when compared with sequences from Sargasso Sea sample 3 (fig. S10). The fact that Sargasso sample 3 was collected during a period of winter deep-water mixing likely contributes to this higher representation of DW-like homologs. Sargasso Sea homologs of our PZ sequence bin included, as expected, sequences associated with photosynthesis; amino acid transport; purine, pyrimidine and nitrogen metabolism; porphyrin and chlorophyll metabolism; oxidative phosphorylation; glycolysis; and starch and sucrose metabolism (fig. S10).

Tentative taxonomic assignments of PZ or DW sequences (top HSPs from NCBI's nonredundant protein database) were also tabulated (fig. S11). As expected, a high percentage of *Prochlorococcus*-like sequences was found in PZ (~5% of the total), and a greater representation of Deltaproteobacteria-like, *Actinobacteria*-like and *Planctomycete*-like sequences were recovered in DW. Unexpectedly, the single most highly represented taxon category in PZ (~21% of all identified sequences in PZ) was derived from viral sequences that were captured in fosmid clones (fig. S11).

Community Genomics and Host-Virus Interactions

Viruses are ubiquitous and abundant components of marine plankton, and influence lateral gene transfer, genetic diversity, and bacterial mortality in the water column (*37*–*40*). The large number of viral DNA sequences in our dataset was unexpected (Fig. 5; fig. S12), because we expected planktonic viruses to pass through our collection filters. Previous studies using a similar approach found only minimal contributions from viral sources (*19*, *40*). The majority of viral DNA we captured in fosmid clone libraries apparently originates from replicating viruses within infected host cells (*35*). Viral DNA recovery was highest in the photic zone, with cyanophage-like sequences representing 1 to 10% of all fosmid sequences (Fig. 5), and 60 to 80% of total virus sequences there. Below 200 m, viral DNA made up no more than 0.3% of all sequences at each depth. Most photic zone viral sequences shared highest similarity to T7-like and T4-like cyanophage of the Podoviridae and Myoviridae. This is consistent with previous studies (*40*–*42*), suggesting a widespread distribution of these phage in the ocean.

Analyses of 1107 fosmid mate pairs provided further insight into the origins of the viral sequences. About 67% of the viruslike clones were most similar to cyanophage on at least one end, and half of these were highly similar to cyanophage at both termini. Many of the cyanophage clones showed apparent synteny with previously sequenced cyanophage genomes (fig. S12). About 11% of the cyanophage paired-ends contained a host-derived cyanophage "signature" gene (*43*) on one terminus. The frequency and genetic-linkage of phage-encoded (but host-derived) genes we observed, including virus-derived genes involved in photosynthesis (*psbA*, *psbD*, *hli*), phosphate-scavenging genes (*phoH*, *pstS*), a cobalamin biosynthesis gene (*cobS*), and carbon metabolism (*transaldolase*) supports their widespread distribution in natural viral populations and their probable functional importance to cyanophage replication (*43*, *44*).

If we assume that the cyanophages' DNA was derived from infected host cells in which phage were replicating, the percentage of cyanophage-infected cells was estimated to range between 1 and 12% (*35*). An apparent cyanophage infection maxima was observed at 70 m, coinciding with the peak virus:host ratio (Fig. 5). Although these estimates are tentative, they are consistent with previously reported ranges of phage-infected picoplankton cells in situ (*38*, *45*).

About 0.5% of all sequences were likely prophage, as inferred from high sequence similarity to phage-related integrases and known prophage genes (*35*). Paired-end analyses of viral fosmids indicated that ~2.5% may be derived from prophage integrated into a variety of host taxa. A few clones also appear to be derived from temperate siphoviruses, and a number of putative eukaryotic paired-end viral sequences shared highest sequence identity with homologs from herpes viruses, mimiviruses, and algal viruses.

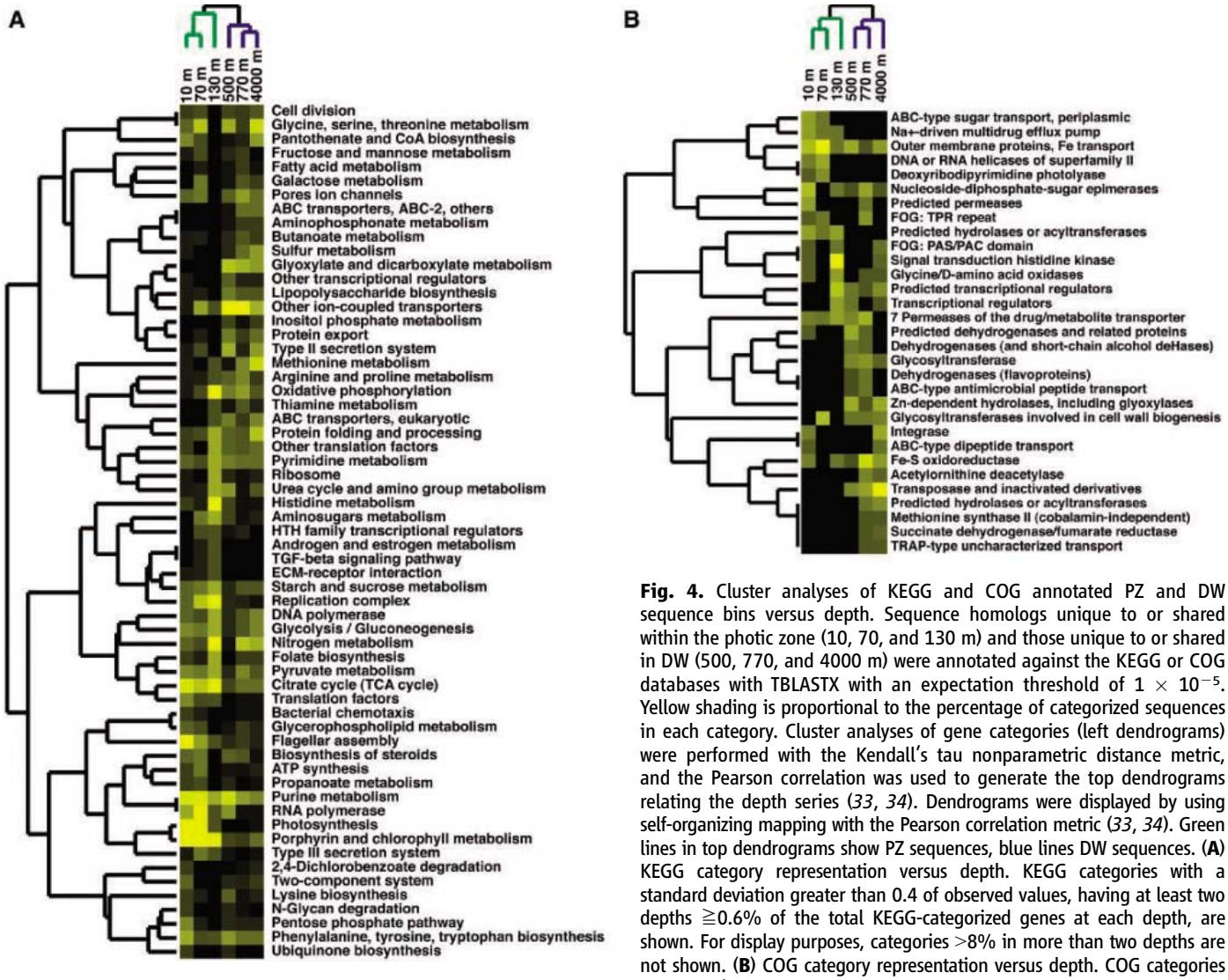

Fig. 4. Cluster analyses of KEGG and COG annotated PZ and DW sequence bins versus depth. Sequence homologs unique to or shared within the photic zone (10, 70, and 130 m) and those unique to or shared in DW (500, 770, and 4000 m) were annotated against the KEGG or COG databases with TBLASTX with an expectation threshold of 1×10^{-5}. Yellow shading is proportional to the percentage of categorized sequences in each category. Cluster analyses of gene categories (left dendrograms) were performed with the Kendall's tau nonparametric distance metric, and the Pearson correlation was used to generate the top dendrograms relating the depth series (*33*, *34*). Dendrograms were displayed by using self-organizing mapping with the Pearson correlation metric (*33*, *34*). Green lines in top dendrograms show PZ sequences, blue lines DW sequences. (**A**) KEGG category representation versus depth. KEGG categories with a standard deviation greater than 0.4 of observed values, having at least two depths ≧0.6% of the total KEGG-categorized genes at each depth, are shown. For display purposes, categories >8% in more than two depths are not shown. (**B**) COG category representation versus depth. COG categories with standard deviations greater than 0.2 of observed values, having at least two depths ≧0.3% of the total COG-categorized genes at each depth, are shown.

Ecological Implications and Future Prospects

Microbial community sampling along well-characterized depth strata allowed us to identify significant depth-variable trends in gene content and metabolic pathway components of oceanic microbial communities. The gene repertoire of surface waters reflected some of the mechanisms and modes of light-driven processes and primary productivity. Environmentally diagnostic sequences in surface waters included predicted proteins associated with cyanophage, motility, chemotaxis, photosynthesis, proteorhodopsins, photolyases, carotenoid biosynthesis, iron-transport systems, and host restriction-modification systems. The importance of light energy to these communities as reflected in their gene content was obvious. More subtle ecophysiological trends can be seen in iron transport, vitamin synthesis, flagella synthesis and secretion, and chemotaxis gene distributions. These data support hypotheses about potential adaptive strategies of heterotrophic bacteria in the photic zone that may actively compete for nutrients by swimming toward nutrient-rich particles and algae (*46*). In contrast to surface-water assemblages, deep-water microbial communities appeared more enriched in transposases, pilus synthesis, protein export, polysaccharide and antibiotic synthesis, the glyoxylate cycle, and urea metabolism gene sequences. The observed enrichment in pilus, polysaccharide, and antibiotic synthesis genes in deeper-water samples suggests a potentially greater role for a surface-attached life style in deeper-water microbial communities. Finally, the apparent enrichment of phage genes and restriction-modification systems observed in the photic zone may indicate a greater role for phage parasites in the more productive upper water column, relative to deeper waters.

At finer scales, sequence distributions we observed also reflected genomic "microvariability" along environmental gradients, as evidenced by the partitioning of high- and low-light *Prochlorococcus* ecotype genes observed in different regions of the photic zone (Fig. 5). Higher-order biological interactions were also evident, for example in the negative correlation of cyanophage versus *Prochlorococcus* host gene sequence recovery (Fig. 5). This relation between the abundance of host and cyanophage DNA probably reflects specific mechanisms of cyanophage replication in situ. These host-parasite sequence correlations we saw demonstrate the potential for observing community-level interspecies interactions through environmental genomic datasets.

Obviously, the abundance of specific taxa will greatly influence the gene distributions observed, as we saw, for example, in *Prochlorococcus* gene distribution in the photic zone. Gene sequence distributions can reflect more than just relative abundance of specific taxa, however.

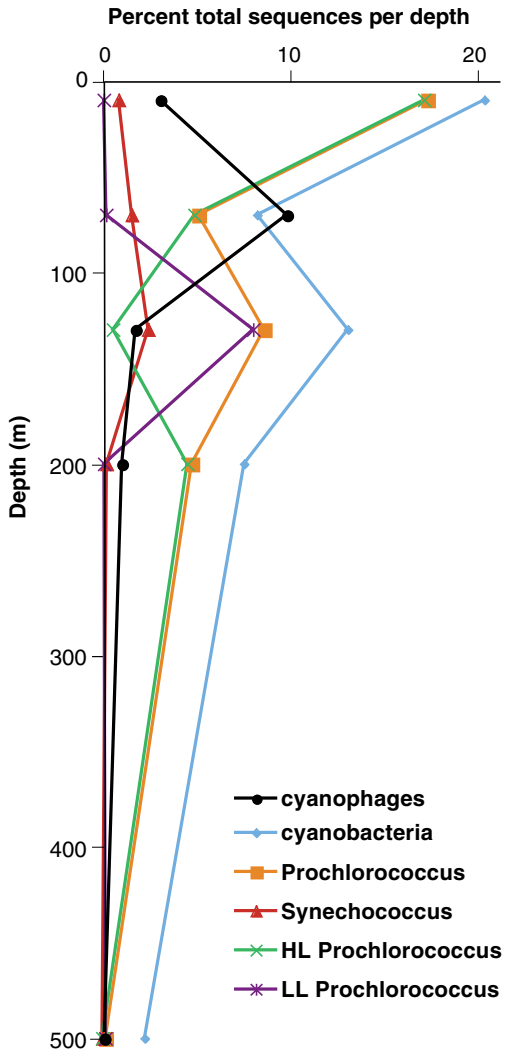

Fig. 5. Cyanophage and cyanobacteria distributions in microbial community DNA. The percentage of total sequences derived from cyanophage, total cyanobacteria, total *Prochlorococcus* spp., high-light *Prochlorococcus*, low-light *Prochlorococcus* spp., or *Synechococcus* spp., from each depth. Taxa were tentatively assigned according to the origin of top HSPs in TBLASTX searches, followed by subsequent manual inspection and curation.

Some depth-specific gene distributions we observed [e.g., transposases found predominantly at greater depths (Fig. 4B; fig. S8)], appear to originate from a wide variety of gene families and genomic sources. These gene distributional patterns seem more indicative of habitat-specific genetic or physiological trends that have spread through different members of the community. Community gene distributions and stoichiometries are differentially propagated by vertical and horizontal genetic mechanisms, dynamic physiological responses, or interspecies interactions like competition. The overrepresentation of certain sequence types may sometimes reflect their horizontal transmission and propagation within a given community. In our datasets, the relative abundance of cyanobacteria-like *psbA*, *psbD*, and transaldolase genes were largely a consequence of their horizontal transfer and subsequent amplification in the viruses that were captured in our samples. In contrast, the increase of transposases from 500 to 4000 m, regardless of community composition, reflected a different mode of gene propagation, likely related to the slower growth, lower productivity, and lower effective population sizes of deep-sea microbial communities. In future comparative studies, similar deviations in environmental gene stoichiometries might be expected to provide even further insight into habitat-specific modes and mechanisms of gene propagation, distribution, and mobility (*27*, *47*). These "gene ecologies" could readily be mapped directly on organismal distributions and interactions, environmental variability, and taxonomic distributions.

The study of environmental adaptation and variability is not new, but our technical capabilities for identifying and tracking sequences, genes, and metabolic pathways in microbial communities is. The study of gene ecology and its relation to community metabolism, interspecies interactions, and habitat-specific signatures is nascent. More extensive sequencing efforts are certainly required to more thoroughly describe natural microbial communities. Additionally, more concerted efforts to integrate these new data into studies of oceanographic, biogeochemical, and environmental processes are necessary (*48*). As the scope and scale of genome-enabled ecological studies matures, it should become possible to model microbial community genomic, temporal, and spatial variability with other environmental features. Significant future attention will no doubt focus on interpreting the complex interplay between genes, organisms, communities and the environment, as well as the properties revealed that regulate global biogeochemical cycles. Future efforts in this area will advance our general perspective on microbial ecology and evolution and elucidate the biological dynamics that mediate the flux of matter and energy in the world's oceans.

References and Notes

1. E. Forbes, in *Physical Atlas of Natural Phenomena*, A. K. Johnston, Ed. (William Blackwood & Sons, London and Edinburgh, 1856).
2. P. W. Hochachka, G. N. Somero, *Biochemical Adaptation* (Princeton Univ. Press, Princeton, NJ, 1984), pp. 450–495.
3. G. Rocap *et al.*, *Nature* **424**, 1042 (2003).
4. Z. I. Johnson *et al.*, manuscript submitted.
5. N. J. West *et al.*, *Microbiology* **147**, 1731 (2001).
6. A. A. Yayanos, *Annu. Rev. Microbiol.* **49**, 777 (1995).
7. N. R. Pace, *Science* **276**, 734 (1997).
8. M. S. Rappé, S. J. Giovannoni, *Annu. Rev. Microbiol.* **57**, 369 (2003).
9. M. T. Suzuki *et al.*, *Microb Ecol* (2005).
10. O. Béjà *et al.*, *Environ. Microbiol.* **2**, 516 (2000).
11. R. M. Morris, M. S. Rappé, E. Urbach, S. A. Connon, S. J. Giovannoni, *Appl. Environ. Microbiol.* **70**, 2836 (2004).
12. S. Y. Moon-van der Staay *et al.*, *Nature* **409**, 607 (2001).
13. J. A. Fuhrman, K. McCallum, A. A. Davis, *Nature* **356**, 148 (1992).
14. E. F. DeLong, *Proc. Natl. Acad. Sci. U.S.A.* **89**, 5685 (1992).
15. M. B. Karner *et al.*, *Nature* **409**, 507 (2001).
16. J. Handelsman, *Microbiol. Mol. Biol. Rev.* **68**, 669 (2004).
17. E. F. Delong, *Nat Rev Microbiol* (2005).
18. G. W. Tyson *et al.*, *Nature* **428**, 37 (2004).
19. J. C. Venter *et al.*, *Science* **304**, 66 (2004).
20. S. G. Tringe *et al.*, *Science* **308**, 554 (2005).
21. S. J. Hallam *et al.*, *Science* **305**, 1457 (2004).
22. D. M. Karl, R. Lukas, *Deep-Sea Res. II* **43**, 129 (1996).
23. D. M. Karl *et al.*, *Deep-Sea Res. II* **48**, 1449 (2001).
24. R. M. Letelier *et al.*, *Limnol. Oceanogr.* **49**, 508 (2004).
25. E. F. DeLong *et al.*, *Appl. Environ. Microbiol.* **65**, 5554 (1999).
26. A. Pernthaler *et al.*, *Appl. Environ. Microbiol.* **68**, 661 (2002).
27. N. U. Frigaard *et al.*, *Nature,* in press.
28. S. M. Barns, C. F. Delwiche, J. D. Palmer, N. R. Pace, *Proc. Natl. Acad. Sci. U.S.A.* **93**, 9188 (1996).
29. M. Kanehisa *et al.*, *Nucleic Acids Res.* **32**, D277 (2004).
30. R. L. Tatusov *et al.*, *BMC Bioinformatics* **4**, 41 (2003).
31. R. Overbeek *et al.*, *Nucleic Acids Res.* **33**, 5691 (2005).
32. S. F. Altschul *et al.*, *J. Mol. Biol.* **215**, 403 (1990).
33. M. J. L. de Hoon *et al.*, *Bioinformatics* **12**, 1453 (2004).
34. M. B. Eisen, P. T. Spellman, P. O. Brown, *Proc. Natl. Acad. Sci. U.S.A.* **94**, 14863 (1998).
35. Materials and methods are available as supporting material on *Science* Online.
36. K. D. Pruitt, T. Tatusova, D. R. Maglott, *Nucleic Acids Res.* **33**, D501 (2005).
37. M. G. Weinbauer, *FEMS Microbiol. Rev.* **28**, 127 (2004).

38. J. Waterbury, F. Valois, *Appl. Environ. Microbiol.* **59**, 3393 (1993).
39. M. B. Sullivan *et al.*, *Nature* **424**, 1047 (2003).
40. R. A. Edwards, F. Rohwer, *Nat. Rev. Microbiol.* **3**, 504 (2005).
41. J. Filee, F. Tetart, C. A. Suttle, H. M. Krisch, *Proc. Natl. Acad. Sci. U.S.A.* **102**, 12471 (2005).
42. M. Breitbart, J. H. Miyake, F. Rohwer, *FEMS Microbiol. Lett.* **236**, 249 (2004).
43. M. B. Sullivan *et al.*, *PLoS Biol.* **3**, e144 (2005).
44. D. Lindell *et al.*, *Proc. Natl. Acad. Sci. U.S.A.* **101**, 11013 (2004).
45. M. G. Weinbauer, I. Brettar, M. G. Hofle, *Limnol. Oceanogr.* **48**, 1457 (2003).
46. F. Azam, *Science* **280**, 694 (1998).
47. C. R. Woese, *Microbiol. Mol. Biol. Rev.* **68**, 173 (2004).
48. E. F. DeLong, D. M. Karl, *Nature* **437**, 336 (2005).
49. (http://hahana.soest.hawaii.edu/hot/parameters.html).
50. (http://hahana.soest.hawaii.edu/hot/hot-dogs).
51. This work was supported by a grant from the Gordon and Betty Moore Foundation, NSF grants MCB-0084211, MCB-0348001, and MCB-0509923 to E.F.D., and OCE-0326616 to D.M.K., and sequencing support from the U.S. Department of Energy Microbial Genomics Program. We thank Dennis Ryan for help with scripting and sequence analyses, the officers and crew of the R/V Ka'imikai-O-Kanaloa and the HOT team for assistance at sea, and L. Fujieki for help with oceanographic data display. J. Chapman, A. Salamov, and P. Richardson of the DOE Joint Genome Institute provided advice and assistance in DNA sequencing and analyses. Sequences have been deposited in GenBank with accession numbers DU731018-DU796676 and DU800850-DU800864 corresponding to fosmid end sequences, and accession numbers DQ300508-DQ300926 corresponding to SSU rRNA gene sequences.

Supporting Online Material

www.sciencemag.org/cgi/content/full/311/5760/496/DC1
Materials and Methods
Figs. S1 to S12
Table S1
References and Notes

16 September 2005; accepted 21 December 2005
10.1126/science.1120250

REPORTS

Pairing and Phase Separation in a Polarized Fermi Gas

Guthrie B. Partridge, Wenhui Li, Ramsey I. Kamar, Yean-an Liao, Randall G. Hulet*

We report the observation of pairing in a gas of atomic fermions with unequal numbers of two components. Beyond a critical polarization, the gas separates into a phase that is consistent with a superfluid paired core surrounded by a shell of normal unpaired fermions. The critical polarization diminishes with decreasing attractive interaction. For near-zero polarization, we measured the parameter $\beta = -0.54 \pm 0.05$, describing the universal energy of a strongly interacting paired Fermi gas, and found good agreement with recent theory. These results are relevant to predictions of exotic new phases of quark matter and of strongly magnetized superconductors.

Fermion pairing is the essential ingredient in the Bardeen, Cooper, and Schrieffer (BCS) theory of superconductivity. In conventional superconductors, the chemical potentials of the two spin states are equal. There has been great interest, however, in the consequences of mismatched chemical potentials that may arise in several important situations, including, for example, magnetized superconductors (*1*–*3*) and cold dense quark matter at the core of neutron stars (*4*). A chemical potential imbalance may be produced by several mechanisms, including magnetization in the case of superconductors, mass asymmetry, or unequal numbers. Pairing is qualitatively altered by the Fermi energy mismatch, and there has been considerable speculation regarding the nature and relative stability of various proposed exotic phases. In the Fulde-Ferrel-Larkin-Ovchinnikov (FFLO) phase (*2*, *3*), pairs possess a nonzero center-of-mass momentum that breaks translational invariance, whereas the Sarma (*1*), or the breached pair (*5*), phase is speculated to have gapless excitations. A mixed phase has also been proposed (*6*–*8*) in which regions of a paired BCS superfluid are surrounded by an unpaired normal phase. Little is known experimentally, however, because of the difficulty in creating magnetized superconductors. Initial evidence for an FFLO phase in a heavy-fermion superconductor has only recently been reported (*9*, *10*). Opportunities for experimental investigation of exotic pairing states have expanded dramatically with the recent realization of the Bose-Einstein condensate (BEC)–BCS crossover in a two spin state mixture of ultracold atomic gases. Recent experiments have demonstrated both superfluidity (*11*–*13*) and pairing (*14*–*17*) in atomic Fermi gases. We report the observation of pairing in a polarized gas of ^{6}Li atoms. Above an interaction-dependent critical polarization, we observed a phase separation that is consistent with a uniformly paired superfluid core surrounded by an unpaired shell of the excess spin state. Below the critical polarization, the spatial size of the gas was in agreement with expectations for a universal, strongly interacting paired Fermi gas.

Our methods for producing a degenerate gas of fermionic ^{6}Li atoms (*18*, *19*) and the realization of the BEC-BCS crossover at a Feshbach resonance (*17*) have been described previously (*20*). An incoherent spin mixture of the $F = 1/2$, $m_F = 1/2$ (state $|1\rangle$) and the $F = 1/2$, $m_F = -1/2$ (state $|2\rangle$) sublevels (where F is the total spin quantum number and m_F is its projection) is created by radio frequency (rf) sweeps, where the relative number of the two states can be controlled by the rf power (*20*). The spin mixture is created at a magnetic field of 754 G, which is within the broad Feshbach resonance located near 834 G (*21*, *22*). The spin mixture is evaporatively cooled by reducing the depth of the optical trap that confines it, and the magnetic field is ramped adiabatically to a desired field within the crossover region. States $|1\rangle$ and $|2\rangle$ are sequentially and independently imaged in the trap by absorption (*20*). Analysis of these images provides measurement of N_i and polarization $P = (N_1 - N_2)/(N_1 + N_2)$, where N_i is the number of atoms in state $|i\rangle$. We express the Fermi temperature, T_F, in terms of the majority spin state, state $|1\rangle$, as $k_B T_F = \hbar\overline{\omega}\,(6N_1)^{1/3}$, where $\overline{\omega} = 2\pi\,(\upsilon_r^2\upsilon_z)^{1/3}$ is the mean harmonic frequency of the cylindrically symmetric confining potential with radial and axial frequencies υ_r and υ_z, respectively. For $P \approx 0$, we find that $N_1 \approx N_2 \approx 10^5$, giving $T_F \approx$ 400 nK for our trap frequencies. Because of decreasing evaporation efficiency with increasing polarization, there is a correlation between P and total atom number (fig. S1).

For fields on the low-field (BEC) side of resonance, real two-body bound states exist, and molecules are readily formed by three-body recombination. For the case of $P = 0$, a molecular Bose-Einstein condensate (MBEC) is observed to form with no detectable thermal molecules (*17*). On the basis of an estimated MBEC condensate fraction of >90%, we place an upper limit on the temperature $T < 0.1T_F$ at a field of 754 G (*17*). However, the gas is expected to be cooled further during the adiabatic ramp for final fields greater than 754 G (*17*). By using similar experimental methods, we previously measured the order parameter of the gas in the BCS regime and found good agreement with $T =$ 0 BCS theory (*17*), indicating that the gas was well below the critical temperature for pairing.

Images of states $|1\rangle$ and $|2\rangle$ at a field of 830 G are shown (Fig. 1) for relative numbers

Department of Physics and Astronomy and Rice Quantum Institute, Rice University, Houston, TX 77251, USA.

*To whom correspondence should be addressed. E-mail: randy@rice.edu

corresponding to $P = 0.14$. The strength of the two-body interactions is characterized by the dimensionless parameter $k_F a$, where k_F is the Fermi wave vector and a is the s-wave scattering length. For a field of 830 G, $k_F a$ is greater than 10, corresponding to a unitarity limited interaction. We contend that the gas has separated into a uniformly paired, unpolarized inner core surrounded by a shell of the excess, unpaired state $|1\rangle$ atoms. In this case, the distribution of the difference, $|1\rangle - |2\rangle$ (Fig. 1), represents the location of these unpaired state $|1\rangle$ atoms.

Axial profiles of a sequence of images (Fig. 2) correspond to increasing values of P, again for 830 G. These axial profiles are the result of integrating the column density over the remaining radial coordinate. They are insensitive to the effect of finite imaging resolution in the radial dimension as well as to probe-induced radial heating of the second image in the sequence (*20*). On the left of Fig. 2 are distributions for both states $|1\rangle$ and $|2\rangle$, whereas the right side shows the corresponding difference distributions. Also shown in Fig. 2 are fits to a noninteracting $T = 0$ integrated Thomas-Fermi (T-F) distribution for fermions, $A\left(1-\frac{z^2}{R^2}\right)^{\frac{5}{2}}$, where A and R are adjustable fitting parameters and z is the axial position. Although the distributions are expected to differ somewhat from that of a noninteracting Fermi gas, we find that the fits are qualitatively good and provide a useful measure of the spatial size of the distributions. For $P = 0$ (Fig. 2A), the two spin components have identical distributions. We previously found that the gas was paired under the same conditions (*17*). As P increases (Fig. 2B), the peak height and width of the state $|2\rangle$ distributions initially diminish with respect to state $|1\rangle$, but their shapes are not fundamentally altered. When the polarization is increased beyond a critical value, however, the shapes of the two clouds become qualitatively different (Fig. 2C): The inner core, reflected by the distribution of the $|2\rangle$ atoms, is squeezed and becomes taller and narrower. This narrowing is noticeable in the wings of the state $|2\rangle$ distribution in comparison with the T-F fit. The squeezing of the state $|2\rangle$ distribution is accompanied by the excess, unpaired state $|1\rangle$ atoms being expelled from the center of the trap. These unpaired atoms form a shell that surrounds the inner core. As P approaches 1 (Fig. 2D), the contrast in the center hole in the difference distribution decreases because of the contribution to the axial density of unpaired atoms in the shell surrounding the core. The observation of difference distributions with a center hole and two peaks on either side is consistent with phase separation. Although more exotic redistributions of atoms cannot be ruled out, a separation between a uniformly paired phase and the excess unpaired atoms is the simplest explanation and is consistent with theoretical predictions (*6*–*8*).

To gain a more quantitative understanding of the phase separation as a function of P, we plot the ratio R/R_{TF} against P, where $R_{TF} = \left(\frac{2k_B T_F}{m\omega_z^2}\right)^{\frac{1}{2}}$ is the axial T-F radius for noninteracting fermions (*23*) and m is the atomic mass, $\omega_z = 2\pi\upsilon_z$, and T_F is calculated for each state from the measured numbers N_1 and N_2. Figure 3 shows the results for all of the 830 G data. At a critical polarization $P_c = 0.09 \pm 0.025$, R/R_{TF} for states $|1\rangle$ and $|2\rangle$ diverges in opposite directions from its value at small P. R/R_{TF} for state $|2\rangle$, which corresponds to the distribution of the pairs, decreases continuously to ~0.4 for the maximum attained polarization of $P \sim 0.86$. For state $|1\rangle$, R/R_{TF} jumps from its initial value to near unity at the critical polarization. Because $P = 1$ corresponds to a noninteracting gas, one expects R/R_{TF} to approach unity in this limit.

In the case of $P \approx 0$, the observation that the axial extent of the paired cloud is smaller than that of a noninteracting Fermi gas can be explained by the universal energy of strongly interacting paired fermions at the unitarity limit, where $k_F|a| \gg 1$ (*24*). In this limit, the chemical potential of the gas is believed to have the universal form $E_F(1+\beta)^{1/2}$, where β is a universal many-body parameter that

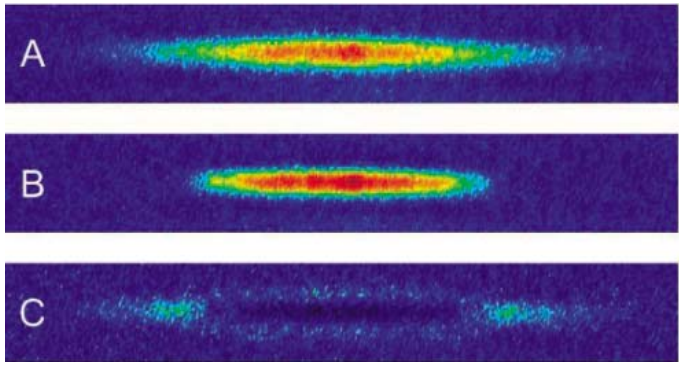

Fig. 1. In situ absorption images showing phase separation at a field of 830 G. A false-color scale is used to represent the column density. The trapping frequencies are $\upsilon_r = 350$ Hz and $\upsilon_z = 7.2$ Hz. These images correspond to $P = 0.14$. **(A)** Majority spin state, $|1\rangle$, with $N_1 = 8.6 \times 10^4$. **(B)** Minority spin state, $|2\rangle$, with $N_2 = 6.5 \times 10^4$. **(C)** Difference distribution, $|1\rangle - |2\rangle$, corresponding to the excess unpaired $|1\rangle$ atoms. These excess atoms reside in a shell surrounding an inner core of unpolarized pairs. We observe that the excess state $|1\rangle$ atoms preferentially reside at large z, whereas relatively few occupy the thin radial shell at small z. We speculate that this may be a consequence of the high aspect ratio trapping potential. (A) and (B) were obtained sequentially by using probe laser beams of different frequencies. Probe-induced radial heating of the second image in the sequence (state $|1\rangle$, in this case), caused by off-resonant excitation by the first probe, produces a slight reduction in peak height (*20*). As a result, the difference distribution is slightly negative at the center. The size of each image in the object plane is 1.41 mm horizontally and 0.12 mm vertically. The displayed aspect ratio has been rescaled for clarity.

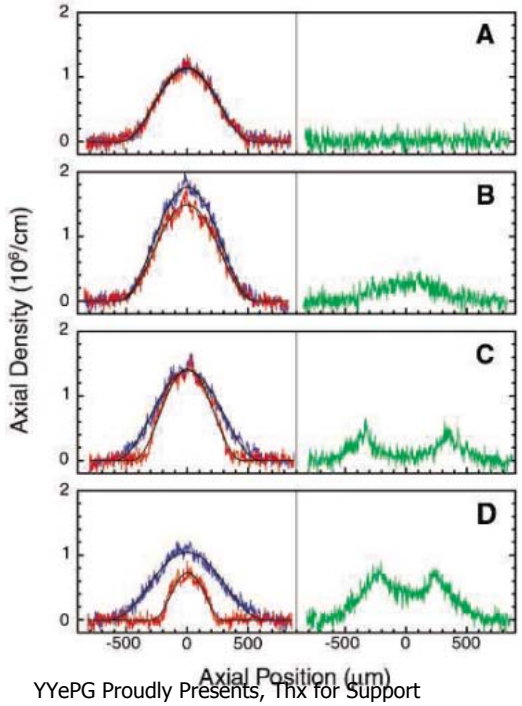

Fig. 2. Axial density profiles at 830 G. For the curves on the left, the blue data correspond to state $|1\rangle$ and the red data correspond to state $|2\rangle$, whereas the green curves on the right show the difference distributions, $|1\rangle - |2\rangle$. The axial density measurements are absolute and without separate normalization for the two states. The solid lines on the left curves are fits to a T-F distribution for fermions, where the fitted parameters are A and R. **(A)** $P = 0.01$, $N_1 = 6.4 \times 10^4$; **(B)** $P = 0.09$, $N_1 = 1.0 \times 10^5$; **(C)** $P = 0.14$, $N_1 = 8.6 \times 10^4$; and **(D)** $P = 0.53$, $N_1 = 6.8 \times 10^4$. The state $|2\rangle$ distributions reflect the distribution of pairs, whereas the difference distributions show the unpaired atoms. Phase separation is evident in (C) and (D). The profiles in (C) are derived from the images given in Fig. 1.

can be determined from $\beta = (R/R_{TF})^4 - 1$ (*25*–*27*). For P near zero, we found that $R/R_{TF} = 0.825 \pm 0.02$, giving $\beta = -0.54 \pm 0.05$ (uncertainties discussed in Fig. 3 legend). This value is in excellent agreement with previous measurements (*24*, *26*, *28*, *29*) but with substantially improved uncertainty. Our measurement is also consistent with $\beta = -0.58 \pm 0.01$ obtained from two Monte Carlo calculations (*8*, *30*, *31*) and with $\beta = -0.545$ from a calculation reported in (*27*). Not surprisingly, the measurement is in disagreement with $\beta = -0.41$ obtained with BCS mean-field theory (*27*).

We believe that the data are consistent with a quantum phase transition from a homogenous paired superfluid state to a superfluid-normal phase separated state. For $P = 0$, the excellent agreement between the measured value of β and theory, combined with our previous measurement of pair correlations in an unpolarized gas (*17*), is strong evidence that the gas is paired. Furthermore, superfluidity has been observed in the same system under similar conditions (*11*–*13*). The fact that the size of the gas, which is strongly dependent on the gas being paired, does not change appreciably for $0 < P < P_c$ suggests that it may remain paired in this regime, which is remarkable (*32*). For $P > P_c$, the excess unpaired atoms prefer to reside in a shell outside the inner core. Such a phase separation may be explained in the BEC regime (*33*) where the atoms and weakly bound dimers are believed to have a large repulsive three-body interaction (*34*); however, application of this theory to the strongly interacting regime would be incorrect because it also gives a large repulsive dimer-dimer interaction (*34*) that is inconsistent with a negative value of β. Therefore, we conclude that the phase separation is a consequence of the energy cost of accommodating unpaired atoms within the paired core (*6*–*8*). Vortices have also been used to explore superfluidity in ^{6}Li with mismatched Fermi surfaces (*35*). Although hints of phase separation are reported in that work, a critical polarization was not observed.

We also performed the experiment at 920 G, which is on the BCS side of the resonance where $k_F a = -1.1$. We found a phase separation at this field as well. However, the value of R/R_{TF} at $P \approx 0$ is larger, 0.92 ± 0.02, a consequence of smaller but still strong interactions, and the critical polarization for phase separation is considerably smaller, $P_c < 0.03$, consistent with zero to within our experimental sensitivity. Observation of phase separation at small P demonstrates the sensitivity of our determination of phase separation. In the BEC regime at a field of 754 G where $k_F a = 0.6$, we find that P_c is somewhat larger than 0.10, but at this field probe-induced radial heating prevents an accurate determination (*20*). The critical polarization value diminishes going from the BEC to BCS regimes, as expected (*8*). In the BCS regime, very little Fermi energy mismatch is tolerated before phase separation occurs. For samples prepared at higher temperature ($T \approx 0.7 T_F$), no phase separation was observed.

The nature of the coexistence phase where $P < P_c$ is still unknown, so the existence of the FFLO and the breached pair states are not excluded by these observations. Recent calculations suggest that a homogeneous gapless superfluid state may be preferred for small polarizations in the unitarity regime (*8*). These results help to clarify the long-open question of how Fermi superfluids respond to mismatched Fermi surfaces.

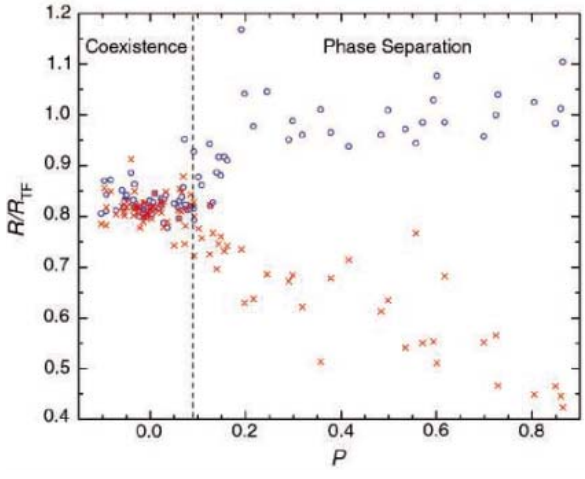

Fig. 3. R/R_{TF} versus P. The ratios of the measured axial radius to that of a noninteracting T-F distribution are shown as blue open circles for state $|1\rangle$ and as red crosses for state $|2\rangle$. The data combine 92 independent shots. The dashed line corresponds to the estimated critical polarization, $P_c = 0.09$, for the phase transition from coexisting to separated phases. The images are of sufficient quality that the assignment of phase separation is ambiguous in only two of the shots represented. Our contention for a phase transition at P_c has its basis in statistical evidence: None of the 31 shots deliberately prepared as $P = 0$ and only one with a measured $P < 0.07$ is phase separated, whereas all but two shots with $P > 0.11$ are. The width of this transition region is consistent with our statistical uncertainty in the measurement of P. Although fluctuations in absolute probe detuning lead to 15% uncertainty in total number, the difference in the two probe frequencies is precisely controlled, resulting in lower uncertainty in P. We estimate the uncertainty in a single measurement of P to be 5%, which is the standard deviation of measurements of P for distributions prepared as $P = 0$. Also from these distributions, we find no significant systematic shift in detection of relative number. The uncertainty in the ratio R/R_{TF} is estimated to be 2.5%, due mainly to the uncertainty in measuring υ_z (*20*). The uncertainty in R/R_{TF} for state $|2\rangle$ grows with increasing P because of greater uncertainty in the fitted value of R with decreasing N_2.

References and Notes

1. G. Sarma, *J. Phys. Chem. Solids* **24**, 1029 (1963).
2. P. Fulde, R. A. Ferrell, *Phys. Rev.* **135**, A550 (1964).
3. A. I. Larkin, Y. N. Ovchinnikov, *Sov. Phys. JETP* **20**, 762 (1965).
4. R. Casalbuoni, G. Nardulli, *Rev. Mod. Phys.* **76**, 263 (2004).
5. W. V. Liu, F. Wilczek, *Phys. Rev. Lett.* **90**, 047002 (2003).
6. P. F. Bedaque, H. Caldas, G. Rupak, *Phys. Rev. Lett.* **91**, 247002 (2003).
7. H. Caldas, *Phys. Rev. A.* **69**, 063602 (2004).
8. J. Carlson, S. Reddy, *Phys. Rev. Lett.* **95**, 060401 (2005).
9. H. A. Radovan *et al.*, *Nature* **425**, 51 (2003).
10. K. Kakuyanagi *et al.*, *Phys. Rev. Lett.* **94**, 047602 (2005).
11. J. Kinast *et al.*, *Phys. Rev. Lett.* **92**, 150402 (2004).
12. M. Bartenstein *et al.*, *Phys. Rev. Lett.* **92**, 203201 (2004).
13. M. W. Zwierlein *et al.*, *Nature* **435**, 1047 (2005).
14. C. A. Regal, M. Greiner, D. S. Jin, *Phys. Rev. Lett.* **92**, 040403 (2004).
15. M. W. Zwierlein *et al.*, *Phys. Rev. Lett.* **92**, 120403 (2004).
16. C. Chin *et al.*, *Science* **305**, 1128 (2004); published online 22 July 2004 (10.1126/science.1100818).
17. G. B. Partridge *et al.*, *Phys. Rev. Lett.* **95**, 020404 (2005).
18. A. G. Truscott, K. E. Strecker, W. I. McAlexander, G. B. Partridge, R. G. Hulet, *Science* **291**, 2570 (2001); published online 1 March 2001 (10.1126/science.1059318).
19. K. E. Strecker, G. B. Partridge, R. G. Hulet, *Phys. Rev. Lett.* **91**, 080406 (2003).
20. Materials and methods are available as supporting material on *Science* Online.
21. M. Houbiers *et al.*, *Phys. Rev. A* **57**, R1497 (1998).
22. M. Bartenstein *et al.*, *Phys. Rev. Lett.* **94**, 103201 (2005).
23. C. J. Pethick, H. Smith, *Bose–Einstein Condensation in Dilute Gases* (Cambridge Univ. Press, Cambridge, 2002), pp. 402.
24. K. M. O'Hara, S. L. Hemmer, M. E. Gehm, S. R. Granade, J. E. Thomas, *Science* **298**, 2179 (2002); published online 7 November 2002 (10.1126/science.1079107).
25. M. E. Gehm *et al.*, *Phys. Rev. A* **68**, 011401 (2003).
26. M. Bartenstein *et al.*, *Phys. Rev. Lett.* **92**, 120401 (2004).
27. A. Perali, P. Pieri, G. C. Strinati, *Phys. Rev. Lett.* **93**, 100404 (2004).
28. T. Bourdel *et al.*, *Phys. Rev. Lett.* **93**, 050401 (2004).
29. J. Kinast *et al.*, *Science* **307**, 1296 (2005); published online 27 January 2005 (10.1126/science.1109220).
30. J. Carlson *et al.*, *Phys. Rev. Lett.* **91**, 050401 (2003).
31. G. E. Astrakharchik *et al.*, *Phys. Rev. Lett.* **93**, 200404 (2004).
32. T.-L. Ho, personal communication.
33. L. Viverit, C. J. Pethick, H. Smith, *Phys. Rev. A.* **61**, 053605 (2000).
34. D. S. Petrov, C. Salomon, G. V. Shlyapnikov, *Phys. Rev. Lett.* **93**, 090404 (2004).
35. M. W. Zwierlein, A. Schirotzek, C. H. Schunck, W. Ketterle, *Science* **311**, 492 (2006); published online 22 December 2005 (10.1126/science.1122318).

36. We acknowledge support from the NSF, Office of Naval Research, NASA, and the Welch Foundation. The authors are grateful for stimulating interactions with Y. Chen, C. Lobo, K. Machida, E. Mueller, and H. Stoof.

Supporting Online Material

www.sciencemag.org/cgi/content/full/1122876/DC1
Materials and Methods
Fig. S1
References

21 November 2005; accepted 14 December 2005
Published online 22 December 2005;
10.1126/science.1122876
Include this information when citing this paper.

Ethanol Can Contribute to Energy and Environmental Goals

Alexander E. Farrell,[1]* Richard J. Plevin,[1] Brian T. Turner,[1,2] Andrew D. Jones,[1] Michael O'Hare,[2] Daniel M. Kammen[1,2,3]

To study the potential effects of increased biofuel use, we evaluated six representative analyses of fuel ethanol. Studies that reported negative net energy incorrectly ignored coproducts and used some obsolete data. All studies indicated that current corn ethanol technologies are much less petroleum-intensive than gasoline but have greenhouse gas emissions similar to those of gasoline. However, many important environmental effects of biofuel production are poorly understood. New metrics that measure specific resource inputs are developed, but further research into environmental metrics is needed. Nonetheless, it is already clear that large-scale use of ethanol for fuel will almost certainly require cellulosic technology.

Energy security and climate change imperatives require large-scale substitution of petroleum-based fuels as well as improved vehicle efficiency (*1*, *2*). Although biofuels offer a diverse range of promising alternatives, ethanol constitutes 99% of all biofuels in the United States. The 3.4 billion gallons of ethanol blended into gasoline in 2004 amounted to about 2% of all gasoline sold by volume and 1.3% (2.5×10^{17} J) of its energy content (*3*). Greater quantities of ethanol are expected to be used as a motor fuel in the future because of two federal policies: a $0.51 tax credit per gallon of ethanol used as motor fuel and a new mandate for up to 7.5 billion gallons of "renewable fuel" to be used in gasoline by 2012, which was included in the recently passed Energy Policy Act (EPACT 2005) (*4*, *5*).

Thus, the energy and environmental implications of ethanol production are more important than ever. Much of the analysis and public debate about ethanol has focused on the sign of the net energy of ethanol: whether manufacturing ethanol takes more nonrenewable energy than the resulting fuel provides (*6*, *7*). It has long been recognized that calculations of net energy are highly sensitive to assumptions about both system boundaries and key parameter values (*8*). In addition, net energy calculations ignore vast differences between different types of fossil energy (*9*). Moreover, net energy ratios are extremely sensitive to specification and assumptions and can produce uninterpretable values in some important cases (*10*). However, comparing across published studies to evaluate how these assumptions affect outcomes is difficult owing to the use of different units and system boundaries across studies. Finding intuitive and meaningful replacements for net energy as a performance metric would be an advance in our ability to evaluate and set energy policy in this important arena.

To better understand the energy and environmental implications of ethanol, we surveyed the published and gray literature and present a comparison of six studies illustrating the range of assumptions and data found for the case of corn-based (*Zea mays*, or maize) ethanol (*11*–*16*). To permit a direct and meaningful comparison of the data and assumptions across the studies, we developed the Energy and Resources Group (ERG) Biofuel Analysis Meta-Model (EBAMM) (*10*). For each study, we compared data sources and methods and parameterized EBAMM to replicate the published net energy results to within half a percent. In addition to net energy, we also calculated metrics for greenhouse gas (GHG) emissions and primary energy inputs (table S1 and Fig. 1).

Two of the studies stand out from the others because they report negative net energy values and imply relatively high GHG emissions and petroleum inputs (*11*, *12*). The close evaluation required to replicate the net energy results showed that these two studies also stand apart from the others by incorrectly assuming that ethanol coproducts (materials inevitably generated when ethanol is made, such as dried distiller grains with solubles, corn gluten feed, and corn oil) should not be credited with any of the input energy and by including some input data that are old and unrepresentative of current processes, or so poorly documented that their quality cannot be evaluated (tables S2 and S3).

Sensitivity analyses with EBAMM and elsewhere show that net energy calculations are most sensitive to assumptions about coproduct allocation (*17*). Coproducts of ethanol have positive economic value and displace competing products that require energy to make. Therefore, increases in corn ethanol production to meet the requirements of EPACT 2005 will lead to more coproducts that displace whole corn and soybean meal in animal feed, and the energy thereby saved will partly offset the energy required for ethanol production (*5*, *18*).

The studies that correctly accounted for this displacement effect reported that ethanol and coproducts manufactured from corn yielded a positive net energy of about 4 MJ/l to 9 MJ/l. The study that ignored coproducts but used recent data found a slightly positive net energy for corn ethanol (*13*). However, comparisons of the reported data are somewhat misleading because of many incommensurate assumptions across the studies.

We used EBAMM to (i) add coproduct credit where needed, (ii) apply a consistent system boundary by adding missing parameters (e.g., effluent processing energy) and dropping extraneous ones (e.g., laborer food energy), (iii) account for different energy types, and (iv) calculate policy-relevant metrics (*19*). Figure 1 shows both published and commensurate values as well as equivalent values for the reference, conventional gasoline.

The published results, adjusted for commensurate system boundaries, indicate that with current production methods corn ethanol displaces petroleum use substantially; only 5 to 26% of the energy content is renewable. The rest is primarily natural gas and coal (Fig. 2). The impact of a switch from gasoline to ethanol has an ambiguous effect on GHG emissions, with the reported values ranging from a 20% increase to a decrease of 32%. These values have their bases in the same system boundaries, but some of them rely on data of dubious quality. Our best point estimate for average performance today is that corn ethanol reduces petroleum use by about 95% on an energetic basis and reduces GHG emissions only moderately, by about 13%. Uncertainty analysis suggests these results are robust (*10*). It is important to realize that actual performance will vary from place to place and that these values reflect an absence of incentives for GHG emission control. Given adequate policy incentives, the performance of corn ethanol in terms of GHG emissions can likely be improved (*20*). However, current data suggest that only cellulosic ethanol offers large reductions in GHG emissions.

The remaining differences among the six studies are due to different input parameters, which are relatively easy to evaluate within the simple, transparent EBAMM framework. For instance, most of the difference between the highest and lowest values for GHG emissions in our data are due to differences in limestone ($CaCO_3$) application rate and energy embodied in farm machinery (table S1). The former is truly uncertain; data for lime application and for the resulting GHG emissions are poor (*15*). In contrast, the higher farm machinery energy values are unverifiable and more than an order of magnitude greater than values reported elsewhere and calculated here, suggesting that the lower values are more representative (*10*) (table S3).

This analysis illustrates the major contribution of agricultural practices to life-cycle GHG emissions (34% to 44%) and petroleum inputs (45% to 80%) to corn ethanol, suggest-

[1]Energy and Resources Group, [2]Goldman School of Public Policy, [3]Renewable and Appropriate Energy Laboratory, University of California, Berkeley, CA 94720–3050, USA.

*To whom correspondence should be addressed. E-mail: aef@berkeley.edu

ing that policies aimed at reducing environmental externalities in the agricultural sector may result in significantly improved environmental performance of this fuel. For example, conservation tillage reduces petroleum consumption and GHG emissions as well as soil erosion and agrichemical runoff (*20*, *21*).

We use the best data from the six studies to create three cases in EBAMM: *Ethanol Today*, which includes typical values for the current U.S. corn ethanol industry and requires the fewest assumptions; *CO_2 Intensive*, which has its basis in current plans to ship Nebraska corn to a lignite-powered ethanol plant in North Dakota (*22*); and *Cellulosic*, which assumes that production of cellulosic ethanol from switchgrass becomes economic as represented in one of the studies (*16*).

The *Cellulosic* case presented here is a preliminary estimate of a rapidly evolving technology and is designed to highlight the dramatic reductions in GHG emissions that could be achieved. In addition, other biofuel technologies and production processes are in active development and, as the data become available, should be the subject of similar energy and environmental impact assessments.

For all three cases, producing one MJ of ethanol requires far less petroleum than is required to produce one MJ of gasoline (Fig. 2). However, the GHG metric illustrates that the environmental performance of ethanol varies greatly depending on production processes. On the other hand, single-factor metrics may be poor guides for policy. With the use of the petroleum intensity metric, the *Ethanol Today* case would be slightly preferred over the *Cellulosic* case (a petroleum input ratio of 0.06 compared with 0.08); however, on the GHG metric, the *Ethanol Today* case is far worse than *Cellulosic* (83 compared to 11). Additional environmental metrics are now being developed for biofuels, and a few have been applied to ethanol production, but several key issues remain unquantified, such as soil erosion and the conversion of forest to agriculture (*18*, *20*).

Looking to the future, the environmental implications of ethanol production are likely to grow more important, and there is a need for a more complete set of policy-relevant metrics. In addition, future analysis of fuel ethanol should more carefully evaluate ethanol production from cellulosic feedstocks, not least because cellulosic ethanol production is undergoing major technological development and because the cultivation of cellulosic feedstocks is not as far advanced as corn agriculture, suggesting more potential for improvement. Such advances may enable biomass energy to contribute a sizeable fraction of the nation's transportation energy, as some studies have suggested (*23*, *24*).

Our study yields both research and policy recommendations. Evaluations of biofuel policy should use realistic assumptions (e.g., the inclusion of coproduct credits calculated by a

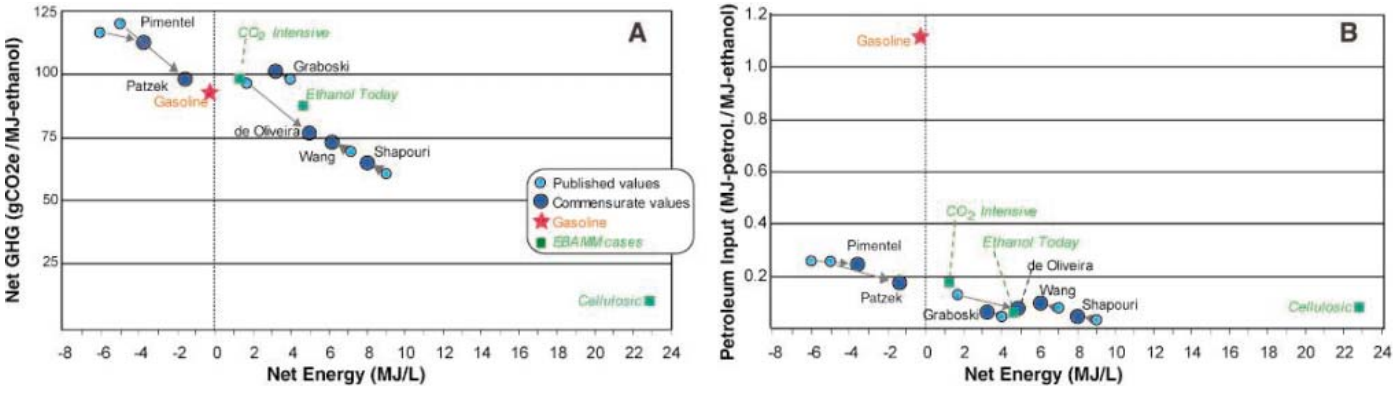

Fig. 1. (**A**) Net energy and net greenhouse gases for gasoline, six studies, and three cases. (**B**) Net energy and petroleum inputs for the same. In these figures, small light blue circles are reported data that include incommensurate assumptions, whereas the large dark blue circles are adjusted values that use identical system boundaries. Conventional gasoline is shown with red stars, and EBAMM scenarios are shown with green squares. Adjusting system boundaries reduces the scatter in the reported results. Moreover, despite large differences in net energy, all studies show similar results in terms of more policy-relevant metrics: GHG emissions from ethanol made from conventionally grown corn can be slightly more or slightly less than from gasoline per unit of energy, but ethanol requires much less petroleum inputs. Ethanol produced from cellulosic material (switchgrass) reduces both GHGs and petroleum inputs substantially.

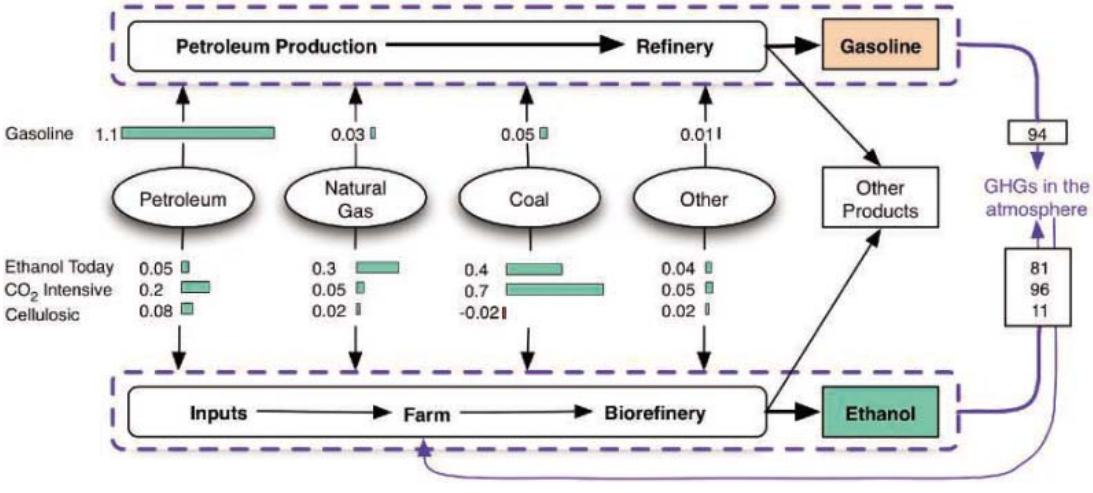

Fig. 2. Alternative metrics for evaluating ethanol based on the intensity of primary energy inputs (MJ) per MJ of fuel and of net greenhouse gas emissions (kg CO_2-equivalent) per MJ of fuel. For gasoline, both petroleum feedstock and petroleum energy inputs are included. "Other" includes nuclear and hydrological electricity generation. Relative to gasoline, ethanol produced today is much less petroleum-intensive but much more natural gas– and coal-intensive. Production of ethanol from lignite-fired biorefineries located far from where the corn is grown results in ethanol with a high coal intensity and a moderate petroleum intensity. Cellulosic ethanol is expected to have an extremely low intensity for all fossil fuels and a very slightly negative coal intensity due to electricity sales that would displace coal.

displacement method), accurate data, clearly defined future scenarios, and performance metrics relevant to policy goals like reducing greenhouse gas emissions, petroleum inputs, and soil erosion. Progress toward attaining these goals will require new technologies and practices, such as sustainable agriculture and cellulosic ethanol production. Such an approach could lead to a biofuels industry much larger than today's that, in conjunction with greater vehicle efficiency, could play a key role in meeting the nation's energy and environmental goals.

References and Notes

1. T. E. Wirth, C. B. Gray, J. D. Podesta, *Foreign Aff.* **82**, 132 (2003).
2. R. A. Kerr, R. F. Service, *Science* **309**, 101 (2005).
3. S. C. Davis, S. W. Diegel, *Transportation Energy Data Book* (Technical Report No. ORNL-6973, Oak Ridge National Laboratory, Oak Ridge, TN, 2004).
4. If only cellulosic ethanol production capacity is added, only 4.8 billion gallons will be required because of preferential credit provisions.
5. "Implications of Increased Ethanol Production for U.S. Agriculture" (Report No. 10-05, Food and Agricultural Policy Research Institute, Univ. of Missouri, Columbia, MO, 2005). Also available at www.fapri.missouri.edu/outreach/publications/2005/FAPRI_UMC_Report_10_05.pdf.
6. By convention, photosynthetic energy is ignored in this calculation.
7. H. Shapouri, J. A. Duffield, M. Wang, *Trans. ASAE* **46**, 959 (2003).
8. R. S. Chambers, R. A. Herendeen, J. J. Joyce, P. S. Penner, *Science* **206**, 789 (1979).
9. C. J. Cleveland, *Energy* **30**, 769 (2005).
10. Materials and methods are available as supporting material on *Science* Online. Additional information is available, including the working EBAMM model, at http://socrates.berkeley.edu/~rael/EBAMM.
11. T. Patzek, *Crit. Rev. Plant Sci.* **23**, 519 (2004).
12. D. Pimentel, T. Patzek, *Nat. Resour. Res.* **14**, 65 (2005).
13. M. E. D. De Oliveira, B. E. Vaughan, E. J. Rykiel, *Bioscience* **55**, 593 (2005).
14. H. Shapouri, A. McAloon, "The 2001 net energy balance of corn ethanol" (U.S. Department of Agriculture, Washington, DC, 2004). Also available at www.usda.gov/oce/oepnu.
15. M. Graboski, "Fossil energy use in the manufacture of corn ethanol" (National Corn Growers Association, Washington, DC, 2002). Also available at www.ncga.com/ethanol/main.
16. M. Wang, "Development and use of GREET 1.6 fuel-cycle model for transportation fuels and vehicle technologies" (Tech. Rep. ANL/ESD/TM-163, Argonne National Laboratory, Argonne, IL, 2001). Also available at www.transportation.anl.gov/pdfs/TA/153.pdf.
17. S. Kim, B. E. Dale, *Int. J. Life Cycle Assess.* **7**, 237 (2002).
18. M. A. Delucchi, "Conceptual and methodological issues in lifecycle analyses of transportation fuels" (Tech. Rep. UCD-ITS-RR-04-45, Univ. of California, Davis, 2004). Also available at www.its.ucdavis.edu/publications/2004/UCD-ITS-RR-04-45.pdf.
19. Factors eliminated were labor transportation, labor food energy, and process water energy. The first two were deemed outside the system boundaries. Process water energy was included in one study but was insufficiently documented. Factors added were farm machinery energy, inputs packaging, and effluent processing energy. The metric for petroleum use included crude oil used as a feedstock for gasoline, and the metric for GHGs included end-use (tailpipe) fossil emissions (*10*).
20. S. Kim, B. E. Dale, *Biomass Bioenergy* **29**, 426 (2005).
21. E. Tegtmeier, M. Duffy, *Int. J. Agric. Sustainability* **2**, 1 (2004).
22. More information is available at www.redtrailenergyllc.com.
23. R. D. Perlack, L. L. Wright, A. Turhollow, R. Graham, B. Stokes, D. Erbach, "Biomass as feedstock for a bioenergy and bioproducts industry: The technical feasibility of a billion-ton annual supply" (Tech. Rep. ORNL/TM-2006/66, Oak Ridge National Laboratory, Oak Ridge, TN, 2005). Also available at http://feedstockreview.ornl.gov/pdf/billion_ton_vision.pdf.
24. L. B. Lave, W. Griffin, H. McLean, *Issues Sci. Technol.* **18**, 73 (2001).

25. This research was made possible through support from the Energy Foundation and the Karsten Family Foundation (both to D.M.K.) and NSF's Climate Decision Making Center at Carnegie Mellon University (SES-034578) (to A.E.F.) and Graduate Research Fellowship program (to A.D.J.). The authors thank J. Thompson, D. Greene, M. DeLucchi, M. Wang, and an anonymous reviewer for assistance and valuable comments.

Supporting Online Material

www.sciencemag.org/cgi/content/full/311/5760/506/DC1
Materials and Methods
SOM Text
Figs. S1 and S2
Tables S1 to S3
References

17 October 2005; accepted 9 January 2006
10.1126/science.1121416

Optical Detection of DNA Conformational Polymorphism on Single-Walled Carbon Nanotubes

Daniel A. Heller,[1] Esther S. Jeng,[2] Tsun-Kwan Yeung,[2] Brittany M. Martinez,[2] Anthonie E. Moll,[2] Joseph B. Gastala,[2] Michael S. Strano[2]*

The transition of DNA secondary structure from an analogous B to Z conformation modulates the dielectric environment of the single-walled carbon nanotube (SWNT) around which it is adsorbed. The SWNT band-gap fluorescence undergoes a red shift when an encapsulating 30-nucleotide oligomer is exposed to counter ions that screen the charged backbone. The transition is thermodynamically identical for DNA on and off the nanotube, except that the propagation length of the former is shorter by five-sixths. The magnitude of the energy shift is described by using an effective medium model and the DNA geometry on the nanotube sidewall. We demonstrate the detection of the B-Z change in whole blood, tissue, and from within living mammalian cells.

Single-walled carbon nanotubes (*1*) are rolled sheets of graphene with nanometer-sized diameters that possess remarkable photostablity (*2*). The semiconducting forms of SWNTs, when dispersed by surfactants in aqueous solution, can display distinctive near-infrared (IR) photoluminescence (*3*) arising from their electronic band gap. The band-gap energy is sensitive to the local dielectric environment around the SWNT, and this property can be exploited in chemical sensing, which was recently demonstrated for the detection of β-D-glucose (*4*).

Among the molecules that can bind to the surface of SWNTs is DNA, which adsorbs as a double-stranded (ds) complex (*5*). Certain DNA oligonucleotides will transition from the native, right-handed B form to the left-handed Z form as cations adsorb onto and screen the negatively charged backbone (*6*–*9*). We now show that an analogous B-to-Z transition for a 30-nucleotide dsDNA modulates the dielectric environment of SWNTs and decreases their near-IR emission energy up to 15 meV. We have used this fluorescence signal to detect divalent metal cations that bind to DNA and stabilize the Z form. The thermodynamics of the conformational change for DNA both on and off the SWNT are nearly identical. These near-IR ion sensors can operate in strongly scattering or absorbing media, which we demonstrate by detecting mercuric ions in whole blood, black ink, and living mammalian cells and tissues.

Near-IR spectrofluorometry was performed on colloidally stable complexes of DNA-encapsulated SWNTs (DNA-SWNTs) buffered at a pH of 7.4 and synthesized by the non-covalent binding to the nanotube sidewall (*10*) of a 30–base pair single-stranded DNA (ssDNA) oligonucleotide with a repeating G-T sequence. This ssDNA can hydrogen bond with itself to form dsDNA. Several types of semiconducting SWNTs are present, but as we show below, they can be identified by their characteristic band gaps. The shift in band gap is similar for each type of SWNT, although there is a diameter dependence. After the addition of divalent cations, we observed an energy shift in the SWNT emission with a relative ion sensitivity of $Hg^{2+} > Co^{2+} > Ca^{2+} > Mg^{2+}$, which is identical for free DNA (Fig. 1A) (*11*). The shift can also be observed by monitoring SWNT photoabsorption bands (fig. S1). The fluorescence peak energy traces a monotonic, two-state equilibrium profile with increasing ionic strength for each case (*12*).

The removal of ions from the system via dialysis returns the emission energy to its initial value, which is indicative of a completely reversible thermodynamic transition (Fig. 1B and

[1]Department of Chemistry, [2]Department of Chemical and Biomolecular Engineering, University of Illinois at Urbana-Champaign, Urbana, IL 61801, USA.

*To whom correspondence should be addressed. E-mail: strano@uiuc.edu

fig. S2) (*10*). Under identical conditions, circular dichroism (CD) spectroscopy confirmed that the unbound DNA undergoes a conformational change from the B to the Z form, and the inversion of the 285-nm peak indicates a reversal of helicity (Fig. 1C) .

We compare the ellipticity of the 285-nm CD peak versus Hg^{2+} concentration with the fluorescent emission energy from the nanotube under identical conditions (Fig. 1D). Assuming identical transitions, the overlapping points of inflection indicate that the difference in the Gibbs free energy (ΔG) changes for the DNA on and off the nanotube is quite small [$\Delta(\Delta G) \sim 0.05\ k_BT$ per phosphate, where k_B is Boltzmann's constant, T is temperature, and k_BT is the thermal energy] (*13*, *14*). Thus, the transitions for DNA in solution or adsorbed on the SWNT appear to be thermodynamically identical.

A critical difference is apparent between the slopes at the inflection. Pohl (*15*) describes the B-Z transition—which requires a double-stranded helix to separate, change helicity, and re-form—as a process of nucleation and propagation in series. The dsDNA strand initially separates with a ratio of rate constants β_B/β_Z, whereas propagation proceeds as a series of equilibrium steps proportional to the number of base pairs, N, as the dislocation proceeds down the chain (*10*). The expression for the fractional transition K (*6*, *15*) contains a scaling factor C_0, which is the ion concentration (C) where K is independent of N

$$K = \left(\frac{C}{C_o}\right)^{aN}\left[\frac{\beta_B}{\beta_Z} + \left(\frac{C}{C_o}\right)^{aN}\right]^{-1}$$

The slope at the inflection is related to the propagation length aN, where a is the ratio of binding sites to oligonucleotide length. Regression of the data in Fig. 1D reveals that DNA on the nanotube precedes through only $\frac{1}{6}$ the number of transitions, as in the case of the free strand. As expected, β_B/β_Z, which is associated with the initiation of the event, is similar for the cases on and off the nanotube (1.21 and 1.04, respectively). If we assume that the same helicity change occurs both on and off the nanotube, our interpretation is one of a transition that propagates in small steps and requires about $\frac{2\pi}{3}$ radians of the strand to unravel for propagation down the nanotube (Fig. 1E and fig. S3).

Examining this phenomenon for SWNTs of different diameters allows us to probe the influence of the cylindrical geometry. Perebeinos and co-workers (*16*) used a numerical solution to the Bethe-Salpeter equation (*17*) to yield a scaling relationship for the exciton binding energy $E = A\mu^{n-1}r_t^{n-2}\varepsilon^{-n}$, where μ is the reduced effective mass (*18*), r_t is the nanotube radius, and ε is the dielectric constant around the nanotube. The constants A and n were determined by fitting nanotubes with diameters in the range of 1 to 2.5 nm and were found to be 24.1 eV $nm^{3/5}$ and 1.4, respectively. With this scaling,

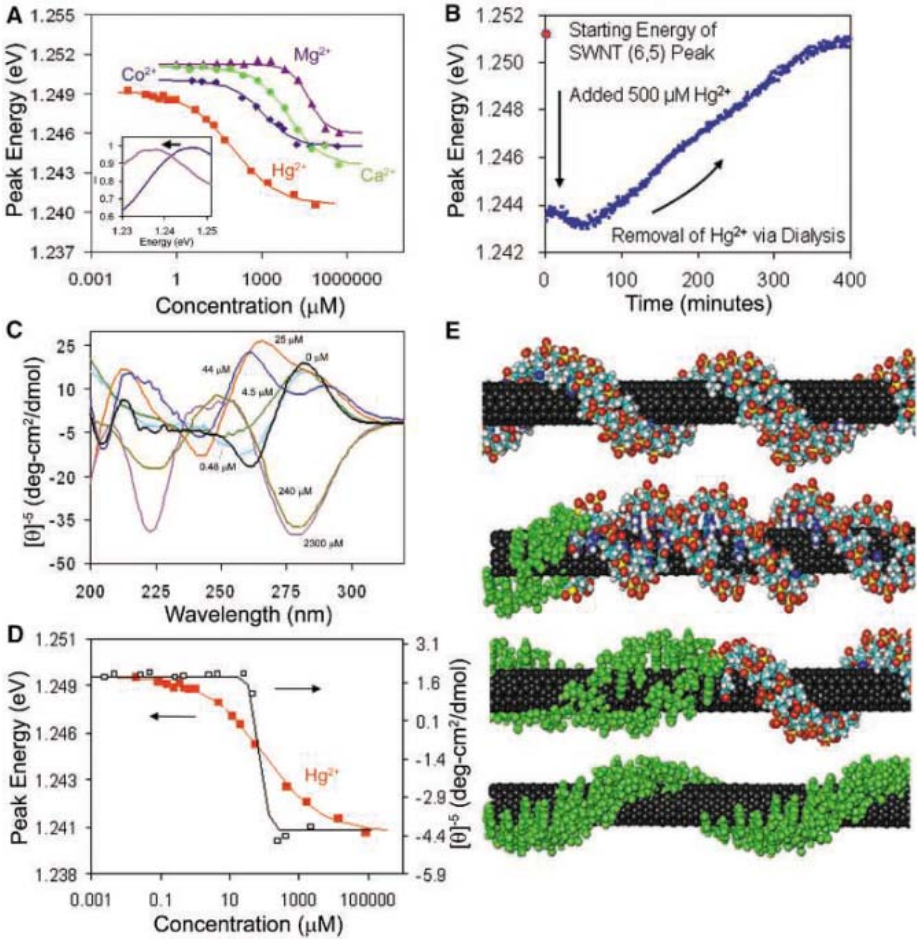

Fig. 1. (**A**) Concentration-dependent fluorescence response of the DNA-encapsulated (6,5) nanotube to divalent chloride counterions. The inset shows the (6,5) fluorescence band at starting (blue) and final (pink) concentrations of Hg^{2+}. (**B**) Fluorescence energy of DNA-SWNTs inside a dialysis membrane upon removal of Hg^{2+} during a period of 7 hours by dialysis. (**C**) Circular dichroism spectra of unbound $d(GT)_{15}$ DNA at various concentrations of Hg^{2+}. (**D**) DNA-SWNT emission energy plotted versus Hg^{2+} concentration (red curve) and the ellipticity of the 285-nm peak obtained via circular dichroism measurements upon addition of mercuric chloride to the same oligonucleotide (black curve). Arrows point to the axis used for the corresponding curve. (**E**) Illustration of DNA undergoing a conformational transition from the B form (top) to the Z form (bottom) on a carbon nanotube.

the change in emission energy from the B to Z form for a DNA wrapped nanotube is then

$$\Delta E_{B\to Z} = A\mu^{n-1}r_t^{n-2}\left(\frac{1}{\varepsilon_Z^n} - \frac{1}{\varepsilon_B^n}\right) \quad (1)$$

Approximating the dielectric constant of the B or Z wrapped nanotube using an effective medium gives

$$\varepsilon_i = \alpha_i\varepsilon_{DNA} + (1 - \alpha_i)\varepsilon_{Water} \quad (2)$$

Here, ε_{DNA} and ε_{Water} are the dielectric constants of DNA (4.0) and water (88.1), and α_i is the ratio of surface area covered by DNA per total area, which increases in transitioning from the B to Z form (*19*). To relate α_i to the geometry of the adsorbed phase, we consider a helical surface described by three parameters: radius r; pitch b; and width of the strand w

$$\alpha = \frac{w\sqrt{r^2 + b^2}}{rb} \quad (3)$$

By describing the mechanics of DNA as a continuum helix (*20*) maintaining an equilibrium curvature (*21*), one can then describe the total energy in terms of its deflection. Adsorbing the DNA to a nanotube of radius r_t perturbs it from the equilibrium radius, r_o, and pitch, b_o. The resulting pitch that minimizes the total energy is

$$b = \sqrt{\left(\frac{r_o + r_t}{r_o}\right)\left(b_o^2 + r_o^2\right) - (r_o + r_t)^2} \quad (4)$$

and the surface area is

$$\alpha = \frac{w}{(r_o + r_t)}\sqrt{\frac{b_o^2 + r_o^2}{b_o^2 + r_o^2 - (r_o + r_t)r_o}} \quad (5)$$

For B DNA, r_o and b_o are 1 and 3.32 nm, respectively; for Z DNA, the values are 0.9 and 4.56 nm, respectively (*19*, *22*).

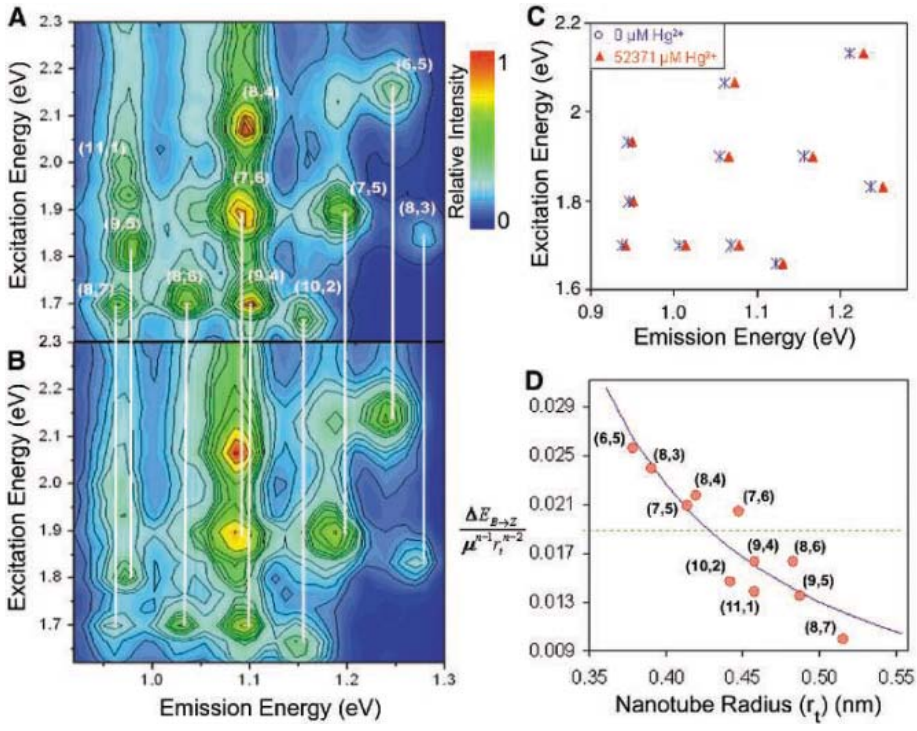

Fig. 2. Fluorescence three-dimensional (3D) profile of excitation versus emission energy of a DNA-SWNT solution with (**A**) 0 μM $HgCl_2$ and (**B**) 52.37 mM $HgCl_2$. Vertical lines highlight the fluorescence red shift of individual SWNT species upon addition of Hg^{2+}. (**C**) Peak centers of the nanotubes present in the 3D profile. (**D**) The energy shift of individual SWNT species modified by the Bethe-Salpeter equation to evince the effective dielectric constant differences caused by DNA geometry (orange points). The model curve (blue line) is based on the radial dependence of the DNA surface area coverage of the nanotube on changing from the B to Z form.

We used fluorescence excitation profiles to experimentally examine the diameter dependence of the transition on the nanotubes. The emission from the B and Z forms (Fig. 2, A and B, with vertical lines comparing the peak centers) shows that the (6,5) nanotube (r_t = 0.38 nm) undergoes a 15-meV decrease, whereas the (8,7) (r_t = 0.51 nm) shifts only 5 meV. This inverse dependence for 11 of the strongest emitting SWNTs in the sample is shown in Fig. 2C. The curve in Fig. 2D is generated by using literature values for the geometric constants and by assuming 0.51 and 1.18 nm for the regressed widths of the bands for B and Z, respectively. Using constant dielectric values in Eq. 1 generates the horizontal line. Despite several limiting assumptions in this treatment (*23*), the model is able to predict the correct magnitude of the energy shift, the trend with radius, and the direction of the shift (red) using only geometric constants for the DNA adsorbed phase (tables S1 and S2) (*10*).

We have shown that the conformational rearrangement of a biomolecule can be transduced directly by the SWNT system. Given the recent discovery of a class of Z-DNA binding proteins and the association of Z-DNA to transcriptional activity and potential biological functions, it will be useful to have new probes to interrogate the conditions under which Z-DNA formation can occur (*9*, *24*). Our previous work has shown that this type of DNA-SWNT complex is found to readily enter mammalian cells upon a 3-hour incubation and localize in the perinuclear region of the cell via endocytosis (*25*). We localized DNA-SWNTs within murine

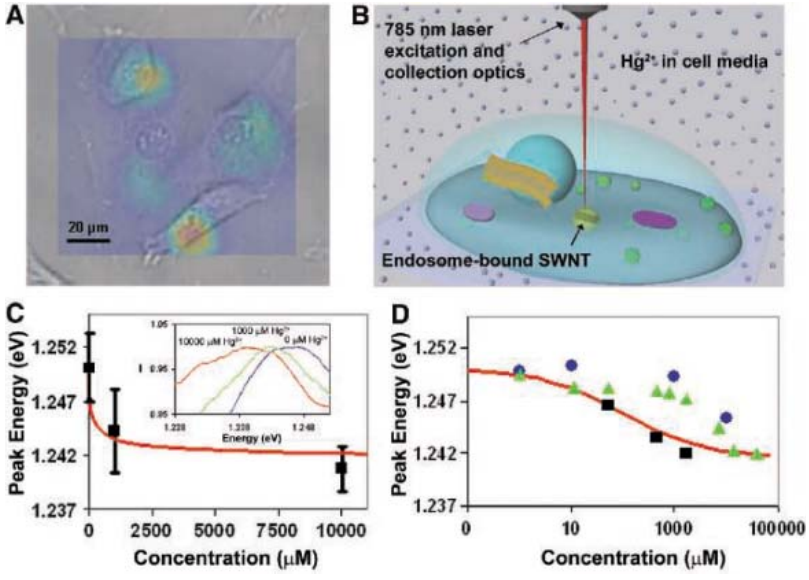

Fig. 3. (**A**) Area map of the (6,5) nanotube peak fluorescence intensity of DNA-SWNTs within murine 3T3 fibroblast cells overlayed on an optical micrograph of the same region. (**B**) Illustration of the experimental method used for ion-binding experiments conducted in mammalian cells. A cell containing endosome-bound DNA-SWNTs undergoes 785-nm excitation through a microscope objective. (**C**) The (6,5) nanotube fluorescence peak energy of DNA-SWNTs in 3T3 fibroblasts plotted versus Hg^{2+} concentration in the cell medium. The fluorescence energy of a population of 8 to 10 cells was averaged for each data point. Error bars indicate 1 SD. The red line shows the model curve from original Hg^{2+} binding experiment conducted in Tris buffer. The inset shows individual spectra at each concentration. (**D**) The (6,5) nanotube fluorescence energy of DNA-SWNTs in the following highly absorptive and scattering media: whole rooster blood (green triangles), black dye solution (black squares), and chicken tissue (blue circles) plotted on a model curve (red) from Hg^{2+} addition to SWNTs in buffer. The ΔE of all blood and tissue data points were corrected for an initial red shift due to the cellular environment.

3T3 fibroblasts (Fig. 3A) and perfused various concentrations of $HgCl_2$ (Fig. 3, B and C) (*10*) in the extracellular buffer space for 5 min. The SWNT emission from the (6,5) nanotube, although shifted by 3 meV already upon uptake within the cell, red shifts additively with in-

creasing Hg^{2+} concentration. After correcting for the initial shift caused by the new environment, the response of cell-bound DNA-SWNTs fits the model curve created by the same complexes in pure buffer (Fig. 3C). Control experiments produced no additional shift. The successful operation of the complex within living mammalian cells creates opportunities for new molecular probes that operate in the near IR and avoid natural autofluorescence of biological media.

Ion detection is also possible in media that already possess a strong ionic background. A 12,000–molecular weight cut off dialysis capillary was filled with DNA-SWNTs and inserted into whole blood and muscle tissue. The complex was added directly to a black dye solution (optical density > 4). The $HgCl_2$ was still detected through these highly absorptive media (Fig. 3D). The near-IR fluorescence of DNA-SWNTs in the dye solution exhibited the same response as SWNTs in pure buffer. In whole blood and tissue, the presence of interfering absorbers of Hg^{2+} (free DNA, proteins, etc.) predictably shifts the observed sensitivity to larger values (C_0 = 3500 μM in blood; 8000 μM in tissue); however, the DNA-SWNTs still provide a measure of the residual ions that are locally bound to the complex in these heterogeneous media (*26*).

References and Notes

1. R. Saito, G. Dresselhaus, M. S. Dresselhaus, *Physical Properties of Carbon Nanotubes* (Imperial College Press, London, 1998).
2. A. Hartschuh *et al.*, *ChemPhysChem* **6**, 577 (2005).
3. M. J. O'Connell *et al.*, *Science* **297**, 593 (2002).
4. P. W. Barone, S. Baik, D. A. Heller, M. S. Strano, *Nat. Mater.* **4**, 86 (2005).
5. M. Zheng *et al.*, *Science* **302**, 1545 (2003).
6. F. M. Pohl, T. M. Jovin, *J. Mol. Biol.* **67**, 375 (1972).
7. S. B. Zimmerman, *Annu. Rev. Biochem.* **51**, 395 (1982).
8. T. M. Jovin, D. M. Soumpasis, L. P. Mcintosh, *Annu. Rev. Phys. Chem.* **38**, 521 (1987).
9. A. Rich, *J. Biol. Chem.* **271**, 11595 (1996).
10. Materials, methods, and discussions of the modeling are available as supporting material on *Science* Online.
11. J. Duguid, V. A. Bloomfield, J. Benevides, G. J. Thomas, *Biophys. J.* **65**, 1916 (1993).
12. Minor variability in the peak energy in the limit of zero ion concentration (Fig. 1A) is apparently caused by batch-to-batch variation in the DNA-SWNT sample.
13. The change in free energy difference (*14*) is taken assuming equal propagation lengths as $[\Delta(\Delta G)] = k_B T \ln(C_f/C_{SWNT})$, where C_f and C_{SWNT} are the free and SWNT-bound DNA inflection concentrations, respectively (Fig. 1D). By comparison, the free energy change from the intramolecular contribution alone is 0.1 $k_B T$ per phosphate. The $[\Delta(\Delta G)]$ normally has three contributions arising from hydration, electrostatic, and intermolecular terms.
14. J. L. F. Abascal, J. C. G. Montoro, *Mol. Phys.* **102**, 2141 (2004).
15. F. M. Pohl, *Cold Spring Harb. Symp. Quant. Biol.* **47**, 113 (1982).
16. V. Perebeinos, J. Tersoff, P. Avouris, *Phys. Rev. Lett.* **92**, 257402-1 (2004).
17. M. Rohlfing, *Phys. Rev. B* **62**, 4927 (2000).
18. V. N. Popov, L. Henrard, P. Lambin, *Phys. Rev. B* **72**, 035436 (2005).
19. R. E. Dickerson *et al.*, *Science* **216**, 475 (1982).
20. C. Tung, S. Harvey, *Nucleic Acids Res.* **12**, 3343 (1984).
21. R. Geballe, *Am. J. Phys.* **26**, 287 (1958).
22. A. Wang *et al.*, *Nature* **282**, 680 (1979).
23. The scaling developed by Perebeinos and co-workers (*16*) has several limitations, including an assumption that the dielectric constant is low and the tube diameters under consideration are greater than 1 nm.
24. S. Rothenburg *et al.*, *Proc. Natl. Acad. Sci. U.S.A.* **102**, 1602 (2005).
25. D. A. Heller, S. Baik, T. E. Eurell, M. S. Strano, *Adv. Mater.* **17**, 2793 (2005).

26. The authors would like to thank S. Denos and M. Gruebele for assistance with circular dichroism experiments, C. Zimmerman and J. Bahr for the donation of rooster blood, and S. McMasters of the School of Chemical Sciences Cell Media Facility for aiding with cell culture and media preparation. This work was supported by NSF grant no. CTS-0330350, DuPont Young Investigator Award 2005, the Defense Advanced Research Projects Agency/Microsystems Technology Office, and the University of Illinois School of Chemical Sciences.

Supporting Online Material

www.sciencemag.org/cgi/content/full/311/5760/508/DC1
Materials and Methods
SOM Text
Figs. S1 to S4
Tables S1 and S2
References

30 September 2005; accepted 18 December 2005
10.1126/science.1120792

Rapid Uplift of the Altiplano Revealed Through ^{13}C-^{18}O Bonds in Paleosol Carbonates

Prosenjit Ghosh,[1] Carmala N. Garzione,[2] John M. Eiler[1]

The elevation of Earth's surface is among the most difficult environmental variables to reconstruct from the geological record. Here we describe an approach to paleoaltimetry based on independent and simultaneous determinations of soil temperatures and the oxygen isotope compositions of soil waters, constrained by measurements of abundances of ^{13}C-^{18}O bonds in soil carbonates. We use this approach to show that the Altiplano plateau in the Bolivian Andes rose at an average rate of 1.03 ± 0.12 millimeters per year between ~10.3 and ~6.7 million years ago. This rate is consistent with the removal of dense lower crust and/or lithospheric mantle as the cause of elevation gain.

Earth scientists have attempted to determine the elevation history of Earth's surface by measuring proxies for barometric pressure (*1*, *2*), the thickness of overlying atmosphere (*3*), the enthalpy of the atmosphere (*4*), ground temperature (*5*, *6*), and the $\delta^{18}O$ value of meteoric water (*7*–*12*). Methods aimed at determining atmospheric pressure/thickness (*1*–*3*) are the most theoretically robust but suffer from difficulties in sample availability and interpretation, and as a result have seen little use. The more practical methods, using isotopic data (*7*–*12*), have difficulty accounting for climate change or changes in the seasonality of precipitation. Paleobotanical methods of constraining atmospheric enthalpy or temperature (*4*–*6*) depend on empirical correlations with plant physiognomy that are of uncertain value when applied to ancient plant communities.

Ghosh *et al.* (*13*) report the calibration of a new kind of carbonate stable isotope paleothermometer that constrains carbonate growth temperature independently of the $\delta^{18}O$ of waters from which they grew. They refer to this method as the "clumped isotope thermometer," because it measures the temperature-dependent clumping of ^{13}C and ^{18}O into bonds with each other in the carbonate mineral lattice. As we show below, this thermometer can (i) constrain the growth temperatures of soil carbonates, which can be compared to a known altitudinal gradient in surface temperature; and (ii) constrain the $\delta^{18}O$ of water from which carbonate grew (because both the growth temperature and $\delta^{18}O$ of carbonate are known), which can be compared to the altitude dependence of the $\delta^{18}O$ of meteoric water; and, by combining these two independent constraints, (iii) constrain the correlation between soil temperature and the $\delta^{18}O$ of soil water exhibited by a suite of related samples. This correlation can discriminate between the effects of altitude, climate, latitude, and seasonality in driving changes in temperature and $\delta^{18}O$ of water, and thus can help identify records that primarily reflect variations in altitude (rather than other factors) or quantify the contributions of altitude changes to those records.

We determined the stable isotope compositions of pedogenic soil carbonate nodules from paleosols collected in the Bolivian Altiplano [an ~300-km-wide (from east to west), ~1200-km-long (from north to south), 4-km-high plateau perched between the Western and Eastern Cordilleras in the central Andes]. Our

[1]Division of Geological and Planetary Sciences, California Institute of Technology, Pasadena, CA 91125, USA. [2]Department of Earth and Environmental Sciences, University of Rochester, Rochester, NY 14627, USA.

analyses include values of Δ_{47}: a measure of the enrichment of mass-47 isotopologs (principally $^{13}C^{18}O^{16}O$) relative to the randomly expected abundance in CO_2 produced by acid digestion of soil carbonate samples (*13*, *14*). The studied samples (Table 1) come from a sequence of interbedded paleosols, sandstones, and mudstones exposed in the Corque syncline near Callapa (north-central Altiplano; approximately at 17.6°S, 68.2°W). Today, these rocks are at elevations between ~3800 and ~3900 m. Carbonate nodules found in paleosols from this section are generally 0.5 to 3 cm in diameter and are found ~25 to 80 cm below the tops of their host paleosols, and some contain root tubules. These features are consistent with their having grown at depths ranging from centimeters to decimeters around tree or shrub roots. The ages of the paleosols we studied vary between 11.4 and 5.8 million years [as constrained by magnetostratigraphy and $^{40}Ar/^{39}Ar$ dates of volcanic rocks within the section (Table 1) (*15*)].

Values of Δ_{47} for CO_2 extracted from 11.4- to 10.3-million-year-old carbonates average 0.631 per mil (‰) (±0.011‰, n = 8 samples), excluding one outlier at 0.546 ± 0.017‰ that we suspect reflects diagenetic resetting (*16*). Carbonates from soils deposited between 7.6 and 7.3 million years ago (Ma) yield CO_2 with Δ_{47} of 0.680‰ (±0.015‰, n = 2), and those from soils deposited between 6.7 and 5.8 Ma yield CO_2 with Δ_{47} of 0.706‰ (±0.029‰, n = 4) (Table 1 and Fig. 1). The data for the 11.4- to 10.3-million-year-old samples are effectively homogeneous in Δ_{47} within analytical precision, and they probably provide our best indication of the current limits of analytical precision for complex natural samples. These data correspond to carbonate precipitation temperatures of 28.4° ± 2.6°C (SE, ±0.9°C) between 11.4 and 10.3 Ma, of 17.7° ± 3.1°C (SE, ±2.2°C) between 7.6 and 7.3 Ma, and 12.6° ± 5.6°C (SE, ±2.8°C) between 6.7 and 5.8 Ma. Measured paleotemperatures between 11.4 and 10.3 Ma are at the high end of measured modern temperatures at low altitudes (200 to 400 m) on the east flanks of the Andes (*17*–*19*), suggesting that they grew at a time when the Altiplano had not yet risen to its current altitude and perhaps suggesting warmer temperatures in the Miocene than at present and/or that paleosol carbonates precipitated during the austral summer. Paleotemperatures determined for soils deposited between 6.7 and 5.8 Ma are similar to those currently typical of the warm season (January and February) in La Paz and El Alto, Bolivia [~8° to 10°C, situated at ~4000 m (*17*–*19*)]. Thus, these data are consistent with the Altiplano having risen to near its modern altitude by 6.7 to 5.8 Ma. Based on the contrast in temperature between the oldest and youngest groups of samples we examined (15.7° ± 2.9°C, 1 SE in the difference between the means) and the vertical gradient in surface temperatures observed in the Andes today [average, 4.66°C/km (*17*–*19*)], these temperature data alone suggest uplift of 3400 ± 600 m over a period of ~3.6 million years (the span between the end of the 11.4 –10.3 Ma period and the start of the 6.7–5.8 Ma period), for an average uplift rate of 0.94 ± 0.17 mm/year. These results are consistent with previous estimates of paleoaltitude for the Altiplano (Fig. 2). This estimate suffers from potential systematic errors due to changes in latitude and/or climate between the Miocene and the present, and/or due to bias toward an extreme of the seasonal variability in temperature (that is, soil carbonate nodules may not grow evenly throughout the year).

We can also estimate paleoelevations by calculating the $\delta^{18}O$ value of the water from which soil carbonates grew (based on the known growth temperatures and the known carbonate-water oxygen isotope exchange equilibrium) and comparing those results with the known altitudinal gradient in $\delta^{18}O$ of meteoric water (*20*). The $\delta^{18}O_{SMOW}$ (SMOW, standard mean ocean water) values of waters in equilibrium with paleosol carbonates that formed between 11.4 and 10.3 Ma average –8.6 ± 1.1‰ (SE, ±0.4); waters in equilibrium with carbonates formed between 7.6 and 7.3 Ma have average $\delta^{18}O_{SMOW}$ values of –11.8 ± 1.8‰ (SE, ±1.3); and waters in equilibrium with carbonates formed between 6.7 and 5.8 Ma have average $\delta^{18}O_{SMOW}$ values of –14.6 ± 1.2‰ (SE, ±0.6) (Table 1 and Fig. 1). On the basis of the contrast in $\delta^{18}O$ of the parent water between the oldest and youngest groups of samples we examined (6.0 ± 0.7‰, 1 SE in the difference of the means) and the altitudinal gradient in the weighted annual mean $\delta^{18}O$ value of meteoric water observed in the Andes today (*21*), these $\delta^{18}O_{water}$ data suggest that the soils were uplifted 3000 ± 300 m (from 700 ± 200 to 3700 ± 200 m) over ~3.6 million years, for an average uplift rate of 0.83 ± 0.08 mm/year. These results are consistent with our estimate of altitude change based on paleothermometry data alone. However, like that estimate,

Table 1. Stable isotope compositions, growth temperatures, and parental water $\delta^{18}O$ values for Altiplano soil carbonates.

Sample	Age (Ma) (*15*)*	$\delta^{13}C_{PDB}$ of carbonate (*14*)	$\delta^{18}O_{PDB}$ of carbonate (*14*)	Δ_{47} of extracted CO_2 (*14*)	Temperature (°C) (*13*)	$\delta^{18}O_{SMOW}$ of water (*20*)
03BL13	11.42	–9.4	–11.4	0.612 (19)	32.8 (4.6)	–7.5 (0.9)
03BL19	11.32	–6.8	–11.1	0.651 (21)	23.8 (4.6)	–9.0 (0.9)
04BL75	10.88	–9.3	–9.8	0.634 (14)	27.7 (3.2)	–6.9 (0.6)
04BL76	10.74	–8.3	–11.7	0.632 (13)	28.2 (3.0)	–8.7 (0.6)
04BL78	10.58	–9.4	–13.0	0.644 (21)	25.6 (4.7)	–10.5 (0.9)
04BL79	10.53	–8.6	–12.3	0.630 (12)	28.6 (2.8)	–9.0 (0.5)
04BL80	10.46	–10.1	–11.6	0.620 (5)	31.0 (1.2)	–8.2 (0.2)
03BL1	10.33	–8.2	–12.5	0.628 (6)	29.2 (1.4)	–9.3 (0.3)
				11.4 to 10.3 Ma average	**28.4 (0.9)**	**–8.6 (0.4)**
04BL2	7.61	–4.6	–13.9	0.695 (9)	14.6 (1.8)	–13.7 (0.4)
04BL10	7.32	–5.9	–11.5	0.665 (10)	20.8 (2.1)	–10.0 (0.4)
				7.6 to 7.3 Ma average	**17.7 (2.2)**	**–11.8 (1.3)**
04BL21	6.74	–7.7	–14.7	0.681 (4)	17.5 (0.8)	–13.9 (0.2)
04BL24	6.64	–6.7	–13.5	0.713 (12)	11.0 (2.3)	–14.1 (0.5)
04BL25	6.53	–7.0	–14.6	0.750 (8)	4.1 (1.4)	–16.7 (0.3)
04BL30	5.83	–6.5	–14.6	0.679 (13)	18.0 (2.7)	–13.7 (0.6)
				6.7 to 5.8 Ma average	**12.6 (2.8)**	**–14.6 (0.6)**
			Suspected of diagenetic alteration			
04BL69	10.95	–9.9	–8.2	0.546 (17)	50.3 (4.9)	–1.1 (0.8)

*Italic numbers in parentheses at the head of each column refer to references explaining the sources, methods, or algorithms on which the data are based. Analytical uncertainties in $\delta^{13}C$ and $\delta^{18}O$ of carbonate average ±0.02 and ±0.1‰, respectively, and are not shown. Analytical uncertainties in Δ_{47} (numbers in parentheses) are shown for each measurement as the standard error of the mean of all mass spectrometric analyses for a given sample. These are propagated to estimate uncertainties in temperature and $\delta^{18}O$ of water.

this one also suffers from potential systematic errors due to latitude and/or climate change between the Miocene and present, and/or due to bias toward an extreme of the seasonal variability in $\delta^{18}O$ of meteoric water. Moreover, it suffers from potential systematic errors due to evaporative fractionation of oxygen isotopes in soil waters.

The relation between growth temperature and the $\delta^{18}O$ of parental waters recorded by our data for paleosol carbonates (Fig. 1) parallels the relation between mean annual surface temperature and the annual weighted average $\delta^{18}O$ of meteoric water recently measured across the Altiplano and surrounding lowlands, but is slightly offset, on average, from the modern trend toward lower $\delta^{18}O$ at any given temperature and extends to higher temperatures than those observed today in eastern Bolivia. The similarity in slope between our data and the modern mean annual trend shown in Fig. 1 suggests that elevation change is the principal cause of variability in carbonate growth temperature and the $\delta^{18}O$ of soil waters seen in our Miocene record, because other factors (such as changes in global climate or latitude and/or changes in the part of the seasonal cycle sampled by soil carbonates) are predicted to lead to slopes that are different from that of the modern mean annual trend in Fig. 1 (*22*). This ability to demonstrate the primary role of altitude change in driving variations in temperature and $\delta^{18}O$ of water is a strength of this approach to paleoaltimetry. Still, we must correct for any second-order effects of climate change and latitude change.

Bolivia was 1° to 2° of latitude north of its current position during the mid-Miocene (*23*), and so its mean annual temperature should have been ~0.3° ± 0.1°C warmer and the $\delta^{18}O$ of its meteoric water 0.9 ± 0.3‰ higher than today (based on modern latitudinal gradients in these variables). Also, low-latitude climate may have been ~1°C warmer in the mid-Miocene (*24*). Finally, the $\delta^{18}O$ of the ocean was ~1‰ lower in the mid- to late Miocene as compared to today, essentially counterbalancing the change in $\delta^{18}O$ of meteoric water expected from change in latitude (*25*). Therefore, the modern mean annual trend in Fig. 1 must be shifted to 1.3°C higher temperature at constant $\delta^{18}O$ to equal the expected trend for the mid-Miocene [the similarity in atmospheric circulation patterns from 10 to 15 Ma to the present suggests that there have been no first-order changes in moisture supply (*26*–*28*)]. Most important, modern meteoric water $\delta^{18}O$ values and surface temperatures vary seasonally by 10 to 15‰ and several degrees, respectively, across most of the Altiplano and surrounding region. It is possible (perhaps even likely) that soil carbonates grow at different rates in different seasons, and thus might be systematically offset from the mean annual trend toward a seasonal extreme in Fig. 1. Seasonal variations in $\delta^{18}O$ and temperature at any one altitude are correlated with one another, and those correlations are at a high angle to the mean annual trend. Therefore, one can contour lines of constant altitude linking the mean annual trend with the seasonal extreme trends in Fig. 1 (as indicated by the fine dashed lines; only the January/February extreme is shown, for simplicity) and use a sample's position in relation to those contours to estimate its paleoelevation. This approach suggests that the

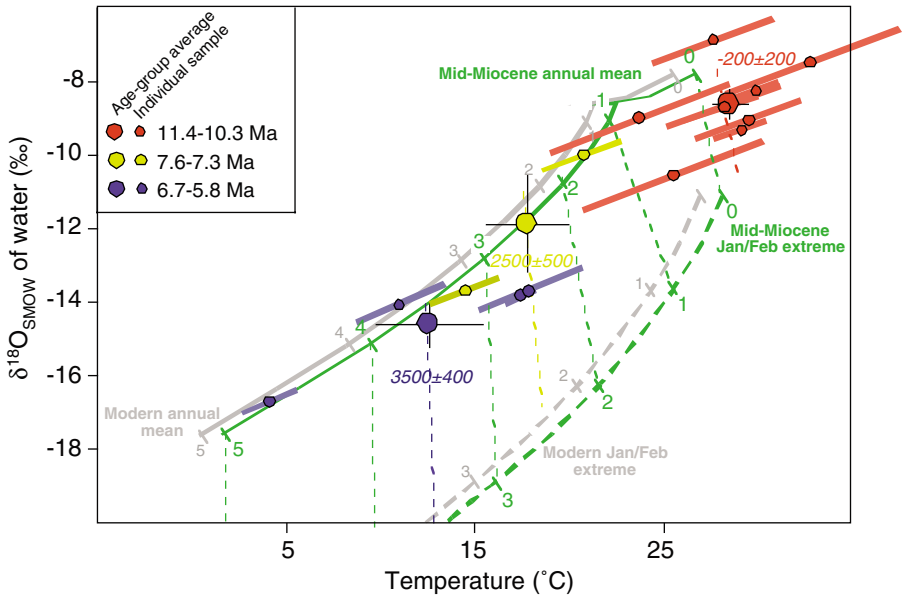

Fig. 1. Plot of the $\delta^{18}O_{SMOW}$ value of water in equilibrium with soil carbonate nodules versus the growth temperatures of those nodules. The small symbols are individual samples from Table 1. The large symbols are averages for the 11.4- to 10.3-Ma, 7.6- to 7.3-Ma, and 6.7- to 5.8-Ma age groups. Error bars for individual measurements are based on external precision in Δ_{47} and $\delta^{18}O$ measurements for acid digestion analyses of carbonates, and they consider the effect of errors in temperature on estimated $\delta^{18}O_{SMOW}$ values of water. Error bars for age groups are ±1 SE of the population. Gray curves show the mean annual trend (solid curve) and trend of January/February (Jan/Feb) extremes (dashed curve) for the relations between surface temperature and the $\delta^{18}O_{SMOW}$ of meteoric water. These curves are contoured for altitude in kilometers. The similar green curves plot the expected location of the mean annual and Jan/Feb extremes in the mid-Miocene, based on inferred changes in the latitude of Bolivia, low-latitude climate change, and secular variation in the $\delta^{18}O$ of seawater. Fine dashed lines connecting the mid-Miocene mean annual trend and Jan/Feb extreme trend show the slopes of seasonal variations in temperature and $\delta^{18}O$ of water at a fixed altitude (we infer that these were the same in the Miocene as today). Paleoaltitudes of age-group averages are estimated by their intersections with this set of altitude contours, as indicated by the red, yellow, and blue dashed lines.

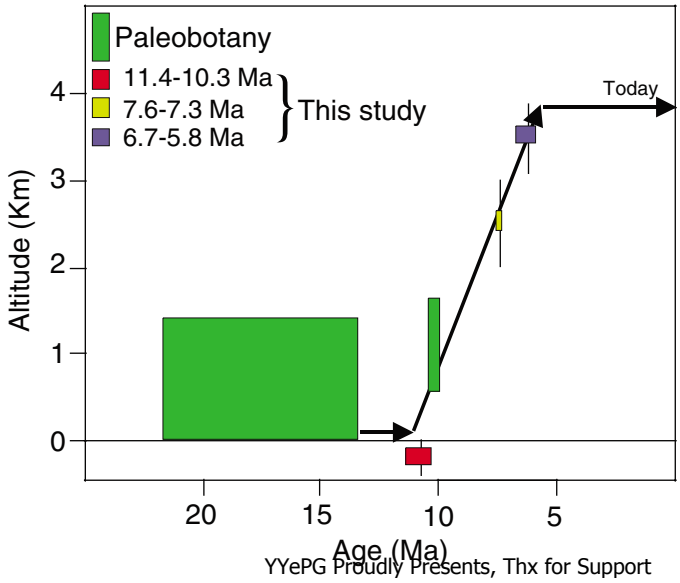

Fig. 2. Constraints on the uplift history of the Altiplano, based on data from this study (colored boxes, with error bars indicating ±1 SE) and paleobotanical constraints (*45*, *46*). Arrows mark the uplift history that is most consistent with both sets of constraints. The average uplift rate between ~10.3 and 6.7 Ma is 1.03 ± 0.12 mm/year, which is approximately three times the rate that could be sustained by crustal shortening driven by plate motions.

soil carbonates examined in this study preferentially sample warm, low-$\delta^{18}O$ conditions that prevail in the Bolivian austral summer. This is the local rainy season, and may be a time of year when the pedogenic carbonate horizon is most likely to be saturated. Finally, it is possible that evaporation has caused the soil waters from which the carbonates grew to have a higher $^{18}O/^{16}O$ ratio than their meteoric water sources. Based on the magnitude of such effects observed in previous studies of modern soils (*29*, *30*) and the relatively high rainfall received by the northern Altiplano (*17*–*19*) (which minimizes evaporative enrichments), we estimate that this effect should be on the order of 0 to 2‰. There is no straightforward way to correct for soil evaporation, but its effects on paleoaltitude estimates using our approach are minimal: If the $\delta^{18}O$ of soil water increased relative to that of meteoric water by 1‰ at a constant temperature, our altitude estimate will be too low by ~200 m at low altitude and by <100 m at high altitude (based on the slopes of isoelevation contours in Fig. 1).

Comparison of our age-group average data (Table 1) with the contours of expected mid-Miocene seasonal variation in temperature and $\delta^{18}O$ of meteoric water (Fig. 1) yields the following paleoaltitude estimates (Fig. 2): –200 ± 200 m between 11.4 and 10.3 Ma, 2500 ± 500 m between 7.6 and 7.3 Ma, and 3500 ± 400 between 6.7 and 5.8 Ma.

The negative altitude obtained by our method for 11.4 to 10.3 Ma indicates a systematic error in our estimate of absolute elevations. Because of the steep slopes of isoelevation contours in Fig. 1, this error is unlikely to result from errors in our estimation of the $\delta^{18}O$ of meteoric water alone. The most likely explanation is that ground temperatures during the mid-Miocene in Bolivia were ~1° to 3°C warmer than expected based on previous estimates of global climate change and South American continental drift. Alternatively, if all soil carbonates underwent small amounts of recrystallization during burial metamorphism, then measured paleotemperatures could be biased upward by several degrees (but no more, because it is not plausible that the 6.7 to 5.8 Ma group grew at temperatures substantially below 10°C). Because of this uncertainty, we suggest that our absolute elevation estimates are likely too low by several hundred meters; assuming that the size of this error does not vary systematically with sample age, it should have an insignificant effect on differences in inferred paleoaltitude between sample age groups.

The elevation history implied by our results and paleobotanical constraints (arrows in Fig. 2) suggests that the Altiplano underwent 3700 ± 400 m of uplift over ~3.6 million years, implying an average uplift rate of 1.03 ± 0.12 mm/year. Visual inspection of Fig. 2 suggests that uplift rate was approximately constant over the sampled period. However, it is possible that rates were higher than this for relatively brief times if elevation change occurred in steps lasting less time than the gaps between each sampled time interval.

The rate of major elevation change of the Altiplano has implications regarding the forces responsible for its uplift. Processes of crustal shortening and isostatic compensation of thickened crust could have led to elevation increases of the Altiplano at rates up to 0.3 mm/year (*31*). This is approximately one-third the minimum rate of elevation change constrained by our results, seemingly ruling out crustal shortening as a physical cause of the rise of the Altiplano. A mechanism that could explain the rapid uplift of a region the size of the Altiplano is the removal of dense lower crust and/or mantle lithosphere and its replacement by hot, less dense, asthenospheric mantle and an accompanying isostatic rise of the lower density lithospheric section (*32*–*34*).

Uplift driven by delamination of the dense lower crust and/or mantle lithosphere could have increased vertical compressive stress beneath the Altiplano plateau, decreased deviatoric compressive stress across the plateau, transformed the Andean fold-thrust belt from a critical to a supercritical state, and increased the forces applied to the lowlands surrounding the plateau (*15*). We suggest that these changes in the stress field that occurred between ~10 and ~7 Ma in and around the Altiplano contributed to the decrease in the rate of shortening across the Altiplano [independently estimated to have occurred at ~7 Ma (*35*)], to the eastward propagation of deformation into the sub-Andean zone in late Miocene time [by ~7.6 Ma (*36*)], and to a late-Miocene decrease in the convergence rate between the Nazca and South American plates (*15*).

References and Notes

1. D. L. Sahagian, A. A. Proussevitch, W. D. Carlson, *J. Geol.* **110**, 671 (2002).
2. J. C. McElwain, *Geology* **32**, 1017 (2004).
3. J. C. Gosse, F. M. Phillips, *Quat. Sci. Rev.* **20**, 1475 (2001).
4. C. E. Forest, J. A. Wolfe, P. Molnar, K. A. Emanuel, *Geol. Soc. Am. Bull.* **111**, 497 (1999).
5. K. M. Gregory, C. G. Chase, *Geology* **20**, 581 (1992).
6. J. A. Wolfe, *Annu. Rev. Earth Planet. Sci.* **23**, 119 (1995).
7. C. N. Drummond, B. H. Wilkinson, K. C. Lohmann, G. R. Smith, *Palaeogeogr. Palaeoclimatol. Palaeoecol.* **101**, 67 (1993).
8. C. P. Chamberlain, M. A. Poage, D. Craw, R. C. Reynolds, *Chem. Geol.* **155**, 279 (1999).
9. D. L. Dettman, K. C. Lohmann, *Geology* **28**, 243 (2000).
10. C. N. Garzione, J. Quade, P. G. DeCelles, N. B. English, *Earth Planet. Sci. Lett.* **183**, 215 (2000).
11. M. A. Poage, C. P. Chamberlain, *Am. J. Sci.* **301**, 1 (2001).
12. D. B. Rowley, R. T. Pierrehumbert, B. S. Currie, *Earth Planet. Sci. Lett.* **188**, 253 (2001).
13. The Ghosh *et al*. (*37*) thermometer is based on the abundances in carbonate minerals of carbonate ion groups that contain both a ^{13}C and an ^{18}O atom (that is, $^{13}C^{18}O^{16}O_2^{-2}$). These ionic groups have lower zero-point energies than their isotopically "normal" and singly-substituted relatives ($^{12}C^{16}O_3^{-2}$, $^{13}C^{16}O_3^{-2}$, $^{12}C^{17}O^{16}O_2^{-2}$, and $^{12}C^{18}O^{16}O_2^{-2}$), leading to a thermodynamic driving force that promotes the clumping of rare isotopes into bonds with each other as opposed to being randomly dispersed throughout the mineral lattice. This effect can be described using an isotope exchange reaction among isotopologs of the carbonate ion: $^{12}C^{18}O^{16}O_2^{-2} + {}^{13}C^{16}O_3^{-2} = {}^{13}C^{18}O^{16}O_2^{-2} + {}^{12}C^{16}O_3^{-2}$. The equilibrium constant for this reaction increases with decreasing temperature and can be determined by digesting a carbonate mineral in phosphoric acid and measuring the $\delta^{18}O$, $\delta^{13}C$, and abundance of Δ_{47} isotopologs (mostly $^{13}C^{18}O^{16}O$) in the product CO_2. From these data, one can calculate the enrichment of Δ_{47} isotopologs in product CO_2 relative to the stochastic, or random, distribution of all C and O isotopes among all possible isotopologs. This enrichment, termed the Δ_{47} value, is proportional to the equilibrium constant for the reaction above in reactant carbonate and varies with carbonate growth temperature by the relation $\Delta_{47} = 59{,}200/T^2 - 0.02$, where Δ_{47} is in units of per mil and T is the temperature in kelvin. Analytical errors in Δ_{47} are on the order of ±0.01 to 0.02, leading to errors in temperature of ~2° to 4°C. The key feature of this thermometer is that it is based on a homogeneous equilibrium within carbonate rather than on a heterogeneous equilibrium between carbonate and water or some other phase. Therefore, unlike conventional carbonate-water oxygen isotope thermometry, it does not require knowledge of the isotopic composition of water from which carbonate grew or of any other phase with which it might have undergone isotopic exchange.
14. Values of $\delta^{18}O$ and $\delta^{13}C$ of soil carbonates were determined using conventional phosphoric acid digestion techniques (*38*, *39*) and were standardized by comparison with similar analyses of the NBS-19 standard distributed by the International Atomic Energy Agency (IAEA). Values of $\delta^{18}O$ measured for carbonates are reported versus the Pee Dee belemnite (PDB) standard, and values of $\delta^{18}O$ calculated for meteoric and soil waters are reported versus the SMOW standard (as indicated by the subscripts on the $\delta^{18}O$ symbol used in the text, table, and figures). Measurements of Δ_{47} were made on these same aliquots of CO_2 generated by phosphoric acid digestion, using instrumentation and methods described in (*40*) and (*13*), including changes in sample preparation described in (*41*). Values of Δ_{47} were calculated based on raw measurements of R^{45}, R^{46}, and R^{47}, using methods described in (*41*, *42*).
15. C. N. Garzione, P. Molnar, J. C. Libarkin, B. MacFadden, *Earth Planet. Sci. Lett.*, **241**, 543 (2006).
16. Sample 04BL69 (depositional age, 10.95 Ma) is significantly lower in Δ_{47} and higher in $\delta^{18}O_{PDB}$ than other samples in the 11.4- to 10.3-Ma age range (Δ_{47} is 0.546 versus 0.612 to 0.651 and $\delta^{18}O$ is –8.2 versus –9.8 to –12.5). These data indicate an equilibration temperature for this nodule of 50°C and a coexisting pore water $\delta^{18}O_{SMOW}$ value of –1.1. These results are consistent with reequilibration of this nodule during burial metamorphism at depths of ~1 to 2 km and are inconsistent with any plausible conditions and water sources for original deposition. We suggest that the portion of this nodule sampled for analysis underwent a cryptic recrystallization event during burial metamorphism and after its original growth near Earth's surface.
17. R. Garreaud, M. Vuille, A. C. Clement, *Palaeogeogr. Palaeoclimatol. Palaeoecol.* **194**, 5 (2003).
18. R. Gonfiantini, M.-A. Roche, J.-C. Olivry, J.-C. Fontes, G. M. Zuppi, *Chem. Geol.* **181**, 147 (2001).
19. Recent meteorological data were taken from a compilation of 8 years of measurements for Bolivian cities found at www.climate-zone.com.
20. The $\delta^{18}O_{SMOW}$ value of water in equilibrium with carbonate was calculated based on the measured $\delta^{18}O_{PDB}$ value of carbonate, the inferred temperature of carbonate equilibration based on the Ghosh *et al*. thermometer (*13*), and the equilibrium water-calcite oxygen isotope

fractionation determined experimentally by S. T. Kim *et al*. (*43*).
21. The altitude gradients in $\delta^{18}O$ of meteoric water were fit to data for weighted annual mean precipitation and for the minimum monthly average (always in January or February) collected in 1984 and reported in (*18*). These fits used least-squares methods and second-order polynomial equations, and they fit data with r^2 values of 0.98 for both the annual weighted mean and the minimum monthly average. These data were then combined with measured altitude gradients in mean annual temperature and maximum monthly average temperature [also always in January or February (*17*–*19*)] to yield the relationships between temperature and $\delta^{18}O$ of water plotted as curves in Fig. 1.
22. The slope in Fig. 1 defined by data for carbonate growth conditions and parental waters is 0.34‰/°C. This is indistinguishable from the slope defined by the mean annual altitude gradient in surface temperature and $\delta^{18}O$ of meteoric water in the Altiplano and surrounding area (Fig. 1) (*17*–*19*) and contrasts with slopes in these dimensions associated with low-latitude climate variations (~0‰/°C for temperatures between 29° and 12°C), latitude variations (~3‰/°C or 0.6‰ per degree of latitude), or seasonality at any one altitude [~ −5‰/°C but varying with altitude; see (*18*) and dashed lines in Fig. 1]. For data documenting these trends, see (*44*).
23. A. G. Smith, A. M. Hurley, J. C. Briden, *Phanerozoic Paleocontinental World Maps* (Cambridge University Press, Cambridge, 1981).
24. S. M. Savin, R. G. Douglas, F. G. Stehli, *Geol. Soc. Am. Bull.* **86**, 1499 (1975).
25. J. Zachos, M. Pagani, L. Sloan, E. Thomas, K. Billups, *Science* **292**, 686 (2001).
26. C. N. Alpers, G. H. Brimhall, *Geol. Soc. Am. Bull.* **100**, 1640 (1988).
27. G. D. Hoke, B. L. Isacks, T. E. Jordan, J. S. Yu, *Geology* **32**, 605 (2004).
28. B. K. Horton, *Tectonics* **18**, 1292 (1999).
29. B. Liu, F. M. Phillips, A. R. Campbell, *Palaeogeogr. Palaeoclimatol. Palaeoecol.* **124**, 233 (1996).
30. T. E. Cerling, J. Quade, in *Continental Indicators of Climate, Proceedings of Chapman Conference, Jackson Hole, Wyoming*, P. Swart *et al.*, Eds. [American Geophysical Union (AGU) Monograph 78, AGU, Washington, DC, 1993), pp. 217–231.
31. Crustal shortening accompanied by isostatic compensation of thickened crust leads to elevation change by the relation $\partial H/\partial T = \partial L/\partial T \times Z/W \times [(\rho_m - \rho_c)/\rho_c]$, where $\partial H/\partial T$ is the rate of elevation gain, $\partial L/\partial T$ is the shortening rate (10 mm/year, based on long-term plate motions), Z is the initial crustal thickness (50 km), W is the width of the deforming region (300 km), ρ_c is the density of the crust (assumed to equal 2.7 g/cc), and ρ_m is the density of the mantle (assumed to equal 3.3 g/cc). See (*15*) for explanations of these choices of values for the physical constants. This relation predicts a maximum rate of elevation gain that is, not considering any elevation losses due to erosion) of 0.3 mm/year.
32. P. Bird, *J. Geophys. Res.* **83**, 4975 (1978).
33. P. C. England, G. Houseman, *J. Geophys. Res.* **94**, 17561 (1989).
34. R. W. Kay, S. Mahlburg-Kay, *Geol. Rundsch.* **80**, 259 (1991).
35. S. Lamb, L. Hoke, *Tectonics* **16**, 623 (1997).
36. L. Echavarria, R. Hernandez, R. Allmendinger, J. Reynolds, *AAPG Bull.* **87**, 965 (2003).
37. P. Ghosh *et al.*, *Geochim. Cosmochim. Acta,* in press.
38. J. M. McCrea, *J. Chem. Phys.* **18**, 849 (1950).
39. P. K. Swart, S. J. Burns, J. J. Leder, *Chem. Geol.* **86**, 89 (1991).
40. J. M. Eiler, E. A. Schauble, *Geochim. Cosmochim. Acta* **68**, 4767 (2004).
41. H. Affeck, J. M. Eiler, *Geochim. Cosmochim. Acta,* in press.
42. Z. Wang, E. A. Shauble, J. M. Eiler, *Geochim. Cosmochim. Acta* **68**, 4779 (2004).
43. S. T. Kim, J. R. O'Neil, *Geochim. Cosmochim. Acta* **61**, 3461 (1997).
44. J. R. Gat, W. G. Mook, H. A. J. Meijer, *Environmental Isotopes in the Hydrological Cycle: Principles and Applications. Volume II: Atmospheric Water* (IAEA, Vienna, Austria, 2001); available at www.iaea.org/programmes/ripc/ih/volumes/volume2.htm.
45. K. M. Gregory-Wodzicki, *Geol. Soc. Am. Bull.* **112**, 1091 (2000).
46. K. M. Gregory-Wodzicki, W. C. McIntosh, K. Velasquez, *Am. Earth Sci.* **11**, 533 (1998).

25 August 2005; accepted 31 October 2005
10.1126/science.1119365

Freezing as a Path to Build Complex Composites

Sylvain Deville,* Eduardo Saiz, Ravi K. Nalla,† Antoni P. Tomsia

Materials that are strong, ultralightweight, and tough are in demand for a range of applications, requiring architectures and components carefully designed from the micrometer down to the nanometer scale. Nacre, a structure found in many molluscan shells, and bone are frequently used as examples for how nature achieves this through hybrid organic-inorganic composites. Unfortunately, it has proven extremely difficult to transcribe nacre-like clever designs into synthetic materials, partly because their intricate structures need to be replicated at several length scales. We demonstrate how the physics of ice formation can be used to develop sophisticated porous and layered-hybrid materials, including artificial bone, ceramic-metal composites, and porous scaffolds for osseous tissue regeneration with strengths up to four times higher than those of materials currently used for implantation.

Although the potential of layered materials has long been recognized (*1*), their creation requires solving a two-fold problem, namely the design of optimum microstructures and the development of fabrication procedures to implement these designs. Natural materials such as nacre offer a wealth of information to guide such a design process (*2*, *3*). The unique properties of natural layered materials are achieved through fine control of the layer thickness, selection of the right components, and manipulation of roughness and adhesion at the organic-inorganic interface (*4*, *5*). The ideal fabrication process has to be not only simple but also adaptable enough to fabricate layers with a large number of material combinations and a wide range of layer dimensions. Previous techniques for mimicking nacre are bottom-up chemical approaches (*6*, *7*) that are intrinsically limited to a narrow range of materials exhibiting the proper interfacial reactions and compatibility. Other techniques offer only a coarse control of the layer thickness or have practical limitations regarding the number of layers that can be fabricated (*7*, *8*).

In sea ice, pure hexagonal ice platelets with randomly oriented horizontal *c* crystallographic axes are formed, and the various impurities originally present in sea water (salt, biological organisms, etc.) are expelled from the forming ice and entrapped within channels between the ice crystals (*9*). We apply this natural principle to ceramic particles dispersed in water to build sophisticated, nacre-like architectures in a simple, two-step approach. Ice-templated (IT), porous, layered materials with layers as thin as 1 μm are first fabricated through a freeze-casting process, which involves the controlled unidirectional freezing of ceramic suspensions. These porous scaffolds are then filled with a selected second phase (organic or inorganic) to fabricate dense composites. By using a natural, self-organizing phenomenon, we allow nature to guide the design and processing.

The physics of water freezing has drawn the attention of scientists for a long time. With few exceptions (*10*), much of this work has concentrated on the freezing of pure water or very dilute suspensions (*9*, *11*). This phenomenon is critical for various applications, such as cryo-preservation of biological cell suspensions (*12*) and the purification of pollutants (*13*). An important observation in these studies is that, during the freezing of such suspensions, there is a critical particle size (*11*) above which the suspended particles will be trapped by the moving water-ice front. Another important observation is that the hexagonal ice crystals exhibit strong anisotropic growth kinetics, varying over about two orders of magnitude with crystallographic orientation. Under steady-state conditions, it is possible to grow ice crystals in the form of platelets with a very high aspect ratio. The ice thus formed will have a lamellar microstructure, with the lamellae thickness depending mainly on the speed of the freezing front. We designed a simple experimental setup (fig. S1) that allowed us to precisely control the freezing kinetics. By freezing concentrated suspensions containing ceramic particles with suitable granulometry, we were

Materials Sciences Division, Lawrence Berkeley National Laboratory, Berkeley, CA 94720, USA.

*Present address: Intel Corporation, 5000 West Chandler Boulevard, Chandler, AZ 85226, USA.

†To whom correspondence should be addressed. E-mail: sdeville@lbl.gov

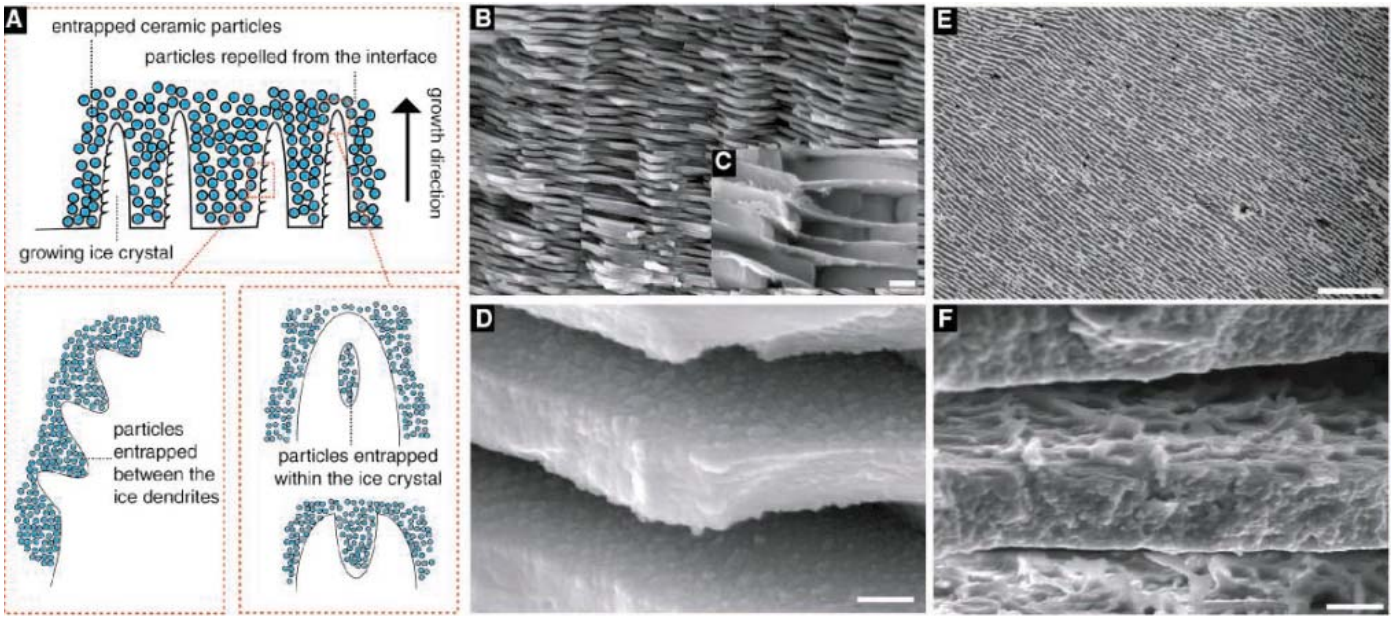

Fig. 1. Processing principles and materials. While the ceramic slurry is freezing, the growing ice crystals expel the ceramic particles, creating a lamellar microstructure oriented in a direction parallel to the movement of the freezing front (**A**). For highly concentrated slurries, the interaction between particles becomes critical: A small fraction of particles are entrapped within the ice crystals by tip-splitting and subsequent healing (A), leading to the formation of inorganic bridges between adjacent walls. Dense composites are obtained by infiltrating the porous lamellar ceramic with a second phase (e.g., a polymer or a liquid metal). Natural nacre has a brick-mortar-bridges microstructure where inorganic calcium carbonate layers are held together by organic protein "glue" (**B** and **C**); the roughness of the inorganic walls (**D**) is a key contributor to the final mechanical properties of nacre. The layered microstructure of the IT dense composites resembles that of nacre [for example, the alumina–Al-Si composite in (**E**)]. The particles entrapped between the ice dendrites generate a characteristic roughness on the lamella surface (**F**) that mimics that of the inorganic component of nacre. Scale bars indicate (B) 5 μm, (C) 0.5 μm, (D) 0.3 μm, (E) 300 μm, and (F) 10 μm.

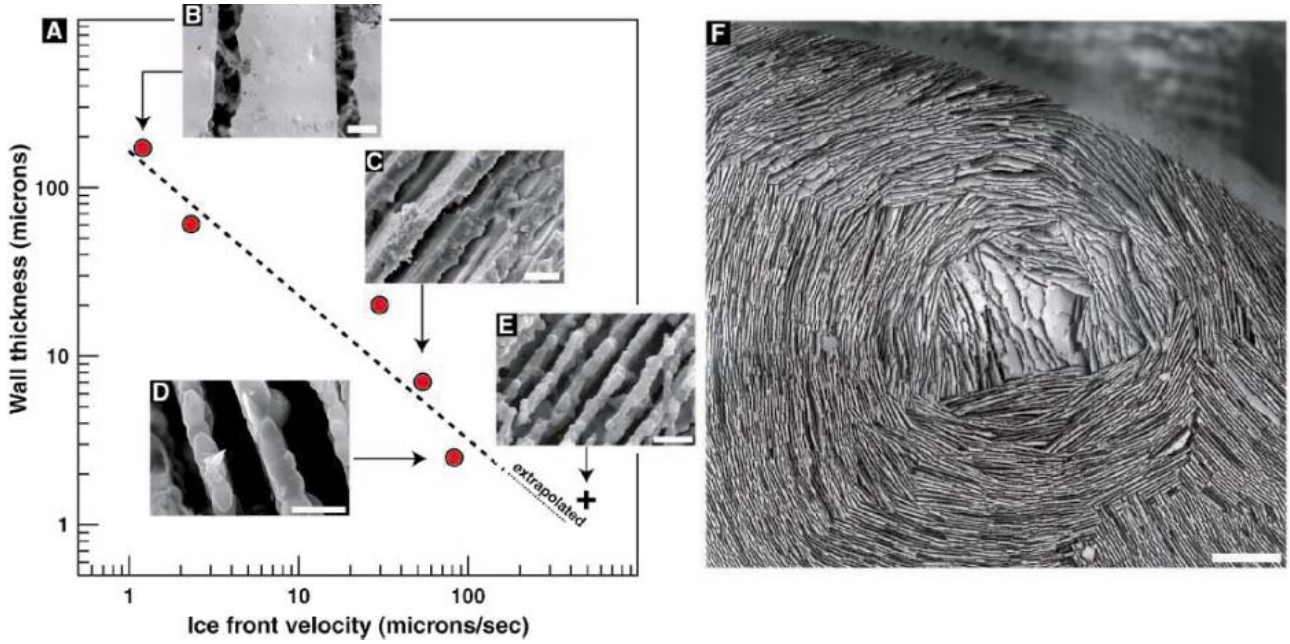

Fig. 2. Microstructural control at several levels. (**A**) Effect of the speed of the solidification front on the thickness of the lamellae for alumina samples fabricated from powders with an average grain size of 0.3 μm (**B** to **E**). The scanning electron micrographs shown in the graph correspond to cross sections parallel to the direction of movement of the ice front. Sample (E) was obtained with ultrafast freezing to gauge the thickness limit achievable by this technique. The approximate ice front velocity for this extreme case is in agreement with the extrapolation of the controlled freezing results. In addition, it is possible to control the materials mesostructure, for example in alumina (**F**), by patterning the surface of the cold fingers on which the ice crystals grow. Scale bars indicate (B) 50 μm, (C) 10 μm, (D) 5 μm, (E) 5 μm, and (F) 500 μm.

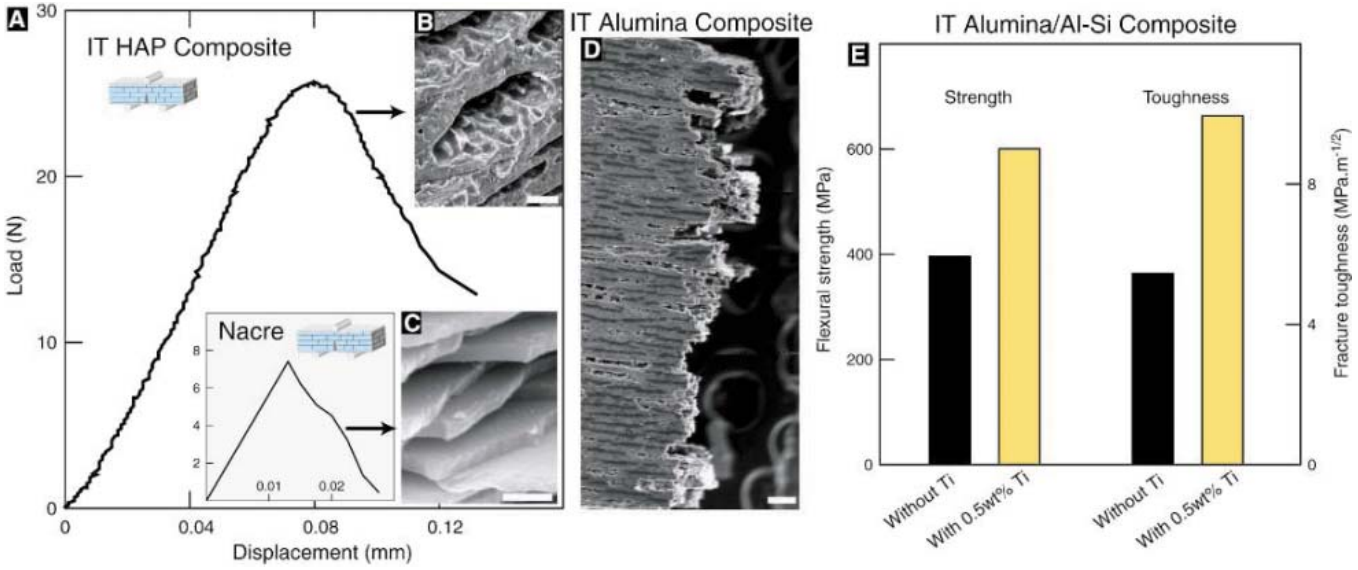

Fig. 3. Mechanical response of natural and synthetic IT composites. The three-points bending load-displacement data for IT HAP-epoxy composites (**A**) was qualitatively very similar to that of nacre (**C**) (*17*), with a gradually decreasing load after the elastic limit—characteristic of a stable crack propagation and active toughening—for cracks propagating in the direction perpendicular to the inorganic layers. Typical scanning electron micrographs of the IT composites (**B**) and nacre of abalone shell (C) reveal similar features on the fracture surface, with mode I cracks moving away from the notch and deflecting at the lamellae. Extensive crack deflection at the organic-inorganic interface results in tortuous crack paths and contributes to the toughening in both cases [as can be observed for the IT alumina-epoxy composite in (**D**)]. The role of the interfacial chemistry in the bonding between layers and the final mechanical properties of the material is illustrated in the data (**E**) for alumina–Al-Si composites (45/55 vol %); the addition of 0.5 wt % titanium to the aluminum alloy significantly increases the strength and toughness of the materials. Scale bars indicate (B) 40 μm, (C) 1 μm, and (D) 100 μm.

able to build homogeneous, layered, porous scaffolds.

In the method proposed here (Materials and Methods), directional freezing of the ceramic slurries is achieved by pouring them into polytetrafluoroethylene molds placed between two copper cold fingers (fig. S1) whose temperature is regulated to control the speed of the solidification front (fig. S2). As in nature, during the freezing of sea water, the ceramic particles concentrate in the space between the ice crystals (Fig. 1A). When the freezing rate increases, the magnitude of supercooling ahead of the solidifying interface is increased, and as a result the tip radius of the ice crystals decreases. A finer microstructure is thus obtained without affecting the long-range order of the entire structure. Afterwards, the ice is sublimated by freeze drying, such that a ceramic scaffold whose microstructure is a negative replica of the ice is produced (Fig. 1F). We controlled the growth of lamellar ice by adjusting the freezing kinetics. In this way, we achieved a layered microstructure with relevant dimensions that vary over two orders of magnitude (Fig. 2A) from 1 μm (almost the same as nacre, typically ~0.5 μm) (*14*) to 200 μm while affecting the ordered architecture. To a large extent, the mesostructure of natural materials determines their mechanical response (*15*), and this mesostructure has been difficult to replicate synthetically. Our results indicate that, by controlling the freezing kinetics and patterns of the cold finger, it is also possible to build mesostructural features and gradients (Fig. 2F) that could optimize the mechanical response of the final materials, for example, by stiffening the structure and limiting torsion (*15*).

The IT porous scaffolds obtained by this process exhibit strong similarities to the meso- and microstructure of the inorganic component of nacre (Fig. 1, B and C). The inorganic layers are parallel to each other and very homogeneous throughout the entire sample (Fig. 1E). Particles trapped in between the ice dendrites (Fig. 1A) lead to a dendritic surface roughness of the walls (Fig. 1F), just as in nacre (Fig. 1D) (*16*). Lastly, some dendrites span the channels between the lamellae (Fig. 2B), mimicking the tiny inorganic bridges linking the inorganic platelets of nacre, which are believed to increase the fracture resistance (*17*).

The inorganic portion represents 95% of the volume of nacre, but its highly specific properties (in particular its great toughness) are due to the interaction of this inorganic component with the organic phase (protein) that is found between the calcium carbonate platelets (*14*). To obtain similar synthetic materials, we next filled the porous ceramic scaffolds with a second phase. For example, we filled the IT scaffolds with a simple organic phase (epoxy) or with an inorganic component (metal) (Fig. 1E). Nature shows that the optimum fracture properties are encountered not only when the organic/inorganic interface is strong but also when delamination at the organic/inorganic interface occurs before the crack goes across the stiff, brittle layer. In the IT composites, extensive crack deflection at the interface between layers was observed (Fig. 3, B and D). As in nacre (Fig. 3C), this delamination creates tortuous cracks that propagate in a stable manner (Fig. 3A) and increases the toughness of the materials. It is believed that nature manipulates adhesion in two ways, mechanical and chemical. In nacre, this is done by controlling the roughness and the highly specific properties of the polymer adhesive phase (*4*). Our process allows us to control the morphology of the inorganic layers and the chemistry of the interface. For example, the mechanical response of alumina–Al-Si [45/55 volume (vol) %] layered composites (Fig. 1E) can be manipulated by controlling the interfacial bonding. By adding as little as 0.5 weight (wt) % Ti [known to segregate at the metal-ceramic interfaces (*18*)] to the aluminum eutectic, the strength increases from 400 to 600 MPa and fracture toughness increases from 5.5 to 10 $MPa/m^{\frac{1}{2}}$ (Fig. 3E).

Our technique shows promise for a large number of applications that require tailored composite materials. One such scientific challenge that could be solved is the development of new biomaterials for orthopedic applications (*19*). Despite extensive efforts in the development of porous scaffolds for bone regeneration, all porous materials have an inherent lack of strength associated with porosity. By applying freezing to commercial hydroxyapatite (HAP, the mineral component of bone) powder

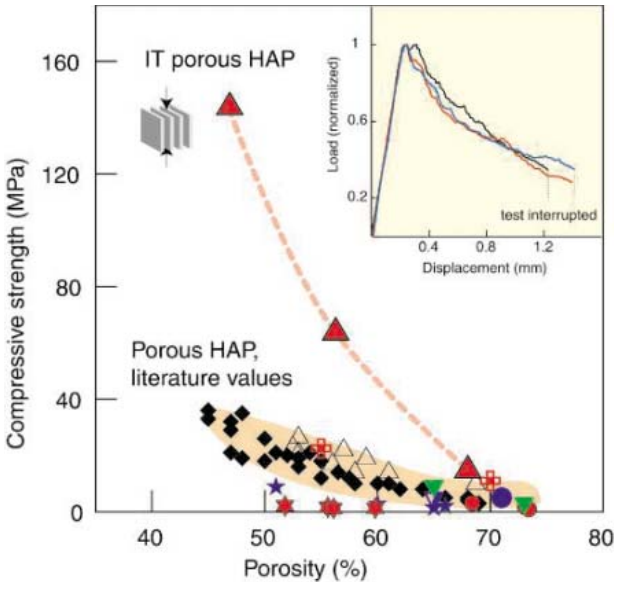

Fig. 4. Compressive strength of porous HAP scaffolds. Results from literature [blue stars (*22*), red stars (*23*), inverted green triangles (*24*), black triangle (*25*), blue circle (*26*), inverted blue triangle (*27*), diamonds (*28*), cross (*29*), and red circles (*30*)] versus IT porous HAP scaffolds. The typical pore sizes of conventional porous HAP scaffolds are on the order of 100 to 800 μm in order to allow bone ingrowth. In the IT materials exhibiting the greatest strength, the pores are typically ~20 by ~200 μm wide and several millimeters long; previous studies have indicated that these dimensions are adequate for bone tissue engineering (*20*). For the IT porous materials, compression is applied in the direction parallel to the ceramic layers. The presence of inorganic bridges between the ceramic layers (a feature that parallels the microstructure of nacre) prevents Euler buckling of the ceramic layers and contributes to the high strength. **(Inset)** Typical compression load-displacement curves for materials with 56% porosity (three different samples shown here). The samples fail gradually, and, because of the large degree of control of hierarchical architecture, the mechanical behavior is very consistent from one sample to another.

suspensions, we processed IT highly porous lamellar scaffolds that are four times stronger in compression than conventional porous HAP (Fig. 4). These IT scaffolds exhibit well-defined pore connectivity along with directional and completely open porosity of an adequate size to allow bone ingrowth (*20*). Hence, most of the current shortcomings (low strength, random organization, multiple pore size, and uncontrolled pore connectivity) that plague bone substitutes are eliminated by this innovative approach.

Current ceramic and metallic implant materials have serious shortcomings because of the mismatch of physical properties with those of bone. In bone, intrinsically weak materials, such as calcium phosphates and collagen, are combined into composites exhibiting intermediate modulus (10 to 20 GPa), fairly high strength (30 to 200 MPa), and high work of fracture (100 to 1000 J/m^2) (*21*). The unique properties of bone arise from the controlled integration of the organic (collagen) and inorganic (apatite) components (*5*) with a sophisticated architecture from the nano- to mesolevels. Our approach to the problem is to infiltrate the IT porous HAP scaffolds with a second organic phase with tailored biodegradability. Because the biodegradation rates of the scaffold and the infiltrated compound can be designed to be different, porosity can be created in situ to allow bone ingrowth. By using this approach, we have been able to fabricate HAP-based composites with stiffness (10 GPa), strength (150 MPa), and work of fracture (220 J/m^2) that match that of compact bone for an equivalent mineral/organic content (around 60/40 vol %).

References and Notes

1. G. Mayer, *Science* **310**, 1144 (2005).
2. C. Sanchez, H. Arribart, M. M. G. Guille, *Nat. Mater.* **4**, 277 (2005).
3. L. Addadi, S. Weiner, *Nature* **389**, 912 (1997).
4. B. L. Smith *et al.*, *Nature* **399**, 761 (1999).
5. G. E. Fantner *et al.*, *Nat. Mater.* **4**, 612 (2005).
6. Z. Y. Tang, N. A. Kotov, S. Magonov, B. Ozturk, *Nat. Mater.* **2**, 413 (2003).
7. A. Sellinger *et al.*, *Nature* **394**, 256 (1998).
8. W. J. Clegg, *Science* **286**, 1097 (1999).
9. M. G. Worster, J. S. Wettlaufer, *J. Phys. Chem. B* **101**, 6132 (1997).
10. S. W. Sofie, F. Dogan, *J. Am. Ceram. Soc.* **84**, 1459 (2001).
11. H. Ishiguro, B. Rubinsky, *Cryobiology* **31**, 483 (1994).
12. J. O. M. Karlsson, *Science* **296**, 655 (2002).
13. G. Gay, M. A. Azouni, *Cryst. Growth Des.* **2**, 135 (2002).
14. A. P. Jackson, J. F. V. Vincent, R. M. Turner, *Proc. R. Soc. Lond. Ser. B* **234**, 415 (1988).
15. J. Aizenberg *et al.*, *Science* **309**, 275 (2005).
16. R. Z. Wang, Z. Suo, A. G. Evans, N. Yao, I. A. Aksay, *J. Mater. Res.* **16**, 2485 (2001).
17. F. Song, A. K. Soh, Y. L. Bai, *Biomaterials* **24**, 3623 (2003).
18. E. Saiz, R. M. Cannon, A. P. Tomsia, *Acta Mater.* **48**, 4449 (2000).
19. L. L. Hench, J. M. Polak, *Science* **295**, 1014 (2002).
20. T. Dutta Roy, J. L. Simon, J. L. Ricci, E. D. Rekow, V. P. Thompson, J. R. Parsons, *J. Biomed. Mater. Res.* **66A**, 283 (2003).
21. Y. H. An, in *Mechanical Testing of Bone and the Bone-Implant Interface* (CRC Press, Boca Raton, FL, 2000), pp. 41–63.
22. A. Almirall *et al.*, *Biomaterials* **25**, 3671 (2004).
23. R. P. del Real, J. G. C. Wolke, M. Vallet-Regi, J. A. Jansen, *Biomaterials* **23**, 3673 (2002).
24. Y. Ota, T. Kasuga, Y. Abe, *J. Am. Ceram. Soc.* **80**, 225 (1997).
25. A. Bignon, thesis, National Institute of Applied Science, Lyon, France (2002).
26. H. R. Ramay, M. Q. Zhang, *Biomaterials* **24**, 3293 (2003).
27. M. Sous *et al.*, *Biomaterials* **19**, 2147 (1998).
28. D. M. Liu, *Ceram. Int.* **23**, 135 (1997).
29. M. Milosevski, J. Bossert, D. Milosevski, N. Gruevska, *Ceram. Int.* **25**, 693 (1999).
30. M. Kawata *et al.*, *J. Mater. Sci. Mater. Med.* **15**, 817 (2004).

31. This work was supported by the NIH National Institute of Dental and Craniofacial Research under grant 5R01 DE015633 ("Complex nanocomposites for bone regeneration") and by the Director, Office of Science, Office of Basic Energy Sciences, Division of Materials Sciences and Engineering of the U.S. Department of Energy under contract DE-AC03-76SF00098 (Metal/Ceramic Composites). The authors wish to thank R. O. Ritchie for useful discussions and J. Wu for help with the synthesis of the aluminum-infiltrated composites.

Supporting Online Material

www.sciencemag.org/cgi/content/full/311/5760/515/DC1
Materials and Methods
Figs. S1 and S2

4 October 2005; accepted 6 December 2005
10.1126/science.1120937

The Cellular Basis of a Corollary Discharge

James F. A. Poulet[1,2]* and Berthold Hedwig[2]

How do animals discriminate self-generated from external stimuli during behavior and prevent desensitization of their sensory pathways? A fundamental concept in neuroscience states that neural signals, termed corollary discharges or efference copies, are forwarded from motor to sensory areas. Neurons mediating these signals have proved difficult to identify. We show that a single, multisegmental interneuron is responsible for the pre- and postsynaptic inhibition of auditory neurons in singing crickets (*Gryllus bimaculatus*). Therefore, this neuron represents a corollary discharge interneuron that provides a neuronal basis for the central control of sensory responses.

An animal's behavior generates a constant flow of sensory information that can update or fine-tune ongoing motor activity (*1*) but can also desensitize the animal's own sensory pathways and/or be confused with external stimuli. One solution to these problems is to forward a signal, or corollary discharge, from motor to sensory regions during behavior to counter the expected, self-generated sensory feedback (*2*, *3*). A role for corollary discharges

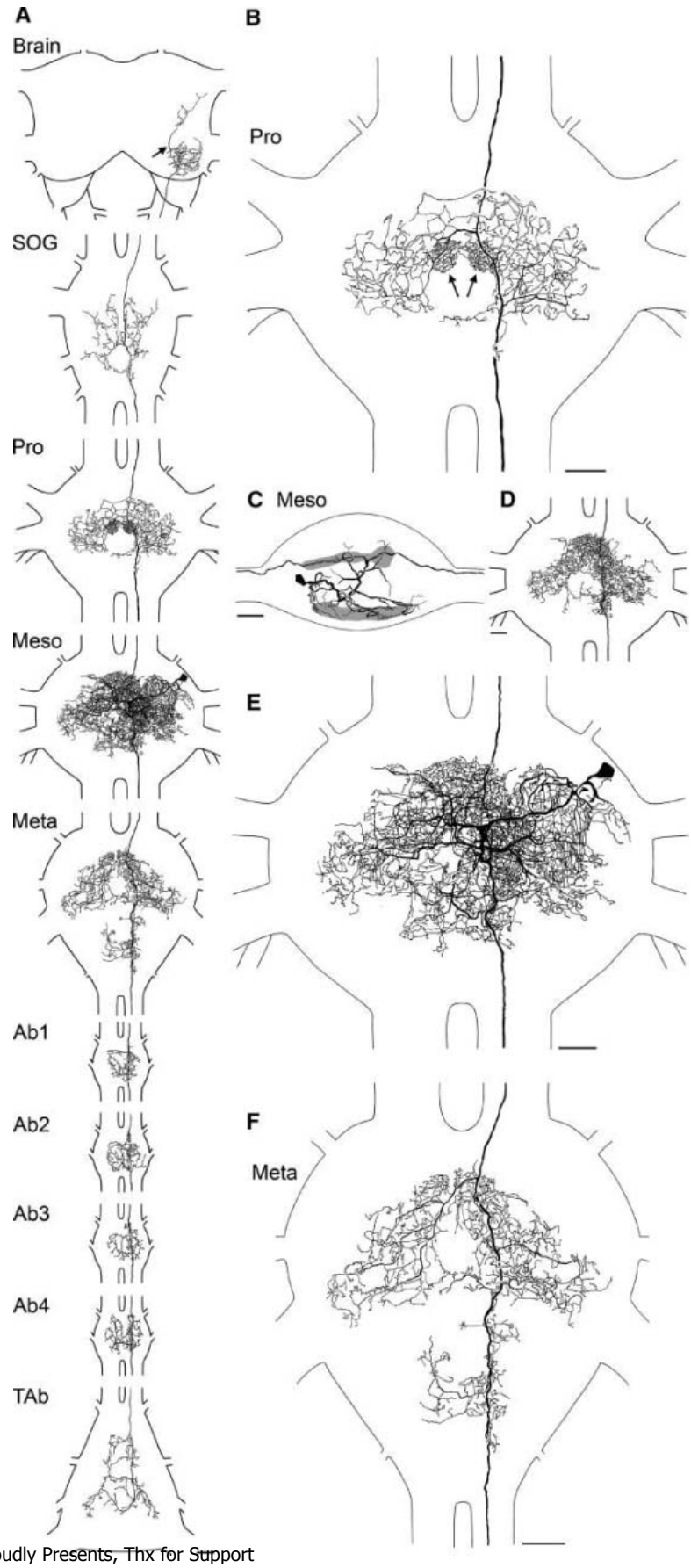

Fig. 1. Morphology of CDI. (**A**) A whole-mount staining of CDI in the CNS of an adult male *G. bimaculatus* in ventral view. The soma and dendrites are located in the mesothoracic ganglion, and two axons project throughout the whole CNS with extensive varicose arborizations that are bilateral in every ganglion except the brain. Arrow in brain indicates anterior branch of CDI stained in two of six stainings of its axon in the brain. (**B**) Axonal arborizations in the prothoracic ganglion; arrows indicate overlap with the auditory neuropils. (**C**) Lateral view of CDI in mesothoracic ganglion. The soma is positioned medially near the dorsolateral edge of the ganglion. From the soma the primary neurite extends in a loop toward the middle of the ganglion and gives off a widespread bilateral array of smooth branches typical of insect dendrites. Two axons originate centrally in the ganglion and extend both anteriorly and posteriorly. (**D**) Ventral axonal arborizations in the mesothoracic ganglion. (**E**) Dendritic (dorsal) and axonal (ventral) arborizations of CDI in the mesothoracic ganglion. (**F**) Axonal arborizations of CDI in the metathoracic ganglion have a similar morphology to those in the mesothoracic ganglion. Abbreviations: SOG, suboesophageal ganglion; Pro, prothoracic ganglion; Meso, mesothoracic ganglion; Meta, metathoracic ganglion; Ab1 to Ab4, abdominal ganglia 1 to 4; TAb, terminal abdominal ganglion. Scale bars, 100 μm.

in modifying sensory processing during behavior has been identified in many sensory systems (*4*–*11*). Despite their ubiquity and importance, however, very little is known about the neurons mediating corollary discharges.

An ideal model system to analyze a corollary discharge is the singing male cricket (*6*, *12*). Cricket song is composed of a series of 100 dB SPL chirps, repeated every 300 to 500 ms, each containing three to five sound pulses or syllables. Sound is generated during the closing movements of the wing. The crickets' ears are located on their forelegs and remain fully sensitive during singing (*13*). Therefore the cricket's central nervous system (CNS) has to deal with a massive influx of auditory, proprioceptive, and mechanoreceptive information during sound production. Crickets maintain auditory sensitivity during singing by inhibiting their central auditory pathway with a corollary discharge in phase with sound production (*14*). In this study, we identify the neuron that mediates this corollary discharge.

The corollary discharge interneuron (CDI) was physiologically identified by simultaneous intracellular recordings of auditory neurons in the prothoracic ganglion, where primary auditory signals are processed, and systematic probing of interneurons in the mesothoracic ganglion, which houses part of the singing pattern generating network. Consecutive stainings (n = 12 crickets) revealed its extensive branching pattern throughout the CNS (Fig. 1) (*15*).

[1]Laboratory of Sensory Processing, Brain Mind Institute, École Polytechnique Fédérale de Lausanne, CH-1015 Lausanne, Switzerland. [2]Department of Zoology, University of Cambridge, Cambridge CB2 3EJ, UK.

*To whom correspondence should be addressed. E-mail: james.poulet@epfl.ch

The morphology of CDI highlights three major structural properties that are crucial for its function. First, its cell body and extensive dendritic arborization is in the mesothoracic ganglion; therefore, it can receive synaptic input from the singing central pattern generator (CPG). Second, the neuron has profuse axonal arborizations that overlap with the auditory neuropil in the prothoracic ganglion, a prerequisite to forming direct output synapses with auditory neurons. Third, its axon targets widespread areas of the CNS and could affect other sensory pathways activated during singing.

Recordings from CDI were made from its dendritic branches during pharmacologically elicited fictive singing, with all thoracic sensory and motor nerves cut except for the auditory nerves (*3*, *15*). CDI generates bursts of spikes in synchrony with the wing motoneuron activity indicating the chirps (Fig. 2A). CDI spikes reach frequencies of 131 ± 16 Hz during the first syllable of the chirp and a maximum of 178 ± 9 Hz during the following syllables (mean ± SEM; n = 18). Quantitative analysis reveals that each burst of spikes occurred during wing-closing motor activity (stippled lines in Fig. 2B). This corresponds to the phase of wing movements when sound is produced and also with the timing of inhibitory inputs in auditory neurons during singing (*14*). To test whether CDI is part of the singing CPG, we used 100-ms depolarizing current pulses to elicit spikes and measured any effect on the singing motor pattern (Fig. 2C). Elicited bursts of spikes in CDI never had an effect on the timing of the ongoing singing motor pattern (n = 10) (Fig. 2D). Singing also continued normally when CDI was prevented from spiking by injection of hyperpolarizing current (n = 10). We therefore conclude that CDI is not part of the singing CPG but instead is driven by it.

Because CDI receives excitatory input during wing-closing movements, we tested whether it might also be activated during flying. When the crickets generated the flight motor pattern (n = 7), CDI was always inhibited by a barrage of inhibitory postsynaptic potentials (IPSPs) (Fig. 2, E and F), as were some of the neurons thought to be part of the cricket singing CPG (*16*). CDI did not respond to 85 dB SPL acoustic stimulation at 4.8 kHz, the carrier frequency of cricket song (n = 10) (Fig. 2G).

CDI's anatomy and physiology strongly suggested that it could mediate pre- and postsynaptic inhibition of the auditory pathway during singing (*3*). Paired intracellular recordings from CDI's dendrite and auditory neurons revealed the synaptic connectivity. About 60 auditory afferent neurons extend from the cricket's ears in the forelegs into prothoracic ganglion, where they terminate in a median-ventral auditory neuropil (*17*). Here they forward excitatory information onto a small number of auditory interneurons such as the local omega neuron 1 (ON1) (*18*). Paired recordings from CDI and auditory afferent axonal arborizations demonstrated that spikes in CDI occurred in synchrony with primary afferent depolarizations (PADs) during wing-closing motor activity (Fig. 3A). PADs cause a reduction in spike height in cricket auditory afferents (*14*) and mediate presynaptic inhibition in a number of sensory systems (*19*–*21*). When depolarizing current was injected into CDI, each spike in CDI reliably elicited a PAD of 2.0 ± 0.2 mV in the auditory afferent after a constant latency of 3.8 ± 0.1 ms (n = 7) (Fig. 3, B and C). Paired recordings of CDI and ON1 (Fig. 3D) revealed that ON1 received IPSPs when CDI spiked during a chirp. Injection of current into CDI revealed that each CDI spike elicited an IPSP of 1.6 ± 0.2 mV in ON1 after a delay of 3.5 ± 0.2 ms (n = 8) (Fig. 3, E and F). CDI has bilateral arborizations in the pro-

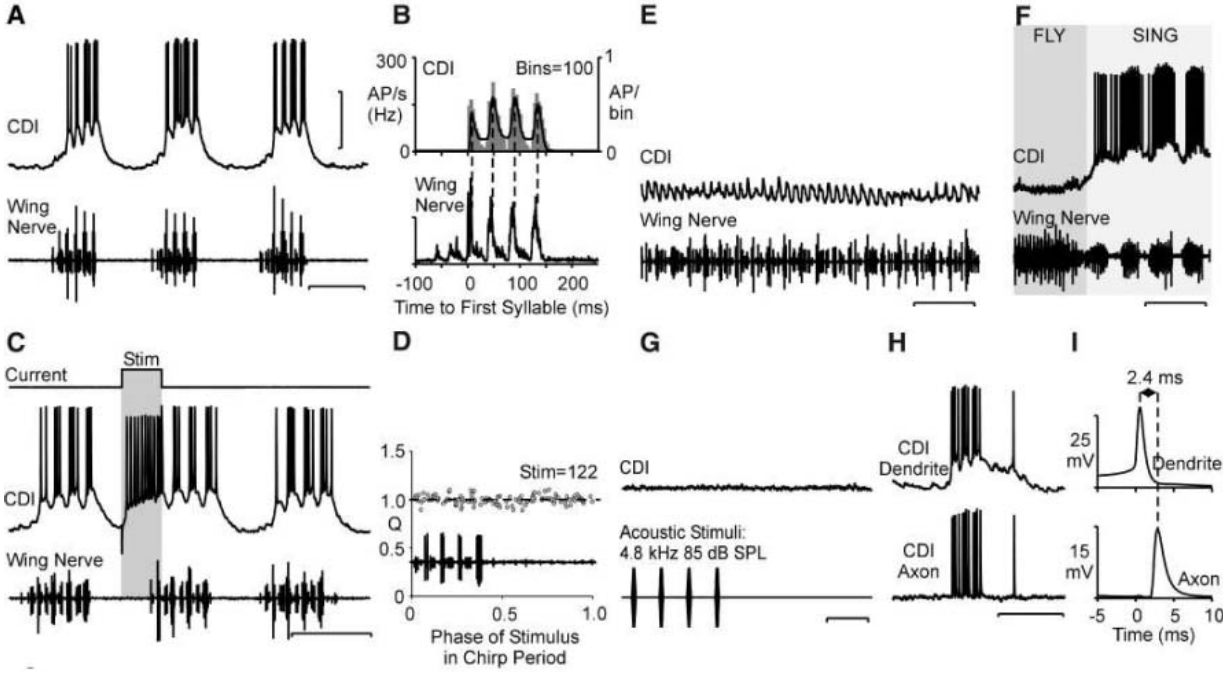

Fig. 2. Recordings of CDI and wing motor nerve during fictive singing and flight. (**A**) Spikes in CDI as recorded in the dendrite during fictive chirps. (**B**) The PSTH and superimposed instantaneous spike rate (n = 59 chirps, 759 spikes) with the averaged wing motor nerve activity demonstrate that CDI fires bursts of spikes during the wing-closing motor activity of each chirp, as indicated by the stippled lines. (**C**) Injection of depolarizing current into CDI elicited bursts of spikes but did not change the ongoing singing pattern. (**D**) Phase response curve. Q = (duration of ongoing chirp period N)/(duration of chirp period N + 1) at the phase of stimulation of CDI with a current pulse of 100 ms. Analysis shows no modulation in the duration of chirps by CDI stimulation. (**E**) CDI is rhythmically inhibited during fictive flight. (**F**) Transition from fictive flight to fictive singing demonstrates the change in activity. (**G**) CDI does not respond to acoustic stimulation with 4.8 kHz, 85 dB SPL pulses 21 ms in duration. (**H**) Paired recording from the dendrite in the mesothoracic ganglion and axon in the prothoracic auditory neuropil of the same CDI. (**I**) Average of paired recording from the same CDI shows, in this example, a delay of 2.4 ms from spike recorded in the dendrite to spike recorded in the axon in the prothoracic ganglion (n = 181 spikes). CDI, intracellular CDI recording; Wing Nerve, activity of mesothoracic nerve 3A. Vertical scale bars, 20 mV [(A), (C), (F), (G), and dendrite in (H)], 10 mV [(E) and axon in (H)]; horizontal scale bars, 250 ms [(A), (G), (H)], 200 ms [(C) and (E)], 1 s (F).

thoracic ganglion, and spikes in CDI elicited IPSPs and PADs in both the left- and right-side ON1s and afferents. Paired recordings of CDI in its dendrite and prothoracic axon showed that CDI spikes take 2.8 ms to reach the auditory neuropil (n = 4) (Fig. 2, H and I), which leaves less than 1 ms from the spike in the prothoracic ganglion to the release of IPSPs or PADs. We never recorded a failure of an IPSP or PAD in response to a CDI spike. Therefore, both the anatomical evidence of axonal arborizations of CDI in the auditory neuropil and the physiological evidence suggest that the connection from CDI to auditory afferents and to ON1 is monosynaptic.

What effect does CDI have on auditory processing? Paired recordings were obtained from CDI and ON1 during continuous presentation of computer-generated sound pulses at the carrier frequency of cricket song (Fig. 4). In resting crickets, when CDI was not spiking, the sound pulses elicited a train of spikes in ON1. When CDI was depolarized to make it spike, the auditory response in ON1 was inhibited (Fig. 4, A and B). During silent, fictive singing, ON1's response to the external sound stimuli was suppressed during the chirps, even when one CDI was prevented from spiking by injecting hyperpolarizing current (n = 8) (*22*). Because CDI exists as a bilateral pair of neurons, both with bilateral outputs, the persisting inhibition was most likely due to spikes in CDI's contralateral partner cell. However, we could not rule out the possibility of parallel inhibitory neurons. To examine whether the CDIs are the only neurons mediating the inhibition of the auditory pathway, we made a paired recording of CDI and ON1 during singing and then cut the contralateral prothoracic-to-mesothoracic connective, which contained the axon of the partner CDI (n = 2). When the animal's singing recovered, ON1 was inhibited by CDI during fictive singing and failed to respond to the ongoing auditory stimuli (Fig. 4, C and D). When CDI was hyperpolarized and prevented from spiking, ON1 responded to the sound pulses both in the chirp interval and in the chirp (Fig. 4, E and F). This confirmed that CDI is both sufficient and necessary to mediate the corollary discharge inhibition during singing, and there is no evidence for any parallel inhibitory pathways.

Over the past 50 years, investigation into the cellular basis of corollary discharges and efference copies has been hampered by a lack of data on identified neurons mediating these signals. There are now only a small number of neurons thought to mediate corollary discharges (*5*, *23*–*26*). The synaptic connectivity has been explored with intracellular recordings in only two populations of neurons (*25*, *26*). CDI is a rare example of a functionally and anatomically identified neuron that extends throughout the entire insect nervous system. Simultaneously, CDI mediates the presynaptic inhibition of auditory afferents with PADs and the postsynaptic inhibition of an identified auditory interneuron with IPSPs. This twofold inhibition reduces the auditory response to self-generated sounds and protects the cricket's auditory pathway from desensitization during sound production, allowing it to remain sensitive to environmental sounds (*6*, *12*, *14*). Thus, even in the small nervous system of the cricket, self-generated sensory signals are processed in a similar way to more complex vertebrate nervous systems (*27*, *28*). During flight, CDI is inhibited and prevented from firing; hence, flying crickets' hearing will not be impeded by CDI and they can listen for signaling conspecifics or echolocating calls from predating bats (*29*). The singing cricket also generates substantial nonauditory sensory feedback [e.g., (*30*)]. The complex and widespread branches of CDI indicate that it may also inhibit other sensory pathways. CDI therefore provides an opportunity to understand not only the role of timing in corollary discharge signals but also the computation by which motor and sensory signals are integrated.

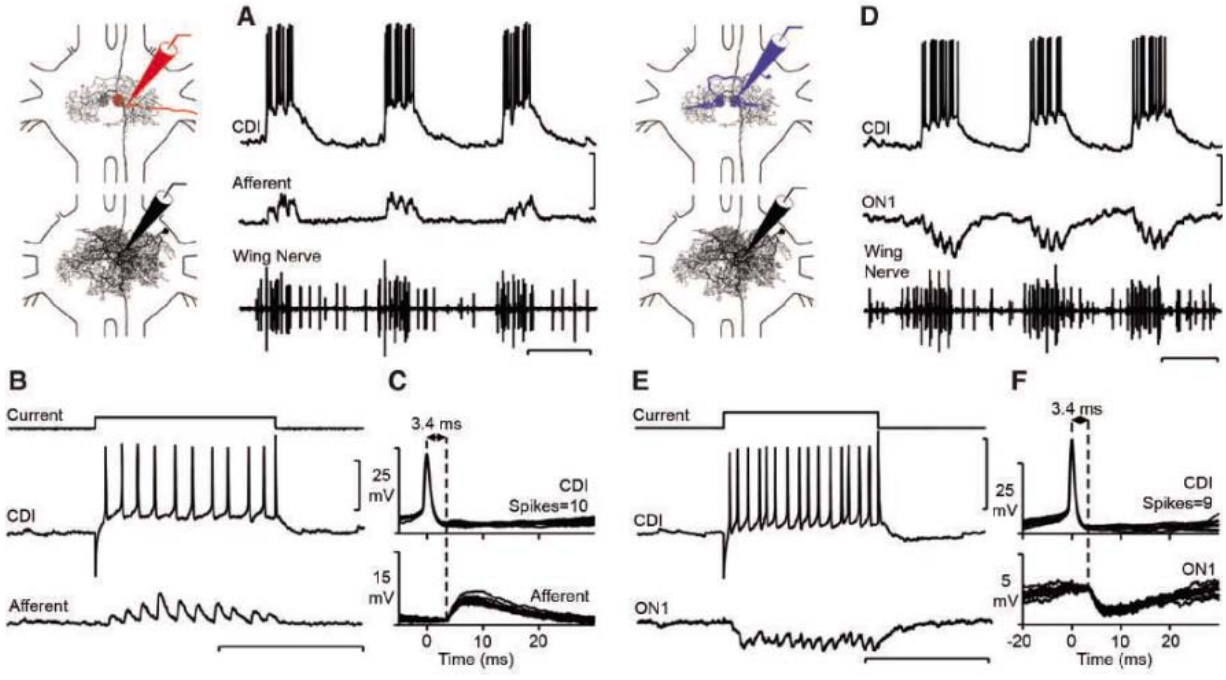

Fig. 3. Inhibitory inputs in auditory neurons are elicited by CDI spikes. (**A**) Paired recording of CDI and an auditory afferent during singing. Spikes in CDI coincide with PADs in the afferent. (**B**) Stimulation of CDI with intracellular depolarizing current injection. Each CDI spike elicits a PAD in the afferent. (**C**) Superposition of CDI and afferent recording triggered by spikes in CDI. In this example, PADs were elicited after a constant delay of 3.4 ms from CDI spike. (**D**) Paired recording of CDI and ON1 during singing. Spikes in CDI coincide with IPSPs in ON1. (**E**) Every spike elicited by depolarizing current injection in CDI elicits an IPSP in ON1. (**F**) Superimposed traces of CDI and ON1 show a constant latency (in this example 3.4 ms) from CDI spike to the IPSP. Afferent: intracellular auditory afferent recording; ON1, intracellular ON1 recording. Vertical scale bars, CDI: 15 mV (A), 30 mV (B), 20 mV (D), 25 mV (E); ON1: 15 mV (D), 5 mV (E); afferent: 20 mV (A), 10 mV (B); current: 5 nA; horizontal scale bars, 250 ms [(A) and (D)], 200 ms [(B) and (E)].

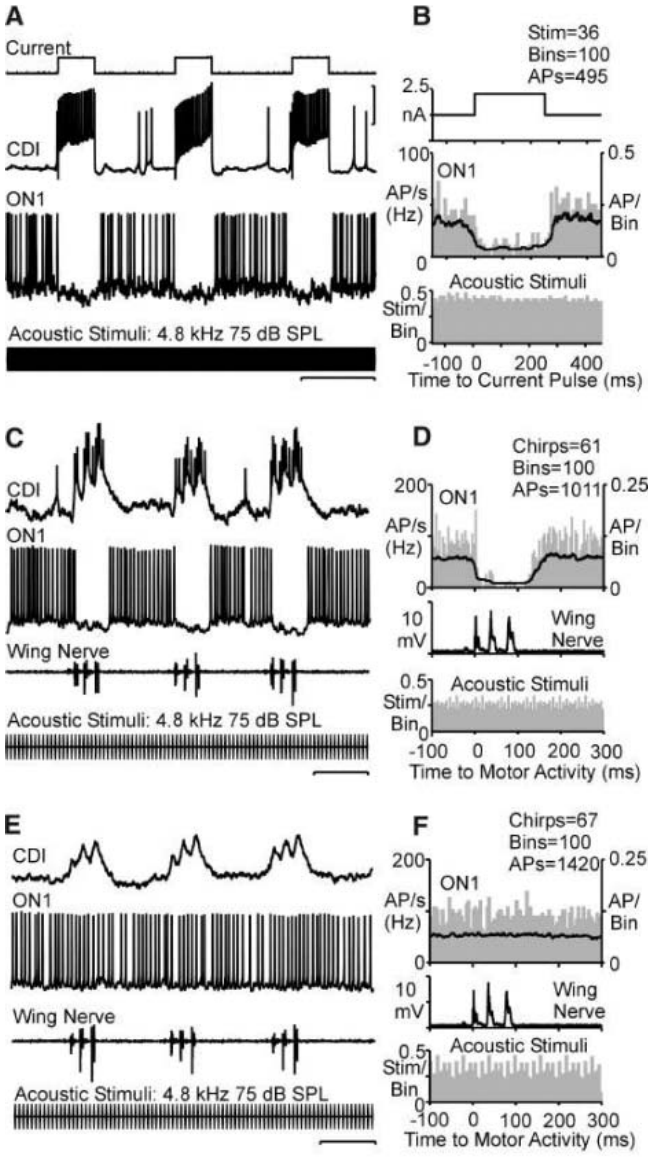

Fig. 4. The effect of CDI on sound processing. (**A**) ON1's response to a continuous sequence of 4.8 kHz, 75 dB SPL sound pulses, 8 ms in duration with intervals of 7 ms, is completely inhibited during periodic current injection in CDI. (**B**) PSTH and superimposed instantaneous spike frequency of ON1 averaged over 36 trials demonstrate that ON1 activity is reduced during CDI stimulation. (**C**) In an animal with the contralateral prothoracic-to-mesothoracic connective cut, ON1 responds with a train of spikes during the chirp intervals, but it fails to respond during the chirp if CDI is spiking. (**D**) The PSTH and instantaneous spike frequency of ON1 highlights the reduction in ON1 response during the chirp. (**E**) When CDI is prevented from spiking by hyperpolarizing current injection, ON1 responds to sound during the chirp and the chirp interval. (**F**) When CDI spikes were suppressed by inhibitory current injection, the PSTH and instantaneous spike frequency show no reduction in the activity of ON1 during chirps. Vertical scale bar, current: 2.5 nA (A); CDI: 20 mV [(A) and (E)], 10 mV (C); ON1: 20 mV [(A), (C), and (E)]; horizontal scale bars, 500 ms (A), 200 ms [(C) and (E)].

References and Notes

1. K. G. Pearson, *Annu. Rev. Neurosci.* **16**, 265 (1993).
2. R. W. Sperry, *J. Comp. Physiol. Psychol.* **43**, 482 (1950).
3. E. von Holst, H. Mittelstaedt, *Naturwissenschaften* **37**, 464 (1950).
4. M. Zaretsky, C. H. F. Rowell, *Nature* **280**, 583 (1979).
5. M. A. Sommer, R. H. Wurtz, *Science* **296**, 1480 (2002).
6. J. F. A. Poulet, B. Hedwig, *Nature* **418**, 872 (2002).
7. K. T. Sillar, P. Skorupski, *J. Neurophysiol.* **55**, 678 (1986).
8. K. T. Sillar, A. Roberts, *Nature* **331**, 262 (1988).
9. S. J. Blakemore, D. Wolpert, C. D. Frith, *Nat. Neurosci.* **1**, 635 (1998).
10. C. C. Bell, *Science* **214**, 450 (1981).
11. J. E. Roy, K. E. Cullen, *J. Neurosci.* **24**, 2102 (2004).
12. J. F. A. Poulet, B. Hedwig, *J. Neurosci.* **23**, 4717 (2003).
13. J. F. A. Poulet, B. Hedwig, *J. Exp. Biol.* **204**, 1281 (2001).
14. J. F. A. Poulet, B. Hedwig, *J. Neurophysiol.* **89**, 1528 (2003).
15. See supporting material on *Science* Online.
16. R. M. Hennig, *J. Comp. Physiol. A* **167**, 629 (1990).
17. K. Michel, *Z. Morph. Tiere* **77**, 285 (1974).
18. K. Schildberger, D. W. Wohlers, F. Huber, in *Cricket Behavior and Neurobiology*, F. Huber, T. E. Moore, T. E. Loher, Eds. (Cornell Univ. Press, Ithaca, NY, 1989), pp. 423–458.
19. M. D. Kirk, J. J. Wine, *Science* **225**, 854 (1984).
20. F. Clarac, D. Cattaert, *Exp. Brain Res.* **112**, 163 (1996).
21. P. Rudomin, R. F. Schmidt, *Exp. Brain Res.* **129**, 1 (1999).
22. J. F. A. Poulet, B. Hedwig, data not shown.
23. M. G. Weeg, B. R. Land, A. H. Bass, *J. Neurosci.* **25**, 5967 (2005).
24. C. C. Bell, K. Dunn, C. Hall, A. Caputi, *J. Comp. Physiol. A* **177**, 449 (1995).
25. W. C. Li, S. R. Soffe, A. Roberts, *J. Neurosci.* **22**, 10924 (2002).
26. S. C. Rosen, M. W. Miller, E. C. Cropper, I. Kupfermann, *J. Neurophysiol.* **83**, 1621 (2000).
27. K. E. Cullen, *E. Curr. Op. Neurobiol*. **14**, 698 (2004).
28. C. C. Bell, K. Grant, *J. Neurosci.* **9**, 1029 (1989).
29. T. G. Nolen, R. R. Hoy, *Science* **226**, 992 (1983).
30. M. Dambach, H.-G. Rausche, G. Wendler, *Naturwissenschaften* **70**, 417 (1983).

31. We thank S. Atkinson, M. Burrows, C. Petersen, and S. Rogers for comments on the manuscript. Supported by the UK Biotechnology and Biological Sciences Research Council, the Royal Society, and the Human Frontier Science Program.

Supporting Online Material

www.sciencemag.org/cgi/content/full/311/5760/518/DC1
Materials and Methods
References

3 October 2005; accepted 20 December 2005
10.1126/science.1120847

Scaling of Connectivity in Marine Populations

R. K. Cowen,[1]* C. B. Paris,[1] A. Srinivasan[2]

Defining the scale of connectivity, or exchange, among marine populations and determining the factors driving this exchange are pivotal to our understanding of the population dynamics, genetic structure, and biogeography of many coastal species. Using a high-resolution biophysical model for the Caribbean region, we report that typical larval dispersal distances of ecologically relevant magnitudes are on the scale of only 10 to 100 kilometers for a variety of reef fish species. We also show the importance of the early onset of active larval movement mediating the dispersal potential. In addition to self-recruitment, larval import from outside the local area is required to sustain most populations, although these population subsidies are very limited in particular systems. The results reveal distinct regions of population isolation based on larval dispersal that also correspond to genetic and morphological clines observed across a range of marine organisms.

Identifying the scale of marine larval dispersal remains one of the fundamental challenges to marine ecology and oceanography. Most coastal marine species have limited adult movement, so the relatively short, pelagic larval phase represents the primary opportunity for dispersal. Although larvae have the potential for long-distance dispersal (*1*, *2*), evidence is mounting that larval dispersal may be limited (*3*–*11*). These studies challenge assumptions about the dominant distance mode of dispersal for marine populations (whether larvae typically travel a long or short distance) (*12*, *13*). The rates, scale, and spatial structure of successful exchange, or connectivity, among local populations of marine organisms drive population replenishment and, therefore, have profound implications for population dynamics and genetics of marine organisms; spatially oriented resource management (e.g., marine protected areas); and the

[1]Marine Biology and Fisheries, [2]Meteorology and Physical Oceanography, Rosenstiel School of Marine and Atmospheric Science, University of Miami, 4600 Rickenbacker Causeway, Miami, FL 33149, USA.

*To whom correspondence should be addressed. E-mail: rcowen@rsmas.miami.edu

spread of invasive species (*9*, *14*, *15*). However, realistic scaling estimates of connectivity are lacking. With major declines in fishery stocks, rapid degradation of natural coastal habitat, and calls for ecosystem-based management, identification of the spatial scale of population connectivity over demographically relevant time scales is critical.

Data on dispersal distances have been collected for only a handful of species, mostly those with short larval durations (hours to days) and very short distance dispersal (*16*, *17*). These studies generally provide a snapshot of dispersal, representing only one possible dispersal scenario. It is impossible to capture empirically the full range of spatial and temporal variability that is expressed as a result of oceanographic conditions and larval behavior. Thus, the task of estimating dispersal kernels (the spatial probability of dispersal) for multiple species from a variety of potential spawning sites is only feasible with the use of high-resolution, hydrodynamic models.

For marine systems, early estimates of dispersal have relied on either simplified advection-diffusion models or passive particle models that use mean currents to define the potential for spread (*18*, *19*). Advection-diffusion modeling studies and those based on statistics of oceanographic flow fields provide good theoretical frameworks for viewing potential scaling issues related to larval dispersal, such as spacing of marine reserves (*15*, *20*–*22*); yet, such studies do not provide realistic renditions of ocean circulation or reveal how biological factors may mediate the dispersal outcome driven by ocean conditions. Critical evaluation of the role of behavior in modifying flow-mediated trajectories, as well as assessing variability in seasonal and spatial aspects of flow over and among heterogeneous coral reef systems along complex coastlines, requires more realistic, coupled biological-physical models (*23*–*26*).

We used flow trajectories from a high-resolution ocean circulation model in a Lagrangian stochastic scheme, generating an individual-based model (IBM) for larval dispersal (*27*). To evaluate the spatial scales over which larvae may be dispersed, that is, the effective geographic distances among reef fish populations, under realistically varying spatial and temporal oceanographic conditions, we ran the circulation model for 5 years of real wind data, resolving interannual variability in transport within the entire region. The IBM model includes a number of biological parameters such as pelagic larval duration (PLD), larval behavior (vertical and horizontal swimming capabilities), and adult spawning strategies (season and frequency). Successful dispersal also requires larvae (real or virtual) to encounter suitable settlement habitat, which is fragmented and often covers a small proportion of the area of potential dispersal by currents. Therefore, we included benthic habitat defined by the presence of coral reefs throughout the spatial domain of the model—the wider Caribbean including the Bahamas and Florida. Contiguous coral reef habitat was further divided into 9-km by 50-km segments, setting the spatial scale for self-recruitment in this study. Virtual larvae had to be near (within 9 km of) available settlement habitat at the end of their larval period in order to be considered successful, that is, able to settle.

Although dispersal of a few organisms may be widespread, ecologically significant levels of dispersal—those necessary to replenish annual mortality—may be substantially more restricted in spatial extent (*12*, *20*). In order to make reasonable predictions of ecologically meaningful dispersal curves or kernels, the required number or relative level of successful settlers arriving at any destination population must be estimated. This level was set to reflect the settlement rates required to replenish the local population, so as to maintain it at a constant population level by balancing the natural juvenile and adult mortality and by accommodating any additional mortality, such as from fishing. Settlement rates (the number of settlers per year), therefore, were matched to estimated adult mortality rates by using simple population growth models ($N_t = N_0 e^{rt}$) set to a constant age 1+ population size. On the basis of these estimates (*27*) (table S1), we found that the required level of potential settlers, those that survived their entire pelagic stage, ranges between 10 and 100% for long-lived and short-lived species (longevity >15 years to ~1 year), respectively. Increasing mortality due to fishing pressure would similarly increase the required level of potential settlers, but would generally fall within this range. Estimating relevant recruitment levels is essential to scaling the extent of dispersal, which otherwise would be meaningless at ecological time scales.

We show for the wider Caribbean—a large region with complex, highly diverse flow re-

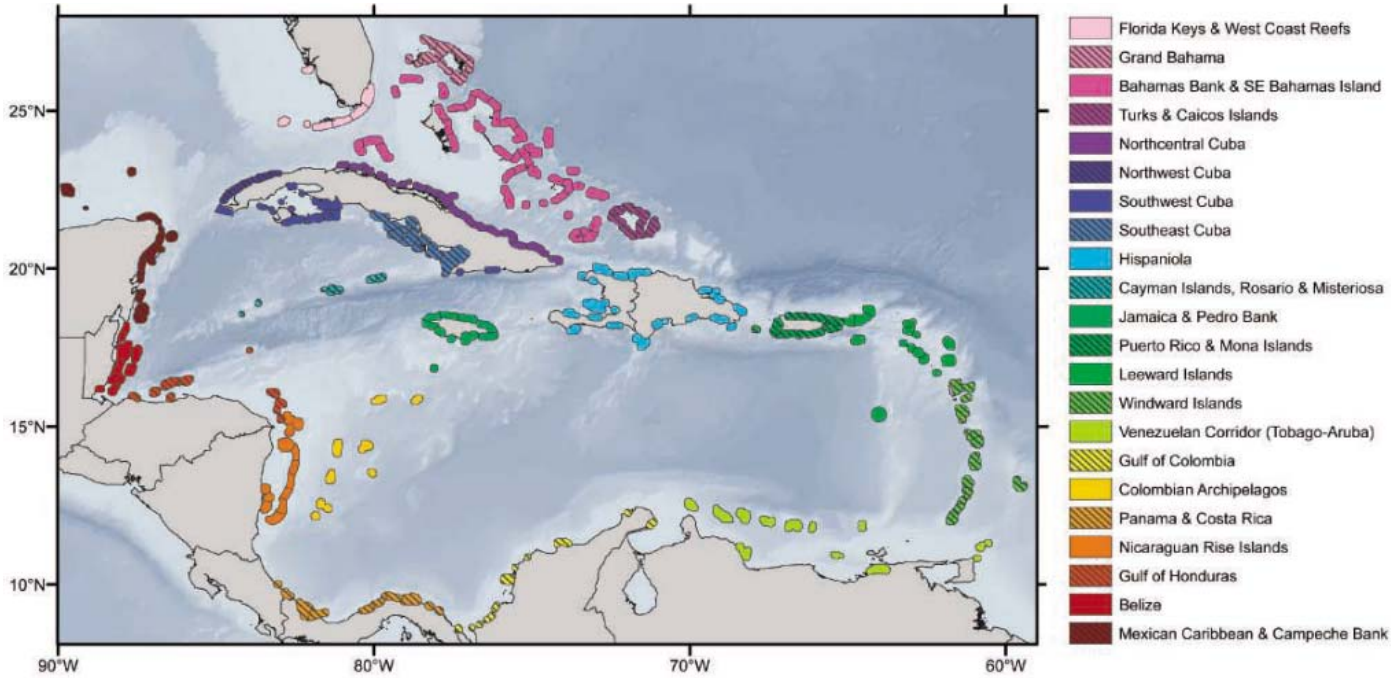

Fig. 1. Coral reef fish settlement habitat in the Caribbean region buffered by a 9-km larval sensory zone. The coral reef mosaic is largely fragmented and restricted to shallow water near continental coastlines or around islands and isolated seamounts, and it represents a small fraction of the entire oceanic and coastal areas. Subregions within the wider Caribbean region are color coded and segmented into a total of 260 polygons (9 km by 50 km) or nodes (N_i).

gimes and spatially heterogeneous habitat (8°N to 28°N, 57°W to 90°W, about 2100 km × 3300 km) (Fig. 1)—that typical larval dispersal distances providing ecologically significant numbers of settlers were only on the scale of 50 to 100 km for most species, with a relatively high rate of local retention or recruitment from adjacent locations. The role of population subsidy from distant locations was greatest for species with high natural (or fishing-related) mortality rates. Across the region, the relative importance of locally retained versus imported larvae varied, as a result of variation in the abundance of imported larvae. Consequently, some populations experience generally less recruitment than others. The fine scale of dispersal, on top of specific suitable settlement habitat and oceanographic boundaries, creates several subregions that are ecologically isolated from each other, which may translate into biogeographic regions of genetic heterogeneity.

At the broadest scale of comparison, there was considerable spatial variation in the exchange of larvae among sites, which interacted strongly with the degree of larval active movement. These results suggest that passive dispersal is insufficient for population replenishment. The foremost difference between a purely passive model and one incorporating larval active movement is the prevalence of local or self-recruitment enhanced with early onset of swimming behavior and modified by the fragmentation pattern of available settlement habitat, whether clustered or isolated, whereas the converse of greater long-distance dispersal under the passive scenario was not realized (Fig. 2). Overall, the passive scenario resulted in recruitment levels that were one to two orders of magnitude below that necessary for successful population replenishment and considerably reduced population connectivity (Fig. 2C). Greater dispersal distances can be achieved with longer duration of the larval stage, which also increases connectivity. These results underscore the role of larval traits and behavior when both dispersal and recruitment are modeled and demonstrate that biological and physical constraints (such as oceanographic boundaries) are equally important in resolving dispersal kernels and connectivity among fish populations.

In most areas, when active larval movement was invoked in the model, total recruitment [subsidy recruitment and self-recruitment] met or exceeded the demographic minimum required to sustain stable populations of long-lived species, but only a few locations were able to regularly sustain short-lived or severely fished

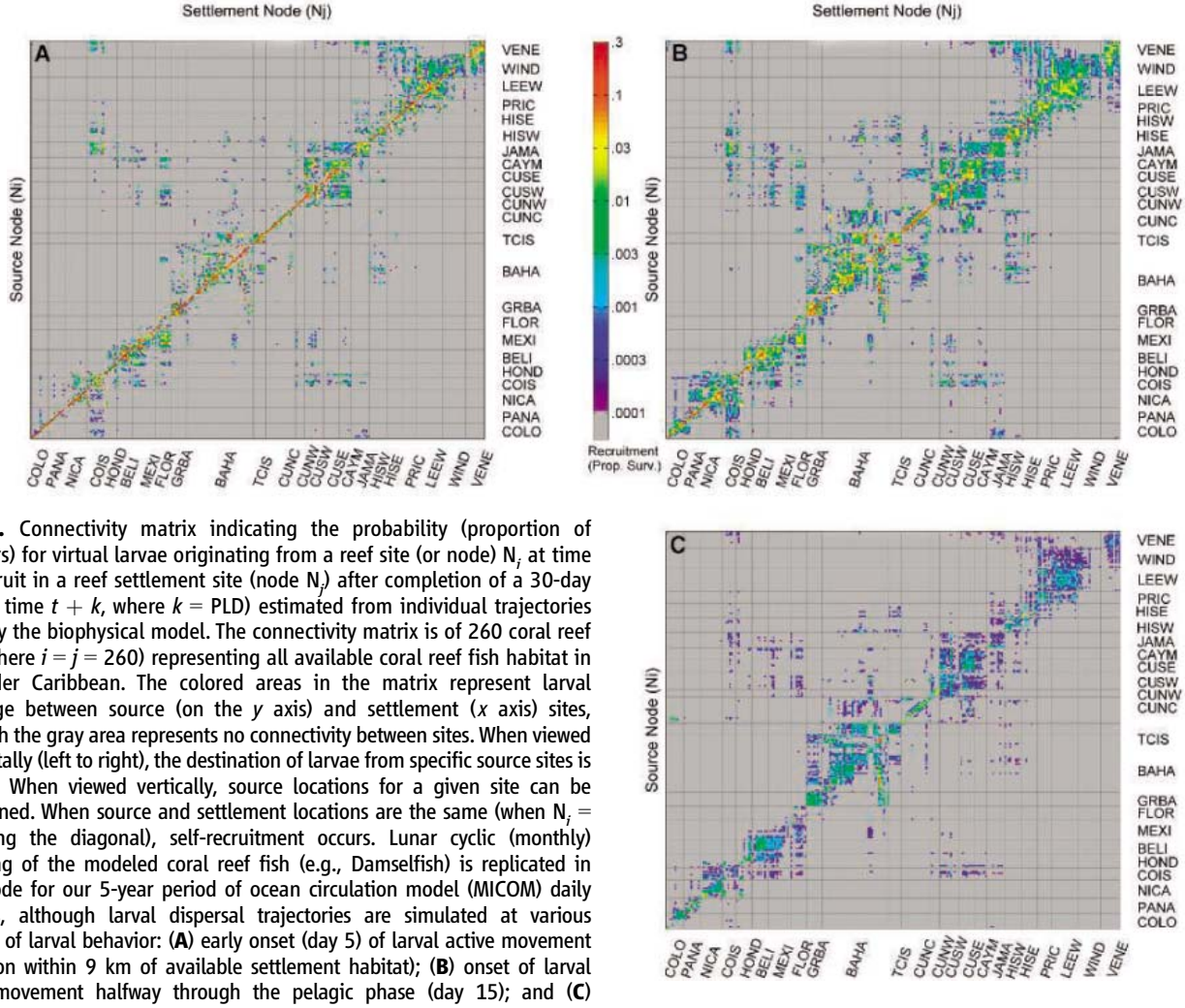

Fig. 2. Connectivity matrix indicating the probability (proportion of survivors) for virtual larvae originating from a reef site (or node) N_i at time t to recruit in a reef settlement site (node N_j) after completion of a 30-day PLD (at time $t + k$, where k = PLD) estimated from individual trajectories given by the biophysical model. The connectivity matrix is of 260 coral reef sites (where $i = j = 260$) representing all available coral reef fish habitat in the wider Caribbean. The colored areas in the matrix represent larval exchange between source (on the y axis) and settlement (x axis) sites, although the gray area represents no connectivity between sites. When viewed horizontally (left to right), the destination of larvae from specific source sites is evident. When viewed vertically, source locations for a given site can be determined. When source and settlement locations are the same (when $N_i = N_j$, along the diagonal), self-recruitment occurs. Lunar cyclic (monthly) spawning of the modeled coral reef fish (e.g., Damselfish) is replicated in each node for our 5-year period of ocean circulation model (MICOM) daily currents, although larval dispersal trajectories are simulated at various degrees of larval behavior: (**A**) early onset (day 5) of larval active movement (retention within 9 km of available settlement habitat); (**B**) onset of larval active movement halfway through the pelagic phase (day 15); and (**C**) delayed onset of active swimming for passive larvae at the end of PLD (day 30). The model domain is grouped (thin gray lines) into 23 subregions: VENE, Venezuelan Corridor (from Tobago to Aruba); WIND, Windward Islands; LEEW, Leeward Islands; PRIC, Puerto Rico and Mona Island; HISW, Hispaniola West (Haiti); HISE, Hispanola East (Dominican Republic); JAMA, Jamaica Island and Pedro Bank; CAYM, Cayman Islands and Rosario and Misteriosa Banks; CUSE, southeast Cuba; CUSW, southwest Cuba; CUNW, northwest Cuba; CUNC, north central Cuba; TCIS, Turks and Caicos Islands; BAHA, Bahamas Bank and southeast Bahamian Islands; GRBA, Grand Bahamas; FLOR, Florida Keys and west coast reefs; MEXI, Mexican Caribbean and Campeche Bank; BELI, Belize; HOND, Gulf of Honduras; COIS, Colombian Archipelagos (from San Andres to Serrena Bank); NICA, Nicaraguan Rise Islands (from Mosquito Coast to Cabo Gracias á Dios); PANA, Panama and Costa Rica; COLO, Gulf of Colombia. Prop. surv., proportion surviving.

(high-turnover) species (Fig. 3A). Two regions, the Windward Islands and the Mexican Caribbean and Campeche Bank, stood out as being strongly recruitment-limited (total recruitment falls well below that necessary for sustaining populations), while most regions appear to receive sufficient recruitment levels such that post-settlement, density-dependent processes may be important at moderating population fluctuation. When parsed between recruitment from local sources (i.e., self-recruitment) versus importation from adjacent or distant sources, the pattern is highly variable across space, as well as in recruitment intensity (Fig. 3, B and C). Self-recruitment was close to sufficient for supplying adequate numbers of young only with active larval movement, but a variety of sites appear to be poor at self-seeding. In contrast, population subsidy is generally less variable, particularly under passive scenarios, though certain sites (e.g., the Windward Islands and the Yucatan Peninsula in northern Mexico) are apparently devoid of sources within a critical upstream distance, which results in low recruitment levels. Life histories and larval capabilities emerge as factors that strongly influence self-recruitment, whereas oceanographic regimes appear to control population subsidies.

Caribbean-wide self-recruitment accounted for ~21% of the recruits to an average site, with subsidy from within 50 km or less—since 50 km is the resolution of the Geographic Information Systems (GIS)–based habitat model—necessary to achieve recruitment levels required to sustain long-lived species and within 200 km at the most to sustain typical reef-fish life histories (Table 1). These values robustly simulate dispersal distances over the wider Caribbean, strongly suggesting that the relevant scaling of dispersal is much smaller than believed. Regionally, self-recruitment varied from 9% (off Mexico in proximity to a strong western boundary current) to almost 57% (off Colombia in proximity to the semipermanent Panama-Colombia Gyre). In the latter case, the high proportion of self-recruitment was partially due to low importation from upstream locations, which resulted in generally low overall recruitment. Generally, important additional contributions of recruits do not accumulate from farther than 200 to 300 km. The exception is in regions upstream of strong western boundary currents (such as those along Florida). However, even though additional larvae accumulated from well upstream in such areas (e.g., Mexico), the overall recruitment was relatively low (Fig. 2). The typical shape of the cumulative dispersal curve, therefore, is strongly skewed near the origin, with a near-zero tail starting as close as a few hundred kilometers (fig. S1).

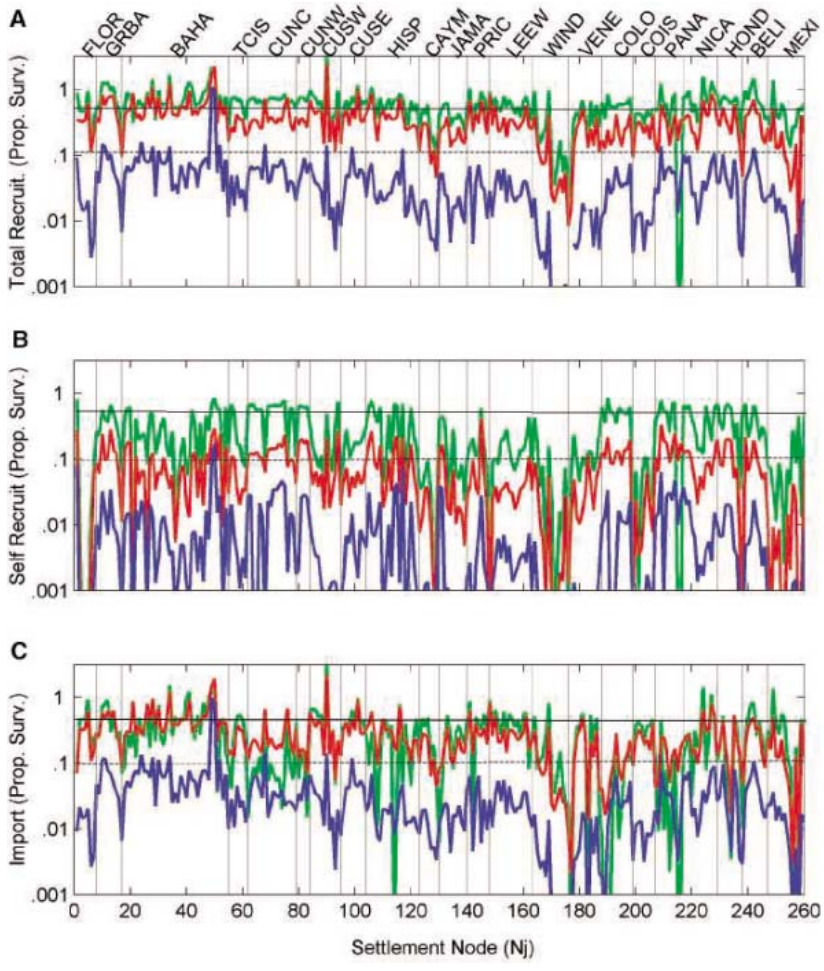

Fig. 3. Simulated larval (**A**) total recruitment, (**B**) self-recruitment, and (**C**) subsidy recruitment (importation) as a proportion of surviving virtual larvae reaching each coral reef settlement site (node N_j) within subregions of the wider Caribbean. Larval dispersal trajectories were simulated at various degrees of larval activity, whereby the onset of active movement is on day 5 (green line), day 15 (red line), and day 30 (blue line; same as passive). Threshold levels required to sustain damselfish (30% of surviving larvae) and snapper (10% of surviving larvae) populations are indicated by the solid and dotted black lines, respectively. Although recruitment levels from passive larvae rarely met the threshold, the early onset of active larval movement typically enhanced both self-recruitment and subsidy. Abbreviations for the subregions are the same as for Fig. 2; prop. surv., proportion surviving.

Population connectivity via larval dispersal can produce biogeographic patterns within the broader Caribbean region (Fig. 4). The western and eastern Caribbean are moderately isolated from each other along a meridional break centered at about 67° to 70°W, or from the western end of Puerto Rico south to Aruba off the coast of Venezuela, which may constitute a clear ecological barrier from the Colombian gyre area to the west. The northeast Caribbean (Puerto Rico, Leeward Islands) is relatively isolated from the remainder of the eastern Caribbean; the Leeward Islands are mostly self-recruiting and constitute a sink for north-south larval exchange with the Windward Islands. However, there is also westerly exchange among the more southern Windward Islands and those along the north coast of South America. The Bahamas and the Turks and Caicos Islands form an enclave of high connectivity in the northern Caribbean, which is largely isolated from the remaining Caribbean domain, except for minor exchange from the north coast of Cuba and Haiti. The southern Mesoamerican (or Gulf of Honduras) reef area, including Belize and Honduras, is weakly isolated from the northernmost Mesoamerican Barrier Reef and strongly isolated from islands along the coast of Nicaragua to the east and south. Reefs along the Panama-Colombia Gyre are also isolated from the remainder of the Caribbean.

The Caribbean region emerges as four broadly defined regions of connectivity, the eastern Caribbean, the western Caribbean, the Bahamas and the Turks and Caicos Islands, and the region at the periphery of the Colombia-Panama Gyre, with lesser areas of isolation within each region. The more central portion of the Caribbean, including Hispaniola and Ja-

maica, represents a zone of mixing among several of these other regions. The prominence of the boundaries of these regions is highlighted in genetic-based and morphological studies. These regions roughly define the same regions of genetically (and morphologically) distinct populations of the goby, *Elacatinus evelynae* (*7*, *11*), and the coral, *Acropora palmata* (*28*). Thus, short-distance, stepping-stone population connectivity (*29*) may occur within regions, but the finding of limited exchange among regions over 5 years of monthly spawning appears sufficiently robust to allow regional scale genetic isolation as shown in other oceanographically and geographically complex regions (*8*). Faunal breaks, which are typically attributed to temperature or salinity differences inferring physiological constraints, may, in fact, be influenced (or alternatively, driven) by circulation constraints on dispersal (*17*, *30*–*32*).

Ecological connections may be extended in some situations by rare, extreme dispersal events in which unusually large numbers of larvae are exported to distant locations (*30*, *33*). When such events occur frequently enough (in terms of the demographic longevity of a species), populations may be sustained by the storage effect (*34*). Extending longevity in a species has been suggested as a means of capturing dispersal-related variability in flow events (*20*, *21*, *33*). In these simulations, which only covered 5 years, long-term rare events (25-, 50-, and 100-year events) were not evident. However, when viewed as cohort-specific events for short-lived species that spawn on a monthly (or more frequent) basis, rare events (defined as recruitment intensity of demographic relevance) occurred ~5% of the time at distances up to 200 km, but less than 1% (less than 1 out of 100 cohorts) at distances greater than 200 km. Thus, the storage effect may occur more as a range extension [e.g., extension of the short-lived blue-phase goby into Turks and Caicos waters (*7*)], with local scale processes maintaining the population thereafter, than as occasional events maintaining a population. Moreover, lengthening adult life does not necessarily increase opportunity to capture variability (as from rare events) if the frequency of spawning decreases as compared with that of short-lived species.

The modeling approach taken in this study used an advanced combination of theoretical tools (*26*) that allowed an unprecedented overview of the spatial and temporal context over which population connectivity in marine species occurs. The passive (water circulation) component of this model has been well validated (*27*). Moreover, results of this model suggest testable hypotheses, with specific pre-

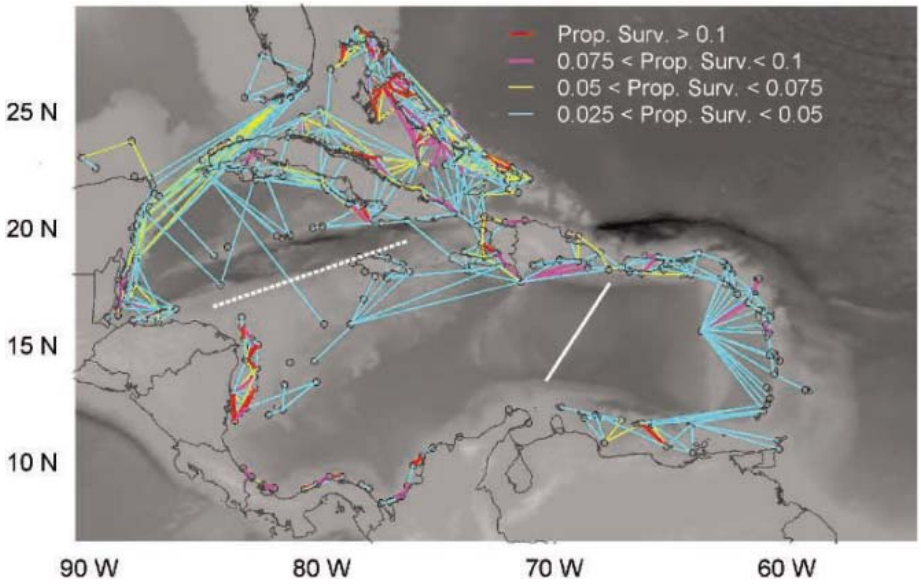

Fig. 4. Connectivity network for reef fish populations in the wider Caribbean plotted for various levels of larval exchange (proportion surviving) between each reef site (or node N_i, where center location is represented by a small gray circle; note that there is no directionality represented in the exchange). Two major meridional biogeographic breaks are identified: one in the eastern Caribbean Sea (white line) and the other one at the northern edge of the Nicaraguan Rise (dotted white line), which separate the eastern and western Caribbean. Two enclaves stand out: the Bahamas Bank, including the Turks and Caicos Islands, and the Nicaraguan Archipelago, which are both strongly intraconnected. The Panama-Colombian Gyre subregion is also largely isolated from the rest of the Caribbean, with little connection between Panama and Colombia. Note that connections at levels below 0.05% (proportion surviving) are not likely contributing appreciably to ecological connectivity but are shown here because they may become important when accumulated from different sources at one particular location.

Table 1. Estimates of total recruitment, proportion of self-recruitment, and dispersal distances at which various thresholds of recruitment are met, those necessary to replace the adult populations of each representative species, in the wider Caribbean region and for subregions (e.g., individual islands, groups of islands, and complex continental shelf and lagoon areas). N/A means not attainable: Not enough larvae could accumulate at a site to accommodate such high levels of recruitment.

Region	Total recruitment (proportion surviving)	Self-recruitment (% total recruitment)	Source distance (km) for recruitment levels			
			0.01	0.1	0.3	1
Caribbean	0.39	20.7	<50	<50	200	N/A
Bahamas	0.63	21.5	<50	<50	100	N/A
Haiti	0.45	26.9	<50	<50	100	N/A
Cuba	0.43	25.0	<50	<50	150	N/A
Belize	0.37	26.4	50	<100	<100	N/A
Dominican Republic	0.36	27.0	<50	<50	300	N/A
Honduras	0.33	36.2	<50	<100	100	N/A
Florida	0.32	14.9	<50	300	950	N/A
Panama-Colombia	0.24	55.2	<50	<50	<100	N/A
Greater Antilles	0.23	12.9	<50	50	<250	N/A
Venezuela Corridor	0.22	16.4	50	<150	N/A	N/A
Jamaica	0.22	24.4	50	100	N/A	N/A
Cayman	0.18	9.8	50	200	N/A	N/A
Mexico	0.17	9.0	50	250	N/A	N/A

dictions about dispersal distances, the role of larval traits, and biogeographic and genetic patterns, which are consistent with emerging empirical data (*6*, *28*, *35*). Further experimental tests of model predictions, as well as incorporation of higher resolution biophysical models, will serve to improve the predictability of dispersal kernels, our understanding of the processes driving the dispersal outcome for explicit locations, and, ultimately, application of appropriate scaling to spatial management of marine populations.

References and Notes

1. G. Thorson, *Meddr. Kommn. Danm. Fisk.-og Havunders. (Ser. Plankton)* **4**, 1 (1950).
2. R. S. Scheltema, *Bull. Mar. Sci.* **39**, 290 (1986).
3. G. P. Jones, M. J. Milicich, M. J. Emslie, C. Lunow, *Nature* **402**, 802 (1999).
4. S. E. Swearer, J. E. Caselle, D. W. Lea, R. R. Warner, *Nature* **402**, 799 (1999).
5. S. R. Thorrold, C. Latkoczy, P. K. Swart, C. M. Jones, *Science* **291**, 297 (2001).
6. C. B. Paris, R. K. Cowen, *Limnol. Oceanogr.* **49**, 1964 (2004).
7. M. S. Taylor, M. E. Helberg, *Science* **299**, 107 (2003).
8. P. H. Barber, S. R. Palumbi, M. V. Erdmann, M. K. Moosa, *Nature* **406**, 692 (2000).
9. S. Palumbi, *Ecol. Appl.* **13**, S146 (2003).
10. G. P. Jones, S. Planes, S. R. Thorrold, *Curr. Biol.* **15**, 1314 (2005).
11. P. L. Colin, *Neon Gobies* (TFH Publications, Neptune, NJ, 1975).
12. R. K. Cowen, K. M. M. Lwiza, S. Sponaugle, C. B. Paris, D. B. Olson, *Science* **287**, 857 (2000).
13. R. R. Warner, R. K. Cowen, *Bull. Mar. Sci.* **70**, 245 (2002).
14. J. Roughgarden, S. D. Gaines, H. P. Possingham, *Science* **241**, 1460 (1988).
15. L. Botsford, W. A. Hastings, S. D. Gaines, *Ecol. Lett.* **4**, 144 (2001).
16. P. W. Sammarco, J. C. Andrews, *Limnol. Oceanogr.* **34**, 896 (1989).
17. A. L. Shanks, B. A. Grantham, M. H. Carr, *Ecol. Appl.* **13**, S159 (2003).
18. A. E. Hill, *Mar. Ecol. Prog. Ser.* **64**, 217 (1990).
19. C. M. Roberts, *Science* **278**, 1454 (1997).
20. J. L. Largier, *Ecol. Appl.* **13**, S71 (2003).
21. S. D. Gaines, B. Gaylord, J. L. Largier, *Ecol. Appl.* **13**, S32 (2003).
22. D. A. Seigel, B. P. Kinlan, B. Gaylord, S. D. Gaines, *Mar. Ecol. Prog. Ser.* **260**, 83 (2003).
23. F. E. Werner, J. A. Quinlan, R. G. Lough, D. R. Lynch, *Sarsia* **86**, 411 (2001).
24. E. Wolanski, P. Doherty, J. Carleton, *Naturwissenschaften* **84**, 262 (1997).
25. M. K. James, P. R. Armsworth, L. B. Mason, L. Bode, *Proc. Biol. Sci.* **269**, 2079 (2002).
26. B. deYoung *et al.*, *Science* **304**, 1463 (2004).
27. Materials and Methods are available on *Science* Online.
28. I. B. Baums, M. W. Miller, M. E. Hellberg, *Mol. Ecol.* **14**, 1377 (2005).
29. M. H. Carr, D. C. Reed, *Can. J. Fish. Aquat. Sci.* **50**, 2019 (1993).
30. R. K. Cowen, *J. Mar. Res.* **43**, 719 (1985).
31. W. R. Coe, *Ecology* **34**, 225 (1953).
32. I. E. Efford, *Crustaceana* **18**, 293 (1970).
33. B. Gaylord, S. D. Gaines, *Am. Nat.* **155**, 769 (2000).
34. R. R. Warner, P. L. Chesson, *Am. Nat.* **125**, 769 (1985).
35. S. Planes, in *The Ecology of Fishes on Coral Reefs*, P. F. Sale, Ed. (Academic Press, San Diego, 2002), pp. 201–220.

36. The authors thank S. Sponaugle, J. Llopiz, J. Kool, and D. Richardson for discussion and review of an earlier draft of this paper. We also thank K. Lindeman of Environmental Defense and the National Science Foundation (OCE-0119976 and OCE-0095955) for supporting this work. Z. Garraffo and E. Chassignet provided help and support with using the output of the Miami Isopycnal Coordinate Ocean Model (MICOM).

Supporting Online Material

www.sciencemag.org/cgi/content/full/1122039/DC1
Materials and Methods
Fig. S1
Table S1
References and Notes

31 October 2005; accepted 18 November 2005
Published online 15 December 2005;
10.1126/science.1122039
Include this information when citing this paper.

Nonrandom Processes Maintain Diversity in Tropical Forests

Christopher Wills,[1]* Kyle E. Harms,[2,3] Richard Condit,[3] David King,[4] Jill Thompson,[5] Fangliang He,[6] Helene C. Muller-Landau,[7] Peter Ashton,[4] Elizabeth Losos,[8] Liza Comita,[9] Stephen Hubbell,[9] James LaFrankie,[10] Sarayudh Bunyavejchewin,[11] H. S. Dattaraja,[12] Stuart Davies,[4] Shameema Esufali,[13] Robin Foster,[14] Nimal Gunatilleke,[13] Savitri Gunatilleke,[13] Pamela Hall,[15] Akira Itoh,[16] Robert John,[17] Somboon Kiratiprayoon,[18] Suzanne Loo de Lao,[3] Marie Massa,[8] Cheryl Nath,[12] Md. Nur Supardi Noor,[19] Abdul Rahman Kassim,[19] Raman Sukumar,[12] Hebbalalu Satyanarayana Suresh,[12] I-Fang Sun,[20] Sylvester Tan,[21] Takuo Yamakura,[16] Jess Zimmerman[5]

An ecological community's species diversity tends to erode through time as a result of stochastic extinction, competitive exclusion, and unstable host-enemy dynamics. This erosion of diversity can be prevented over the short term if recruits are highly diverse as a result of preferential recruitment of rare species or, alternatively, if rare species survive preferentially, which increases diversity as the ages of the individuals increase. Here, we present census data from seven New and Old World tropical forest dynamics plots that all show the latter pattern. Within local areas, the trees that survived were as a group more diverse than those that were recruited or those that died. The larger (and therefore on average older) survivors were more diverse within local areas than the smaller survivors. When species were rare in a local area, they had a higher survival rate than when they were common, resulting in enrichment for rare species and increasing diversity with age and size class in these complex ecosystems.

Most of the mechanisms that have been proposed for the maintenance of species diversity in ecosystems do not assume that locally rare species will survive preferentially. These mechanisms include the intermediate disturbance hypothesis and classic niche differentiation (*1*); lottery competition for space, coupled with storage effects, which can take place in a variable environment or when recruitment is limited (*2*); the source-sink hypothesis (*3*); and the neutral theory of biodiversity (*4*). The last of these assumes that within a trophic level of an ecosystem—such as the trees of a tropical forest—ecological drift governs local community dynamics.

Three important models invoke frequency-dependent mechanisms that lead to higher survival of locally rare species. The first of these is the Janzen-Connell hypothesis (*5*, *6*), in which diversity is maintained by frequency- or density-dependent interactions between hosts and specialized pathogens, herbivores, or predators. The Janzen-Connell model predicts that diversity should increase as a group of individuals ages, because more common species are selectively removed by pathogens and predators. The mix of surviving species will also depend on the past history of local host-pathogen or plant-resource interactions, so that it is likely to vary over both time and space. There is experimental evidence for the Janzen-Connell model (*7*–*11*).

The second of these models, the niche complementarity hypothesis (*12*, *13*), posits that species differ in the sub-environments or resources they exploit, and as a result, individuals compete more intensively with conspecifics than with individuals of other species. Because locally rare species are subject to relatively less conspecific competition than more common species, they are at a relative advantage (*14*). In this model, an increase in diversity can be traced to variations in the physical characteristics of the environment rather than the effects of pathogens and predators. In the third model, facilitation (*15*), diversity may increase if an individual facilitates (benefits) nearby nonconspecifics. Similar to the niche complementarity hypothesis, facilitation has the effect of making interspecific interactions more positive than intraspecific interactions and thus provides an advantage to locally rare species.

Possible frequency-dependent effects have recently been proposed for six forest sites (*16*), but these postulated effects are based on extrapolations from theory rather than actual birth and death rates. Frequency-dependent recruitment and mortality have been observed

in common species of forests in Barro Colorado Island (BCI), Panama and in Pasoh, peninsular Malaysia (*17*–*19*), but such observations are unable to distinguish the Janzen-Connell model from the two other models that depend on local frequency-dependent effects. The relative importance of each of these three frequency-dependent models in the maintenance of diversity can only be determined by detailed studies of ecosystems exhibiting a range of diversities (*20*). In all three of these mechanisms, species diversity can increase in a way analogous to the frequency-dependent advantage of rare alleles that can increase the number of alleles and the average heterozygosity at a genetic locus (*21*). If these processes act throughout the lifetimes of the organisms, they will lead to an increase in diversity with age class.

All three of these mechanisms should act locally rather than globally. If infections by pathogens are responsible for the differential survival of locally rare and common species, such infections are likely to be local in extent. Similarly, niche complementarity and facilitation would be expected to have their strongest effects among near-neighbor trees. A complex ecosystem can be thought of as a mosaic in which local diversity is increasing everywhere, regardless of the local mix of species that is present.

We investigated whether local diversity patterns in tropical forests were consistent with the presence of local frequency dependence by carrying out a quadrat-based analysis of seven tropical forest dynamics plots (FDPs). The FDPs, located in the New and Old World tropics, range in size from 16 to 52 ha. They have a wide range of species richnesses and tree densities and have all been censused more than once (Fig. 1). Each is managed by a host-country institution belonging to a research network that is coordinated by the Center for Tropical Forest Science based at the Smithsonian Tropical Research Institute.

For each FDP census, the locations of all trees with diameters $\geq$ 1 cm at 1.3 m above the ground (DBH) were determined, and the trees were identified to the species level. Trees that were recorded as recruits in the second census but not the first were therefore not new seedlings but trees that had reached 1 cm DBH during the census interval. We divided the FDPs into quadrats with dimensions 10, 20, 30, 40, or 50 m. Censuses used in the present analysis were separated by 10 years in two FDPs (BCI and Pasoh) and by 5 years in the other FDPs. The intermediate BCI census was examined, and the two successive 5-year intervals yielded the same pattern as the 10-year interval but with lower significance levels.

To quantify diversity, we used the rarefaction index, which estimates the average number of species to be expected in samples of a fixed number of individuals taken from a quadrat. Other commonly used diversity measures are correlated with tree density, which varies widely among quadrats in all the FDPs and confounds the analysis. In the present study, rarefaction is not correlated with densities of trees in the quadrats (*22*).

We examined the diversities of four demographic categories of tree within each quadrat. The first two of these categories consisted of the trees that died and the trees that were recruited during the census period. The third and fourth categories consisted of the younger and older surviving trees (those observed at both censuses), respectively. Although it was not possible to partition the survivors directly into age classes, we noted that within each species small survivors were likely to be younger than large survivors. We therefore grouped into the small-survivor category the members of the survivors of each species in a quadrat that fell within the smallest quartile of DBH values for the survivors of that species at the first census. The large-survivor category was made up of the remaining three quarters of the survivors of each species in the quadrat. Only trees that increased in size or stayed the same size during the census period, usually more than 90% of the surviving stems (table S1), were included in the analysis. By partitioning the tree size data within species, we avoided the problem that some species are shorter-lived than others. Differences in life span alone would result in diversity differences between small and large individuals if a cutoff were applied equally across all species. Division of the survivors into size classes within species avoided this possible source of bias and provided a comparison uninfluenced by species life history differences.

The within-quadrat differences in diversity of trees in each of the four demographic categories are shown in Fig. 2. In almost all cases, the diversities of the trees that died, the recruits, and the small survivors were significantly lower than the diversities of the large survivors. In most of the cases in which the differences were not significant, the number of degrees of freedom was low. These patterns were seen at all five quadrat sizes, but in general the most pronounced and most highly significant differences were seen at small quadrat sizes. This observation is in agreement with the prediction of the Janzen-Connell,

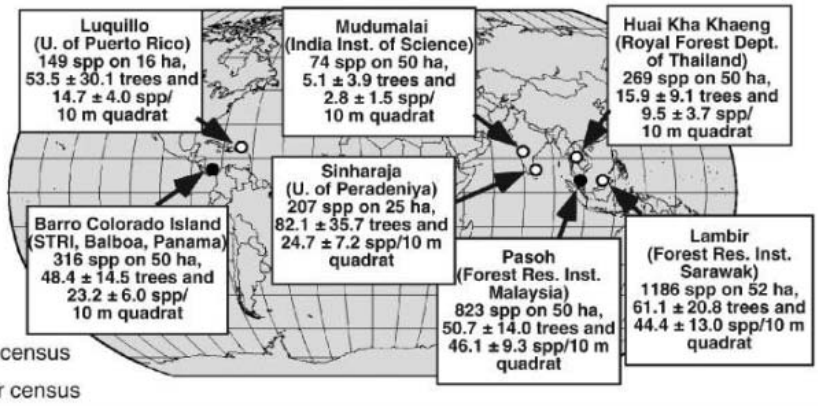

Fig. 1. Locations and species diversities of the seven FDPs included in this analysis. Shown in parentheses are the host-country institutions that manage the plots for the Smithsonian Tropical Research Institute. Means ± SD are shown for number of trees and number of species (spp) per 10-m quadrat.

[1]Division of Biological Sciences, University of California, San Diego, La Jolla, CA 92093–0116, USA. [2]Department of Biological Sciences, Louisiana State University, Baton Rouge, LA 70803, USA. [3]Smithsonian Tropical Research Institute, Unit 0948, APO AA 34002-0948, Panama. [4]Center for Tropical Forest Science, Arnold Arboretum Asia Program, Harvard University, Herbaria, 22 Divinity Avenue, Cambridge, MA 02138, USA. [5]Institute for Tropical Ecosystem Studies, University of Puerto Rico, Post Office Box 21910, San Juan, PR 00931–1910, USA. [6]Department of Renewable Resources, University of Alberta, Edmonton AB, T6G 2H1, Canada. [7]Department of Ecology, Evolution, and Behavior, University of Minnesota, St. Paul, MN 55108, USA. [8]Center for Tropical Forest Science, Smithsonian Tropical Research Institute, 1100 Jefferson Drive, Suite 3123, Washington, DC 20560–0705, USA. [9]Department of Plant Sciences, University of Georgia, 2502 Miller Plant Sciences Building, Athens, GA 30602, USA. [10]Center for Tropical Forest Science, Arnold Arboretum Asia Program, National Institute of Education, Nanyang Technological University, 1 Nanyang Walk, 637616, Singapore. [11]Thai National Park Wildlife and Plant Conservation Department, Silviculture Research, 61 Phaholyothin Road, Chatuchak Bangkok 10900, Thailand. [12]Center for Ecological Sciences, Indian Institute of Science, Bangalore 560012, India. [13]Department of Botany, Faculty of Science, University of Peradeniya, Peradeniya 20400, Sri Lanka. [14]Botany Department, The Field Museum, Roosevelt Road at Lake Shore Drive, Chicago, IL 60605–2496, USA. [15]Department of Biology, Florida State University, 5051 Quail Valley Road, Tallahassee, FL 32309, USA. [16]Plant Ecology Lab, Faculty of Science, Osaka City University, Sugimoto 3-3-138, Sumiyoshi-ku, Osaka 558, Japan. [17]Department of Plant Biology, University of Illinois, 505 South Goodwin Avenue, 265 Morrill Hall, Urbana, IL 61801, USA. [18]Faculty of Science and Technology, Thammasat University (Rangsit), Klongluang, Patumtani, 12121, Thailand. [19]Forest Environment Division, Forest Research Institute Malaysia, Kepong, Kuala Lumpur 52109, Malaysia. [20]Center for Tropical Ecology and Biodiversity, Tunghai University, 407 Taipei, Taiwan. [21]Forest Research Center, Sarawak Forest Department, Km10 Jalun Datak Amar Kalong Ningkan, 93250 Kuching, Sarawak, Malaysia.

*To whom correspondence should be addressed. E-mail: cwills@ucsd.edu

niche-complementarity, and facilitation models that locally rare species should be at an advantage. The size of the effects diminishes at larger quadrat sizes because species that are common in some small quadrats are rare in others; when larger quadrats were examined, the diverse small quadrats were pooled together.

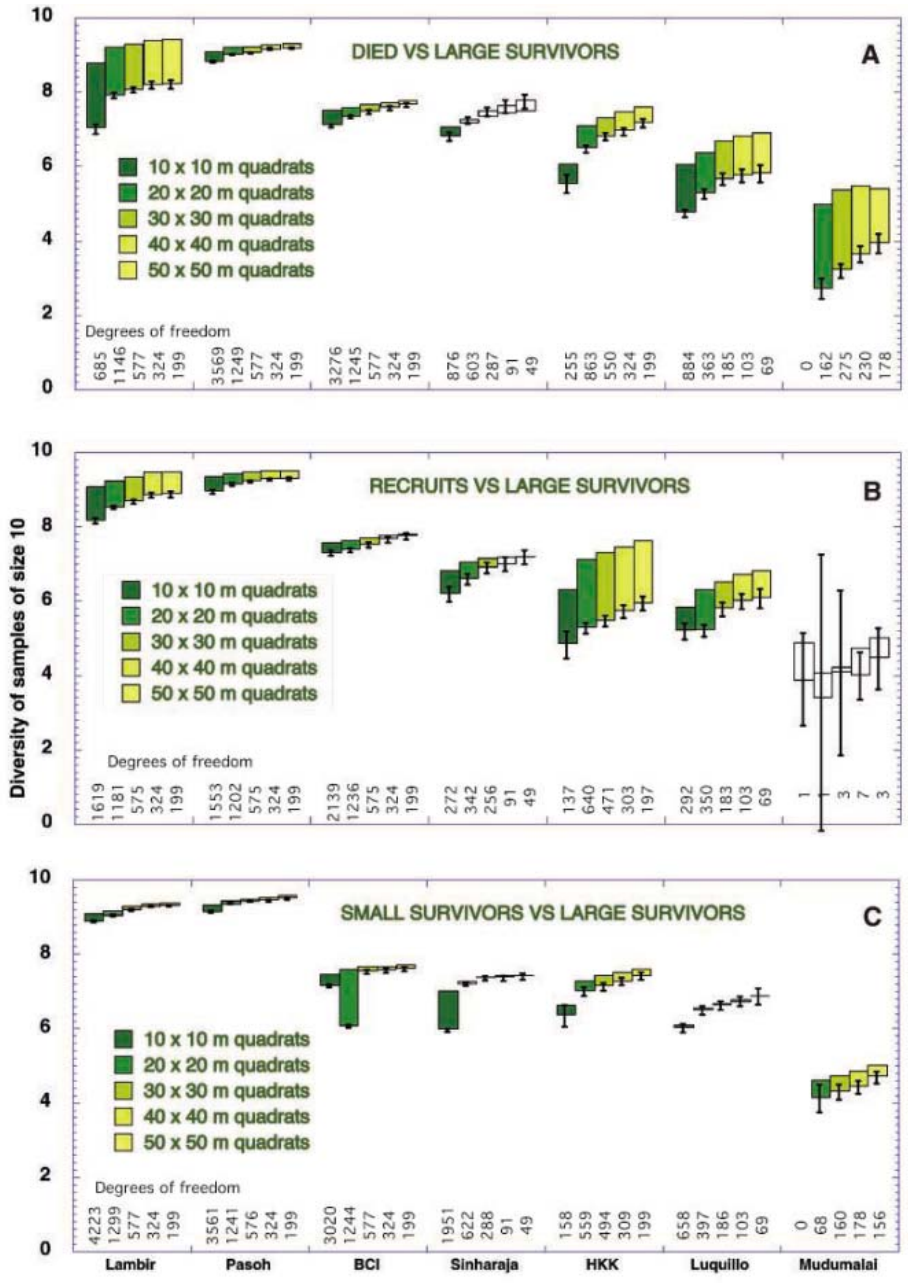

Fig. 2. Comparisons of diversities between different categories of tree, measured as rarefaction samples of size 10. The FDPs were divided into quadrats of dimensions 10, 20, 30, 40, or 50 m, and comparisons were made for all quadrats in which there were at least 10 trees in each category. The differences between the mean diversities are shown as colored bars. The top of each bar indicates the mean diversity of the large survivors, and the bottom of that bar indicates the mean diversity of the category of trees that is being compared to the large survivors. Nonsignificant differences are shown as white bars. Error bars are the 95% confidence intervals for pairwise *t* tests, and the degrees of freedom are given below each bar. Similar results were obtained for rarefaction values of 2 and 5. The diversities vary among FDPs because of differences in species richness. (**A**) Comparisons between the diversities of trees that died during the census period and those of large survivors. (**B**) Comparisons between the diversities of trees that were recruited during the census period and those of large survivors. (**C**) Comparisons between the diversities of small survivors (the smallest quartile of each species) and large survivors (the largest three quarters of each species).

The smallest differences were seen between small survivors and large survivors. Thus, diversity tended to increase from the recruits through the smaller survivors to the larger survivors. The trees that died also had low diversity, as expected if commoner species were disproportionately subject to mortality.

As a further check that these diversity estimates were not biased by the densities of trees in the quadrats, we examined size-equivalent subsamples of the quadrat data (Fig. 3). These subsamples consisted of pairs of quadrats chosen such that the numbers of survivors in one quadrat were matched with a different quadrat from the same FDP that had the same number of trees that died or were recruited during the census period. The differences in diversity between the equal-sized demographic categories in these pairs of quadrats were, with a few exceptions, statistically significant when compared by unpaired *t* tests. The magnitudes of the differences were similar to those found with the use of the entire data set. Only 10- and 20-m quadrats could be used in this analysis, because larger quadrats had large numbers of survivors, making it impossible to find pairs of quadrats with the same number of trees in different categories.

We then examined whether species that are locally common have higher mortality than those that are locally rare and whether this effect diminishes at larger quadrat sizes. We also examined whether species that are locally common recruit at a higher rate than those that are locally rare, so that in the absence of other factors recruitment should diminish diversity over time. We carried out these analyses for all FDPs and all quadrat sizes.

We obtained the frequencies of each of the species in all of the quadrats, and then correlated this set of frequencies against a matched set of differences in mortality or recruitment rates. Each of these differences consisted of the difference between the observed mortality or recruitment rate of the species in the quadrat and the mortality or recruitment rate of that species in the FDP as a whole. If a species had lower-than-average mortality or recruitment when it was locally rare, then the difference between the two rates would be negative. If it had higher-than-average mortality or recruitment when it was locally common, then this difference would be positive. The result would be a positive correlation between these differences and the local frequencies of each species in each quadrat.

Figure 4 shows a typical analysis presented in graphical form. Table 1 lists the correlation coefficients and degrees of freedom of all these analyses. In each case, the correlation was positive and highly significant, but the strength of the correlation diminished as quadrat size increased. Species that were locally common had higher mortality than would be predicted from their overall mortality rates and higher recruitment than would be predicted from their

Table 1. Within-quadrat frequency for each species, correlated with the excess or deficiency of within-quadrat mortality or recruitment for that species when compared with recruitment or mortality for the species in the entire FDP (see Fig. 4 for an example of this analysis in graphical form). df, degrees of freedom.

FDP	10-m quadrats		20-m quadrats		30-m quadrats		40-m quadrats		50-m quadrats	
	r	df	*r*	df	*r*	df	*r*	df	*r*	df
Mortality										
Lambir	+0.545	231,127	+0.319	162,337	+0.257	123,548	+0.201	95,043	+0.157	74,863
Pasoh	+0.750	230,993	+0.485	155,412	+0.415	112,558	+0.331	83,765	+0.261	63,849
BCI	+0.488	115,815	+0.204	67,012	+0.182	45,088	+0.132	32,310	+0.098	23,741
Sinharaja	+0.446	61,786	+0.221	31,642	+0.199	20,408	+0.110	8,053	+0.070	5,277
HKK	+0.562	47,611	+0.295	30,098	+0.264	21,201	+0.212	15,724	+0.162	12,093
Luquillo	+0.302	23,616	+0.127	11,924	+0.112	7,582	+0.088	5,152	+0.068	3,874
Mudumalai	+0.509	14,389	+0.296	8,454	+0.221	5,674	+0.161	4,098	+0.124	3,092
Recruitment										
Lambir	+0.638	238,007	+0.406	165,849	+0.216	125,552	+0.135	96,172	+0.090	75,558
Pasoh	+0.764	216,478	+0.549	148,567	+0.478	108,588	+0.389	81,589	+0.304	62,441
BCI	+0.577	111,902	+0.290	64,535	+0.250	43,429	+0.194	31,029	+0.151	22,877
Sinharaja	+0.541	59,223	+0.332	30,632	+0.280	19,875	+0.136	7,837	+0.181	5,141
HKK	+0.491	43,407	+0.294	27,846	+0.247	19,800	+0.203	14,820	+0.173	11,379
Luquillo	+0.517	22,147	+0.251	11,325	+0.232	7,157	+0.168	4,886	+0.140	3,682
Mudumalai	+0.767	11,693	+0.676	7,253	+0.702	4,983	+0.652	3,683	+0.569	2,806

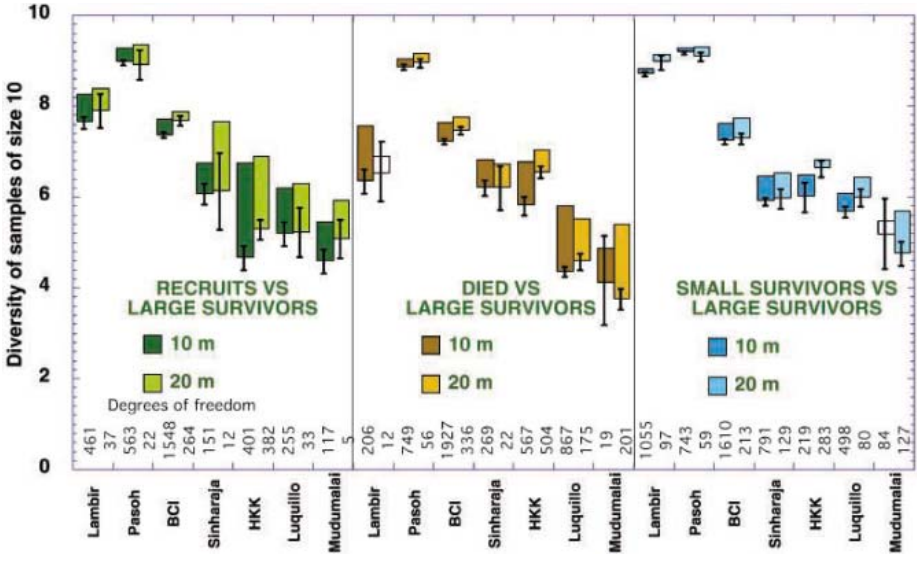

Fig. 3. A test for whether numbers of trees in each quadrat influenced the diversity estimates. Here, the comparisons have been made between matched pairs of quadrats that had the same number of trees in each of the two categories being compared. In these comparisons the *t* tests used to obtain the 95% confidence intervals were unpaired because the comparisons were made between different quadrats.

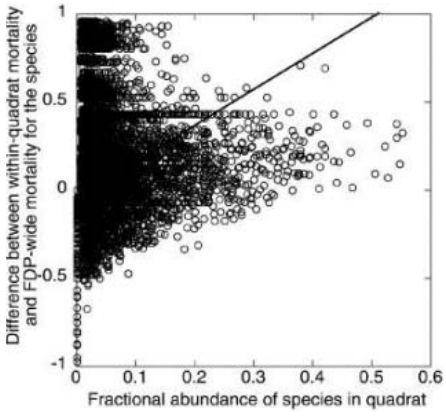

Fig. 4. Plot of Luquillo 10-m quadrat mortality data, in which the frequency of each species in a quadrat (abscissa) is plotted against the difference between the mortality rate of the species in that quadrat and the mortality rate of the species in the FDP as a whole (ordinate). Solid line, linear regression fit to the data. Summaries of analyses of this type for all FDPs at five quadrat sizes are shown in Table 1.

overall recruitment rates. When species were locally rare, this pattern was reversed. The correlations diminished with increasing quadrat size, showing that these nonrandom effects were primarily acting at the local level.

We next asked whether changes in diversity in the FDPs were evenly distributed or concentrated in certain areas. An overall increase in diversity with age throughout the FDPs would be predicted if increases in diversity were being driven by local factors that operated everywhere in the FDPs. Figures S1 and S2 show filled contour plots of the differences in diversity between demographic categories in the Luquillo and BCI FDPs, with the use of the data from the 10-by-10-m quadrats. The overall trend was for diversity to increase relatively uniformly throughout the FDPs.

In a previous detailed survey of the BCI FDP, the diversity of seedlings was found to be greater than the diversity of the seeds from which they came (*23*). Our findings extend the BCI seed-to-seedling results to include cohorts of trees at later stages of maturity and show that the same increase in diversity has taken place in six other FDPs from around the world. The increase in diversity from trees that died and recruits to survivors may be due in part to differences in life history between rare and common species, but the diversity differences between relatively larger and relatively smaller survivors can be due only to local frequency-dependent processes.

Further censuses planned for these and other FDPs should let us follow in detail increases in diversity over a span of decades, to determine whether these gains are sufficient to maintain diversity in the FDPs. We will also be able to measure more precisely why the changes in diversity vary in their magnitude from plot to plot (Fig. 2).

Is the low diversity of recruits in the FDPs the result of recent worldwide environmental

changes, possibly generated by human activity? Recent changes in weather patterns and a wide variety of anthropogenic effects (*24*, *25*), along with losses of pollinators and herbivores from all tropical ecosystems (*26*), may have contributed to a reduced diversity of recruits in all these FDPs. Such effects cannot be ruled out, but the increase in diversity observed from seeds to seedlings at BCI (*23*) and the low diversity of trees that died during the census interval at all the FDPs in the current study indicate that the changes in diversity reported here have largely been the result of ongoing natural processes. It remains to be discovered, however, what fraction of these increases in local diversity can be attributed to Janzen-Connell effects, to the ability of rare tree species to take advantage of a complex local environment, and to positive interactions among rare tree species themselves. Thorough testing of these possibilities may require experimental manipulation of small areas within mature tropical forests through the deliberate introduction of large numbers of seeds or seedlings of a variety of common or rare species followed by a detailed examination of the fate of these introductions over time.

The nonrandom maintenance of diversity has two consequences, one short term and one longer term. In the short term, ecosystems that have lost diversity after temporary damage may be able to recover their former diversity levels rapidly, provided that any extinctions that have taken place in the affected ecosystems are local and diversity can be restored through immigration. Such a rapid recovery in diversity would not be possible if individuals of different species replaced each other at random (*4*). In the longer term, natural selection will tend to increase morphological and biochemical differences among host species (*27*, *28*). In the case of Janzen-Connell effects, these differences will be selected because they result in pathogen range restriction. This restriction will in turn increase the effectiveness of frequency-dependent selection for host species that are rare, because their pathogens will also be rare (*29*). In the case of niche complementarity and facilitation, differences between tree species will increase over time because these differences will aid the efficient utilization of different physical environments or will increase the benefit of interspecific interactions. Thus, the evolutionary result of frequency-dependent mechanisms for the maintenance of ecosystem diversity will be the generation of further diversity among the species of each trophic level.

References and Notes

1. J. H. Connell, *Science* **199**, 1302 (1978).
2. G. C. Hurtt, S. W. Pacala, *J. Theor. Biol.* **176**, 1 (1995).
3. H. R. Pulliam, *Am. Nat.* **132**, 652 (1988).
4. S. P. Hubbell, *The Unified Neutral Theory of Biodiversity and Biogeography* (Princeton Univ. Press, Princeton, NJ, 2001).
5. D. H. Janzen, *Am. Nat.* **104**, 501 (1970).
6. J. H. Connell, in *Dynamics of Populations*, P. J. Den Boer, G. Gradwell, Eds. (PUDOC, New York, 1971), pp. 298–312.
7. C. K. Augspurger, *J. Ecol.* **71**, 759 (1983).
8. K. E. Mills, J. D. Bever, *Ecology* **79**, 1595 (1998).
9. A. Packer, K. Clay, *Nature* **404**, 278 (2000).
10. M. R. Silman, J. W. Terborgh, R. A. Kiltie, *Ecology* **84**, 431 (2003).
11. L. A. Hood, M. D. Swaine, P. A. Mason, *J. Ecol.* **92**, 816 (2004).
12. T. E. Shelly, *Oecologia* **67**, 57 (1985).
13. A. Hector *et al.*, *Science* **286**, 1123 (1999).
14. P. Chesson, *Theor. Pop. Biol.* **58**, 211 (2000).
15. J. F. Bruno, J. J. Stachowicz, M. D. Bertness, *Trends Ecol. Evol.* **18**, 119 (2003).
16. I. Volkov, J. R. Banavar, F. He, S. P. Hubbell, A. Maritan, *Nature* **438**, 658 (2005).
17. C. Wills, R. Condit, R. Foster, S. P. Hubbell, *Proc. Natl. Acad. Sci. U.S.A.* **94**, 1252 (1997).
18. C. Wills, R. Condit, *Proc. R. Soc. London Ser. B* **266**, 1445 (1999).
19. H. A. Peters, *Ecol. Lett.* **6**, 757 (2003).
20. D. Tilman *et al.*, *Science* **294**, 843 (2001).
21. C. Wills, D. R. Green, *Immunol. Rev.* **143**, 263 (1995).
22. Materials and methods are available as supporting material on *Science* Online.
23. K. E. Harms, S. J. Wright, O. Calderon, A. Hernandez, E. A. Herre, *Nature* **404**, 493 (2000).
24. W. F. Laurance *et al.*, *Conserv. Biol.* **16**, 605 (2002).
25. S. J. Wright, *Trends Ecol. Evol.* **20**, 553 (2005).
26. I. R. Noble, R. Dirzo, *Science* **277**, 522 (1997).
27. P. Feeny, in *Coevolution Between Plants and Animals*, L. E. Gilbert, P. H. Raven, Eds. (Univ. of Texas Press, Austin, TX, 1975), pp. 3–19.
28. D. F. Rhoades, R. G. Cates, *Recent Adv. Phytochem.* **10**, 168 (1976).
29. C. Wills, *New Scientist* **149**, 38 (1996).

30. This work was carried out during the Center for Tropical Forest Science (CTFS) Analytical Workshop Series. Supported by NSF grant no. 0090311 of the Research Coordination Network Program and the CTFS Research Grant Program. Data collections were funded, in part, by the Smithsonian Tropical Research Institute, Centre for Ecological Sciences of the Indian Institute of Science, Forest Research Institute Malaysia, Royal Forest Department (Thailand), Sarawak Forest Department (Malaysia), University of Puerto Rico (USA), International Institute for Tropical Forestry (Puerto Rico), NSF grants to the Luquillo Long Term Ecological Research site, Arnold Arboretum of Harvard University, National Institute of Environmental Studies (Japan), and other grants from the NSF, The John D. and Catherine T. MacArthur Foundation, the Andrew W. Mellon Foundation, the U.S. Agency for International Development, the Agora Foundation, and the Frank H. Levinson Donor-Advised Fund at the Peninsula Community Foundation. The authors are grateful to J. Kohn, D. Holway, W. Jetz and three anonymous reviewers for helpful comments.

Supporting Online Material

www.sciencemag.org/cgi/content/full/311/5760/527/DC1
Materials and Methods
Figs. S1 and S2
Tables S1 and S2
References

20 July 2005; accepted 21 December 2005
10.1126/science.1117715

An Architectural Framework That May Lie at the Core of the Postsynaptic Density

Marisa K. Baron,[1] Tobias M. Boeckers,[2] Bianca Vaida,[2] Salem Faham,[1] Mari Gingery,[1] Michael R. Sawaya,[1] Danielle Salyer,[1] Eckart D. Gundelfinger,[3] James U. Bowie[1]*

The postsynaptic density (PSD) is a complex assembly of proteins associated with the postsynaptic membrane that organizes neurotransmitter receptors, signaling pathways, and regulatory elements within a cytoskeletal matrix. Here we show that the sterile alpha motif domain of rat Shank3/ProSAP2, a master scaffolding protein located deep within the PSD, can form large sheets composed of helical fibers stacked side by side. Zn^{2+}, which is found in high concentrations in the PSD, binds tightly to Shank3 and may regulate assembly. Sheets of the Shank protein could form a platform for the construction of the PSD complex.

Signaling pathways in eukaryotic cells are often physically linked in large protein complexes (*1*). A particularly dramatic example is the PSD, a disk-shaped protein assembly on the postsynaptic side of neuronal synapses, which is roughly 40 to 50 nm thick, up to 500 nm wide, and contains more than 100 different proteins (*2*–*5*). The PSD likely aids the appropriate communication of incoming signals to cytoplasmic targets and contributes to neuronal plasticity by readily changing its composition and structure in response to neural activity (*6*–*9*).

A number of scaffolding proteins link components of the PSD (*10*). The Shank family of proteins (also known as ProSAP, SSTRIP, CortBP, Synamon, or Spank) are considered master scaffolding proteins in the PSD, because they bind to a number of other scaffolding proteins including guanylate kinase–associated protein/SAP90/PSD-95–associated proteins (GKAP/SAPAPs),

[1]Department of Chemistry and Biochemistry, Molecular Biology Institute and University of California at Los Angeles–U.S. Department of Energy Institute for Genomics and Proteomics, University of California, Los Angeles, 611 Charles E. Young Drive East, Los Angeles, CA 90095-1570, USA. [2]Institute of Anatomy and Cell Biology, University of Ulm, Ulm, Germany. [3]Leibniz Institute for Neurobiology, Post Office Box 1860, D-39008 Magdeburg, Germany.

*To whom correspondence should be addressed. E-mail: bowie@mbi.ucla.edu

α-fodrin, Homer, Cortactin, and Abp-1 (*11*–*14*). Shank proteins are located deep within the PSD, wedged between scaffolding proteins that are bound to either neurotransmitter receptors or the actin cytoskeleton (*15*, *16*). They are therefore well positioned to nucleate the underlying structure of the PSD. Moreover, Shank3 expression increases the number and size of synaptic contacts in induced dendritic spines, which suggests that it plays a fundamental role in organizing the PSD (*17*). Among the conserved domains of Shank, a likely candidate for generating a higher order structure is the sterile alpha motif (SAM) domain, which in some cases is known to form a polymer through self-association (*18*–*21*). The SAM domain of Shank is also known to self-associate (*22*) and is required for the localization of Shank2 and Shank3 to the PSD (*23*).

Examination of purified rat Shank3 SAM domains by electron microscopy (EM) revealed large sheets of parallel fibers (Fig. 1A). Each fiber is approximately 70 Å in diameter and has a striated surface suggesting a helical structure, similar to other SAM polymers. In contrast to other SAM polymers, however, over 25 fibers could be seen to stack tightly side by side in a highly ordered array (Fig. 1B).

To learn in more detail how this sheet was constructed, we sought a high-resolution structure but were stymied by the poor solubility and heterogeneous assembly of Shank-SAM. To improve solubility, we changed 10 potential surface hydrophobic residues to Glu one at a time. Four of the mutants [W5E (where Trp^5 is replaced by Glu), S6E, V52E, and M56E] (*24*) increased solubility, and we were able to crystallize and solve the structure of M56E at 2.1 Å (*25*). Shank-SAM forms polymeric fibers in the crystal structure, which was previously seen with other SAM domains (Fig. 1C). The individual fibers form a left-handed helix with six subunits per turn, a pitch of ~40 Å, and a width of ~70 Å, consistent with the EM images. The M56E mutation is in the intrapolymer interface, where it can disrupt polymerization and solubilize the protein, but sufficient binding affinity remains to drive recreation of this interface in the crystal.

The fibers in the crystal structure also stack side by side in a manner that closely resembles the EM images (compare Fig. 1, B and C). Although SAM domains are known to form helical polymers very much like the individual fibers of Shank-SAM, side-by-side packing of these fibers into a sheet has not been observed before. Polymeric fibers often associate, but the formation of a flat sheet like we see for Shank-SAM is an improbable organization, suggesting that the sheet structure is a design feature of the protein. Moreover, two of the mutations (W5E and S6E) that effectively solubilize the protein are found only in the interfiber interface, suggesting that inter- and intrafiber assembly occur in concert.

To further test the requirement for cooperative assembly, we generated a series of 18 mutations that we predicted, based on the structure, might destabilize either intra- or interfiber interfaces, and we analyzed their aggregation behavior by gel filtration chromatography (*25*). On the basis of their elution profiles, the mutants were classified as perfect monomers (M), partially monomeric (PM), or aggregates (A). Of the 18 mutants, we obtained 6 M mutants (W5E, S6E, F8E, L47E, V52E, and M56E), 4 PM mutants (L4A, H22A, L36E, and V45E), and 8 A mutants (L2E, E21A, R23A, I31E, L39A, D43R, H54A, and L65E) (*24*).

As shown in Fig. 2, A to C, the side chains of the 6 M mutants are involved in creating both the interfiber and intrafiber interaction surfaces. Three of the M mutants (L47E, V52E, and M56E) and one of the PM mutants (V45E) occur in the intrafiber interface (Fig. 2B), whereas the other three M mutants (W5E, S6E, and F8E) and one PM mutant (L4A) are in the interfiber interface (Fig. 2C). The remaining two PM mutants (H22A and L36E) are not directly in the interface. L36 is 100% buried, and the mutation is likely to distort the structure; whereas H22 is a ligand to the Zn^{2+} site, which provides additional stability to the sheet (discussed below). The ability of single-point mutations in either inter-

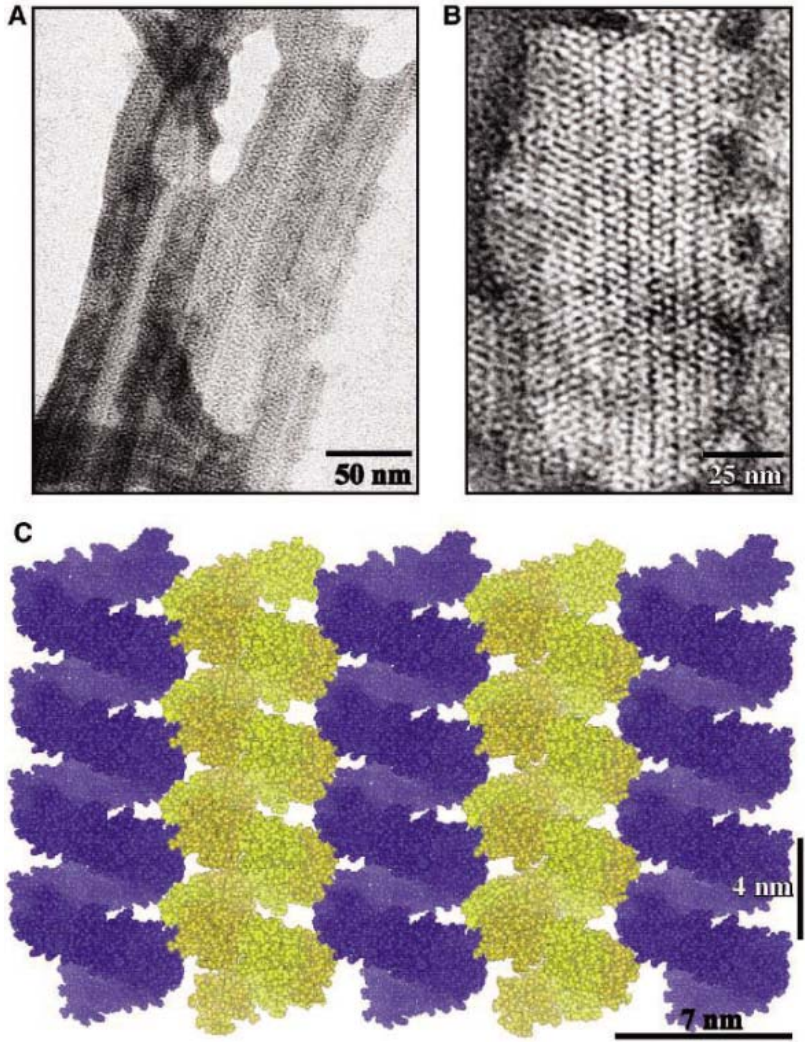

Fig. 1. The Shank3 SAM domain forms large sheets of helical fibers. (**A**) An EM image of Shank-SAM reveals over 25 fibers stacked side by side in a two-dimensional sheet. (**B**) At higher magnification, the well-ordered nature of the sheet can be seen as individual subunits that are arranged in a highly ordered array. (**C**) The packing of Shank-SAM into a sheet is also evident in the crystal structure of Shank-SAM M56E (a soluble mutant) solved to 2.1 Å. Yellow and blue depict fibers stacked in opposite orientations. Both the antiparallel and parallel orientations are seen in the crystal, but we believe the antiparallel orientation is physiologically relevant for several reasons. First, the interfiber interface buries more surface area in the antiparallel orientation (1264 $Å^2$ versus 852 $Å^2$). Second, the position of a mutation that solubilizes the protein (W5E) is in the interface between antiparallel fibers (Fig. 2C) but not parallel fibers. Finally, Zn^{2+}, which has a dramatic effect on sheet organization, stabilizes salt bridges between antiparallel fibers but not parallel fibers (Fig. 3C). In the numbering scheme used for the crystal structure, residue 1 corresponds to residue 174 in the full rat Shank3 sequence.

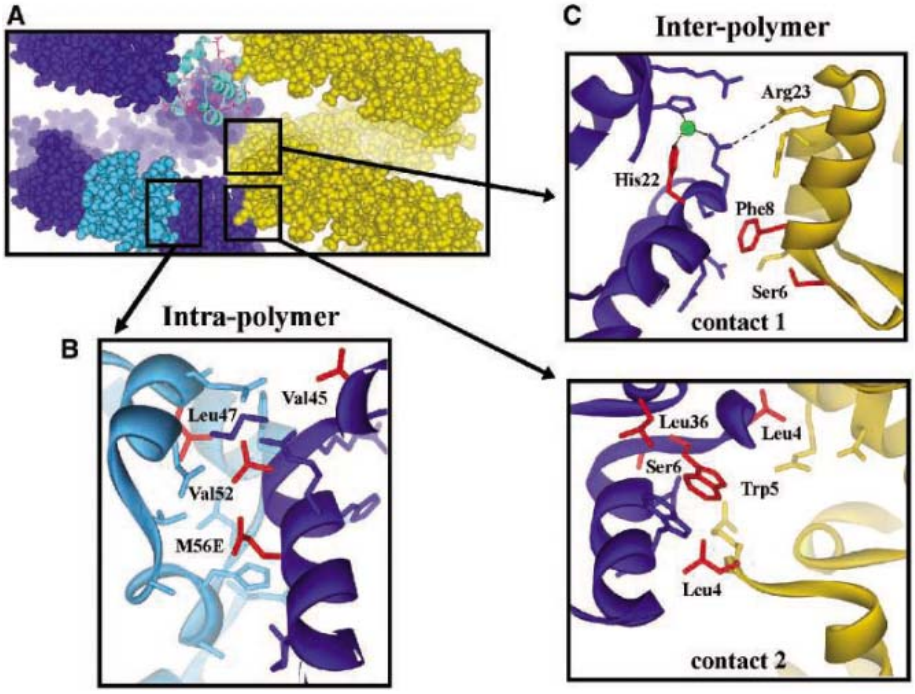

Fig. 2. Mutations of Shank-SAM that disrupt assembly are located in the inter- and intrapolymer interfaces of the sheet. (**A**) Designed mutants are spread out over the monomer (pink) and have the potential to disrupt two types of interfaces, intra- and interpolymer. (**B**) The intrapolymer interface is between SAM domains within a polymer. Three M mutants (V52E, M56E, and L47E) and one PM mutant (V45E) are located in this interface (shown in red). We solved the structure of the M56E mutant; therefore, a Glu side chain is found at position 56. (**C**) The interpolymer interface (for which there are two contact points) is between SAM domains of neighboring polymers. The remaining three M mutants (W5E, S6E, and F8E) and three PM mutants (L4A, H22A, and L36E) are found in or near one of these two contact sites (shown in red). Although peripheral, H22A may destabilize the interpolymer interface by weakening the salt bridge that strengthens this interface.

face to prevent the formation of the sheet strongly suggests that stable assembly requires favorable interactions both within and between the fibers.

Is the observed sheet assembly compatible with the full-length protein? The SAM domain is at the C terminus of a large, 1806-residue protein, raising a question of whether the helical SAM polymers could associate into a sheet with such a huge protein arrayed in a radial fashion on the outside. Examination of the crystal structure indicates that all the N termini can escape steric clash. To test experimentally whether the sheet structure could accommodate a large protein at the N terminus, we constructed a fusion protein, called MBP-Shank, composed of a maltose binding protein (MBP) linked to the C-terminal 353 amino acids of Shank (1454 to 1806) that includes the SAM domain. Thus, MBP-Shank adds approximately 670 residues to the SAM domain. When MBP-Shank was refolded and examined by EM, huge sheets were observed that contained over 100 long fibers stacked side by side (Fig. 3, A and B). These sheets exhibited local order, although the order broke down over long distances.

Zn^{2+} is found in the PSD and is apparently important for PSD assembly (*26*, *27*), so we were intrigued by the observation of a potential Zn^{2+} binding site in Shank-SAM. We noticed that in the Au^{2+} derivative used to solve the structure, Au^{2+} bound at a site that resembled the Zn^{2+} binding sites seen in zinc metalloproteases (*28*, *29*). We therefore tested the ability of Shank-SAM and two monomeric double mutants

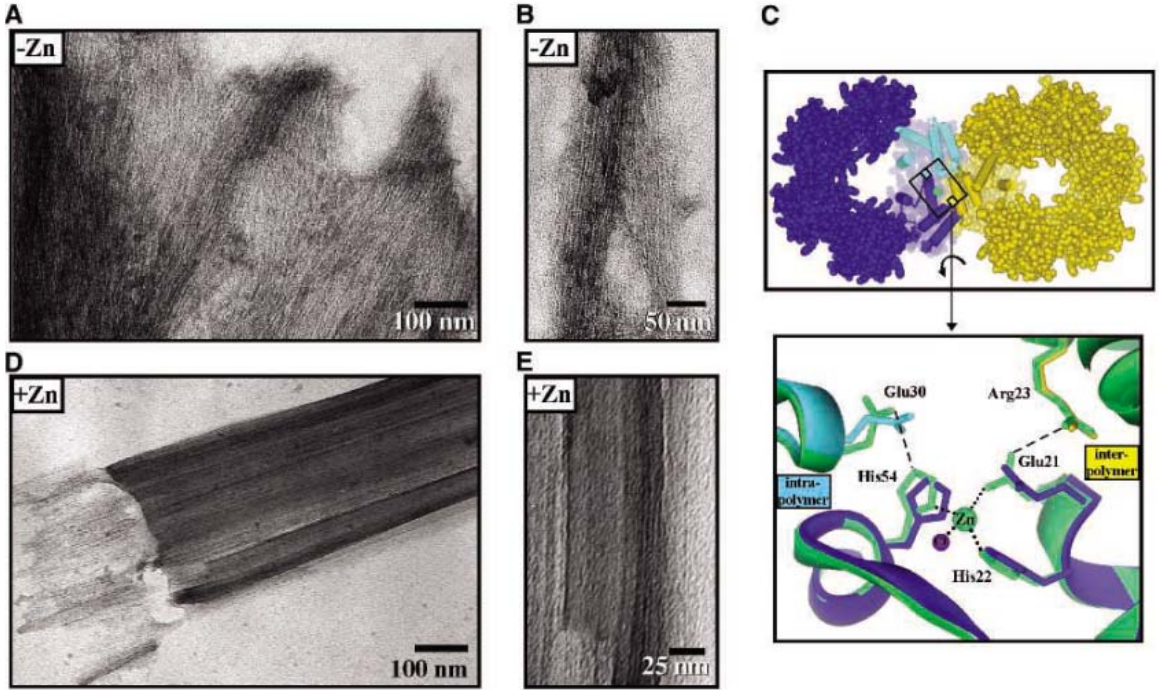

Fig. 3. The sheet structure can accommodate a large fusion protein at the N terminus, and the sheet becomes well ordered upon binding Zn^{2+}. (**A**) An EM image of MBP-Shank displayed a wide sheet consisting of hundreds of fibers. (**B**) The side-by-side packing of individual fibers can be seen, although order breaks down over long distances. (**C**) The crystal structure of Shank-SAM bound to Zn^{2+} shows that Zn^{2+} is coordinated in a tetrahedral geometry to Glu^{21}, His^{22}, His^{54}, and a chloride ion. The Zn^{2+} site is located where the intra- and interpolymer interfaces meet and appears to stabilize salt bridges across two interfaces: His^{54} with Glu^{30} and Glu^{21} with Arg^{23}, respectively. Only minor conformational changes are seen when the Zn^{2+} structure (green) is overlaid with the apo structure (yellow and blue). (**D**) The arrangement of MBP-Shank into a sheet becomes highly ordered in the presence of Zn^{2+}. (**E**) At high resolution, the helices appear more stiff, clearly defined, and woven together over longer distances than those in the absence of Zn^{2+}.

(W5E/S6E and V52E/M56E) to bind Zn^{2+} by using inductively coupled plasma (ICP) analysis (*30*, *31*). Even after overnight dialysis, we found 43, 53, and 54% Zn^{2+} occupancy for wild type, W5E/S6E, and V52E/M56E, respectively, indicating that Shank-SAM does have a high affinity Zn^{2+} binding site.

To visualize how Zn^{2+} binds to Shank-SAM, we re-solved the structure of Shank-SAM in the presence of Zn^{2+}. Zn^{2+} was indeed bound in the same pocket as was Au^{2+}, and is coordinated in a tetrahedral geometry by E21, H22, H54, and electron density that we attribute to a chloride ion (Fig. 3C) (*28*). Superposition of the apo and Zn^{2+} structures (Fig. 3C) indicates that only minor conformational changes occur upon binding Zn^{2+}. The Zn^{2+} pocket is located where the inter- and intrapolymer interfaces meet. Furthermore, the ligands that coordinate Zn^{2+} form salt bridges across these two interfaces: E21 with R23 (intrapolymer) and H54 with E30 (interpolymer). Thus, the binding of Zn^{2+} may stabilize these salt bridges, mitigating the entropy cost of assembly.

To investigate whether Zn^{2+} affects the formation of the SAM sheet, MBP-Shank was refolded in the presence of zinc acetate. Massive sheets were again seen, but they were remarkably better organized in the presence of Zn^{2+} (Fig. 3, D and E). The sheets are over 300 nm wide, containing more than 50 fibers packed together. In contrast to the sheets without Zn^{2+}, the interdigitation of pairs of helical fibers can be traced almost the entire length of the sheet (over 700 nm). The dramatically improved ordering of the sheet suggests that Zn^{2+} plays an important structural role in organizing Shank and further demonstrates that the sheet is compatible with a very large protein.

To determine whether sheet construction is required for the integration of Shank into the PSD, we tested the effect of assembly mutants on Shank localization in hippocampal neurons of rats. Shank-416-GFP is a construct, consisting of green fluorescent protein (GFP) fused to the C-terminal 416 residues of Shank, that localizes to synapses (*23*). Seven Shank-SAM mutants that disrupt sheet assembly (W5E, F8E, H22A, M56E, W5E/F8E, W5E/M56E, and L47E/M56E) (*24*) were introduced into Shank-416-GFP, expressed in hippocampal neurons, and examined for synaptic clustering. Synaptic localization was quantified by two parameters: (i) the synaptic clustering ratio (SCR), which is the ratio of GFP fluorescence in dendritic shafts versus spines, and (ii) the percentage of colocalization of clustered Shank3 with the presynaptic marker Bassoon (P/B) (*23*).

All seven assembly mutants disrupted localization (Table 1 and Fig. 4). The point mutants W5E and M56E (located in the inter- and intrapolymer interfaces, respectively), and all three double mutants completely prevented localization, suggesting that both interfaces of the sheet must be functional for Shank to be properly assembled in the PSD. Another interpolymer interface mutant, F8E, was found to partially disrupt localization. The elimination of the Zn^{2+} ligand in the H22A mutant also precluded localization, consistent with our in vitro findings of an important role for Zn^{2+} in sheet construction. Sheet-disrupting mutations also fail to localize to the synapse, which suggests that sheet formation is important for assembly of Shank3 in the PSD.

We propose that Shank3 (and possibly other Shanks) creates a platform for the construction of the massive complex of proteins at the PSD.

Table 1. Synaptic clustering ratios (SCR) and percentage colocalization with the presynaptic marker Bassoon (P/B) for Shank-416-GFP and variants. SCR < 0.5 indicates synaptic clustering and SCR ≥ 0.7 indicates no clustering. The wild-type Shank-416-GFP has an SCR of 0.35 and a P/B between 67 and 94%, which is essentially the same as for the full-length Shank3 (*23*). Only those variants that showed significant clustering to synapses were analyzed for colocalization with Bassoon. Five mutations in the interfaces of the sheet (W5E, M56E, and all three double mutants) and a mutant that replaces a Zn^{2+} ligand (H22A) dramatically reduce localization. The remaining mutation, F8E, which is also located in the sheet interface, partially inhibits localization. Errors are SD.

Protein	SCR	P/B
Wild-type	0.35 ± 0.09	67 to 94%
W5E	0.80 ± 0.10	-
F8E	0.56 ± 0.05	9 to 53%
H22A	0.70 ± 0.08	-
M56E	0.90 ± 0.01	-
W5E/F8E	0.77 ± 0.04	-
W5E/M56E	0.75 ± 0.05	-
L47E/M56E	0.75 ± 0.08	-

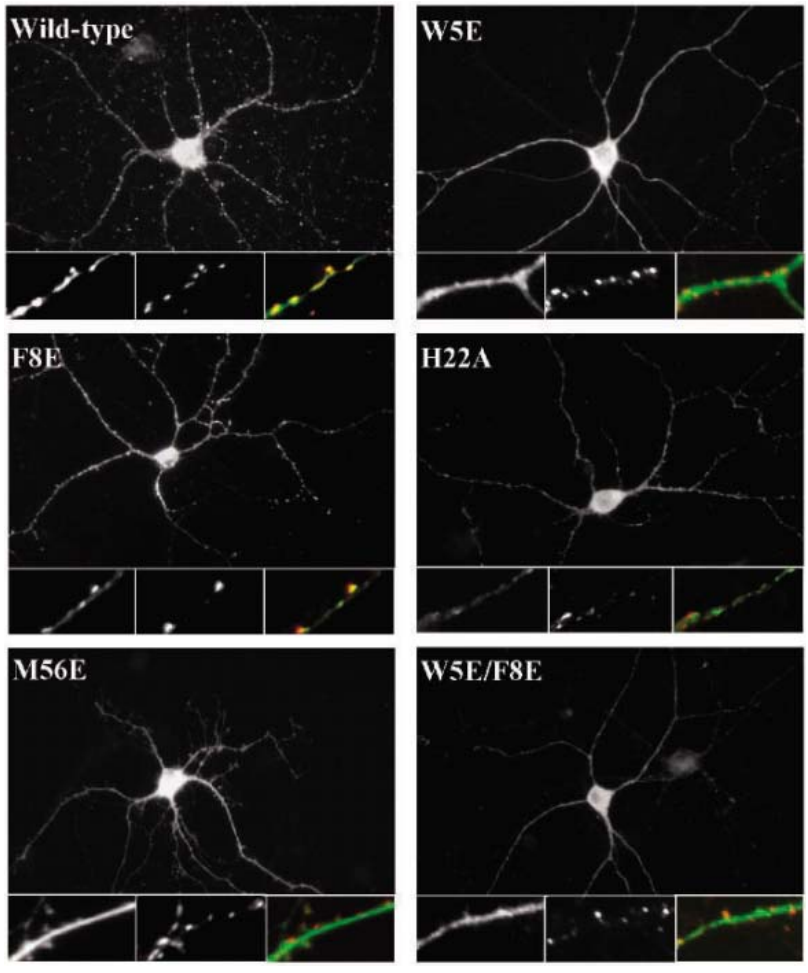

Fig. 4. Assembly mutants prevent the localization of Shank to the synapse. Visualization of Shank variant distributions in transfected hippocampal neurons is shown. The wild-type Shank-416-GFP construct (green) clusters in neuronal dendrites and colocalizes with Bassoon (red) in transfected hippocampal neurons (insets: left, GFP; middle, Bassoon; right, merge). In contrast, mutants (W5E, H22A, M56E, and all three double mutants) display a diffusely distributed green fluorescence, indicating no preferential localization to synaptic sites as indicated by Bassoon staining (insets). F8E shows partial clustering and partial colocalization with Bassoon (inset).

Recent cryogenic EM imaging of the PSD in intact synapses revealed a regular row of electron-dense material running parallel to the postsynaptic membrane at ~6-nm spacings, by our measurement (*32*). Although the nature of this array is not yet known, it could correspond to a view of a Shank organized sheet looking either down the ends of the fibers (~6-nm spacings due to fiber interdigitation). The proposed sheet structure, with radially projecting protein interaction domains, appears to be an ideal architecture for a protein that must contact both membrane and cytoplasmic components at a two-dimensional cell surface. The ability of Zn^{2+} to aid the organization of the Shank sheet raises the possibility that Zn^{2+} ions, which are released during neuronal activity (*33*–*35*), could directly modulate the PSD structure by regulating the assembly of Shank SAM domains.

References and Notes

1. H. J. Carlisle, M. B. Kennedy, *Trends Neurosci.* **28**, 182 (2005).
2. M. B. Kennedy, *Science* **290**, 750 (2000).
3. K. W. Li *et al.*, *J. Biol. Chem.* **279**, 987 (2004).
4. J. Peng *et al.*, *J. Biol. Chem.* **279**, 21003 (2004).
5. A. I. Matus, D. H. Taff-Jones, *Proc. R. Soc. London Ser. B* **203**, 135 (1978).
6. M. Sheng, M. J. Kim, *Science* **298**, 776 (2002).
7. A. Matus, *Science* **290**, 754 (2000).
8. P. M. Okamoto, C. Gamby, D. Wells, J. Fallon, R. B. Vallee, *J. Biol. Chem.* **276**, 48458 (2001).
9. T. Bresler *et al.*, *J. Neurosci.* **24**, 1507 (2004).
10. M. D. Ehlers, *Trends Neurosci.* **25**, 64 (2002).
11. E. Kim, M. Sheng, *Nat. Rev. Neurosci.* **5**, 771 (2004).
12. T. M. Boeckers, J. Bockmann, M. R. Kreutz, E. D. Gundelfinger, *J. Neurochem.* **81**, 903 (2002).
13. S. Lim *et al.*, *J. Biol. Chem.* **274**, 29510 (1999).
14. B. Qualmann *et al.*, *J. Neurosci.* **24**, 2481 (2004).
15. J. G. Valtschanoff, R. J. Weinberg, *J. Neurosci.* **21**, 1211 (2001).
16. F. G. Wouterlood, T. Bockers, M. P. Witter, *J. Neurosci. Methods* **128**, 129 (2003).
17. G. Roussignol *et al.*, *J. Neurosci.* **25**, 3560 (2005).
18. F. Qiao, J. U. Bowie, *Sci. STKE* **2005**, re7 (2005).
19. J. Behlke, D. Labudde, O. Ristau, *Eur. Biophys. J.* **30**, 411 (2001).
20. C. D. Thanos, K. E. Goodwill, J. U. Bowie, *Science* **283**, 833 (1999).
21. C. A. Kim *et al.*, *EMBO J.* **20**, 4173 (2001).
22. S. Naisbitt *et al.*, *Neuron* **23**, 569 (1999).
23. T. M. Boeckers *et al.*, *J. Neurochem.* **92**, 519 (2005).
24. Single-letter abbreviations for the amino acid residues are as follows: A, Ala; C, Cys; D, Asp; E, Glu; F, Phe; G, Gly; H, His; I, Ile; K, Lys; L, Leu; M, Met; N, Asn; P, Pro; Q, Gln; R, Arg; S, Ser; T, Thr; V, Val; W, Trp; and Y, Tyr.
25. Materials and methods are available as supporting material on *Science* Online.
26. H. H. Jan, I. T. Chen, Y. Y. Tsai, Y. C. Chang, *J. Neurochem.* **83**, 525 (2002).
27. C. J. Chang *et al.*, *Chem. Biol.* **11**, 203 (2004).
28. D. S. Auld, *Biometals* **14**, 271 (2001).
29. L. A. Finney, T. V. O'Halloran, *Science* **300**, 931 (2003).
30. F. Vanhaecke, M. Resano, L. Moens, *Anal. Bioanal. Chem.* **374**, 188 (2002).
31. J. A. Caruso, M. Montes-Bayon, *Ecotoxicol. Environ. Saf.* **56**, 148 (2003).
32. B. Zuber, I. Nikonenko, P. Klauser, D. Muller, J. Dubochet, *Proc. Natl. Acad. Sci. U.S.A.* **102**, 19192 (2005).
33. Y. Li, C. J. Hough, S. W. Suh, J. M. Sarvey, C. J. Frederickson, *J. Neurophysiol.* **86**, 2597 (2001).
34. J. H. Weiss, S. L. Sensi, *Trends Neurosci.* **23**, 365 (2000).
35. D. W. Choi, J. Y. Koh, *Annu. Rev. Neurosci.* **21**, 347 (1998).

36. Coordinates have been deposited in the Protein Data Bank with accession codes 2F3N and 2F44. This work was supported by NIH grant no. RO1 CA081000 to J.U.B., an NIH Cellular and Molecular Biology Training Grant to M.K.B., by the Deutsche Forschungsgemeinschaft (grants SFB 497/B8 and SFB 426/A1) to T.M.B. and E.D.G., and by the State of Baden-Württemberg (grant 1423/74) to T.M.B. J.U.B. is a Leukemia and Lymphoma Society Scholar.

Supporting Online Material

www.sciencemag.org/cgi/content/full/311/5760/531/DC1
Materials and Methods
References

17 August 2005; accepted 28 December 2005
10.1126/science.1118995

Design and Evolution of New Catalytic Activity with an Existing Protein Scaffold

Hee-Sung Park,[1] Sung-Hun Nam,[1] Jin Kak Lee,[2]* Chang No Yoon,[2] Bengt Mannervik,[3] Stephen J. Benkovic,[4] Hak-Sung Kim[1]†

The design of enzymes with new functions and properties has long been a goal in protein engineering. Here, we report a strategy to change the catalytic activity of an existing protein scaffold. This was achieved by simultaneous incorporation and adjustment of functional elements through insertion, deletion, and substitution of several active site loops, followed by point mutations to fine-tune the activity. Using this approach, we were able to introduce β-lactamase activity into the αβ/βα metallohydrolase scaffold of glyoxalase II. The resulting enzyme, evMBL8 (evolved metallo β-lactamase 8), completely lost its original activity and, instead, catalyzed the hydrolysis of cefotaxime with a $(k_{cat}/K_m)^{app}$ of 1.8×10^2 (mole/liter)$^{-1}$ second^{-1}, thus increasing resistance to *Escherichia coli* growth on cefotaxime by a factor of about 100.

Enzymes with new functions targeted at practical applications have long been a goal of protein engineering, and advances have been made with methods involving structure-based rational design or directed evolution (*1*–*4*). These approaches allow improvement of specific enzyme characteristics such as folding and stability (*5*), substrate specificity and enantioselectivity (*6*), and catalytic activity (*7*), but the design of enzymes with new functions remains a challenge. Computational design of proteins has had notable successes, culminating in Hellinga and co-workers' report (*8*) introducing triose phosphate isomerase activity into a noncatalytic ribose-binding protein. However, a lack of understanding of structure-function relations continues to hinder rational design, and methods relying on accumulation of point mutations remain desirable.

We have used an approach designated SIAFE (simultaneous incorporation and adjustment of functional elements), in conjunction with directed evolution, to introduce new catalytic activity into an existing scaffold. A schematic illustration of the SIAFE process is presented in fig. S1. SIAFE consists of insertion, deletion, and substitution of gene segments in addition to the conventional directed evolution method of accumulating point mutations, mimicking natural protein evolution (*9*, *10*). Functional elements (catalytic and substrate-binding elements) that constitute the active site are designed on the basis of sequence, mechanistic, and structural information and are incorporated into a template scaffold in a programmed and combinatorial manner. Using this approach, we generated β-lactamase activity from the glyoxalase II αβ/βα metallohydrolase scaffold.

The αβ/βα four-layer sandwich scaffold is proposed to have diverged extensively during evolution to give rise to a superfamily of metallohydrolase enzymes that are distributed over Eukarya, Archaea, and Bacteria. This superfamily catalyzes a variety of diverse reactions and includes metallo β-lactamase (MBL), glyoxalase II (GlyII), flavoprotein, arylsulfatase, type II polyketide synthase, β-CASP family, cytidine monophosphate (CMP)-N-acetylneuraminate hydroxylase, and phosphodiesterase (*11*). GlyII and MBL catalyze unrelated metabolic reactions, but their marginal structural similarity and conserved metal-binding site suggest that they are evolutionarily related (*12*) so that they present a typical example of the differentiation of a progenitor scaffold. GlyII (EC 3. 1. 2. 6) is involved in the hydrolysis of the thiolester bond of S-D-lactoylglutathione (Fig. 1A), a critical step in the conversion of cytotoxic 2-oxoaldehyde into 2-hydroxycarboxylic acids that occurs in the cyto-

[1]Department of Biological Sciences, Korea Advanced Institute of Science and Technology, 373-1, Kusung-Dong, Yusung-Gu, Daejon 305-701, Korea. [2]Bioanalysis and Biotransformation Research Center, Korea Institute of Science and Technology, Post Office Box 131, Cheongryang, Seoul 130-650, Korea. [3]Department of Biochemistry, Uppsala University, Biomedical Center, Box 576, SE-751 23 Uppsala, Sweden. [4]Department of Chemistry, The Pennsylvania State University, 104 Chemistry Building, University Park, PA 16802, USA.

*Present address: Nanormics Inc., Seoul, Korea.
†To whom correspondence should be addressed. Email: hskim76@kaist.ac.kr

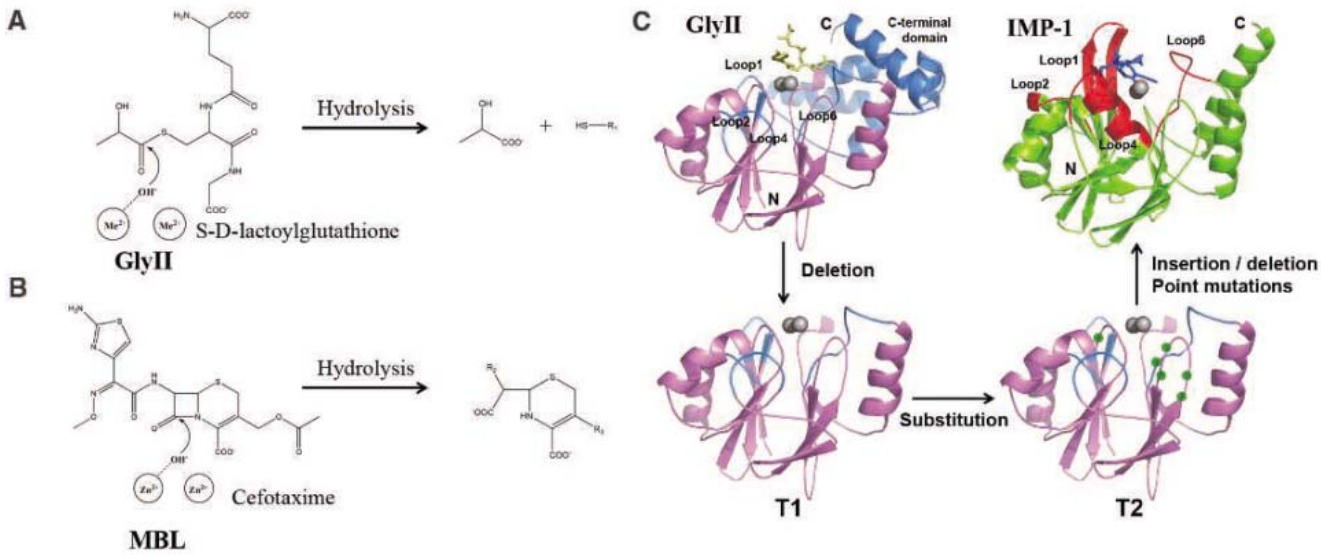

Fig. 1. Strategy for generation of MBL activity from GlyII. Catalytic mechanisms of (**A**) GlyII and (**B**) MBL. (**C**) Reconstruction of the active site of GlyII for generation of IMP-1 activity with the SIAFE process. As the first step, the C-terminal domain was deleted to produce template T1, and the catalytic elements (marked by green circles) were substituted to yield T2. Substrate-binding elements consisting of predesigned functional loops with different lengths and sequences were inserted, and random point mutations were induced for further adjustment. Functional loops constituting the active site of IMP-1 [Protein Data Bank (PDB) entry, 1DDK)] are shown in red, and the corresponding loops of GlyII (PDB entry, 1QH5) are in blue. The C-terminal domain to be deleted is shown in blue. Substrates for GlyII and IMP-1, S-(N-hydroxy-N-bromophenylcarbamoyl)glutathione and cefotaxime, are shown in yellow and blue, respectively

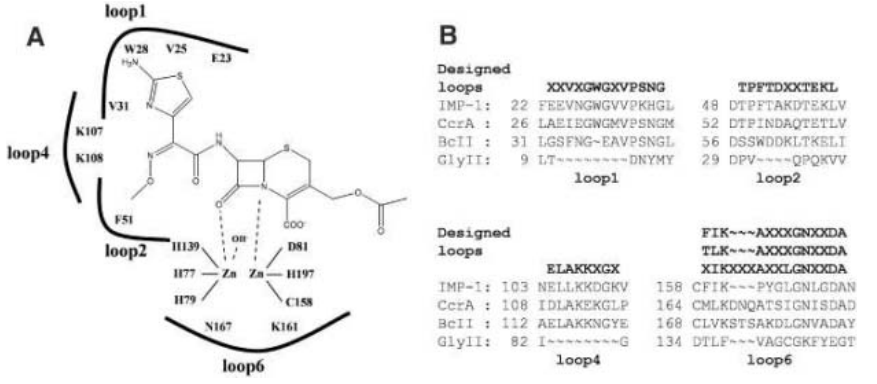

Fig. 2. Design of the MBL active site architecture. (**A**) Schematic diagram of the IMP-1 active site. Metal coordination and the active site pocket are shown. (**B**) Newly designed loops from the sequences of MBL family enzymes. IMP-1, MBL from *P. aeruginosa*; CcrA, MBL from *Bacteroides fragilis*; BcII, MBL from *Bacillus cereus* (*13*); GlyII, GlyoxalaseII from human (*12*).

plasm (*12*), whereas MBL (EC 3. 5. 2. 6) catalyzes the hydrolysis of the β-lactam amide bond to inactivate β-lactam antibiotics in the periplasmic space (Fig. 1B), giving rise to bacterial resistance against β-lactam antibiotics (*13*).

Human GlyII (260 amino acids, 29 kD) and IMP-1 (228 amino acids, 25 kD), an MBL family member from *Pseudomonas aeruginosa*, share a low sequence identity (13% for regions between 1 and 177 of GlyII and regions between 14 and 201 of IMP-1), but the overall folds are similar (Fig. 1C). Both contain αβ/βα sandwich structures and binuclear metal ions essential to the hydrolysis reaction. The active sites, however, differ in metal coordination and substrate binding. Typically, IMP-1 contains two Zn ions linked by a hydroxide molecule. Zn1 has tetrahedral coordination (H77, H79, and H139), and Zn2 has trigonal bipyramidal coordination (D81, C158, and H197) (*14*). GlyII, on the other hand, can have various metal ions, such as iron, manganese, or zinc, in its binuclear site (*15*). Metal 1 in GlyII is coordinated with three histidine residues similarly to Zn1 in MBL. However, for metal 2, C158 is replaced by D134, and H59 acts as an additional ligand (*12*). There are no common characteristics to substrate binding between GlyII and IMP-1. The IMP-1 substrate-binding site is composed mainly of loops 1, 2, and 6. Loop 1 (E23, V25, W28, and V31) and loop 2 (F51) constitute a hydrophobic pocket for β-side chain substituents of antibiotics (Fig. 2A) (*16*). Loop 6 contains K161 and N167, which are crucial for binding and activation of the β-lactam substrate during catalysis (*17*). Preliminary studies revealed that mutations (K107E and K108E) in IMP-1 loop 4 caused specific activity to decrease by a factor of about 100, which suggests that this loop plays some role in β-lactam binding or catalysis from a distance. In GlyII, loop 4 (K143 and Y145) and the C-terminal helical domain (Y175, R248, and K252) are implicated in binding (*12*). Thus, the distinct catalytic reactions derive from different active site architectures.

On the basis of sequence, mechanistic, and structural information, we used the SIAFE process to reconstruct the active site of GlyII (Fig. 1C) to bind and catalyze the hydrolysis of a typical substrate for MBL, cefotaxime. The C-terminal glutathione-binding domain of GlyII (residues 178 to 260) sterically prevents binding of a new substrate. Therefore, the first step was the deletion of this binding domain to create a template T1. The loss of critical substrate-binding elements caused the T1 template to lose all GlyII activity. Catalytic and substrate-binding elements for the new active site were designed in the next step. The catalytic elements of metallohydrolase superfamily enzymes mainly consist of metal-binding ligands and residues for stabilization of metal coordination. The T1 template was substituted with the following catalytic elements to produce T2: H59C and D134C for Zn affinity, A106Y, insertion of glycine between T107 and P108, S112T, and G113D for Zn stabilization (*18*). We also constructed a new active site pocket based on the sequence alignment of respective loops in MBL family enzymes. For loop 6, there is consider-

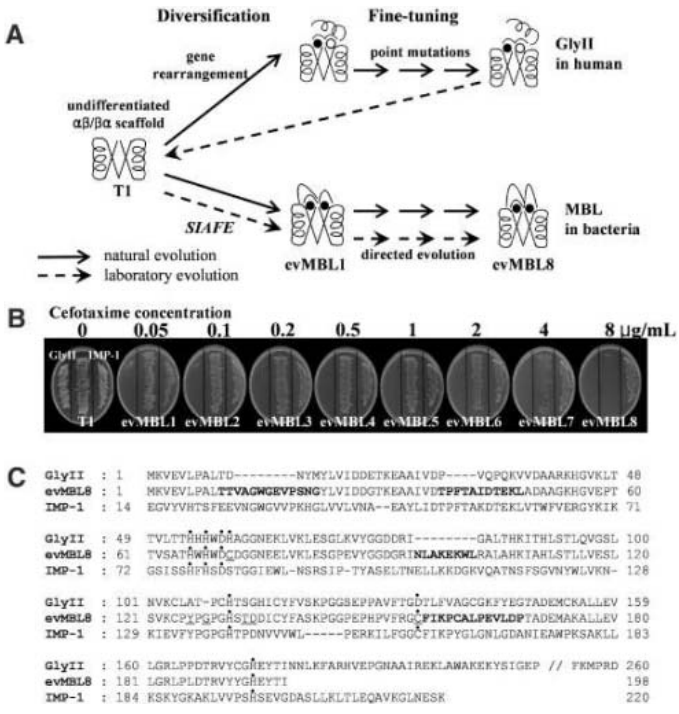

Fig. 3. Evolutionary trajectory of β-lactamase activity from the GlyII scaffold through SIAFE and directed evolution. (**A**) Schematic diagram showing the trajectories of the natural and artificial laboratory evolution of αβ/βα scaffold enzymes. (**B**) Cefotaxime resistance pattern of evolved enzymes selected at each round of evolution on selective plates with increasing concentrations of cefotaxime. (**C**) Sequence alignment of evMBL8 with GlyII and IMP-1. The specific mutations introduced by SIAFE are underlined, and newly designed loops are presented in bold. Residues essential for metal coordination are indicated with dots.

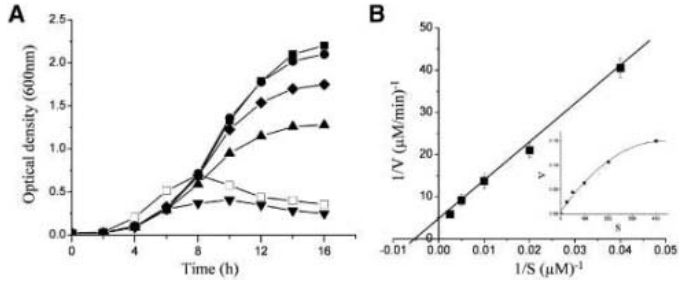

Fig. 4. Characteristics of evMBL8. (**A**) Growth patterns of *E. coli* cells with GlyII and evMBL8 on various cefotaxime concentrations. For evMBL8, cefotaxime concentrations are 0 (■), 0.2 (●), 0.5 (◆), 1.0 (▲), and 2.0 (▼) μg/ml. In the case of GlyII (□), the cefotaxime concentration was 0.02 μg/ml. (**B**) Steady-state kinetics (Lineweaver-Burke plot) of evMBL8 for cefotaxime.

Table 1. Kinetic constants and metal content of various enzymes.

Enzymes	k_{cat}* (s^{-1})	K_m* (μM)	k_{cat}/K_m ($M^{-1}s^{-1}$)	Metal (mol/mol of enzyme)*	
				Zn	Iron
GlyII	–	–	–	1.32 ± 0.27	0.10 ± 0.03
evMBL8	0.042 ± 0.003†	229 ± 36‡	1.84 × 10^2§	1.63 ± 0.43	0.46 ± 0.14
IMP-1	6.3 ± 0.8	7.9 ± 1.2	8.01 × 10^5	2.10 ± 0.50	–

*Values measured from at least three independent experiments †Apparent turnover number, k_{cat}^{app} ‡Apparent Michaelis-Menten constant, K_m^{app} §Apparent catalytic efficiency, $(k_{cat}/K_m)^{app}$

able variation among MBL family enzymes; accordingly, a mixture of three different oligonucleotides was used when designing this loop. Figure 2B shows the resulting loops: loop 1 (XXVXGWGXVPSNG), loop 2 (TPFTDXXTEKL), loop 4 (ELAKKXGX), and loop 6 (FIKAXXXGNXXDA, TLKAXXXGNXXDA, and XLKXXXAXXLGNXXDA). The loops contain residues that are in MBL family enzymes and several random residues for fine adjustment. The four sets of functional loops were incorporated into T2 with overlapping extension polymerase chain reaction (PCR) under error-prone conditions that also induce point mutations. Topology of the template scaffold GlyII and locations where the designed functional elements were incorporated are shown in fig. S2. The SIAFE approach allowed the constituents of the active site of GlyII to be replaced with newly designed functional elements in a planned and combinatorial manner. Mutation rates during mutagenic PCR were controlled at low levels (1 to 2 amino acid changes) and high levels (as many as 5 to 6 amino acid changes) throughout the gene to induce cumulative and synergistic effects on catalytic and substrate-binding sites.

From a library of 2.1 × 10^7 transformants, we first isolated 13 positive clones after two steps of selection on 0.2 μg/mL cefotaxime. All selected clones contained the segment (FIKAXXXGNXXDA) in loop 6 (fig. S3). Eight additional random mutations occurred in the active site loops. Further changes (2 to 9 amino acids) were randomly distributed in regions away from the active site. When functional elements were incorporated without additional mutations, no positive clones were isolated. The positive clones had undetectable β-lactamase activity. Thus, the isolated clones were subjected to directed evolution to increase their catalytic activities. Because the efficiency of directed evolution is highly dependent on the diversity of the starting clones, the library size was increased up to 1.5 × 10^8 with only the loop 6 segment (FIKAXXXGNXXDA). The resulting 312 positive clones were subjected to an additional seven rounds of directed evolution with DNA shuffling. To maintain high diversity, we selected positive clones from the library of more than 10^7 mutants at each round of in vitro evolution (table S1). As the evolution process progressed, selection pressure (cefotaxime concentration) was gradually increased from 0.2 to 4.5 μg/ml. In the seventh round of directed evolution, only 15 clones were isolated from the 7.0 × 10^7 mutant library at a cefotaxime concentration of 4.5 μg/ml. Of 15 positive clones, the one showing the most improved growth pattern on selective plates was selected. Additional rounds only resulted in a marginal increase in growth resistance for cefotaxime.

The overall evolution process to generate β-lactamase activity from template T1 is schematically represented in Fig. 3A. The figure also illustrates the trajectories of natural evolution and artificial laboratory evolution of the αβ/βα scaffold enzymes, GlyII and MBL. At the stage of SIAFE and each round of directed evolution, the clones showing the highest resistance against cefotaxime were selected as representatives and designated evMBL1 to evMBL8. The increasing resistance caused by these evMBL mutants was demonstrated by the comparison of growth between host cells expressing evolved enzymes and wild-type GlyII and IMP-1 on various dosages of cefotaxime (Fig. 3B). The observed growth resistance of evolved enzymes was somewhat higher than their actual resistance because of a confluence effect. Nonetheless, overall growth resistance of selected mutants gradually increased from 0.05 to 8 μg/ml, so antibiotic resistance was increased by a factor of about 160 through artificial evolution of the GlyII scaffold. The possibility of contamination by wild-type IMP-1 in the bacterial population carrying evMBL8 was checked and ruled out (*19*).

The amino acid sequence of the finally selected evMBL8 was determined and compared with those of GlyII and IMP-1 (Fig. 3C). Interestingly, evMBL8 carries only a 59% amino acid identity with GlyII, even though it has evolved from the GlyII scaffold. This indicates that 81 of the 198 amino acid residues were changed through insertion, deletion, and substitution of functional elements in addition to accumulation of point

mutations by SIAFE and directed evolution. Meanwhile, the amino acid sequence identity of evMBL8 with IMP-1 (25%) was almost double that of GlyII with IMP-1 (13%). As expected from the design strategy, more than 60% (49 amino acids) of mutations were concentrated in the catalytic and substrate-binding regions. In addition, many originally designed conserved residues in functional loops were changed during evolution. Nonetheless, the residues responsible for metal coordination (H66, H68, and H131 for metal 1; D70, C155, and H194 for metal 2) were not changed despite extensive mutagenesis. Replacement of any of these residues in evMBL8 with Ala resulted in loss of catalytic activity (*19*). Mutations C71H and C155D, which were attempts to restore GlyII-like metal coordination (H59 and D134) in evMBL8, also resulted in complete loss of catalytic activity (*19*). Thus, as evMBL8 evolved to have β-lactamase activity, it retained the designed metal coordination of IMP-1 that is essential for catalysis.

To further confirm the evolution of β-lactamase activity from the GlyII scaffold, evMBL8 was characterized in terms of in vivo biological activity, kinetic constants, and metal content. When *E. coli* cells expressing the evMBL8 were grown in liquid medium, distinct cell growth was observed up to cefotaxime concentrations of 1.0 μg/ml (Fig. 4A). A further increase in cefotaxime concentration (>2.0 μg/ml) caused a serious inhibition of cell growth due to cell lysis. On the other hand, cells expressing GlyII showed growth inhibition even at cefotaxime concentrations of 0.02 μg/ml. To study enzyme kinetics, evMBL8 was expressed as a fusion with maltose-binding protein (MBP) to improve stability (fig. S4). evMBL8 exhibited a typical saturation profile for cefotaxime, and k_{cat}^{app} and K_m^{app} were calculated to be 0.042 s^{-1} and 229 μM, respectively, from the reciprocal plot (Fig. 4B and Table 1). These values are lower by a factor of 150 and higher by a factor of 30 than the k_{cat} and K_m values of wild-type IMP-1, respectively, with the difference in K_m providing evidence against contamination by IMP-1 in conjunction with their relative activities for various substrates (table S2). Consequently, overall catalytic efficiency $(k_{cat}/K_m)^{app}$ of evMBL8 for cefotaxime was estimated to be 1.8×10^2 $M^{-1}s^{-1}$, which is about 3 to 4 orders of magnitude lower than that of wild-type IMP-1. Nonetheless, evMBL8 was active enough to provide *E. coli* cells a resistance against cefotaxime that is higher by a factor of 100 compared with cells having no evMBL8 (Fig. 4A). To check whether evMBL8 was still able to bind metal ions in its fused form with MBP, the total metal content of the enzyme was measured. Mutation H59C of GlyII was reported to cause a loss of zinc while maintaining iron content at a normal level, which suggests that H59C severely impaired the metal-binding site for zinc (*15*). However, evMBL8 with mutation H59C was found to bind both zinc (1.6 mol) and iron (0.4 mol) essential for hydrolytic reaction at levels comparable to GlyII (Table 1). It is likely that the disruption of metal coordination was reversed by other mutations during the directed evolution process.

Molecular modeling of evMBL8 with either an MBL family member (CcrA) or GlyII as the template gave an evMBL8 structure that is similar to that of the target IMP-1 (fig. S5A) but shows a distinct active site architecture compared with the template GlyII (fig. S5B). The model of the evMBL8-cefotaximne complex shows well-organized metal coordination (H66, H68, and H131 for metal 1; D70, C155, and H194 for metal 2) at the bottom of the active site (fig. S5C), which is consistent with the mutation study on putative metal ligands described above. Within the active site, loop 2 (T38-L48) and loop 6 (F156-P168) constitute two walls of the substrate-binding pocket, and loop 1 (T10-G22) forms the ceiling. Thus, we suggest that evMBL8 has acquired a new active site architecture with well-defined metal coordination and a substrate-binding pocket for new catalytic activity through the SIAFE and directed evolution process.

The design strategy presented here enabled the conversion of an enzyme in the metallohydrolase superfamily into a new family member with a different catalytic function, providing experimental support for the divergent evolution of mechanistically diverse family enzymes. We hope that the developed process can be extended to other scaffolds and create a larger variety of catalytic lineages performing diverse reactions and perhaps even reactions not found in nature.

References and Notes

1. S. J. Benkovic, S. Hammes-Schiffer, *Science* **301**, 1196 (2003).
2. F. H. Arnold, *Nature* **409**, 253 (2001).
3. A. Schmid *et al.*, *Nature* **409**, 258 (2001).
4. A. C. Joerger, S. Mayer, A. R. Fersht, *Proc. Natl. Acad. Sci. U.S.A.* **100**, 5694 (2003).
5. H. S. Park, K. H. Oh, H. S. Kim, *Methods Enzymol.* **388**, 187 (2004).
6. Y. H. Cheon *et al.*, *Biochemistry* **43**, 7413 (2004).
7. L. Tang *et al.*, *Biochemistry* **44**, 6609 (2005).
8. M. A. Dwyer, L. L. Looger, H. W. Hellinga, *Science* **304**, 1967 (2004).
9. S. Leopoldseder, J. Claren, C. Jurgens, R. Sterner, *J. Mol. Biol.* **337**, 871 (2004).
10. A. Aharoni *et al.*, *Nat. Genet.* **37**, 73 (2005).
11. H. Daiyasu, K. Osaka, Y. Ishino, H. Toh, *FEBS Lett.* **503**, 1 (2001).
12. A. D. Cameron, M. Ridderström, B. Olin, B. Mannervik, *Struct. Fold. Des.* **7**, 1067 (1999).
13. Z. Wang, W. Fast, A. M. Valentine, S. J. Benkovic, *Curr. Opin. Chem. Biol.* **3**, 614 (1999).
14. N. O. Concha *et al.*, *Biochemistry* **39**, 4288 (2000).
15. T. M. Zang *et al.*, *J. Biol. Chem.* **276**, 4788 (2001).
16. Z. Wang, W. Fast, S. J. Benkovic, *Biochemistry* **38**, 10013 (1999).
17. M. P. Yanchak, R. A. Taylor, M. W. Crowder, *Biochemistry* **39**, 11330 (2000).
18. S. D. Scrofani *et al.*, *Biochemistry* **38**, 14507 (1999).
19. Materials and methods are available as supporting material on *Science* Online.

20. We thank R. Sterner, M. Meyer, and F. Arnold for helpful comments, and J. H. Kim and S. C. Lee for technical assistance. Supported by National Research Laboratory program and Microbial Genomics and Application Center of Ministry of Science and Technology, Nano-Medical Project of Ministry of Health and Welfare, R & D program of Fusion Strategies for Advanced Technologies of Ministry of Commerce, Industry and Energy, and Brain Korea 21 of Ministry of Education and Human Resources Development, Korea.

Supporting Online Material

www.sciencemag.org/cgi/content/full/311/5760/535/DC1
Materials and Methods
SOM Text
Figs. S1 to S6
Tables S1 and S2
References

16 August 2005; accepted 7 December 2005
10.1126/science.1118953

A Virus Reveals Population Structure and Recent Demographic History of Its Carnivore Host

Roman Biek,[1]*† Alexei J. Drummond,[3] Mary Poss[1,2]

Directly transmitted parasites often provide substantial information about the temporal and spatial characteristics of host-to-host contact. Here, we demonstrate that a fast-evolving virus (feline immunodeficiency virus, FIV) can reveal details of the contemporary population structure and recent demographic history of its natural wildlife host (*Puma concolor*) that were not apparent from host genetic data and would be impossible to obtain by other means. We suggest that rapidly evolving pathogens may provide a complementary tool for studying population dynamics of their hosts in "shallow" time.

The genetic population structure of human pathogens often reflects known patterns of human migration (*1–4*). Moreover, the rapid evolutionary rate of many viral parasites means that this information can manifest itself over months or years (*5*). With HIV, for example, the origin and demographic history of epidemics have been determined retrospectively

from genetic data (*6*–*8*). Especially because of their high temporal resolution, viruses hold great potential as genetic tags of their hosts. Yet, this exciting potential remains largely unexplored for the study of wildlife populations where such an approach could be used to address questions in numerous disciplines, ranging from epidemiology to conservation.

Many wild feline species are natural hosts to species-specific types of feline immunodeficiency virus (FIV), analogous to simian immunodeficiency viruses (SIVs) in wild primates (*9*, *10*). Cougars (*Puma concolor*), a large New World feline species, are commonly infected by their own type of FIV (FIV_{Pco}) (*11*, *12*), apparently without suffering major fitness consequences (*13*). Transmission, which requires direct contact between individuals, occurs vertically and horizontally (*14*) and causes persistent infections. Exchange of virus with other cat species in the wild either does not occur or must be extremely rare (*10*). Importantly, FIV_{Pco} measurably evolves within years (*14*) and thus has the potential to be informative about virus and host dynamics over extremely short periods.

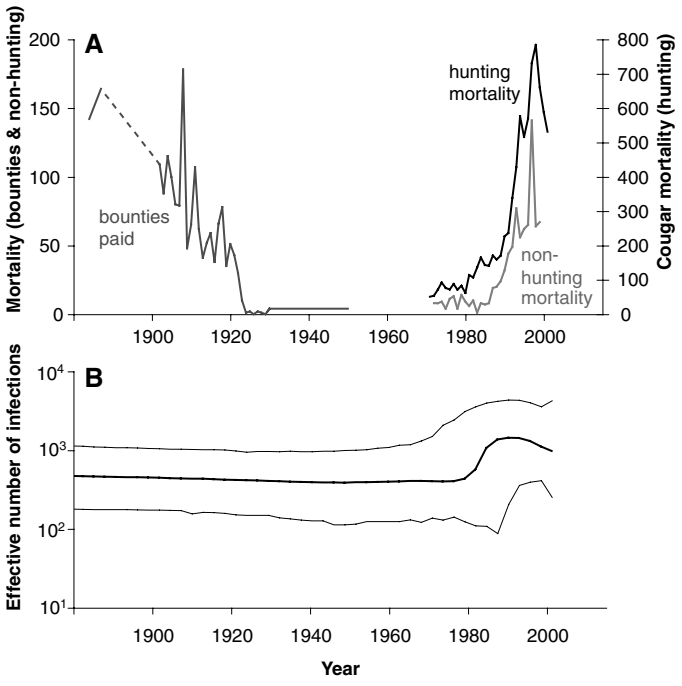

Fig. 1. Demographic trends for cougars and FIV_{Pco}, 1880 to 2001. (**A**) Cougar population indices for Montana. Dashed line indicates years with incomplete records. Nonhunting mortality represents cougars that died primarily as a result of animal control and road mortality. Numbers are taken from Riley (*17*) and from public records by Montana Fish Wildlife and Parks. (**B**) Median effective number of FIV_{Pco} infections (thin lines indicate 95% highest posterior density interval) as estimated from virus sequence data in program BEAST (*24*) using a Bayesian skyline plot technique (*22*). Estimates for years before 1880 remained essentially unchanged and are omitted.

As in most parts of North America, cougar populations in the northern Rocky Mountains underwent drastic declines during the early 20th century as a consequence of human persecution and depleted prey populations (*15*, *16*). In Montana, for example, the number of cougar carcasses annually submitted for bounty payments plummeted between 1908 and 1929 from more than 170 to zero and stayed extremely low for decades thereafter despite the bounty incentive remaining in place (*17*) (Fig. 1A). Populations in neighboring states and provinces apparently experienced a similar fate (*16*). More recently, cougar populations throughout the region have shown signs of recovery following legislation that limits the take of both cougars and their ungulate prey (*15*) (Fig. 1A). This strong demographic signal of decline followed by rapid growth offered a unique opportunity to test whether the dynamic history of cougars in Montana in the recent past could be discerned from the genetic structure of its obligate viral parasite.

We collected samples from 352 cougars across western Montana, as well as adjacent areas [Wyoming, British Columbia, and Alberta (*18*); table S1, Fig. 2A), and conducted genetic analysis of 11 host microsatellite loci using different individual-based methods [i.e., without relying on predefined populations (*18*)]. Despite samples being collected over distances exceeding 1000 km, results revealed little population structure. Although a southern and northern group could be distinguished, both overlapped substantially, indicating genetic admixture (fig. S2). This result was confirmed by a weak but significant isolation-by-distance pattern of cougar relatedness (*18*). Low genetic differentiation has also been noted among cougar populations in neighboring areas (*19*, *20*). Evidently, low population densities in the recent past, possibly associated with reduced movement, have not resulted in pronounced genetic structure for cougars in the northern Rocky Mountains.

More than one-quarter of the cougars we sampled were infected with FIV_{Pco} (98 or 28%; Fig. 2A, table S1), consistent with prevalence levels found in previous studies (*11*, *14*). Phylogenetic analysis based on combined sequence data (~1400 base pairs) from two viral genes identified two major virus clades with >20% divergence. Within clades, a total of eight FIV_{Pco} lineages (L1 to L8) could be distinguished that were up to 5% divergent and had high bootstrap and/or posterior support (Fig. 2B). Seven cougars yielded sequences of more than one lineage, indicative of coinfection or potentially circulating recombinants (*18*).

Consistent with cougar host genetics, FIV lineages fell into a northern (L1 to L4) and a southern group (L5 to L8) (Fig. 2A). However, in contrast to host genetics, spatial structure of viral populations was much more pronounced. All lineages exhibited more or less contiguous ranges, and these ranges were often spatially exclusive (Fig. 2A) such as for northern (L1 to L4) versus southern lineages (L5 to L8). Furthermore, individual lineages were restricted to smaller geographic areas. For example, L1 dominated the central part of our study area, whereas L3, L4, L5, and L8 were found only in small areas at the periphery. Lineage L2 was exceptional in that it co-occurred with all other lineages even though it was found only in 14% of infected cougars. All seven individuals yielding virus sequences from more than one lineage were found where ranges of these lineages overlapped (Fig. 2A).

The lack of spatial admixture of most virus lineages was clearly at odds with the microsatellite results because high levels of cougar movement should tend to quickly randomize virus distributions. Therefore, we hypothesized that the current virus pattern may be a direct consequence of previously low cougar population sizes and thus a rather recent, and potentially transient, phenomenon. To determine how long ago the most recent common ancestor (MRCA) of each of the FIV lineages had existed, we estimated evolutionary rates for the two FIV_{Pco} genes, *pol* and *env*, on the basis of temporally spaced sampling of cougars. Both genes were found to evolve at a rate of about 4×10^{-4} per site per year [*pol*: 2.9 (95% highest posterior density interval, HPD: 1.2 to 4.8) $\times 10^{-4}$; *env*: 4.0 (HPD: 1.6 to 6.3) $\times 10^{-4}$], slightly lower than but generally consistent with previous estimates from a different cougar data set (*14*).

On the basis of the estimated rate, diversification of all eight viral lineages had occurred within the last 20 to 80 years (Fig. 3). Because this interval coincides with the period of low cougar densities (Fig. 1A), it seems likely that the FIV_{Pco} lineages currently found are survivors of a demographic bottleneck that must have resulted in frequent local extinction and severe spatial restriction of lineages. Moreover, the time elapsed since the MRCA was posi-

[1]Wildlife Biology Program, [2]Division of Biological Sciences, University of Montana, Missoula, MT 59812, USA. [3]Department of Computer Science, University of Auckland, Auckland, New Zealand.

*Present address: Department of Biology, Emory University, Atlanta, GA 30322, USA.

†To whom correspondence should be addressed. E-mail: rbiek@emory.edu

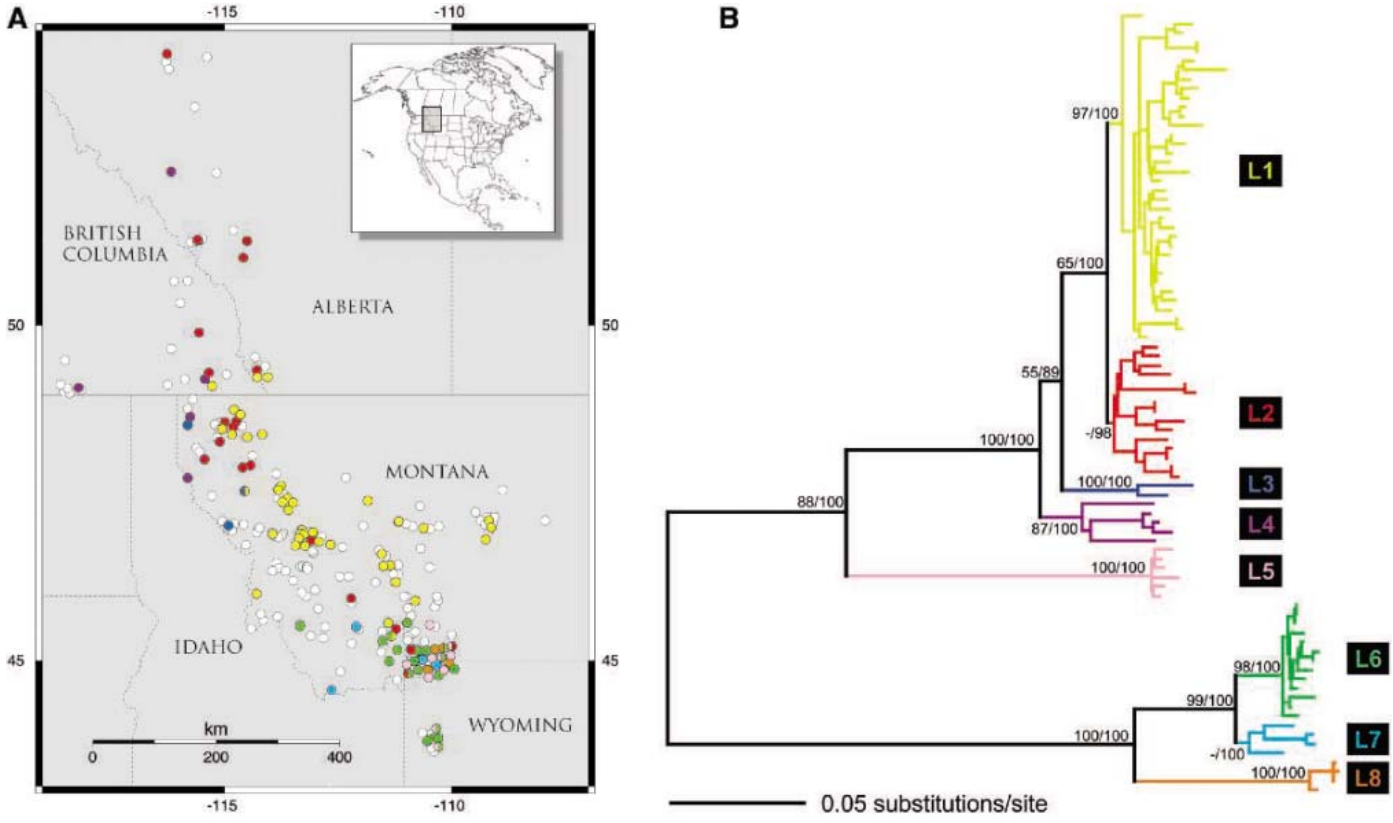

Fig. 2. FIV_{Pco} lineages and their spatial distribution. (**A**) Origin of FIV_{Pco}-positive [colors as in (B)] and -negative samples (white circles). The map was generated using Online Map Creator (*25*). The area covered by samples in Montana roughly reflects distribution of cougar habitat (forest). (**B**) Phylogeny of FIV_{Pco} in the northern Rocky Mountains constructed from concatenated *pol* and *env* sequences (n = 85) and designation of eight viral lineages based on >5% divergence. Labeled nodes represent bootstrap support based on 1000 neighbor-joining trees generated from maximum-likelihood distances estimated from the original likelihood model and posterior proportions from the Bayesian analysis. Values for within-lineage nodes are omitted for clarity.

tively correlated with the distribution of virus lineages, in that samples of more recently diverged lineages exhibited smaller maximum geographic distances (P = 0.012) (Fig. 3A). This suggests that, concurrent with cougar population recovery, surviving lineages have consistently expanded their range. This scenario of spatial expansion was supported by a separate analysis in which the geographic distance between the sampled viruses and their inferred ancestors was regressed against the corresponding time separating the sample from the origin of its lineage. This regression of geographic distances against times revealed an estimated mean viral diffusion rate of 3.7 km per year (Fig. 3B). Interestingly, the recovery of cougar populations in Alberta is thought to have started earlier than it did further south, possibly during the 1930s (*21*). This may explain the particularly wide distribution of lineage L2, which is the dominant type in Alberta today and which may have benefited, in terms of spread, from the earlier expansion of cougars in that area (Fig. 2A).

If the population dynamics of cougars had affected the current spatial distribution of FIV_{Pco}, it should also have had a discernable effect on virus demography. We estimated changes in the effective number of infections through time from the distribution of coalescent events in the genealogy using a Bayesian skyline plot (*22*). Results support an exponential increase in the absolute number of infections after 1980, i.e., during the demographic recovery of cougars in Montana (Fig. 1B). The maximum number of infections, as well as indexes of cougar abundance, was reached during the late 1990s (Fig. 1, A and B). Although this result fits expectations in terms of correlated demographic trends for both cougars and virus, evidence of a decline in infections before 1950 was weak (Fig. 1B). We suspect that this inability to detect a signature of decline during the early 20th century was due to the scarcity of coalescent events (and hence data points) in our phylogeny for this time period.

In principle, an increase in FIV_{Pco} infections could reflect elevated prevalence rather than changes in host population size; however, we believe that this alone is unlikely to explain the observed trend. For example, data collected from cougars in and around Yellowstone National Park between 1990 and 2004 show that the proportion of infected individuals remained relatively stable (~20%) throughout this period (*13*). It is important to stress, however, that our results only allow us to infer a simultaneous increase in virus and cougar host qualitatively, because reliable estimates of cougar population sizes do not exist and the proportion of infected hosts through time ultimately remains unknown.

In conclusion, we have shown that FIV_{Pco} genetics are highly informative about the recent history of its cougar host, whereas the same information was either not apparent or could not have been inferred from host genetic data. Given that lineages appear to be spatially expanding, we predict that the fine-scale spatial structure currently characterizing FIV_{Pco} will likely disappear in the near future, assuming cougar population sizes and movement remain sufficiently high. Maintaining functional populations and natural levels of gene flow remain important priorities for the conservation of wildlife populations. Monitoring the distribution and diversity of FIV_{Pco} in cougars may therefore represent a future tool for wildlife managers to ensure that these goals are met.

More generally, rapid evolutionary rates and host specificity are traits not limited to FIV_{Pco} but are typical of many parasites. Although our knowledge of parasite diversity in nondomestic species is still limited, the approaches described here should be applicable to a wide range of species and systems (*23*), provided that the ecology of interaction between parasite and host is sufficiently well understood. Natural ecosystems and populations are currently undergoing changes

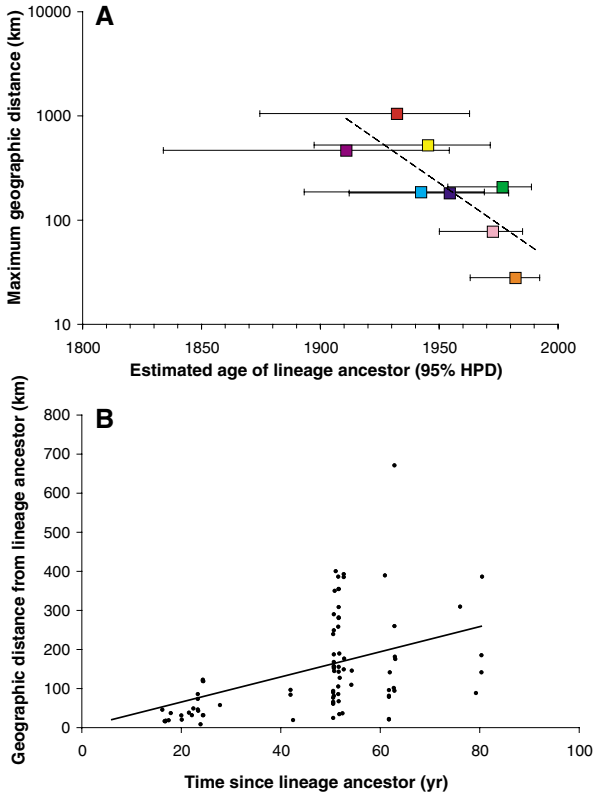

Fig. 3. Space-time relationships of virus distributions. (**A**) Median age of common ancestor (95% highest posterior density interval; HPD) for eight FIV_{Pco} lineages is correlated with their spatial range (expressed as maximum pairwise geographic distance) [$R^2 = 0.61$, $P = 0.023$; log(distance) = 0.0182(years before present) + 1.4847]. (**B**) Spatial diffusion of viruses over time. Temporal divergence for each sequence was calculated as number of years elapsed between the median age of lineage ancestor [as in (A)] and sampling date. Similarly, spatial divergence was calculated relative to the putative location of the respective lineage ancestor determined through ancestral reconstruction in COMPARE (*26*). Regression parameter estimates were obtained by comparative analysis, also using COMPARE (*26*), and excluded zero for slope ($\beta_1 = 3.74$; confidence interval: 1.04 to 6.44) but not intercept ($\beta_0 = -43.41$; confidence interval: −188.67 to 101.85); therefore, the regression line shown is based on a model without intercept. See supporting online material for details.

at unprecedented rates owing to human activities. Molecular markers with an equally short temporal resolution will be of increasing value to researchers trying to understand and mitigate these changes.

References and Notes

1. T. Wirth, A. Meyer, M. Achtman, *Mol. Ecol.* **14**, 3289 (2005).
2. D. Falush *et al.*, *Science* **299**, 1582 (2003).
3. E. C. Holmes, *Mol. Ecol.* **13**, 745 (2004).
4. C. Sugimoto, T. Kitamura, J. Guo, *Proc. Natl. Acad. Sci. U.S.A* **94**, 9191 (1997).
5. A. J. Drummond, O. G. Pybus, A. Rambaut, R. Forsberg, A. G. Rodrigo, *Trends Ecol. Evol.* **18**, 481 (2003).
6. V. V. Lukashov, J. Goudsmit, *J. Mol. Evol.* **54**, 680 (2002).
7. P. Lemey *et al.*, *Proc. Natl. Acad. Sci. U.S.A* **100**, 6588 (2003).
8. B. Korber *et al.*, *Science* **288**, 1789 (2000).
9. R. A. Olmsted *et al.*, *J. Virol.* **66**, 6008 (1992).
10. J. L. Troyer *et al.*, *J. Virol.* **79**, 8282 (2005).
11. M. A. Carpenter *et al.*, *J. Virol.* **70**, 6682 (1996).
12. R. J. Langley *et al.*, *Virology* **202**, 853 (1994).
13. R. Biek, thesis, University of Montana (2004).
14. R. Biek *et al.*, *J. Virol.* **77**, 9578 (2003).
15. K. A. Logan, L. L. Sweanor, *Desert Puma: Evolutionary Ecology and Conservation of an Enduring Carnivore* (Island Press, Washington, DC, 2001).
16. R. M. Nowak, "The cougar in the United States and Canada" (U.S. Department of Interior Fish and Wildlife Service and New York Zoological Society, 1976).
17. S. J. Riley, thesis, Cornell University (1998).
18. Materials and methods are available as supporting material on *Science* Online.
19. C. R. J. Anderson, F. G. Lindzey, D. B. McDonald, *J. Mammal.* **85**, 1207 (2004).
20. E. A. Sinclair *et al.*, *Anim. Conserv.* **4**, 257 (2001).
21. M. G. Jalkotzy, "Management plan for cougar in Alberta" (Alberta Forestry, Land and Wildife, Fish and Wildlife Division, 1992).
22. A. J. Drummond, A. Rambaut, B. Shapiro, O. G. Pybus, *Mol. Biol. Evol.* **22**, 1185 (2005).
23. N. K. Whiteman, P. G. Parker, *Anim. Conserv.* **8**, 175 (2005).
24. A. J. Drummond, A. Rambaut, BEAST, version 1.2; available at http://evolve.zoo.ox.ac.uk/beast/ (2003).
25. Online Map Creator available at www.aquarius.geomar.de/omc/.
26. E. P. Martins, Computer programs for the statistical analysis of comparative data. Distributed by the author at http://compare.bio.indiana.edu/ (2004).

27. For help collecting cougar samples, we thank T. K. Ruth, K. Murphy, R. DeSimone, R. Grey, C. Chetkiewicz. T. Shury, A. Kortello, H. Schwantje, M. Hall, Montana Fish Wildlife and Parks, Montana State Houndsmen Association, and Alberta Tree Hound Association. See supporting online material for more extensive acknowledgements. Research was funded by the Wilburforce Foundation, the Yellowstone to Yukon Conservation Initiative, and the NSF. We thank S. Painter, K. Pilgrim, K. Samuel, and N. Akamine for lab assistance and L. A. Real and M. K. Schwartz for comments. Sequences have been submitted to GenBank under accession numbers DQ106985 to DQ107160.

Supporting Online Material

www.sciencemag.org/cgi/content/full/311/5760/538/DC1
Materials and Methods
SOM Text
Figs. S1 and S2
Table S1
References

14 October 2005; accepted 21 December 2005
10.1126/science.1121360

Automated Bioreactor Sampling

The 2700 ARS (automated reactor sampling) and 7100 ARS automated online biochemistry analyzers offer real-time online monitoring. Capable of round-the-clock monitoring without the need for manual intervention, the ARS allows up to four reactors to be sampled simultaneously, eliminating the high cost of manual sampling. The fully programmable automated cleaning system guarantees sterility by use of bioreactor isolation, remote dual valve interface, and steamable probes. These analyzers provide precise, accurate measurements of the key nutrients and by-products in the fermentation and cell culture process. Frequent sampling and analysis increases knowledge of the process, leading to improved quality of the finished product and reduced costs.

Analytical Technologies

For information 01252 514711 www.analyticaltechnologies.co.uk

Receiver Plates

Two new receiver plates facilitate high-throughput, artificial membrane layer transport assays. These assays are being widely adopted in the drug discovery process to accelerate compound profiling. The rapid access to high-quality, lipid-layer permeability data augments the selection process prior to more expensive cell-based assays. The disposable MultiScreen Transport Receiver plate is a precision-injection, molded accessory that eliminates the need for cleaning steps between assays. The low-evaporation design accommodates in-plate mixing or stirring and exhibits high drug recovery. Also available is the made-to-order, reusable MultiScreen PTFE Acceptor plate, which offers broad chemical compatibility and low drug binding.

Millipore

For information 800-MILLIPORE
www.millipore.com/bioscience

Plasmid-Safe DNase

Plasmid-Safe ATP-Dependent DNase provides a fast and easy method for the removal of bacterial genomic DNA from vector preparations. This unique deoxyribonuclease (DNase) selectively digests linear double-stranded DNA but has no activity on nicked, closed circular double-stranded DNA or supercoiled DNA. It can be used as a final purification step when preparing cloning vectors and to avoid ligating contaminating DNA fragments that can result in false positives and high background.

Epicentre Biotechnologies

For information 800-284-8474 www.EpiBio.com

Mammalian Lysis Buffer

The Mammalian Cell-PE LB Kit has been developed for extraction of total soluble protein from mammalian cultured cells. The product is based on organic buffering agents, which make use of a mild, non-ionic detergent, and a proprietary combination of various salts and agents to enhance extraction and stability of proteins. Depending on the application, additional agents, such as chelating agents, reducing agents, and protease inhibitors, can be added. It is compatible with most applications, including enzyme assays, various chromatography procedures, and electrophoresis.

G-Biosciences/Genotech

For information 314-991-6034 www.GBiosciences.com

Taq DNA Polymerase

HotStart-IT Taq DNA Polymerase makes use of a novel hot start method called primer-sequestration. The manufacturer has combined high-quality Taq DNA polymerase with a recombinant protein that binds and sequesters primers at lower temperature, making them unavailable for use by Taq DNA polymerase. This primer-sequestration technique effectively blocks DNA synthesis from mis-priming events at lower temperatures. Following the initial denaturation step during polymerase chain reaction, the protein is inactivated and the primers are free to participate in the amplification reaction.

USB Corp

For information 216-765-5000 www.usbweb.com

Zoom Microscope System

The Olympus MacroView MVX10 macro zoom microscope combines maximum detection sensitivity at the lowest magnifications with a high-magnification zoom for imaging fluorescence specimens at the cellular level. It combines the best features of compound and stereo microscopes, allowing zoom macro- to micro-level fluorescence imaging of the same specimen. The MVX10 offers large working distances and fields of view similar to stereomicroscopes, making it well-suited for visualizing whole organisms and large tissue slices. It also provides high numerical aperture (NA) objectives for enhanced resolution and light-gathering ability; it is optimized to handle low-light fluorescence for imaging cellular features. The MVX can be used with any of three parfocal, high-NA objectives. The 0.63x/0.15NA objective provides a field of view ranging up to 55 mm. The 1x/0.25NA sets a record among life science zoom microscopes for both working distance (65 mm) and light-gathering ability for objectives of its magnification. The 2x/0.5NA objective has a correction collar for adjusting to aqueous media with a depth of up to 5 mm above the specimen.

Olympus

For information 800-446-5967
www.olympusamerica.com/microscopes

Newly offered instrumentation, apparatus, and laboratory materials of interest to researchers in all disciplines in academic, industrial, and government organizations are featured in this space. Emphasis is given to purpose, chief characteristics, and availability of products and materials. Endorsement by *Science* or AAAS of any products or materials mentioned is not implied. Additional information may be obtained from the manufacturer or supplier by visiting www.science.labvelocity.com on the Web, where you can request that the information be sent to you by e-mail, fax, mail, or telephone.

POSITIONS OPEN

WUHAN INSTITUTE OF VIROLOGY
Chinese Academy of Sciences

Wuhan Institute of Virology, Chinese Academy of Sciences (CAS), founded in 1956, is the only comprehensive institute carrying out fundamental research on virology in CAS with scientific research elitists. Wuhan Institute of Virology has recently extended its emphasis from general virology to medical virology and emerging infectious diseases. The Institute invites applications for multiple principal investigator positions, including CAS Hundred Talents Program. Our priority is for candidates interested in viral immunology, virus-host interaction, HIV/AIDS, epidemiology and emerging infectious diseases, vaccines and antiviral drugs, but we will consider strong applications in all areas of virology. These positions offer the opportunity to join a rapidly growing group of virologists in an institute that focuses on the research of virology and provides a highly interactive, interdisciplinary research environment, and excellent research support facilities.

The successful candidates will receive attractive startup packages, spaces, and highly competitive salaries that are commensurate with experiences and qualifications. All appointments require a Ph.D. and/or M.D. degree, strong publications, and evidence of outstanding research potential and the ability to develop a vigorous, independently funded program. Applicants under the age of 45 have priority for consideration.

Interested applicants should submit complete curriculum vitae, a copy of certification for the Ph.D. degree, a copy of appointment for the current position, and five representative publications, a two-page summary of research interests related to the applied position, and three letters of recommendation by March 25, 2006. Review of applications will begin after that date and will continue until the positions are filled.

The Institute anticipates additional hires in these and related areas this year, and for the next several years for the level of Associate and Assistant Professors for existing research programs that include tumor virology, hepatitis, influenza virus, viral zoonosis, et cetera.

Further information can be reviewed at **website: http://www.whiov.ac.cn.**

Applicants are encouraged to contact the Institute.

Contact: **Ms. Naxin Shang, Dr. Zhiming Yuan**
Personnel Office, Wuhan Institute of Virology
Chinese Academy of Sciences
44 Xiao Hongshan Middle District
Wuhan 430071 China
Telephone: 86-27-87199413; 86-27-87199145
Fax: 86-27-87198072
E-mail: shang@pentium.whiov.ac.cn or **yzm@wh.iov.cn**

PLANT OR ALGAL BIOLOGY
Colgate University

We are seeking a **VISITING ASSISTANT PROFESSOR** to fill a one-year position starting August 2006. Ph.D. or expectation of completion this academic year required, teaching experience desirable. The appointee will join a biology faculty committed to innovative teaching in the liberal arts setting and involvement of students in research. The successful candidate will contribute to a foundation course in evolution, ecology, and diversity, teach a course in phycology in the fall, and teach a course in plant biology in the spring. Please forward a letter of application with curriculum vitae and transcripts, along with a statement of teaching philosophy and interests to: **Dr. Randy Fuller, Department of Biology, Colgate University, 13 Oak Drive, Hamilton, NY 13346-1398,** and also arrange to have three letters of recommendation sent to this address. Review of applications will begin February 20, 2006, and continue until the position is filled. We intend to begin interviewing candidates by mid-March, 2006. *Colgate University is an Equal Opportunity/Affirmative Action Employer. Developing and maintaining a diverse faculty and staff further the University's academic mission. Women and minorities are especially encouraged to apply.*

POSITIONS OPEN

Applicants are invited to apply for an **ASSISTANT/ASSOCIATE PROFESSOR** position (12 month, non-tenure track) in **functional genomics, proteomics or metabolomics** in the **Center of Excellence for Poultry Science** (**website: http://www.poultryscience.uark.edu**) at the **University of Arkansas** (Fayetteville, Arkansas). The successful candidate will develop an extramurally funded research program in the area of poultry biology, with specific emphasis on using emerging technologies of global expression analysis directed towards enhancing productivity, disease resistance, and/or genetics in commercial poultry. Individuals with expertise in growth and development, obesity, disease, immunogenetics, or muscle structure/quality are encouraged to apply. The candidate will mentor M.S. and Ph.D. students, and teach at the undergraduate and/or graduate level. Demonstrated research ability, effective oral and written communication, and evidence of successful grantsmanship are essential. Excellent opportunities exist for interdisciplinary and collaborative research with faculty within the Department, College and campus. Scientists in the Center are housed in a state-of-the-art laboratory/office complex that contains a campus-wide DNA resource Center, a Cell Sorting and Characterization Center, and a state-wide Mass Spectrometry Laboratory. Salary will be commensurate with experience. Review of applicants will commence March 15, 2006, and continue until a suitable applicant is obtained. Submit resume and at least three letters of reference to: **Dr. Robert F. Wideman, Jr. (Chair, Search Committee, e-mail: rwideman@uark.edu), Department of Poultry Science, University of Arkansas, Fayetteville, AR 72701 (telephone: 479-575-4397 or 575-3699).**

FACULTY POSITIONS IN MOLECULAR AND COMPUTATIONAL BIOLOGY
University of Southern California

The Molecular and Computational Biology Section of the Department of Biological Sciences in the College of Letters, Arts and Sciences at the University of Southern California (USC) invites applications for multiple open-rank tenure-track Faculty Positions. We are seeking outstanding colleagues who use modern molecular, genetic and/or computational approaches to address fundamental biological questions in diverse model systems that enhance and complement our current research strengths. Our program is undergoing significant expansion, including recent occupancy of a new molecular and computational biology research building.

Disciplines of major interest include, but are not limited to, cell and developmental biology; computational biology and bioinformatics; plant molecular biology; neurobiology; evolutionary biology; systems biology.

Review of applications will begin immediately. Please send curriculum vitae, statement of research objectives, and three letters of recommendation to **e-mail: msearch@usc.edu.** For additional information about our program, visit our **website: http://www.usc.edu/dept/LAS/biosci/mcb/.**

USC is an Affirmative Action/Equal Opportunity Employer.

BIOCHEMISTRY, HENDRIX COLLEGE

Tenure-track **ASSISTANT PROFESSOR** in biochemistry, beginning August 2006. Ph.D. required, postdoctoral experience preferred. Candidates must be committed to excellence in teaching and research. Competitive startup funding and research time assignment provided in new facilities. Details regarding this position are available at **website: http://www.hendrix.edu/chemsearch.** Hendrix College is a selective liberal arts college with particular strength in the sciences. Send letter, curriculum vitae, undergraduate and graduate transcripts, teaching philosophy, and detailed research plans, and arrange for three letters of reference to be sent to: **Dr. Randall Kopper, Department of Chemistry, Hendrix College, 1600 Washington Avenue, Conway, AR 72032.** *Hendrix is an Equal Opportunity Employer. Women and members of minority groups are especially encouraged to apply.*

Positions @ NIH
THE NATIONAL INSTITUTES OF HEALTH

Office of the Director
Office of Behavioral and Social Sciences Research

The Office of Behavioral and Social Sciences Research (OBSSR), a component of the National Institutes of Health (NIH) and the Department of Health and Human Services, is seeking a dynamic individual to serve as a Medical Officer to advise the Director and Deputy Director, OBSSR on programmatic issues relating to clinical and preventive medicine, social and behavioral determinants of health, and health services research, as well as other social and behavioral sciences areas to strengthen the NIH's research and training initiatives relating to human behavior in order to promote health and prevent diseases. Applicants will be evaluated on the extent to which their application shows possession of the knowledges, skills, and abilities defined below.

- Knowledge of clinical, preventive, occupational, and environmental medicine, especially with respect to social and behavioral determinants of health. This includes broad comprehension of the principles, theories and methodological approaches in the biomedical, behavioral and social science disciplines in order to combine approaches from the different disciplines to understand health and well being.
- Ability to communicate orally and in writing, with senior management officials and scientists, for the purpose of interpreting and explaining research studies, results, initiatives and opportunities which impact the conduct of a research program.
- Ability to plan, direct and guide the policy development and operations of a major research project or research initiative.

Additional information and application procedures may be obtained by visiting **www.usajobs.opm.gov**. Click **"search"**, then insert the vacancy announcement number **OD-06-105003** in the **'key word search'** box. Applications must be received by **MIDNIGHT on February 28, 2006**. Questions regarding this vacancy may be addressed to **Beverly Davis on 301 496-1443**.

Division of Cancer Biology
Cancer Etiology Branch
Chemist/Microbiologist/Biologist

With nation-wide responsibility for improving the health and well being of all Americans, the Department of Health and Human Services (DHHS) oversees the biomedical research programs of the National Institutes of Health and those of NIH's research Institutes.

The National Cancer Institute (NCI) at the NIH is seeking a Chemist, Microbiologist, or Biologist to fill the position of Chief in the Cancer Etiology Branch (CEB). This branch administers a large portfolio of research grants covering a broad spectrum of topics directed at understanding the biological basis of cancer, emphasizing cancer etiology, biological and chemical carcinogenesis. The Branch Chief uses expert knowledge of the research field and administrative experience to provide the Branch with leadership, direction, coordination and perspective as well as to respond to NCI leadership. The Chief develops initiatives in the area of scientific responsibility, establishes program priorities, evaluates program effectiveness, provides information, advice and consultation to individual scientists and institutional management officials relative to NIH and NCI funding, provides NCI leadership with recommendations concerning funding needs, priorities and strategies, and organizes meetings and workshops to further program objectives.

A full Civil Service package of benefits (including health and life insurance options, retirement, paid holidays, vacation and sick leave) is available.

The NCI vacancy announcement for this position contains complete application procedures and lists all mandatory information, which you must submit with your application. To obtain the vacancy announcement for this position which will be available on **01/06/2006** and posted under announcement **#NCI-05-104816**, you may visit the website **https://www.usajobs.opm.gov**. Questions can be directed to **Eugene McDougal on (301) 435-5722**. Please see vacancy announcement for application submission requirements.

The NIH Director's Wednesday Afternoon Lecture Series

Biomedical scientists around the world are invited to join us online to hear leading investigators present their latest results to the NIH Intramural Research community. Lectures may be viewed live at 3:00 p.m., EST (20:00 GMT) on Wednesdays, from September through June. Live webcasts can be viewed under "Today's Events" at: <http://videocast.nih.gov/>

The current schedule of lectures is available at: <http://www1.od.nih.gov/wals/schedule.htm>

Upcoming Lectures:

- **February 1:** Michael Rossmann, Purdue University: The Structure and Function of Flaviviruses
- **February 8:** Michael Stryker, University of California, San Francisco: Making Maps in the Brain
- **February 15:** Rena Wing, The Miriam Hospital, Providence: Winning at Losing: The Art and Science of Long-Term Weight Control
- **February 22:** Enrique Rodriguez-Boulan, Cornell University: Epithelial Cell Polarity: Life in Between Two Worlds

The lecture series has archived more than 240 lectures since 1998. Archived lectures can be viewed under ""Wednesday Afternoon Lectures" at: <http://videocast.nih.gov/PastEvents.asp>

WWW.NIH.GOV

NIDDK

POSTDOCTORAL FELLOWSHIPS IN DNA REPAIR AND RECOMBINATION AT THE NIH

We are a group of molecular and structural biologists whose main interests are in the areas of DNA repair and recombination. We are all located in a single building on the main intramural campus of the NIH in Bethesda, Maryland, a 20-minute ride from Washington, D.C. The intramural program of the NIH offers an outstanding research environment and many opportunities for collaborations. Applications are invited from individuals of the highest caliber with Ph.D., M.D., or M.D., Ph.D. degrees. Salary and benefits will be commensurate with experience of the candidate. The current research interests of the group include:

-Biochemistry and molecular biology of double-strand break repair and homologous recombination. Current interests include mouse meiosis (Dev Cell (2003) **4**: 497; NSMB (2005) **12**: 449; JCS (2005) **118**: 3233) and evolutionary genomics (Nature Genetics (2004) **36**: 642). (**Dan Camerini-Otero**).

-Molecular mechanism of retroviral DNA integration. Biochemical, structural and functional analysis of HIV integrase and other proteins and nucleoprotein complexes involved in retroviral integration (http://orac.niddk.nih.gov/www/craigie/crahome.html). (**Bob Craigie**: bobc@helix.nih.gov)

- Structural Biology of Site-Specific DNA Recombination. Current interests include the Adeno-Associated Virus (Mol. Cell (2002) **10**:327; (2004) **13**:403), and other eukaryotic and prokaryotic recombination systems. (Nature (2004) **432**:995; Mol. Cell (2005) **20**:143; NSMB (2005) **12**:715). (**Fred Dyda**: Fred.Dyda@nih.gov)

- Molecular Mechanisms of DNA Mismatch Repair. Biochemistry and molecular biology of mismatch repair and the cellular response to DNA damage. (Nature (2000) **407**:703; J. Mol. Biol. (2003) **334**:949; Proc. Natl. Acad. Sci. (2003) **100**:14822). (**Peggy Hsieh**: ph52x@nih.gov)

- Single-molecule biochemical study of macromolecular complex assembly/disassembly dynamics involved in DNA transposition, site-specific recombination and related reactions. (Mol. Cell (2002) **10**: 1367). (**Kiyoshi Mizuuchi**: kmizu@helix.nih.gov)

Interested candidates should send a letter stating their interests, their curriculum vitae and list of publications, and arrange to have letters from three references emailed to one of the investigators above or if you would like to be considered for more than one lab to **Dan Camerini-Otero (camerini@ncifcrf.gov) at: Bldg. 5, Rm 201, 5 Memorial Dr MSC 0538, National Institutes of Health, Bethesda, MD 20892-0538.**

NIDDK

NIDDK Tenure-Track Investigator: Modeling of Cell Biological and Physiological Systems

The National Institute of Diabetes and Digestive and Kidney Diseases (NIDDK), National Institutes of Health (NIH), Department of Health and Human Services, invites applications for tenured or tenure track positions in the Laboratory of Biological Modeling. The Laboratory is currently comprised of scientists who use computational approaches to understand cell biological and physiological systems. Specific areas of research interest will include mathematical modeling at the subcellular, cellular, tissue and system levels. Excellent computational facilities and resources for rapid achievement of research goals are available. LBM is in close proximity in particular to the NIDDK Computational Chemistry Core Facility, engaged in molecular modeling. The position offers unparalleled opportunities for interdisciplinary collaboration within NIDDK and throughout NIH. For further information about NIDDK, see **http://www.niddk.nih.gov**.

Candidates must have a Ph.D., M.D., or equivalent degree in the physical or biomedical sciences. He or she should have an outstanding record of research accomplishments in mathematical modeling and will be expected to propose and pursue an innovative and independent research program. Salary and benefits will be commensurate with the experience of the individual. Applicants should send a curriculum vitae and list of publications, copies of three major publications, a plan for future research, and three letters of reference by **February 15, 2006 to Dr. Robert Tycko, Chair of the Search Committee, Laboratory of Chemical Physics, Building 5, Rm. 112, 5 Memorial Drive, NIH, Bethesda, MD 20892-0520, tel.: 301-402-8272, fax: 301-496-0825, email: Tycko@helix.nih.gov.**

Position Description:

The successful candidate will establish an independent group with research interests focused on mathematical modeling at the subcellular, cellular, tissue, or organism levels. Other members of the Laboratory of Biological Modeling (**http://lbm.niddk.nih.gov**) conduct basic research on a wide variety of topics including insulin secretion (A. Sherman), insulin action (A. Sherman, C. Chow), metabolism (K. Hall), adipocyte differentiation (V. Periwal), calcium homeostasis (A. Sherman) and neuroscience (C. Chow), all relevant to diabetes and obesity. Interaction is expected with experimental laboratories or other computational groups in NIDDK or other NIH institutes.

ÉCOLE POLYTECHNIQUE
FÉDÉRALE DE LAUSANNE

Faculty Positions in Microbiology and Infectious Diseases

The School of Life Sciences at EPFL invites applications for faculty positions in Microbiology and Infectious Diseases within the framework of its newly established Global Health Institute. We are primarily seeking candidates for **tenure track assistant professorships**, but suitably qualified applicants may also be considered at **associate and full professor level**.

Successful candidates will develop an independent and vigorous research program, participate in both undergraduate and graduate teaching, and supervise PhD students.

Candidates from all areas of Microbiology and Infectious Diseases will be considered, but preference will be given to applicants with interests in **cellular and molecular mechanisms of microbial pathogenesis** (bacteria, viruses, parasites and fungi), **genetics of host-pathogens interactions, innate and adaptive immunity to pathogens, therapeutics, diagnostics and vaccine development**. Candidates working on topics of primary relevance for major worldwide infectious threats (malaria, tuberculosis, viral diseases) are particularly encouraged to apply.

Significant start-up resources and state-of-the-art research infrastructure will be available, within the framework of a campus that fosters very strong interactions between life sciences, basic science, informatics and engineering. Salaries and benefits are internationally competitive.

Applications should be submitted by e-mail to monika.loperiol@epfl.ch, and should include the following documents in PDF format: curriculum vitae, publication list, brief statement of research and teaching interests, names and addresses (including e-mail) of 3 references for junior positions, 6 for senior positions. Screening will start on **March 1st, 2006**.

Further questions may be addressed to:
Professor Didier Trono, Dean
EPFL, School of Life Sciences, Station 15, CH-1015 Lausanne, Switzerland

For additional information on EPFL, please consult http://www.epfl.ch

EPFL is an equal opportunity employer

THE UNIVERSITY OF MAINE

Dean, College of Natural Sciences, Forestry, and Agriculture and Director, Maine Agricultural and Forest Experiment Station

The University of Maine invites applications and nominations for the position of Dean of the College of Natural Sciences, Forestry, and Agriculture, and Director of the Maine Agricultural and Forest Experiment Station (MAFES).

The Dean is the chief executive officer of the College and reports to the Provost. The Dean/Director provides leadership for the College and the Station and fosters excellence in teaching, research, and service to the community. The Dean represents the College, MAFES, and the University to external agencies, constituents, and legislative delegations at the local, state, and federal levels.

A complete list of duties and qualifications is online at **www.umaine.edu/eo/jobs**.

MAINE'S LAND GRANT AND SEA GRANT UNIVERSITY
A Member of the University of Maine System

The University of Maine is an Equal Opportunity, Affirmative Action Employer. Minorities and women are strongly encouraged to apply.

ASSOCIATE DIRECTOR AND ENDOWED CHAIR FOR CLINICAL RESEARCH

THE METHODIST HOSPITAL RESEARCH INSTITUTE

The Methodist Hospital Research Institute of The Methodist Hospital, Houston, Texas, seeks an exceptional physician scientist to lead its effort in clinical research. The Methodist Hospital System consists of 1,450 beds, including 950 located in the Texas Medical Center in Houston. Together with our partners at Weill Cornell Medical College and New York-Presbyterian Hospital in New York City, there are 3,500 beds available for clinical investigation and clinical trials. The successful applicant will be responsible for organizing and leading the Institute's clinical research in Houston and collaborating with our Cornell and NYP colleagues. We encourage applications from individuals who currently lead substantial programs conducting clinical research. The hospital is in an unprecedented expansion phase, which includes building a new 560,000 SF outpatient facility and 300,000 SF research building. These state-of-the art facilities are designed to foster extensive collaboration between clinical and basic scientists.

The successful applicant will hold an endowed chair and receive a generous salary, fringe benefits, and a relocation package. Individuals interested in this unique career opportunity should send via e-mail a curriculum vitae, including grant funding information and the names of five references to:

Michael W. Lieberman, M.D., Ph.D., c/o Ms. Patricia Sandler
Director, The Methodist Hospital Research Institute
6565 Fannin, Mail Stop B154
Houston, TX 77030
psandler@tmh.tmc.edu

Methodist The Methodist Hospital Research Institute

LEADING MEDICINE

University of Massachusetts Medical School
UMASS

TENURE-TRACK NEUROSCIENCE POSITION

The Brudnick Neuropsychiatric Research Institute (BNRI), established as part of the unprecedented research expansion at the University of Massachusetts Medical School, invites applications for a tenure-track position at the level of Assistant/Associate Professor. The BNRI was established in 2000 as a division of the Department of Psychiatry and is committed to broad based research investigating basic neurobiological principles underlying psychiatric disorders. Faculty interests focus on a variety of neurobiological problems and psychiatric disorders, with a common theme in the neurobiology of addiction. Applicants whose interests focus on addiction are especially welcomed, particularly those with a strong behavioral component. The BNRI is integrated into the Interdepartmental Neuroscience Program, which provides opportunities for graduate training and interactions with a large group of multidisciplinary neuroscientists. The BNRI is housed in a state-of-the-art laboratory facility, which includes magnets for high resolution functional brain imaging. The successful candidate is expected to establish an independent research program and play an integral role in new program initiatives. The position is highly competitive with regard to salary, start-up funds, and laboratory space.

Applicants should send a CV, statement of research interests, and names and addresses of three references to:

Dr. Steven Treistman, Director
Brudnick Neuropsychiatric Research Institute
University of Massachusetts Medical School
303 Belmont Street
Worcester, MA 01604

E-mail: bnri@umassmed.edu
www.umassmed.edu/bnri

An Equal Opportunity/Affirmative Action Employer.

Pacific Northwest National Laboratory

Operated by Battelle for the U.S. Department of Energy

PNNL's innovations in the computational sciences result in tools that allow scientists to understand data in real time using high-performance, data-intensive computing. Our leading-edge capabilities in informatics, modeling, and simulation enable scientific discoveries that lead to solutions in the areas of Computational Biology and Bioinformatics, Computational Chemistry, and Computational Materials Science. To learn about the Computational and Information Sciences Directorate at PNNL, visit: **http://cisd.pnl.gov/**.

Our vision is to be nationally recognized for leadership in providing computational and information sciences, and secure science-driven, high-end computing research and development. We are seeking exceptional candidates to fill the following positions:

Full Time Research Positions:
- 110750 – Senior Scientist: Biomolecular Modeling and Simulation
- 110851 – Senior Scientist: Computational Biology
- 110852 – Senior Scientist: Bioinformatics

Student / Post Doc Positions:
- 107123 – Post Doc: Computational Chemistry
- 110251 – Post Doc: Computational Biology
- 110567 – Post Doc: Biomolecular Modeling and Simulation
- 110578 – Post Doc/Grad Student: High Performance Parallel Computing

To learn more about these positions and apply, visit our Careers Website - **http://www.jobs.pnl.gov** - and search for the job number listed.

PNNL offers a comprehensive salary and benefits package. All positions are located in Richland, WA; relocation assistance is available.

We are an EEO/AA Employer.

HUMAN MICROBIAL PATHOGENESIS
FACULTY POSITIONS — OPEN RANK
CENTER FOR MOLECULAR & TRANSLATIONAL HUMAN MICROBIAL PATHOGENESIS RESEARCH
THE METHODIST HOSPITAL RESEARCH INSTITUTE

The Methodist Hospital Research Institute at The Methodist Hospital in Houston, Texas, seeks several exceptional scientists studying the molecular basis of human microbial pathogenesis. Individuals who currently lead multiple-PI teams and collaborating PIs who desire to co-locate also will be considered.

The Methodist Hospital System consists of 1,450 beds, including 950 located in the Texas Medical Center in Houston. With our partners at Weill Cornell Medical College and New York-Presbyterian Hospital in New York City, there are 3,500 beds and many outpatients available for human microbial pathogenesis research. Collaborative opportunities also are available with the University of Houston and other local institutions.

The hospital has entered an unprecedented expansion phase that includes building a 300,000 SF state-of-the-art research building with bio-containment and non-human primate facilities, and a 560,000 SF ambulatory care building, both designed to foster interdisciplinary collaboration.

We are interested in candidates using new technologies to study molecular events occurring at the host-pathogen interface.

Successful applicants will be responsible for establishing or expanding nationally recognized, externally funded research programs.

Applicants must have an advanced degree (PhD, DVM, MD, or MD/PhD). Successful applicants will receive an outstanding recruitment package. Interested individuals should send via e-mail a curriculum vitae; description of research interests, future directions, and grant funding information; and the names of at least three references to:

James M. Musser, M.D., Ph.D. c/o Ms. Irene Harrison
Co-Director and Executive Vice President
The Methodist Hospital Research Institute
6565 Fannin, Mail Stop B154, Houston, TX 77030
E-mail: iaharrison@tmh.tmc.edu

Methodist The Methodist Hospital Research Institute

LEADING MEDICINE℠

ACADEMIA SINICA, TAIPEI, TAIWAN
POSITION ANNOUNCEMENT

POSITION: The Institute of BioAgricultural Sciences (IBS), at Academia Sinica, Taipei, invites applications for two tenured ASSISTANT RESEARCH FELLOW positions. Candidates must have a Ph.D. (or equivalent) and an outstanding record of research achievement. The successful candidates are expected to develop state-of-the-art research programs in the area of integrative plant stress biology. Preference will be given to candidates whose approaches incorporate molecular biochemistry and secondary metabolites, or systems biology. An important mission of the IBS is to engage in translational research and platform technologies. The successful candidate will be required to participate in collaborative research projects that will contribute to these goals.

LOCATION: Academia Sinica, the most prominent academic institution in Taiwan, is located in Taipei, Taiwan. The Academy is comprised of world-class institutes. The infrastructure for research is excellent, and Research Fellows are afforded well-equipped laboratories and access to excellent research funding opportunities.

IBS: The Institute of BioAgricultural Sciences pursues basic and translational research in bioagricultural sciences that have the potential to generate new platform technologies or develop into novel systems or products in biotechnology. Plant stress biology and herbal medicine are two major research areas within the IBS. For more information, please visit our website at http://ibs.sinica.edu.tw/E_www/

TO APPLY: Applicants should submit the following materials, online, at http://ibs.sinica.edu.tw/jobs/ (a) Cover letter; (b) Curriculum vitae, including publications; (c) Summary of research accomplishments; (d) Clearly focused description of future research plans; (e) PDF copies of major publications; (f) Names and contact information for four referees.

Closing date: Open until filled although to assure full consideration, applications should be received prior to March 30, 2006.

Candidates should arrange four letters of recommendation to be submitted by e-mail to: ibshire@gate.sinica.edu.tw or sent by regular mail to:

Ning-Sun Yang, Director, Institute of BioAgricultural Sciences, Academia Sinica, No. 128, Academia Rd. Sec. 2, Nankang, Taipei 11529, Taiwan ROC

UNIVERSITY of VIRGINIA HEALTH SYSTEM

CHAIR, DEPARTMENT OF MOLECULAR PHYSIOLOGY AND BIOPHYSICS

The University of Virginia School of Medicine is seeking an established scientist to assume the position of Chair. The department has a history of national prominence with established strengths in smooth muscle physiology, structural biology and cardiovascular disease (see: **www.healthsystem.virginia.edu/internet/physio**). The successful candidate requires an internationally recognized research program, a record of scholarly achievement, and outstanding leadership abilities. We invite either applications or nominations. Review of applications commences March 1, 2006 and will continue until the position is filled. Communications will be kept in confidence.

Please submit a letter describing interest and qualifications and current CV to:

Professor David L. Brautigan
Chair, School of Medicine MP&BP Chair Search
UVA School of Medicine
P.O. Box 800419
Charlottesville, VA 22908-0419

The University of Virginia is an Equal Opportunity/Affirmative Action Employer that seeks to promote diversity and tolerance in the University community.

UNIVERSITY OF KENTUCKY
PROFESSOR
ENVIRONMENTAL CHEMISTRY/TOXICOLOGY

As part of a Provost's Initiative in Environmental Sciences, the University of Kentucky is searching for a nationally recognized individual with an established, exciting interdisciplinary research program focused on the fate and transport mechanisms that govern bioavailability of organic chemicals and heavy metals in terrestrial or aquatic ecosystems. Research should address important pollutants of national and regional concern, due to their prevalence, tendency to bioaccumulate in food chains, and toxicity to animals and humans. Examples of such pollutants include pesticides, pharmaceuticals, PCBs, mercury, arsenic, chromium, and lead from agricultural, industrial, and domestic sources. The individual is expected to add significant expertise and leadership to a University of Kentucky initiative in Environmental Chemistry.

Areas of research should be competitive and fundable at the federal level and could include, but are not limited to, the creation of 'omics' technologies with applications to toxicology (including DNA microarray expression analysis, proteomics, and metabolomics), development of advanced methods to detect pollutants in environmental samples, and biological and chemical pollutant remediation strategies that decrease exposure risks to susceptible populations and the environment.

The individual will be encouraged to participate as a Senior Research Fellow of the Tracy Farmer Center for the Environment at the University of Kentucky. The Tracy Farmer Center focuses on environmental problems and issues facing the residents of the Commonwealth of Kentucky, the nation, and the world and develops sustainable solutions to these problems. As a Senior Research Fellow the individual will help set scientific priorities and direction for the Center.

An attractive start-up package is associated with this position. Resources are available to relocate and support members of a research team. We expect that this individual would be hired as a Full Professor at the University of Kentucky. The academic College and Department for this individual are flexible and will be based on the candidate's interests, experience, and qualifications. The individual will have the opportunity to collaborate with researchers from several academic units, including the Colleges of Agriculture, Arts and Sciences, Engineering, and Medicine, which administers the Graduate Center for Toxicology.

Candidates should submit a letter of application that includes an overview of their research interests and its relationship to this position at the University of Kentucky, curriculum vitae, selected recent reprints, and names, addresses, phone numbers and e-mail addresses of five references. All materials should be sent to: **John J. Obrycki, Chair of Environmental Chemistry/Toxicology Search Committee, University of Kentucky, Department of Entomology, S-225 Agricultural Science North, Lexington, KY 40546-0091 USA; E-mail: john.obrycki@uky.edu**. Review of applications will begin on **February 28, 2006**, and continue until the position is filled.

The University of Kentucky is an Equal Opportunity Employer and encourages applications from minorities and females.

www.uky.edu

FACULTY POSITION IN SENSORY NEUROSCIENCE

The Department of Physiology, University of Wisconsin School of Medicine and Public Health, invites applications for a tenure-track assistant professor position in sensory neuroscience. We seek to recruit an outstanding investigator with interests that complement our existing strong auditory group (**http://www.physiology.wisc.edu**) and uses integrative approaches to study problems at the molecular, cellular or systems level. The Department encourages applications from individuals working on all aspects of the physiology of the auditory system including inner ear function, development and regeneration, or central processing in the auditory system, although outstanding candidates in other areas of sensory neuroscience will also be considered. The successful candidate will teach in one or more programs in the Department such as team-taught courses in physiology and neuroscience and participate in Ph.D. and post-doctoral training programs. The Department features a breadth of inquiry encompassing molecular to systems level research, a supportive collegial work environment, and a collective commitment to collaborative research programs. Opportunities for participation in campus-wide interdisciplinary research and training programs are excellent.

Applicants should send curriculum vitae, a one to two page summary of research interests and plans, and three letters of reference to: **Alice Puchalski, Faculty Search Committee, Department of Physiology, University of Wisconsin Medical School, 1300 University Avenue, Madison, WI 53706** or electronically to **facsearch@physiology.wisc.edu**. To ensure consideration, please submit complete application by **March 15, 2006**. However, applications will be accepted until the position is filled.

Unless confidentiality is requested in writing, information regarding applicants and nominees must be released upon request. Finalists cannot be guaranteed confidentiality. The UW-Madison is an Equal Opportunity/Affirmative Action Employer.

EaStCHEM
The Edinburgh and St Andrews Research School of Chemistry

THE UNIVERSITY OF EDINBURGH

Chair in Inorganic Chemistry

Salary will be in the professorial range

The School of Chemistry at the University of Edinburgh is internationally renowned and has top quality ratings for both teaching and research. The Universities of Edinburgh and St Andrews have now jointly established a new research school of chemistry, EaStCHEM, which is the premier research school for chemistry in Scotland.

As part of this exciting initiative, EaStCHEM requires a world-class scientist to a Chair of Inorganic Chemistry, to be based at the University of Edinburgh. Edinburgh's School of Chemistry offers an innovative and interdisciplinary approach to traditional chemistry subjects and is at the forefront of research in emerging disciplines. The breadth of research in the School has been further enhanced by the recent appointments of Professors Mark Bradley and Paul Madden FRS. We are seeking an outstanding individual with an established international reputation for excellence and achievement in research to appoint to this Chair.

Apply online, view further particulars or browse more jobs at our website www.jobs.ed.ac.uk Alternatively, telephone the recruitment line on 0131 650 2511. Ref: 3005360SC. Closing date: 24 February 2006. Interviews will be held on 24 March 2006.

Committed to Equality of Opportunity

SCOTT & WHITE

College of Medicine
The Texas A&M University System Health Science Center

Pediatric Hematology-Oncologist

The Section of Pediatric Hematology/Oncology at **Scott and White Clinic** and the **Texas A&M University System Health Science Center College of Medicine** (TAMUS HSC-COM) are seeking a clinician scientist with current research grants for a faculty position in a rapidly growing program. The candidate should be BE/BC in pediatric oncology and committed to an academic career. The successful candidates will join and enhance ongoing efforts in basic and translational research, with an institutional commitment to building a world-class experimental therapeutics program. An outstanding start-up package includes high quality laboratory space, excellent benefits and competitive salaries commensurate with academic qualifications. The position guarantees 75% protected time for research activities.

Scott & White Clinic is a 500+ physician directed multi-specialty group practice that is the leading provider of cancer care in Central Texas. Scott and White Clinic and the 486 bed tertiary Scott & White Memorial Hospital is the main clinical teaching facility for TAMUS HSC-COM. Outstanding clinical practice and laboratory facilities on campus that perform state of the art molecular and cellular biology research, flow cytometry, genomics and biostatistics are in place to support the research effort.

Please contact: **Don Wilson, M.D. Professor and Chairman, Department of Pediatrics, Scott & White, 2401 S. 31st, Temple, TX 76508. (800)725-3627 dwilson@swmail.sw.org Fax (254) 724-4974.**

For more information about Scott & White, please visit www.sw.org For Texas A&M www.tamhsc.edu. Scott & White is an equal opportunity employer.

GOVERNMENT OF INDIA
MINISTRY OF SCIENCE & TECHNOLOGY
DEPARTMENT OF BIOTECHNOLOGY
NEW DELHI - 110 003

INVITES APPLICATIONS FOR THE POST OF DIRECTOR, CENTRE FOR DNA FINGERPRINTING & DIAGNOSTICS (CDFD), HYDERABAD

Applications are invited for the post of Director, Centre for DNA Fingerprinting & Diagnostics (CDFD), Hyderabad, an autonomous institute under the Department of Biotechnology, Government of India, from Indian citizens including those staying abroad and Non-Resident Indians (NRIs). The main activities of the Centre are Research & Development in Genomic Science and Genome based applications including fingerprinting and diagnostics in health care, agriculture and forensic science.

The applicants should be below 55 years of age. The post carries scale of pay of **Rs 22,.400-525-24,500/-** with usual allowances as per the Govt of India Rules. The applications along with detailed curriculum vitae including the date of birth, address for correspondence including telephone, fax and e-mail address, qualifications acquired, professional and research experience, present position and scale of pay with total emoluments, publication details and a 500-words write-up on the candidate's vision of CDFD for the next ten years may be sent to Shri Virendra Kapoor, Deputy Secretary, Department of Biotechnology, Block-2, CGO Complex, Lodi Road New Delhi - 110 003, superscribing the cover "Application for the Post of Director, CDFD" so as to reach him by 6th March, 2006. The detailed advertisement and format of application is available at DBT website www.dbtindia.nic.in and at the CDFD website www.cdfd.org.in

The Department reserves the right to relax any of the requirements prescribed above.

HEALTH EFFECTS INSTITUTE

Science Positions

HEI seeks strong candidates at various levels to strengthen its scientific staff. HEI is a nonprofit organization designed to provide impartial, relevant scientific information about the health effects of air pollution to decisionmakers in government and industry. Its core funds come equally from the U.S. Environmental Protection Agency and industry; HEI also receives funds for some projects from other governments, industries, and foundations. HEI is funding a broad range of epidemiologic, toxicologic, and other research at universities and research centers in many countries. Priorities in HEI's strategic plan are: (1) health effects of air pollution; (2) assessing emerging technologies; (3) evaluating the public health impact of actions to improve air quality; (4) and international health effects research. Additional information about HEI's work can be found at **www.healtheffects.org**.

Epidemiologists/Biostatisticians: HEI has 2 openings for epidemiologists or biostatisticians to work with HEI 's Research and Review Committees and Scientific Staff to develop and implement HEI's research program on air pollution and health. We are looking for scientists with a strong foundation in epidemiologic and statistical methods who are interested in the health effects of air pollution. Experience in air pollution epidemiology is desirable, but not required. These scientists would plan future research directions, participate in selecting and overseeing studies, review and write commentaries on final reports from HEI investigators, and contribute to literature reviews on critical issues. Interesting responsibilities on the horizon are:

- Initiating and overseeing a major research program to investigate which components or sources of particulate air pollution pose greater health risks than others.
- Managing ongoing "accountability" studies in several countries that are measuring the exposure and health impacts of air quality actions designed to improve public health.
- Reviewing final reports of HEI-funded epidemiologic studies on health effects of air pollution from traffic and from particulate air pollution in North America and Europe, and on accountability studies, and writing commentaries, to be published with the reports, that describe strengths, limitations, scientific contributions, and relevance to human health effects of the research in terms understandable to a diverse audience.
- There are also periodically opportunities to contribute as an author of reviews of critical scientific issues.

We seek to hire at the Staff Scientist and Senior Scientist levels. Both require a doctoral degree in epidemiology or biostatistics; the Senior Scientist position requires 5+ years of subsequent experience in epidemiologic research. Experience in project management is a priority. Good written and oral communication skills are essential. Experience on how research is used in public health and/or policy settings is desirable.

Research Assistants: HEI seeks to hire 1 or 2 Research Assistants who would assist Staff Scientists by gathering and organizing information and drafting summaries on topics relevant to current projects. Backgrounds in biology, chemistry, toxicology, epidemiology, mechanical engineering, environmental science, and similar disciplines are of interest. These positions offer an opportunity for someone with initial science training to obtain experience as she or he considers next steps in education and career development.

As part of one of these positions, in addition to work described above, we are also looking for someone to assist in managing HEI's quality assurance (QA) program on funded research, which is conducted by external QA auditors. Previous QA experience is desirable, but not required; HEI is willing to pay for QA training. Applicants interested in the QA aspect should have some research experience. The Research Assistant position requires a bachelor's or master's degree in one of the disciplines listed above.

Applying for These Positions: For all positions, interested applicants should submit a letter, resume, and writing samples no later than **April 30, 2006**. Please send application material to: **Ms. Terésa Fasulo, Manager of Science Administration, Health Effects Institute, Charlestown Navy Yard, 120 Second Avenue, Boston MA 02129, tfasulo@healtheffects.org**.

HEI is an Equal Opportunity Employer.

U.S. Environmental Protection Agency
Office of Research and Development
National Center for
Environmental Assessment (NCEA)

Supv. Biologist/Toxicologist/Health Scientist/Physical Scientist/Mathematical Statistician
Ez hire Announcement #RTP-DE-2006-0048 or RTP-MP-2006-0080

The U.S. Environmental Protection Agency is seeking highly qualified applicants for two Branch Chief positions with the National Center for Environmental Assessment (**http://cfpub.epa.gov/ncea/**) which are located in Cincinnati, Ohio. Duties include supervision and leadership of an interdisciplinary team of scientists conducting high-profile human health and ecological assessments and developing cutting-edge risk assessment methods, with emphasis on water quality and hazardous waste.

Excellent benefits: The selected candidate will be eligible for a full benefits package, including paid relocation, health insurance, life insurance, retirement, and vacation and sick leave. This is a permanent, full time position. U.S. citizenship is required.

Salary Range: The salary range is $91,080 to $139,275 (GS 14/15) per year, commensurate with qualifications.

Qualifications: A bachelor's degree (or higher) is required. Desirable applicants will have an advanced degree and demonstrated experience in conducting research and leading research teams in environmental health, toxicology, biology, physical science, mathematical statistics, or a related field.

How to Apply: Applicants should apply through Ezhire at **http://www.epa.gov/ezhire** Select apply for jobs. If you are already registered in Ezhire@EPA system, access the vacancy announcement through Registered Users. Otherwise, select New Users and complete the registration process. The vacancy announcement will be open through March 13, 2006. Application materials must be submitted with 48 hours from the closing date of the announcement. You need to submit the additional documentation described in the full text vacancy. Questions regarding this vacancy may be directed to **Joann Kelleher, Human Resources Management Division** at **kelleher.joann@epa.gov**.

The US EPA is an Equal Opportunity Employer.

THE UNIVERSITY of WISCONSIN MADISON

NMR Postdoctoral Position Opening

The Center for Eukaryotic Structural Genomics (CESG) at the University of Wisconsin-Madison Biochemistry Department in Madison, Wisconsin, USA, has an open postdoctoral position on its team of NMR structure solvers. For more information about the University of Wisconsin-Madison, see **www.wisc.edu**.

CESG is supported by the National Institute of General Medical Sciences (NIGMS) Protein Structure Initiative (PSI), a federal, university, and industry effort aimed at dramatically reducing the costs and lessening the time it takes to determine a three-dimensional protein structure. The long-range goal of PSI is to make the three-dimensional atomic-level structures of most proteins easily obtainable from knowledge of their corresponding DNA sequences. CESG's targets are chosen to expand knowledge of sequence-structure relationships (60%), to include proteins of biomedical relevance (20%), and to accommodate requests from the scientific community (20%). For more information about CESG, see **www.uwstructuralgenomics.org**.

This is a challenging position for an experienced spectroscopist who enjoys solving structures and developing the technology of high-throughput solution structure determination. The NMR team evaluates labeled proteins produced by CESG's cell-based and cell-free platforms, optimizes solution conditions, solves and refines structures, and prepares data depositions. Data are collected at the National Magnetic Resonance Facility at Madison (**www.nmrfam.wisc.edu**).

The position reports to the CESG NMR Team Leader, who in turn reports to Professor John Markley, CESG's Principal Investigator. Team members are encouraged to write and publish papers on interesting structures and to devise and test hypotheses concerning functions of unknown proteins, often times by developing collaborations. The successful candidate will have the possibility of future promotion to an academic staff position. The position is available immediately, and the project is funded through May, 2010.

Interested candidates are encouraged to send their CV and application to: **markley@nmrfam.wisc.edu**.

POSITIONS OPEN

VISITING ASSISTANT PROFESSOR OF BIOLOGY

The Biology Department at the University of the South, also known as Sewanee, invites applications for a Visiting Assistant Professor for the 2006-2007 academic year. The successful candidate will teach in the Department's introductory cell/molecular/physiology class, in biology classes for nonmajors, and possibly in upper division classes in their area of specialty (nine contact hours per week teaching time). Candidates should be enthusiastic about working in the context of the liberal arts tradition in education. The University, with an undergraduate enrollment of about 1,400, has a highly selective program and is located on a biologically diverse 10,000-acre campus on Tennessee's Cumberland Plateau. Review of applicants will begin February 17, 2006, and applications will be accepted until a suitable replacement is found. Send a letter of application, curriculum vitae, statements of teaching and research interests, transcripts, and three letters of reference to:

Dr. David Haskell
Chair, Biology Department
735 University Avenue
The University of the South
Sewanee, TN 37383

E-mailed applications are not accepted. **Website: http://www.sewanee.edu/biology/top.html.** *The University of the South is an Equal Opportunity Employer. Minorities and women are encouraged to apply.*

POSTDOCTORAL POSITION

An NIH funded position is available at New York University School of Medicine to study structure-functions of tetraspanins and related proteins. Strong background in membrane protein expression and purification is required. Send curriculum vitae and names of references to **e-mail: xiangpeng.kong@med.nyu.edu.**

POSITIONS OPEN

JOHNS HOPKINS BLOOMBERG SCHOOL of PUBLIC HEALTH

VIROLOGIST/IMMUNOLOGIST
Department of Molecular Microbiology and Immunology

The Department of Molecular Microbiology and Immunology invites applications for a tenure-track faculty position at any rank for a virologist or immunologist with expertise in influenza. Candidates should have an appropriate doctoral degree and an outstanding record in research. There will be opportunities to develop an independent research program within an interactive environment of investigators interested in pathogenesis of microbial diseases. Applicants should send curriculum vitae and description of research interests, along with names of three references, by March 15, 2006, to: **Diane E. Griffin, M.D. Ph.D., Johns Hopkins Bloomberg School of Public Health, 615 N. Wolfe Street, Room E5132, Baltimore, MD 21205.**

The Johns Hopkins University actively encourages interest from women and minorities and is an Equal Opportunity/Affirmative Action Employer.

POSTDOCTORAL POSITION at the **University of Connecticut** in **molecular neurobiology** to study brain GABAA receptors and mechanisms involved in receptor trafficking and localization. Experience with recombinant DNA and/or membrane proteins is desirable. Salary commensurate with experience. Send curriculum vitae and three references to: **Dr. Angel L. De Blas, Department of Physiology and Neurobiology, 75 North Eagleville Road, U-3156 Storrs, CT 06269-3156. Fax: 860-486-3303; e-mail: angel.deblas@uconn.edu.** *We encourage applications from under-represented groups, include minorities, women, and people with disabilities.*

POSITIONS OPEN

TENURE-TRACK POSITION, Brain Tumor Program, University of Pittsburgh Cancer Institute. The Brain Tumor Program at the University of Pittsburgh Cancer Institute is seeking an experienced basic/translational researcher for a tenure-track position. Candidates should have a doctoral degree, be actively engaged in an established laboratory research program, and have a strong publication record. Candidates should also have attained recognition in molecular genetics, cellular biology, or neuroimmunologic research at the national level; demonstrated promise in becoming a leader in neuro-oncology research; and have experience in directing students, postdoctoral fellows, and/or residents in research. Strong preference will be given to candidates having an extramurally funded research program. The Program provides a highly collaborative research environment with NIH programmatic funding; and functions within the context of a vibrant NCI-designated Comprehensive Cancer Center and university academic environment. Appointment and salary will be commensurate with experience. Send curriculum vitae and the names and addresses of three references to:

Ian Pollack, M.D.
Director, Brain Tumor Program
University of Pittsburgh Children's Hospital
Suite 3705, Third Floor
Pittsburgh, PA 15213

Genetics, ASSISTANT PROFESSOR OF BIOLOGY (tenure-track). **Grand Valley State University** is seeking a broadly trained Geneticist to teach human genetics and other courses. Application deadline: February 24, 2006. For full position description, see **website: http:// www.gvsu.edu/biology.** *Equal Opportunity Employer.*

International Institute of Molecular and Cell Biology in Warsaw is a modern Polish research institute active in the field of molecular biomedicine, with research focused on molecular biology of cancer, neurobiology/neurodegeneration, cell biology, crystallography/structural biology, biomodelling of membrane proteins and their complexes, bioinformatics/molecular evolution and enzyme engineering.

We are seeking highly motivated scientist ready to start his/her independent career as a

GROUP LEADER

who would complement existing research groups and bridge their interest and activities.

We offer work in a scientifically stimulating environment of a large biomedical campus, start-up funds, furnished laboratory and office space in a modern building, possibility of selecting PhD students from leading Polish universities, access to the Institute's equipment, and a salary for the Group Leader and his/her two PhD students for 5 years initially.

Interested scientists should submit:

- CV
- list of publications
- proposal of research plans (up to 3 pages)
- three letters of recommendation

Apply on-line by March 19, 2006 at SC@iimcb.gov.pl. Details on the competition and the Institute can be viewed on website (www.iimcb.gov.pl).

The **Department of Surgery at the University of California San Francisco** is recruiting an **Assistant Professor** to join the Surgical Research Laboratory. The individual will also be cross-appointed in an appropriate basic science department within the Biomedical Sciences Graduate Program. We are seeking an individual (Ph.D, MD/Ph.D) with a strong basic science background to complement the existing strengths in the Surgical Research Laboratory that include angiogenesis, wound healing, hepatic dysfunction and acute lung disease. Individuals with interests in translational research in tissue repair and regeneration, vascular malformations, stem cell biology, cell-matrix interactions and organotypic and/or mouse models are encouraged to apply. The new appointee will be expected to develop an independent research program and obtain extramural funding.

Applicants should send a CV, description of research interests and the names of three references to:

Surgical Research Laboratory
Search Committee
c/o Nancy Boudreau, Ph.D., Director
Surgical Research Laboratory
Box 1302
Dept of Surgery
University of California San Francisco
San Francisco CA 94143

The University of California, San Francisco is an Equal Opportunity/Affirmative Action Employer. The University undertakes Affirmative Action to assure Equal Employment opportunities for under utilized minorities and women, for persons with disabilities, and for Vietnam-era veterans and special disabled veterans.

UNIVERSITY OF DELAWARE

One of theoldest institutions of higher education in this country, theUniversity of Delaware today combines tradition and innovation, offering students a rich heritage along with the latest in instructional and research technology. The University of Delaware is a Land-Grant, Sea-Grant, Urban-Grant and Space-Grant institution with its main campus in Newark, DE, located halfway between Washington, DC and New York City. Please visit our website at: **www.udel.edu**

Assistant or Associate Professor, Avian Virology

Department of Animal and Food Sciences

Applications are invited for a 12-month tenure track faculty position at the Assistant or Associate Professor level. The position is 65% research and 35% teaching and requires a Ph.D. with postdoctoral experience. The successful candidate will be expected to develop an extramurally funded research program in avian virology focused on the study of immunosuppressive or respiratory RNA viruses. The individual will be responsible for advising undergraduate and graduate students relative to curriculum requirements and is expected to participate in the University's nationally recognized undergraduate student research program. Applicants should submit a letter of application, curriculum vitae, a statement of research and teaching interests, and the names and addresses of three professional references to: Dr. Calvin Keeler, Department of Animal and Food Sciences, University of Delaware, Newark, DE 19716-2150. Application may also be submitted electronically to ckeeler@udel.edu. Application deadline is April 3, 2006.

The curriculum vitae and letters of reference shall be shared with departmental faculty.

The UNIVERSITY OF DELAWARE is an Equal Opportunity Employer which encourages applications from Minority Group Members and Women.

University of California
Santa Barbara
Senior Faculty Position in Organic Chemistry

The University of California, Santa Barbara solicits applications for a senior faculty position beginning in the fall of 2006. Creative and energetic candidates in all areas of organic chemistry who have demonstrated extraordinary accomplishment in research and teaching are encouraged to apply. The search will be conducted within the Department of Chemistry and Biochemistry and this position is also supported by the newly created endowed "Robert and Patricia Duggan Chair in Organic Chemistry". Successful candidates will have the opportunity to interact with scientists and engineers across a broad spectrum of disciplines and are strongly encouraged to build campus-wide interactions and alliances with interdisciplinary programs, University-based Centers and Institutes, and other departments within the Colleges of Letters and Sciences, and Engineering. Applicants should send a complete curriculum vitae, a selection of publication reprints (five or less), and a brief statement of future research plans and teaching interests. Applications should be sent to: **Faculty Recruitment Committee; Department of Chemistry and Biochemistry; University of California, Santa Barbara, CA 93106-9510**. A Ph.D. in Chemistry or a related field is required at the time of appointment. The department is especially interested in candidates who can contribute to the diversity and excellence of the academic community through research, teaching and service. The search will continue until the position has been filled.

The University of California is an Equal Opportunity/Affirmative Action Employer.

Looking for a postdoc position?

Postdoctoral Careers 1

Advertising Supplement

Get the experts behind you.

Be sure to read this special ad supplement devoted to postdoctoral opportunities, in the upcoming **10 February 2006 issue of *Science*.**

You can also read it online on **www.sciencecareers.org.**

To advertise in this issue, please contact:

U.S. Daryl Anderson
phone: 202-326-6543
e-mail: danderso@aaas.org

Europe and International
Tracy Holmes
phone: +44 (0) 1223 326 500
e-mail: ads@science-int.co.uk

Japan Jason Hannaford
phone: +81 (0) 52 789-1860
e-mail: jhannaford@sciencemag.jp

ScienceCareers.org
We know science AAAS

POSITIONS OPEN

The Biological Science Department at Southeastern Louisiana University invites applications for a tenure-track **ASSISTANT PROFESSOR** position available August 2006. Qualifications: Ph.D. in biological sciences. Duties will include coordinating and teaching lectures and labs in human anatomy and physiology, with opportunities to develop and teach upper level courses in your specialty. Establishment of a productive research program is expected. Preference will be given to those with undergraduate teaching experience and a proven record of supervising undergraduate and graduate research. Applicants must be committed to working with diversity. To ensure review, application materials must be received by March 15, 2006. Qualified applicants should send a letter of application, current curriculum vitae, copies of both undergraduate and graduate transcripts (official transcript will be required of finalist), three letters of reference, statement of teaching experience and philosophy, and a summary of research interests and plans. Application materials should be sent to: **Dr. William F. Font, Chairman of the Search Committee, Department of Biological Sciences, Southeastern Louisiana University, SLU Box 10736, Hammond, LA 70402.** Information about the Department of Biological Sciences can be found at **website: http://www.selu.edu/Academics/Depts/Biology/.** *Southeastern is an Affirmative Action/Americans with Disabilities Act/Equal Opportunity Employer.*

TECHNICAL SUPPORT SPECIALIST
Sunnyvale, California

Responsibilities include customer and sales technical support for hardware, software and chemistry, via telephone, and e-mail. Customer and sales technical training in-house, on-site, via telephone, or WebEx. Documentation of customer calls and complaints in accordance with Quality Service Requirement (QSR) and ISO requirements. Preparation and/or editing of all technical support materials including Tech Notes, Application Notes, and Operator Manuals. Laboratory work to develop, troubleshoot, and/or validate Application Notes, UDAs, ASRs and Cepheid reagents. A B.S. in life science and a minimum of two years of laboratory experience with assays required. Experience developing molecular biology or microbiology assays desirable. Experience in medical diagnostics desirable. Excellent oral and written communications in English required. Highly developed analytical skills a must. Technical support experience desirable. Requires ability to multi-task. Some travel may be required. Please submit your resume online at **website: http://www.cepheid.com** or e-mail your resume to **e-mail: talent@cepheid.com.** Be sure to indicate the job code (5822). *Equal Opportunity Employer.*

TWO POSTDOCTORAL POSITIONS AVAILABLE
Massachusetts Institute of Technology

Postdocs will work in a group of experimental and theoretical researchers with the objective of elucidating the mechanisms of self-association of therapeutic antibodies. Research is fundamental and sponsored by a major pharmaceutical company with the potential for direct impact on their therapeutic pipeline. Position One: Some experience in protein expression and purification from cell culture is essential. Experience in site-directed mutagenesis, fluorophore labeling, and fluorescence spectroscopy is desirable. Position Two: Experience in high performance liquid chromatography (HPLC), laser light scattering, and/or other methods for quantifying rates of biochemical processes is desirable.

Candidates will be appointed through MIT's Department of Chemical Engineering, but because of the interdisciplinary nature of the research, Ph.D. can be in biology, biochemistry, chemistry, engineering, et cetera. Send a resume with contact information for references to: **Professor Bernhardt L. Trout, e-mail: trout@mit.edu.**

POSITIONS OPEN

THE DEPARTMENT OF PSYCHIATRY
University of Pennsylvania School of Medicine

Seeks candidates for an **ASSISTANT** or **ASSOCIATE PROFESSOR** position in either the tenure-track or the non-tenure Clinician-Educator track. Track and rank will be commensurate with experience. The successful applicant will have experience in the field of neuropsychiatry with a focus on behavioral neuroscience, functional magnetic resonance imaging (fMRI). Applicants must have a Ph.D. or M.D./Ph.D. degree and have demonstrated excellent qualifications in education and research. Candidate should have research experience in application of fMRI or electrophysiology in human studies, preferably in area of memory and executive function. Individuals with training in developmental neuropsychology are encouraged to apply. Responsibilities include participation in multi-disciplinary team of basic and clinical neuroscientists with opportunities to contribute to study of schizophrenia and other brain disorders while pursuing independent research. Opportunities for clinical and teaching activities are available. Please submit curriculum vitae, a letter of interest, and three reference names to: **Dwight L. Evans, M.D., Professor and Chair; Raquel E. Gur, M.D., Ph.D.; REF#75, c/o A. Plotnick, Department of Psychiatry, University of Pennsylvania School of Medicine, 305 Blockley Hall, 423 Guardian Drive, Philadelphia, PA 19104-6021.**

The University of Pennsylvania is an Equal Opportunity, Affirmative Action Employer. Women and minority candidates are strongly encouraged to apply.

POSTDOCTORAL POSITIONS
Integrative Neurophysiology of Cortical/Basal Ganglia Interactions

(1) Candidates should have experience with patch clamp recordings in brain slices or anatomical methods to map the connectivity of neuronal circuitry that involves multiple brain loci, such as the neocortex and basal ganglia, in the rodent brain. Experience with analysis of rodent behavior is also relevant.

(2) The project is part of a larger effort to use a combination of molecular, genetic, cellular, and systems approaches to analyze the neural circuitry underlying a well-defined behavior. This multidisciplinary effort involves the laboratories of **Doug Nitz, Niraj Desai, Weimin Zheng,** and **Fred Jones** at the Neurosciences Institute. The immediate objective is to relate the electrophysiological properties of neurons with their patterns of connectivity with other brain regions. In addition to more traditional techniques, the project will make extensive use of dynamic clamp methodology and molecular perturbation techniques.

Submit curriculum vitae, statement of research interests, and names of three references to: **Dr. W. Einar Gall, Research Director, The Neurosciences Institute, 10640 John Jay Hopkins Drive, San Diego, CA 92121. E-mail: jobs@nsi.edu.**

STAFF ASSOCIATE/MOLECULAR MECHANISMS OF NEURODEGENERATION
Columbia University, New York, New York

The Department of Neurology at Columbia University is seeking a Staff Associate to work in a laboratory studying molecular and cellular mechanisms of neurodegeneration related to Parkinson's Disease (PD). We are engaged in a wide-ranging research program studying the role of programmed cell death in the neurodegenerative process. The preferred candidate should hold an M.D. or Ph.D., have significant experience in cell/molecular biology, immunohistochemistry, and methods of analysis of genetically modified mice coupled with an interest in mechanisms of neurodegeneration. Send curriculum vitae and the names of three references, along with a description of research interests and experience to: **Dr. Robert E. Burke, Professor, Columbia University, Department of Neurology, 650 W. 168th Street, BB-306, New York, NY 10032.** *Columbia University is an Affirmative Action/Equal Opportunity Employer.*

POSITIONS OPEN

MICROBIOLOGIST
Faculty Position

The Department of Veterinary Pathobiology at Purdue University invites applications for a ten-month tenure-track faculty position in microbial pathogenesis. Responsibilities of the position include the development of an extramurally funded research program and teaching microbiology in the professional veterinary and graduate curriculum. Applicants must have a Ph.D. Postdoctoral experience and a D.V.M. or equivalent degree are preferred. The rank of the position is open and will be determined by the qualifications of the successful candidate. Candidates who are applying for the position at the Associate or Full Professor level are expected to have a record of extramural funding. Primary consideration will be given to candidates who use animal models to study host-pathogen interactions.

The Department of Veterinary Pathobiology has 30 faculty members and 51 graduate students. Faculty have strong expertise in various areas, including microbiology, immunology, epidemiology, host-pathogen interactions, and vaccine development. Interdisciplinary research is strongly encouraged. Purdue University has many interdisciplinary research centers, including the Bindley Bioscience Center, the Center for Aging and the Life Course, the Center for Food Safety Engineering and the Purdue Cancer Center. Core research facilities available on campus include flow cytometry and confocal microscopy, gene array, proteomics, mass spectrometry, and transgenic mouse production and housing.

Applications should be submitted electronically as a single PDF file that includes curriculum vitae, a summary of research interests, a statement on teaching, and names and contact information of three references to **e-mail: microvpb@purdue.edu.** Review of applications will start on February 15, 2006, and will continue until the position is filled.

Purdue University is an Equal Opportunity/Equal Access/Affirmative Action employer. Women and minority applicants are strongly encouraged to apply.

SENIOR POSTDOCTORAL ASSOCIATE
University of Southern California

Senior Postdoctoral position available for molecular research on adipogenic transcriptional regulation of hepatic stellate cell differentiataion or iron-mediated signaling for NF-kB activation in macrophages. Applicants are required to: (1) *be U.S. citizens or permanent residents* and (2) have completed two to four years of postdoctoral training in cell and molecular research. The position is to be filled between June and August 2006. Send curriculum vitae and names of three references by **e-mail: htsukamo@usc.edu** or mail to:

Professor Hide Tsukamoto
Department of Pathology
Keck School of Medicine
University of Southern California
1333 San Pablo Street
MMR Fourth Floor
Los Angeles, CA 90033-9141

An Equal Opportunity/Affirmative Action Employer.

The University of Southern California (USC)/Norris Comprehensive Cancer Center of the Keck School of Medicine at the University of Southern California is undergoing a major expansion and seeks applicants for Faculty Positions at the **ASSISTANT, ASSOCIATE, AND FULL PROFESSOR** level in **tumor immunology/immunotherapy.** Areas of particular interest include, but are not limited to, translational research, human immunology, regulatory T cells, cancer vaccines, and antigen presentation. The positions are to be filled starting in March 2006, and thereafter. All applicants should send curriculum vitae and research plan, along with names of three references to: **Dr. W. Martin Kast, Co-Director, Tumor Micro-environment Program. USC/Norris Comprehensive Cancer Center, ZNI 245, 1501 San Pablo Street, Los Angeles, CA 90033** or **e-mail: judygonz@usc.edu.** *USC is an Equal Opportunity Employer.*

DIRECTOR
RESEARCH RESOURCES CENTER

The University of Illinois at Chicago (UIC) is seeking applicants for the position of Director of the Research Resources Center (RRC). UIC is an ambitious, urban, state-supported, Research I institution with world-renowned programs in biomedical, physical, chemical and engineering research. The RRC is a centrally managed cooperative of research support services that play a key role in the incorporation of new technologies with a growing user base. Given the recent growth of RRC services in the area of biotechnology, the preferred candidate should ideally have a strong background in this area. We seek a director who can effectively lead programmatic growth, has excellent communication skills, and who has demonstrated relevant research and management skills, preferably in an academic environment. Applicants must possess a doctoral degree, five to ten years of related experience, and have knowledge of major instrumentation. Currently, RRC research support services include a DNA sequencing facility, a genomic facility, a protein laboratory, a transgenic production service, electron, confocal and Raman microscopy, NMR spectrometry, mass spectrometry, flow cytometry, X-ray photon spectroscopy, electronic and machine shops, a computer support group and stores facility. The RRC is a campus-wide program that currently has forty full time employees and provides support service to over 800 principal investigators. The RRC is a division of the Office of the Vice Chancellor for Research and the Director reports to the Vice Chancellor for Research.

For fullest consideration, send a letter of application by March 15, 2006, with a complete professional vita, and the names and addresses of at least three references whom we may contact, to: **Dr. Tim Keiderling, Chair, RRC Search Committee, % Ms. Raydell Erin, University of Illinois at Chicago, E102 Medical Science Building MC 937, 835 South Wolcott Avenue, Chicago, Illinois, 60612-7341; email Raydell@uic.edu; http://www.rrc.uic.edu/.**

The University of Illinois at Chicago is an Affirmative Action and Equal Opportunity Employer.

MEETINGS

SEB at Canterbury 2006

SEB

3rd – 7th April
University of Kent
at Canterbury

The Society for Experimental Biology's Annual Main Meeting

REGISTER NOW!
at
www.sebiology.org

Featured Employers

Search **ScienceCareers.org** for job postings from these employers. Listings updated three times a week.

Abbott Laboratories
www.abbott.com

Kelly Scientific Resources
www.kellyscientific.com

Pfizer, Inc.
www.pfizer.com

Pierce Biotechnology, Inc.
www.piercenet.com

Scios
www.sciosinc.com

If you would like to be a featured employer, call 202-326-6543.

ScienceCareers.org
We know science AAAS

BAYLOR
Institute for
Immunology Research
Baylor Research Institute

Junior Investigator to Lead 'Humanized' Mouse Core Facility

Baylor Institute for Immunology Research (BIIR) in Dallas, TX is seeking a PhD-level Junior Investigator to lead the development of the humanized mouse project to model the human immune system (Humouse project). The successful applicant will direct the Humouse Core Facility with the goal of providing novel strains of Humouse for research purposes. Candidates should have extensive experience in genetic manipulation of rodent populations with a solid background in immunology. This position will work closely with BIIR researchers in a variety of existing projects as well as the development of new projects. BIIR is a highly collaborative and energetic research facility that focuses on dendritic cells, the initiators of immune responses. The overarching aim at BIIR is to quickly translate relevant research findings to the clinical setting in the form of novel therapeutic and diagnostic tools.

Ref: **Palucka, A. K. et al.** Human dendritic cell subsets in NOD/SCID mice engrafted with CD34+ hematopoietic progenitors. *Blood* **102:**3302-10, 2003. **Caroline Aspord, Mike Gallegos, Florentina Marches, Jacques Banchereau**, and **A. Karolina Palucka**, OncoHumouse reveals how breast cancer subverts human immune responses.

Contact: **A. Karolina Palucka, MD, PhD; karolinp@baylorhealth.edu.**

Cryo-Electron Microscopist

The Department of Molecular Physiology and Biophysics at Mount Sinai School of Medicine has embarked on developing new research directions and invigorating its research program in Structural Biology. We invite applications from individuals with expertise in Cryo-Electron Microscopy (or related areas of research) to submit their candidacy for a position at the Assistant/Associate Professor level. We seek an outstanding candidate to develop a vigorous research program in the study of macromolecular structure and dynamics of biological assemblies. We are committed to building on our departmental strengths in Structural Biology and Molecular Biophysics, and our ongoing growth of a multidisciplinary and interactive environment for studies of macromolecular structure and physiological function. Generous start-up funding will be provided to the successful applicant. Access to the state of the art Cryo-EM facility at the New York Structural Biology Center is available.

Applications, including a CV, a statement of research interests, copies of 2-3 publications, and three or more letters of reference (sent independently) should be submitted to:

Professor Aneel Aggarwal
Chair, Search Committee
Department of Molecular Physiology and Biophysics
Mount Sinai School of Medicine
Box 1677
1425 Madison Avenue
New York, NY 10029

POSITIONS OPEN

TENURE-TRACK FACULTY POSITION IN PATHOLOGY

Applications are invited for an **ACADEMIC PATHOLOGIST** at the rank of Assistant/Associate/Full Professor. Candidates must have M.D., D.O. D.V.M., Ph.D., or equivalent degree with training in human pathology. Tenure-track faculty candidates are expected to teach general and systemic human pathology to medical students, and to develop a strong research program. Candidates with only teaching credentials in pathology will also be considered for a non-tenure-track faculty position. Apply with curriculum vitae and three references to **Dr. Mitzi Nagarkatti, Chair, Department of Pathology, Microbiology, and Immunology, University of South Carolina School of Medicine, Columbia, SC 29208,** or **e-mail: pathmicro3@med.sc.edu.** The search will start immediately and continue till the position is filled. *University of South Carolina, Columbia is an Equal Opportunity/Affirmative Action Employer.*

University of Illinois at Chicago (UIC), Department of Medicine, ASSISTANT TO ASSOCIATE PROFESSOR, PHYSICIAN SCIENTIST. The Department of Medicine's Center for Cardiovascular Research at the University of Illinois at Chicago is seeking Physician Scientists at the level of Assistant to Associate Professor (rank/tenure commensurate with qualifications) with interests in the broad fields of cardiovascular research. This position emphasizes research with some clinical responsibilities. Salary/benefits are competitive. Junior investigators are encouraged to apply. M.D. is required, M.D./Ph.D preferred. For fullest consideration send curriculum vitae by February 20, 2006, to: **Peter M. Buttrick M.D., University of Illinois at Chicago, 840 S Wood Street, (CSB 929 - MC 715), Chicago, IL 60612. E-mail: buttrick@uic.edu; fax: 312-413-2948.** *UIC is an Affirmative Action/Equal Opportunity Employer.*

POSITIONS OPEN

RESEARCH ASSOCIATE (POSTDOCTORAL)
Medical Biotechnology Center
University of Maryland Biotechnology Institute

The Medical Biotechnology Center (MBC; **website: http://www.umbi.umd.edu**) of the University of Maryland Biotechnology Institute (UMBI) seeks applications for a Research Associate (Postdoctoral position R3-0325) to study presenilin-interacting proteins.

Candidates should possess a Ph.D. and/or M.D. degree in molecular biology, biochemistry, cell biology, or related field. The ideal applicant should have experience in molecular-cell biology and biochemistry. Experience in transgenic and knockout mice is highly desirable. Applicants should send curriculum vitae and names and contact addresses of three references to: **Dr. Mervyn J. Monteiro, 725 West Lombard Street, Baltimore, MD 21201. E-mail: monteiro@umbi.umd.edu.**

MBC/UMBI is an Affirmative Action/Equal Opportunity Employer. Women, minorities, veterans, and candidates with disabilities are encouraged to apply.

GRANTS

BRAIN TUMOR RESEARCH GRANTS
ONE YEAR $100,000 GRANTS
TWO YEAR $200,000 GRANTS
Available in the United States and Canada
Application Deadline: March 16, 2006

The Brain Tumor Society (BTS) is awarding grants to fund basic scientific and translational research directed at finding a cure for brain tumors. Grants are awarded annually at a maximum of $100,000 per year. Grants may be used for startup projects or supplementary funding. Funds cannot be used for indirect costs. Clinical projects will not be funded.

For application packets, visit BTS **website: http://www.tbts.org.**

COURSES AND TRAINING

COURSES AND TRAINING
Third Annual
EXPERIMENTAL NEUROGENETICS OF THE MOUSE
May 8-16, 2006
University of Tennessee Health Science Center
Memphis, Tennessee U.S.A.

This lecture and hands-on workshop is to train students and researchers in the use of mice in the analysis of nervous system structure and function. Topics covered include mouse informatics, genetics of Mendelian and complex disorders of the nervous system, and various approaches to examining gene function (e.g., knockouts, ethyl nitro sourea, mutagenesis, RNA interference, inbred lines).

A significant part of the course will be devoted to phenotypic analysis of mice for neurological traits using behavioral, anatomical, physiological, and molecular screens. Invited speakers include **Ellen Hess, Ilan Golani,** and **Doug Walhsten,** plus faculty affiliated with the Tennessee Mouse Genome Consortium. See **website: http://mouseneurogenetics.utmem.edu,** or contact: **Pat Goss, e-mail: pgoss@utmem.edu.**

Find out about jobs before you get your issue. Sign up for customized e-mail notification of jobs at **website: http://www.sciencecareers.org** by clicking on Job Alerts. You can also post your resume (open or confidentially) and check how many employers have viewed your resume at your own convenience.

MARKETPLACE

Believe it!

DNA Sequencing for $2.50 per reaction.

- Read length up to 900 bases.
- High quality electropherograms.
- Fast turnaround.
- Plasmid and PCR purification available.

$2.50 per reaction!

POLYMORPHIC
Polymorphic DNA Technologies, Inc.℠

Polymorphic exclusively uses ABI 3730XL sequencers.
Data delivered via secure FTP, email or CD.
No charge for standard sequencing primers.
384 sample minimum order.
96 well plates only—no tubes.

www.polymorphicdna.com
info@polymorphicdna.com

1125 Atlantic Ave., Ste. 102
Alameda, CA 94501

888.362.0888

For more information please visit
www.polymorphicdna.com